TOWARDS GASTRIC CANCER IMMUNOTHERAPY: ASSESSMENT OF CANCER IMMUNITY AND POTENTIAL IMMUNE TARGETS

By

ALI GAITHAN AL KHATHAMI

A thesis submitted to
The University of Birmingham
for the degree of
DOCTOR OF PHILOSOPHY

Institute of Cancer and Genomic Sciences
School of Medical and Dental Sciences
University of Birmingham
May 2018

Abstract

Gastric cancer (GC), the fourth most common malignancy worldwide, has poor prognosis and treatment innovation is needed. The aims of this project were to investigate immune targets and treatment strategies for GC. I identified new T-cell epitopes in three Epstein-Barr virus (EBV) tumour antigens, LMP1, LMP2 and BARF1, expressed in the 10% of GC cases positive for EBV. T-cell clones showed that a BARF1-specific CD4 T-cell epitope restricted by HLA-DR51, an allele common in the population, was presented by an EBV-positive epithelial cancer cell line.

Analysing blood and fresh tumour from newly diagnosed GC patients, I detected T-cell responses to MAGEA1, MAGEA4 and NY-ESO-1 tumour antigens in blood but not tumour. Compared to healthy donors, patients had: higher frequencies of LAG3 or CTLA4 positive CD8 T-cells, TIM-3 or CTLA4 CD4+ T-cells, T-regs, NKT-cells and gamma-delta T-cells in blood and tissue. Patients also had high granulocytic MDSC frequencies in PBMC. The CD4:CD8 ratio was low in some patients' blood, potentially indicating immunosenesence, but was always higher in tumour tissue.

I successfully generated tumour infiltrating lymphocytes (TILs) from nine patients' tumours. These comprised high T-cells and NK-cells and low T-reg and MDSC. LAG-3 was increased, but PD1, was decreased on TIL T-cells. Using 3-dimensional organoids established from two patients, I showed that TIL NK-cells, but not TIL T-cells, recognised autologous tumour organoids. My results are the first proof of principle that TILs can readily be generated from gastric tumours, can target tumour cells and therefore be used to treat gastric cancer.

I would like to dedicate this thesis to my parents, who believed in my choices and supported me unfailingly throughout My studies.

Acknowledgments

The most acknowledgment of gratitude I wish to express is to Almighty ALLAH for his uncountable blessing and for giving me the strength and patience to complete my thesis successfully, after all the challenges and difficulties.

I wish, first of all, to extend a sincere gratitude to my supervisor Dr. Graham Taylor, for his supervision, guidance, and for helping me throughout my PhD project. I am tremendously fortunate for having the opportunity to study under his supervision. I would also like to thank my second supervisor Dr. Heather Long for her support and giving such thoughtful feedback.

I would like to express my warmest and deepest thanks to my wife, and my kids for their love and support in every way possible over the past years. They have always been there for me and I am thankful for everything they have made for helping achieved my dreams.

Many people have kindly contributed toward the successful of this project. A special thanks to Tracey Haigh for her help, training, and friendship throughout my PhD. I would also like to acknowledge other colleagues including Dr. Claire Shannon Lowe, Dr. Andy bell, Dr. Alexander Dowell, Joseph and, all T and B cells groups for their ideas, help, and good humor.

I am very much thankful to the Saudi Arabian Cultural Bureau in UK and King Khalid University for offering me the scholarship to continue my studies and supporting me morally and materially.

Table of contents

List of tables

List of figures

Abbreviations

aa	Amino acid
AP-1	Activator protein-1
APCs	Antigen presenting cells
ATP	Adenosine triphosphate
β2m	Beta-2-microglobin
BCR	B cell receptor
BFA	Brefeldin A
BL	Burkett lymphoma
CBF-1	Cp binding factor-1
CLIP	Class II peptide
CSF-1	Colony-stimulating factor-1
CXCL12	C-X-C motif chemokine 12
CEA	Carcinoembryonic antigen
CTL	Cytotoxic lymphocyte
DCs	Dendritic cells
DMSO	Dimethyl sulphoxide
DC	Dendritic cell
DETC	Dendritic epidermal T-cell
DNA	DeoxyribonucleicAcid
DP	Double positive
dsDNA	Double-stranded DNA
ECM	Extracellular matrix
EBERs	EBV-encoded small RNAs
EBNA	EBV nuclear antigen
EBVGC	EBV-positive gastric carcinoma
EBV	Epstein Barr Virus
ELISA	Enzyme linked immunosorbent assay
EBNA1	Epstein-Barr nuclear antigen 1
FasL	Fas-ligand
FcR	Fc receptors
FCS	Foetal calf serum
Gly-Ala	Glycine-alanine
GM-CSF	Granulocyte/macrophage colony-stimulating-factor
HC	Heavy chain
HCMV	Human cytomegalovirus
HD	Healthy donor
HHV	Herpesvirus
HLA	Human leukocyte antigens
HS	Human serum
HSV	Herpes simplex virus
ICAM	Inter-cellular adhesion molecule
IE	Immediate early
IFN	Interferon
FACS	Fluorescence-activated cell sorting
IL	Interleukin
IM	Infection mononucleosis
IMGT	ImMunoGeneTics
IRF	Interferon regulatory factor
LAG-3	Lymphocyte-activation gene 3
LCL	Lymphoblastoid cell lines
LCs	Langerhans cells
LMP	Latent membrane proteins
MDP	Macrophage DC progenitor
MAGE	melanoma associated antigen

MHC	Major histocompatibility complexes
MIIC	MHC class II late endosomal compartment
MDSCs	Myeloid-derived suppressor cells
miRNAs	MicroRNAs
moDCs	Monocyte-derived dendritic cells
MACS	Magnetic-activated cell sorting
MFI Mean	Mean fluorescence intensity
NBD	Nucleotide binding domain
NFkB	Nuclear factor-kB
NK	Natural killer
NK	Cell Natural killer cell
NLR	Nod-like receptor
NY-ESO-1	cancer-testis antigen
NLRs	NOD-like receptors
NOD	Nucleotide oligomerisation domain
NOX2	NADPH-oxidase 2
OriP	Origin of viral replication
PBMCs	Peripheral blood mononuclear cells
PBS	Phosphate buffered saline
PD- L	Programmed death-ligand
PD1	Programmed cell death protein
PCR	Polymerase chain reaction
PSMA	Prostate-specific membrane antigen
PDCs	Plasmacytoid dendritic cells
PHA	Phytohaemagglutinin
PLC	Peptide loading complex
pMHC	Peptide-MHC
PMNs	Polymorphonuclear leukocytes
PTLD	Post-transplant lymphoproliferative disorder
ROS	Reactive oxygen species
RR	Ribonucleotide reductase
RBC	Red blood cell
TAP	Transporter associated with antigen processing
TCR	T cell receptors
TIL	Tumour-infiltrating lymphocytes
TME	Tumour microenvironment
TIR	Toll/Interleukin-1 receptor
TNFR	Tumour necrosis factor receptor
TIM-3	T cell immunoglobulin and mucin domain 3
T-Reg	Regulatory T-cell
TCR	T-cell receptor
TEC	Thymic epithelial cell
TGFβ	Transforming growth factorbeta
Th1	T-helper celltype1
Th17	IL-17-secreting T-helpercell
Th2	T-helper cell type2
TLR	Toll-like receptor
TNF	Tumour necrosis factor
TSA	Tissue specific antigen
Ub	Ubiquitin

CHAPTER 1

INTRODUCTION

1.1 Hallmarks of Cancer

All cancers, including gastric cancer, possess a range of hallmarks that allow their uncontrolled growth [1]. According to Berretta and Moscato, the most common hallmark is the fact that cancer cells have effective growth signals, thus can multiply without inhibition factors[2]. Cancer cells have the capacity to undergo indefinite number of cell divisions because of the ability to alter inhibitory factors, such as enzymes and hormones[3], which control the replication of DNA material. For normal cells, genetic material can only be replicated a limited number of times since the length of chromosomal DNA reduces every time new genetic material is formed. It eventually reaches a point where it cannot be further replicated and the cells die. Sonnenschein and Soto suggest that chromosomal telomeres are linked to growth factors that ensure, even after cell division, their initial size is maintained allowing cancerous cells to be immortal Cancerous cells also become resistant to apoptosis [4], a process that allows the destruction of damaged cells. In addition, cancerous cells initiate angiogenesis[5] which allows a growing tumour to develop new blood vessels allow sufficient nutrients and oxygen for maximum cell growth. Cancerous cells also have the capacity to undergo dysregulated metabolism [6]. Finally, cancers are able to evade immune effector cells that would otherwise eliminate them.

1.2 T Cell Biology

Leucocytes comprise multiple types, which can be divided into innate and adaptive immune cells. Innate cells, including NK and NKT cells have germline coded receptors and are capable of rapid response to infection. Adaptive immune cells are more complex and comprise B cells and T-cells, the latter of which will be described in more detail.

Dendritic cells are professional antigen presenting cells that activate undeveloped naïve T cells, while, macrophages and B cells activate long term memory T cells that have been initially activated by the dendritic cells. This process is continually initiated by the presence of foreign antigens or substances that prove toxic to the body cells. Dendritic cells, part of the innate immune system, are located at the skin, respiratory tract and gastrointestinal mucosa at a resting state waiting for engagement with microorganisms, they then migrate to the lymphatic system where they activate T cells. There two types of signals that have to come from the dendritic cells; signal one – for specific recognition and signal two-co-stimulatory/positive signal. Signal one involves interaction with antigen, co-receptor molecules CD-4 and CD-8 are also involved interaction[7]. Signal two involves CD-28 expressed in resting T cell and B-71 and B-72 on antigen presenting cells. If only signal two occurs (not antigen specific) the signal is not recognized as a positive signal, only signal one occurs T cells recognize the signal are not activated the T-cell become deleted or allergic but not activated therefore the dendritic cell is able to control T-cell inducing its activation and promoting peripheral tolerance. Co-stimulation is critical when it occurs with antigen stimulation; protective and tumor immunity, if absent induction to harmless environmental allergies does not occur, no autoimmunity and acceptance of grafted organs occurs.

Based on [8],hematopoietic precursors from hematopoietic stem cells from which the T cells originate populate the thymus and multiply to bring about large numbers of immature thymocytes. the initial thymocytes are CD4-CD8- that develop further to CD4+ CD8+and finally mature to single positive thymocytes (CD4+ CD8+ or CD4-CD8-) that are released into circulation to organs or peripheral tissues[9]. This

is facilitated by the thymus epithelial cells. In addition, the double negative neither expresses the CD4 nor CD8 co-receptor required for the T cell , but in double negative two stage its becomes a T-cell precursor by losing its ability to become another type of lymphocyte (B cell or natural killer cells) it also begins to develop T cell receptor. In double negative four stage the thymocytes proliferates becomes a double positive that is it acquires the CD4 and CD8 co-receptor and the T cell receptor, they can die (98%) or get into circulation.

There exist several types of T cells with different functions. Helper T-cells (CD4+) aid other lymphocytes in their immunologic processes by activation and maturation of B cells into memory B cells and plasma cells. An effective helper T-cell response is required for an effective long-lived cytotoxic (CD8+) T-cell response. These cells are associated with transplant rejection and destruction of both tumor and virus-infected cells. Regulatory T-cells (T reg) preserve immunological tolerance by suppressing auto reactive T cells. Memory T cells have formerly responded to a cognate antigen, thus have able to combat the infection or even fight cancer cells.

There are a number of inherited T cell disorders that sehd light on T-cell function. . To begin with, 22Q/11.2 deletion, the DiGeorge syndrome where 40 genes in chromosome 22 leading to 3rd and the 4th pharyngeal pouch not developing, which are essential for thymus development thus reduced T-cell[10]. Decreased IL12 function due to its receptor deficiency resulting to recurrent infection by fungi and mycobacterium, hyper IgE syndrome due to mutation of STAT 3 mutations that control cytokines and growth factors[11]. This affects helper T cells 17, thus it cannot release IL12, general cytokines and interferon gamma (IFNg), shows as recurrent infections and cold infections. IL2 deficiency results in reduced T helper1 cells and

increased T helper2 cells, the latter causes increase in IgE and eosinophil[12]. Other diseases due to T-cell deficiencies include, complete insufficiency- cartilage-hair hypoplasia, severe combined immune deficiency and Omenn syndrome; partial insufficiency chromosomal breakage syndrome and acquires immune deficiency syndrome; T cell and B cell combined Wiskott-Aldrich syndrome and ataxia-telangiectasia[13].

1.3 Cancer Immunology

Cancer immunology deals with the s immune system and how it recognises and eliminates cancer. Immunosurveillance of cancer is a hypothesis that operates under the principle that immune system recognizes and kills malignant cells. This policy was contentious until improved animal models were developed for experiments. Mouse models were used in which there was a reduction in the tumors which was a result of elimination of interferons[14]. Hence, Immunoediting was established to show the action of the immune system against the nascent tumor cells. This work brought about the the 'three e's' of cancer immunoediting: elimination of cancer, equilibrium of cancer cells with the host's immune system and, eventually, escape of the immune response allowing cancer to develop.

Cancers express a range of proteins, known as tumour associated antigens. The discovery that tumor cells could be identified by T-cells specific for the MAGE-1 protein led to the discovery of more tumor antigens, which is still an ongoing process., For cancers associated with viruses, viral proteins also serve as tumor antigens.

1.4 Immune Cells and the Cancer Microenvironment

The Tumor microenvironment is complex with many components. In addition to malignant cells there are parenchyma cells, mesenchyme cells, fibroblast, blood, and lymph vessels. The components also constitute cancer-infiltrating immune cells, cytokines, chemokine, cancer cells, stromal tissue and extracellular matrix [15].

Both innate and adaptive immune cells are present. Focusing on the latter, CD8 T cells are cytotoxic effectors capable of recognition of tumor antigen-derived epitopes presented by MHC-I molecules. Their presence in tumours is usually associated with better prognosis. Lung patients with stage 1 and 2 cancers who do not have T cell will have a repeat of the disease within five years afterward. Patients with stage three cancer but who have T cell infiltrate have an extended period without the disease. A prognostic test based on the presence of T-cells in the tumour has been developed for colorectal cancer. This immunoscore immune based biomarker outperforms the traditional TNM staging used to predict patient outcomes [16, 17].

CD4+ T-cells are generally thought to provide help to the CD8 T-cell system, since in the absence of CD4 T-cells a poor quality CD8 T-cell response results. More recent work is starting to appreciate that CD4 T-cells may also act as direct effector cells, with evidence in both mouse models but also humans. Indeed, administration of an NY-ESO-1 specific CD4 T-cell clone results in durable clinical response in a patient with melanoma. In Epstein-Barr positive cancers, administration of CD4 T-cells specific for the EBNA1 viral protein resulted in clinical responses in the majority of patients tested. Therefore CD4 T-cells should also be considered when developing cancer immunotherapies.

1.5 Cancer Immunotherapy

Immunotherapy is the treatment of cancer using the immune system. The immune system targets the cancer cells and kills them. In the past, few years immunotherapy has developed and became an integral part of treating cancer.

Antibodies are a widely used form of immunotherapy. The antibodies attach to cell surface antigens and, once connected, they can potentially call upon other parts of the immune system to fight antigen bound cancer cells. There are several types of monoclonal antibodies which include naked monoclonal, conjugated, and bispecific antibodies [18]. Naked monoclonal antibodies work alone; that is they have nothing attached to them like a drug or radioactive material. An example of such an antibody is alemtuzumab for leukemia[18]. Certain naked antibodies work by boosting the immune system and these will be discussed later. Conjugated antibodies have radioactive or chemotherapy particles joined to them. These antibodies circulate in the body untill they come in contact with specific antigens and bind to them. They then deliver the toxic substances Further, conjugated monoclonal antibodies can be radiolabeled such as anti-CD20 (Ibritumomab tiuxetan) for lymphoma, or chemolabelled such as anti-HER2 (Ado-trastuzumab emtansine) for breast cancer. Bispecific monoclonal antibodies can bind to two different proteins and have been used to activate immune cells and bring them into close proximity of cancer cells, thus redirecting the immune system to attack the cancer cells[19].

A rapidly developing immunotherapy area is the use of various checkpoint inhibitors. The immune system has normal checkpoint processes that act as negative feedback loops to prevent immune responses from escalating out of control.

Often, cancer cells use these the checkpoints to prevent attack by the immune system. Interfering with checkpoints is proving to be an extremely promising strategy. Antibodies targeting two checkpoints, CTLA4 (ipilimumab) or PD-1 (nivolumab, pembrolizumab) are currently licensed as of May 2018. Additional checkpoints, such as TIM-3 and LAG-3 amongst others are currently being investigated for cancer therapy [20].

Chimeric antigen receptors (CAR) T cell therapies are another recently developed approachto fight cancer. The immune cells are engineered in the lab so that they are specific for cancer cells. This is done by generate nove hybrid receptors that redirect T cells to target specific tumor cells[21]. As of 2018, two CD19-specific CAR T-cell therapies have been licensed to treat B-cell malignancies [22].

Cancer vaccines help the immune system to prevent or fight cancer. Examples of preventative vaccines are those that protect against particular oncogenic strains of human papillomavirus, which causes cervical cancer [23]. Liver cancer can also result from chronic infection withhepatitis B virus, thus a vaccine to prevent HBV also protects the individual from cancer development [24]. In contrast, treatment vaccines basically fight the already existing cancer cells. The vaccines are injected into the patient to increase the immune response to cancer cells. Most of them are combined with substances called adjuvants that boost immune response. So far, Sipuleucel-t is the only vaccine licensed to treat cancer [25].

Nonspecific cancer immunotherapies and adjuvants cannot target cancer cells specifically, but rather improve how another immunotherapy works. Interleukins are small proteins that are important for signaling in between leucocytes. Interleukin-2 (IL-2) is often used as a single drug treatment because it helps to support T-cell growth

[26]. Interleukins are joined with chemotherapy or with cytokines such as interferon Alpha (IFNa) [26].

1.6 The role of Tumor Associated Antigens in cancer development

Tumor-associated antigens can be divided into different categories including differentiation, over-expressed and mutated self-antigens. Cancer antigen 125 is a product of the MUC16 gene and has found its way to therapy but is very poor in specificity and sensitivity[27]. Cancer antigen 125 may be overexpresed in other types of cancers, including endometrial cancer, fallopian tube cancer, and cancer of the lungs, breast cancer and cancer of the gastro intestinal tract [28]. Prostate-specific antigen is a tumor-associated antigen[29], which is only identified in the serum of men. It is used as a tumor marker for prostate cancer. The disadvantage with this antigen is that it does not adequately distinguish between cancer and benign enlargement of the prostate gland and its low specificity makes its use as a screening tool controversial, leading to over treatment.

Her2/neu, MUC1, PRAME, survivin and are overexpressed cancer antigens that exhibit heterogonous distribution pattern in normal tissues[30, 31]. Mucin glycosylation pattern antigen is different from tumor cells and healthy cells[30]. CD4 T cells can recognize glycosylated MUC1 peptide epitope pattern and differentiate it from other glycosylated patterns[32].

1.7 Gastric Cancer

The fourth most common cause of cancer-related death in the world is Gastric Cancer[33]. Gastric cancer results from inflammation within the gut region, a condition known as gastritis, which encourages the growth of tumor cells in the stomach lining. This kind of growth may become rapid if the patient is already suffering from irregular stomach cells growth, referred as polyps. Other surrounding factors can also increase the chances of being diagnosed with gastric cancer. For instance, data exists supporting the idea that patients who have underwent stomach surgery to deal with ulcers are exposed to factors causing cell inflammation [34]. In addition, a higher number of the reported cases of gastric cancer involve obese individual because of the extra rectus abdominis layer. These excess fats interfere with digestion and replacement of cells inside the stomach. Additional risk factors include smoking, gene alteration and bacterial and viral infection. Early symptoms of gastric cancer include loss of appetite, indigestion, frequent and severe heartburn, and nausea. The patient develops serious stomach pain, unaccountable loss of weight, the stomach swells, general body weakness occurs, and either the eyes or skin turns yellowish[34]. At this stage, the tumor cells increase and can even affect the duodenum region. Several mechanisms of diagnosis such as blood tests, CT scan, and Upper GI endoscopy have been used to detect this tumor. However, treatment of the disease has often been hindered by the fact that patients are often elderly and unable to tolerate surgery or aggressive chemotherapy treatments.

more than 900,000 new cases reported annually[35], the highest mortality of GC based on its high incidence in Asia, Eastern Europe and South America[36]. In recent years, even with improvements in prognosis after use the application of cisplatin and fluoropyrimidine-based chemotherapies, surgery still the main curative therapy[37]. sadly, highly frequent relapse, in addition to distant metastases ensure that five-year survival of gastric cancer rarely exceeds 10%[36] thus, more effective and efficiency therapeutic approaches are urgently needed for gastric cancer

Pathogenesis and molecular classification of GC

Several classification systems have been used for gastric carcinoma, The Lauren classification is based on microscopic tumor morphology and divides GC into two main types: intestinal type, in which the tumor cells are well differentiated and grow slowly and diffuse type, in which tumor cells are poorly differentiated. The two morphological types have significant differences in clinical outcome[38] and possess different molecular pathogenetic pathways.

The intestinal type is associated with Helicobacter pylori (H. pylori) infection and involves a multistep molecular pathway driving the normal epithelium to intestinal metaplasia, dysplasia, and malignant transformation by chromosomal and/or microsatellite instability (MSI), mutation of tumor suppressor genes, and loss of heterozygosity among others[39, 40]. Detection of certain genetic markers, such as matrix metalloproteinases and MSI, may give prognostic information, especially for intestinal type. The common genetic alterations may provide therapeutic targets for treatment of GC cases.

Regarding the role of H. pylori, this agent frequently colonizes the human stomach, causes gastric ulcers and increases the risk of developing stomach cancer. In addition to genes that help the bacterium neutralize the acid pH of the stomach, virulent H. pylori strains contain a CagA pathogenicity island, which encodes the components of a secretion system that can inject bacterial effectors into adjacent gastric epithelial cells. One of these injected virulence factors, CagA, is highly associated with peptic ulcer disease and the development of stomach cancer [41, 42].It is known that, on entry into the epithelial cell, host kinases phosphorylate CagA at a specific EPIYA protein sequence motif, which then interacts with the host SHP2 tyrosine phosphatase. This interaction increases SHP2 activity, which leads to oncogenic Ras–Erk and Wnt signalling [42, 43] . The binding of SHP1 results in dephosphorylation of the EPIYA motif and thus reduces activation of SHP2 indicating that SHP1 normally opposes the oncogenic activity of SHP2 in these cells [44]

In contrast to the intestinal type, diffuse type GC shows no clear causal relationship with H. pylori infection, but is instead commonly associated with deficiency of cell-cell adhesion due to mutation of the E-cadherin gene (CDH1), and a manifestation of the hereditary gastric cancer syndrome. Thus, the abnormality of CDH1 mutation or loss of expression of E-cadherin may be found in early diagnosis or screening of diffuse type GC development [45] . About 50% of diffuse-type gastric cancer harbour this mutation or gene inactivation[46]. In early hereditary gastric cancer, the wild-type CDH1 allele is lost or suppressed in tumour cells with a second hit in at least 50% of cases, caused by promoter hypermethylation of CDH1. Promoter methylation is considered part of the major mechanism underlying E-cadherin downregulation in

sporadic diffuse GC [47]. in diffuse-type GC, chromosome instability includes gains at 12q, 13q and losses at 4q, 15q, 16q, and 17p[48, 49]. moreover, diffuse type gastric cancer is associated with the mutations or alterations genes, such as met proto-oncogene encoding the hepatocyte growth factor receptor and the SC-1 antigen as apoptosis receptor[50]

An alternative system divides GC into four phenotypes based on mucin (MUC1, MUC2 and CD10) expression: i) intestinal phenotype (I-type), ii) gastric foveolar phenotype (G-type), iii) intestinal and gastric mixed phenotype and iv) neither gastric nor intestinal phenotype[51]. Genetic changes were associated with mucin phenotypic expressions in gastric cancer include TP53 mutations in I-type GC and microsatellite instability in G-type. in addition to epigenetic alterations include methylation of hMLH1 revolving more frequently in MUC2-negative gastric cancer and increase frequently methylated MGMT in MUC2-positive GC than in MUC2-negative GC[52]. A good understanding of the mechanisms implicating cancerous tumour in gastric is critical to conquering the tumor and targeting pathogenic mechanisms has led to improvements in survival [53]. Thus, GC cases can be divided into subtypes defined by biomarkers, such as the overexpression of epidermal growth factor receptor kinase 2 (HER2) protein and amplification of its gene ERBB2. These biomarkers have been used to inform targeted treatment approach of GC. Functional genomic alterations, such as c-MET activation, have also been used as biomarkers to inform personalized treatments. Other potential targets for gastric cancer therapy include the P13K/Akt/mTOR pathway, epidermal growth factor receptor (EGFR), fibroblast growth factor receptor , insulin-like growth factor receptor and VEGF receptor [54] It

is clear from such work that gastric cancer is characterized by molecular complexity.[55, 56].

Finally, a recent classification scheme for gastric cancer has been proposed based on molecular classification of tumor cells. It divides GC into four subtypes: i) genomically stable tumors (GS), ii) tumors with chromosomal instability (CIN), iii) tumors with microsatellite instability (MSI) and iv) tumors positive for Epstein-Barr virus (EBV) (Cancer Genome Atlas Research, 2014)[56]. As might be expected from a molecular classification each subtype possesses distinct genomic features.

GS tumors are consolidated in both the diffuse histological variant and mutations of, RHOA , CDH1 or unification of RHO-family GTPase-activating proteins . CIN tumors are characterised by wide frequencies of CDH1 mutation (37%) and TP53 mutation (71%), marked aneuploidy and focal amplification of receptor tyrosine kinases which are clinically therapeutic targets[57]. MSI tumors display a high prevalence of DNA promoter hypermethylation, for example at the MLH1 promoter, which is different from EBV-associated DNA hypermethylation [58] MSI tumors show elevated mutation frequencies of genes encoding targetable oncogenic proteins : TP53, ARID1A, KRAS PIK3CA, ERBB3, PTEN and HLA-B[57] although few clear targets are noted. Finally, EBV-related tumors are chromosomally stable but, show extensive minimal demethylation and genome-wide hypermethylationand exhibit requent ARID1A, PIK3CA BCOR mutations and 9p chromosome amplification. They have a low rate of TP53 mutations which contrasts with the high TP53 mutation frequency found in CIN and MSI tumors[57]. The unique features of the EBV+ GC subset is explored in greater detail below.

Molecular pathogenesis of Epstein-Barr virus-associated GC

Ten percent of gastric cancer is associated with EBV. The tumour consists of a monoclonal proliferation of EBV infected epithelial cells and, as described above, represents a distinct clinicopathologic subset. Key characteristics are: younger age, male predominance, proximal location, lower rate of lymph node involvement, marked lymphocytic infiltration, and lace pattern within the mucosa[59]. Frequent loss of p16 (CDKN2A), Fhit, smad4 and CD82 (KAI-1) are found[60]. Global CpG island methylation in the PTEN promoter region is considered as a characteristic feature abnormality in EBV-GC[61]. The tumour cells contain non-coding EBV RNAs including EBV-encoded small RNA (EBERs) and Bam H1-A rightward transcripts (BARTs). Several EBV latent genes are also expressed within the tumour cells including EBV nuclear antigen 1, latent membrane protein 2A (LMP2A) and BARF1 [62]. viral gene LMP2A responsible for aberrant hypermethylation through activation of host DNA methyltransferase 1[63] furthermore, LMP2A upregulates Birc5 (survivin) expression by activation of nuclear factor-κB, activates extracellular signal regulated kinases (ERK/MAPK1), and inhibits TGF-β-induced apoptosis via upregulation of the Ras/PI3K/Akt pathway[64] . however, the role of EBV genes in gastric cancer will discuss next with more details.

1.7.1 Role of Immune Cells in Gastric Cancer

Immune cells play an important role in the pathogenesis and progression of many cancer. Several reports suggest the same is true also for gastric cancer[65, 66]. Recently, B cells have been reported to be present at lower levels in cancer patients with different type of cancers include GC [67]. In the peripheral blood the proportion of γδ T cells in GC patients was found to be higher than healthy controls[68].

1.7.2 Tumor Infiltrating Lymphocytes in cancer therapy

Tumor infiltrating lymphocytes are immune cells in tumor site that can isolated from a patient's tumour and expanded in number by culture in vitro. Removal of immunosuppressive factors present in the tumour microenvironment, and the addition of growth promoting cytokines such as IL-2, allows lymphocytes to divide and grow resulting in large numbers of immune cells. The assumption underpinning TIL therapy is that amongst these cells are effector cells specific for the tumour but unable to act in the suppressive tumour microenvironment. Growth conditions can readily be manipulated in vitro to support preferential expansion of desired immune cell types. Administered back to the original patient, the immune cells can re-infiltrate tumors and, being present in higher numbers than before, can overcome the barriers that previously limited their functional capacity to initiate tumor lysis. Most tumor infiltrating lymphocytes (TILs) are T lymphocytes[69]. Tumor infiltrating lymphocytes intended for therapy are usually isolated from tissues and cultured with cytokines such as interleukin 2[70]. This type of adoptive immunotherapy Has proven effective in a number of patients with melanoma. TIL therapy has surpassed a number of existing cancer treatment in a number of ways; it is seen to have a higher response than ipilimumab and works for a longer time than vemurafenib. If there is a therapy

with promising potential to improve outcomes for melanoma, then it is TILs. In addition, scientists have used TILs therapy to define ways through which cell based immunotherapy can be incorporated into cancer treatment[71].

The generation of tumor infiltrating lymphocyte first involves harvesting of a 2 centimeter excisional biopsy. The biopsy is then cut into small fragments that range between 1-3 millimeters and then incubated in a desired growth medium. Interleukin 2(IL-2) is then added and observations made. The presence of lymphocytes will cause death to the adherent tumor cells as the TIL proliferates. Approximately after four weeks, the T-cell phenotype of TILs as well as their action against the patient's tumor cells is tested. TILs are then expanded for about two weeks using a cell expansion protocol; typically these use high concentrations of activating anti-CD3 antibody and interleukin 2. In total it takes between 2-6 weeks to generate TILs.

1.7.3 Gastric Tumour Associated Antigens

There are several known tumor associated antigens in gastric cancer. For instance, Ademuyiwa, *et al.* , indicate that NY-ESO-1 cancer testis (CT) antigen is one of the most likely antigen to be used for immunotherapy surveys based on the fact that it has a high immunogenicity potential[72]. Antibodies specific for NY-ESO-1have been detected in gastric patients' blood[73]. This antigen could be a critical element in improving the immunotherapeutic process for gastric cancer patients.

Another antigen that may be important for the immunotherapy of gastric cancer is mucin 1 (MUC 1), which is a cell surface protein [74]. MUC 1 is involved in establishing mucous layers that shield surfaces of the epithelial cells in the body [75]. Specifically, the protein formed using MUC 1 gene signals the mucous glands to secrete more mucous on internal surfaces such as the stomach lining and pancreatic

region. As a result, the mucous protects the stomach from the possibility of a mechanical breakdown due to excess HCl level. This could be of utmost importance when used as a signal for the action of immune cells. For example, immunotherapeutic technique involving MUC 1 induces rapid formation of mucous within the stomach region[75]. It means that the peptide groups on the surface of these mucous proteins trigger an immune response against malignant cells forming around this region.

Several tumour antigens from the melanoma associated antigen (MAGE) family are thought to be expressed in gastric cancer. Melanoma-associated antigen 1 (MAGE 1) is a protein known to induce the activity of TRIM31, which is inherited in different forms [76]. The activity taking place in this case is referred as E3 ubiquitin-ligase action that is viewed as a target immunological threat to the human body. The amino acid composition of this protein is slightly different from that of the normal proteins synthesised by the cells. Although it has no effect on the individual, cytotoxic T cells view it as a foreign antigen. It stipulates that an immune response would be directed towards the region in which these proteins are synthesized. In addition, MAGEA1 and TRIM31 combine to form a TRIM31-MAGEA-NSE4 complex[76], which seems to hinder the progressiveness of cells around their region. However, this complex can be eliminated within a short duration by reducing the activity of TRIM31. If the same antigen is produced within the tumor region, it would help expose malignant cells to the immune system. This means that the immune system will counter the ability of cancerous cells to protect themselves from being detected by the cytotoxic T cells. According to Sienel, *et al.* , melanoma-associated antigen 3 (MAGE-A3) has been used in the past to initiate the destruction of cancerous cells present in the early stages of lung cancer[77].

Carcinoembryonic antigen (CEA) is another common antigen in cancer therapy[78]. This protein originates within the human body during the early stages of life. However, levels subsequently decrease as an individual grows. Over the years, CEA has been important in the field of medicine and health sciences because it reappears in high levels in cancer patients. A test for CEA has been developed to detect the presence of cancerous cells [78]. a possibility that cytotoxic T cells might end up attacking non-cancerous cells.

Prostate-specific membrane antigen (PSMA) has also been a primary research target for cancer therapy for a long period [79]. This transmembrane protein has features that can indicate the presence of malignancy. Despite its name, PSMA is expressed in other cancers including gastric cancer, where there exists a poor correlation between PSMA expression and survival[80]. Studying the protein could be helpful for gastric cancer because the compound is present in the malignant tissue. Chang et al. [79] describe that the 7E11 antibody has been used for years to target the PSMA. However, the form of this antigen synthesized in cancerous cells is slightly different from the original one. As a result, new studies are being conducted to establish anti-PSMA antibodies that will not only recognize but also bind to the epitope of PSMA around the cancer region. This would suit the process of eliminating any possible malignancies using immunotherapy.

1.7.4 Role of Immunosuppressive cells

The immunosuppressive cell within tumours include the cancer associated fibroblasts that are normally identified by the expression of the membrane protein fibroblast activation protein (FAP). This protein in turn suppresses the anti-tumor immune response by mainly restricting the T cells from the stroma thereby preventing

them from accumulating in the vicinity of the gastric cancer cells. CAFs can act as an immunosuppressive cell through production of a dense extracellular matrix (ECM) that traps T cells in the stroma thus denying them access to the cancer cells. The other mechanism used by CAFs is secretion of CXCL12. The CAF-secreted CXCL12 is known to coat T cells therefore excluding them in the CXCR4-dependent manner[81].

Secondly, tumor associated macrophages (TAMs) are also known to contribute to the immunosuppressive tumor microenvironment. TAMs are not only mostly involved in tumor-promoting angiogenesis but also in fibrous stroma deposition as well as metastasis formation. The two mechanisms that make TAMs have the immunosuppressive abilities are; TGF-beta production that negatively regulates the effector T cells function and at the same time induces T regulatory cell differentiation. EGF and CCL18 production is the second mechanism employed by TAMs that in turn promotes angiogenesis and tumor progression[82, 83].

Thirdly, regulatory T cells (Tregs) are also among the immunosuppressive cells that contribute to immune suppression. Tregs are subsets of CD4+ T cells with suppressive capabilities that are known to have a major role when it comes to maintaining immune homeostasis and self-tolerance as well as dampening inflammation. In addition, T-regs helps prevent autoimmunity diseases. T-regs function by suppressing the function of the effector CD8+ and CD4+ cells and the antigen presenting cells among other important cells through a number mechanisms that includes secretion of immunosuppressive cytokines and production of cytolytic factors[84].

Although immunotherapies have been showing promise in the cancer field, they have failed to meet their ultimate objective. One possible explanation is the

availability of the immunosuppressive cells like the regulatory T cells and the MSDCs that produce signals that prevent tumor associated T cells from effectively attacking and killing the cancer cells[85]. Immunosuppressive cells are known to facilitate ways by which tumors can escape the immune response and they effectively achieve this mostly through stimulation of mechanisms that inhibit anti-tumor immune responses [85].Furthermore, the immunosuppressive cells contribute to the spread and growth of tumor cells by not only their suppressive property but also by inducing cell invasion and intra-vasation. Immunosuppressive cells also establish a pre-metastatic niche and facilitate the transition of epithelial mesenchyme. In addition, immunosuppressive cells also induce angiogenesis at certain metastatic sites. Recent studies have shown that it is possible to inhibit the growth and escape of tumors by blocking the immunosuppressive cells. In addition, the immunosuppressive mechanisms caused by the immunosuppressive cells or tumor cells are also eliminated.[86]

1.7.5 Immune Checkpoint Inhibitors

Immune checkpoints are signaling pathways whose function is to down-regulate immune responses to avoid damage through prolonged immune responses. Cancers frequently express these checkpoint molecules to prevent their elimination by immune effectors. Immune checkpoint inhibitors have been developed as drugs that inhibit these pathways allowing immune responses to act and destroy the cancer cells. The most common example of immune checkpoints are CTLA-4 and PDL-1. In addition, there is the PD-1 that is found on the T cells. When PD-1 binds to PDL-1, it prevents pro-apoptotic signaling and limit T cells function and activation. The immune checkpoint inhibitor CTLA-4 is most often involved during T cell priming in the lymph node and it normally prevents T cell proliferation when T cell receptors (TCRs)

are strongly stimulated with antigen. While PD-1 on the other hand, is involved later in the immune response and acts to dampen the effector T cells mediated inflammatory responses[87] .

The use of monoclonal antibodies when it comes to cancer treatment is currently on the rise, especially those that target the binding of the PD-1 and PD-L1 and block this binding and in turn enhance the immune response against the cancer cells. Notably, these antibodies have the capacity to attach to their activation sites such that they inhibit the process of binding. Therefore, immune checkpoint inhibitors are quite promising in treating certain types of cancer. Examples of drugs that target the PD-1 pathway include Pembrolizumab and Nivolumab that are generating clinical responses in a proportion of patients with several different cancer types. For instance, these two have been used in melanoma of the skin, kidney cancer, and bladder cancer[88].

1.7.6 Myeloid Derived Suppressor Cells (MDSCs)

Myeloid derived suppressor cells (MDSCs) are defined as a heterogeneous population of immature myeloid progenitor cells that have failed to mature into granulocytes, macrophages and dendritic cells. In tumor-bearing hosts, the MDSCs usually move from their site of generation, the bone marrow, to the peripheral lymphoid organs. The myeloid derived suppressor cells also display immunosuppressive properties that are thought to create the immunosuppressive tumor microenvironment (TME)[89]. When an individual gets an inflammation or cancer, the population of MDSCs is known to expand rapidly. In addition, MDSCs are known to regulate the immune responses and facilitate the repair of tissues in healthy

individuals. MDSCs also contribute to tumor growth and inhibition of anti-tumor immune reactions.[90]

As immunosuppressive cells, MSDCs exhibit both immunosuppressive and tumorigenic activities. The functions of MSDCs include but not limited to depriving the T cell of its essential amino acid for proliferation and anti-tumor activity. In addition, MSDCs produce nitric oxide (NO) and the reactive oxygen species (ROS) that causes the nitration of both chemokines that result in lower T cell recruitment as well as damage to T cell receptors inhibiting T-cell function. Moreover, MDSCs can produce interleukin 10 to inhibit immune effector cell functions. Lastly, MDSCs produce growth factors- the matrix metalloproteinase, factors that stimulate the growth of cytokines and activation of Tregs [91]

There are a number of mechanisms associated with the MDSC-mediated immune suppressive and they include; production of Arginase 1 (ARG1) and up-regulation of iNOS. Conversely, ARG1 and iNOS not only metabolize *L-arginine* but also causes the loss of the TCR zeta chain as well as promote nitration of TCR, CD3, CD8 and CCL2. In addition, they also disrupt interleukin 2 signaling and inhibit T cell proliferation. The second mechanism by the MDSC is the secretion of immunosuppressive cytokines. These cytokines include interleukin 10 and TGF-beta leading to the induction of regulatory T cells and inhibition of the functions of natural killer cells and CD8+ T cells. [90] [91].

1.7.7 Organoid and Gastric cancer

According to Tan and Barker, organoids are small forms of tissue that showcase endogenous three-dimensional organ structure, multilineage differentiation, and stem cells which are in a simple in vitro system[92]. Clevers , indicates that organoids of the mouse and human are composed of epithelium, which can be propagated from the previous standard gastrointestinal tissues including the intestines, pancreas, stomach, and liver. The propagation is defined by growth factors that replace stromal signals in a matrix geometry. Murine organoids have the opposite in that it's been propagated in a non-submerged air-liquid interface and contain the mesenchyme and epithelium and can grow without growth factor supplementation. Human-induced stem cells can be divided into intestinal cells and expanded to epithelial or mesenchyme organoids.[93]

Organoids can be wild-type, which gives an opportunity for oncogene validation. Mutations in the oncogene can be introduced to the wild-type organoids, and the effects of the modifications determined[92, 93]

1.8 Epstein Barr Virus: infection and diseases

The Epstein- Barr virus was discovered in 1964 by Epstein and his group in specimens from patients who had Burkett's lymphoma. [94]. In 1968 it was discovered that EBV could immortalize B cell [95]. At this time the link between EBV virus and infectious mononucleosis was also discovered.

EBV infects about 90% of people around world but small proportion can develop tumour. For that EBV consider the first human virus that implicated directly in carcinogenesis[96]. As result EBV associated with different malignancies including

Hodgkin lymphoma, Burkett lymphoma and post-transplant lymphproliferative disease (PTLD) for B cell cancer in addition to T and NK cell lymphoma. Moreover EBV associated with epithelial tumour such as gastric cancer and nasopharyngeal carcinoma NPC[97].

EBV is a gamma herpesvirus, also known as Human herpsvirus 4 (HHV4). The genome is double helix DNA and encodes more than one hundred genes. It is covered by a protein capsid, which is surrounded by tegument protein. This is wrapped by a lipid envelop that contain glycoproteins that allow the virus to bind to cells [98].

Initiation of the infection start when EBV attaches to B cells or epithelial cells using its glycoproteins. EBV interacts with B cells through the binding of EBV glycoprotein gp350 to complement receptor CD21 on the surface of B cell. After that EBV glycoprotein gp42 interacts with cellular B Cell-MHC II molecules. As a result the envelope of virus and cell membrane fuse after EBV forms gH, gL, gp42 glycoproteins complexs on B cell membrane. This fusion allows the viral genome to enter the cytoplasm then the nucleus of the cell. EBV can also infect epithelial cell by the BMRF2 protein binding to β1 integrin with. After that, gH,gL glycoprotein of EBV bind to αvβ6/8 integrin. These interactions lead to fusion of the envelope of the virus with the cell membrane. [98, 99].

EBV has two separate stages as part of its lifecycle which are lytic and latent cycle. The induction of lytic cycle involves three sequential phases of protein expression termed, immediate early, early and late. However (in references *Hudnall, S.D. 2014 and Tsurum et al*), Lytic cycle starts with immediate early genes which are transactivators of viral gene expression. This stage includes two EBV encoded transcription factors, BRLF1 and BZLF1, that bind to lytic origin of replication in

virus (oriLyt) to initiate replication. BZLF1 acts to inhibit expressing of p53 and NF-kB when bind to subset genes [100]. [101, 102]. .

Early lytic genes are responsible for viral genome replication and export of RNA to the cytoplasm such as BNLF2 and BSMLF1. Other early genes, BALF1 and BHRF1 act to prevent apoptosis during replication[103]. The last stage in lytic EBV replication is expression of late lytic genes that are responsible for DNA synthesis and forming the structural components of the virion (Tsurumi, Fujita et al. 2005; Hudnall 2014). There are viral homology genes that particpate during lytic stages of infection such as BCRF1 and BARF1, to inhibtit immune response [104].[101].

In Latent replication EBV persists in memory B cell without viral production. The viral genome persists in the nucleus of infected cells as an episome via host DNA polymerase. In vitro, latent infection of B cells (in the absence of an immune response) generates transformed B cell lymphoblastoid cell lines (LCL) [105]. In tumours, EBV persists in the tumour cells as a latent infection characterised by three different EBV latency programs, termed latency I, II or III[98, 106]. Each program expresses different latent viral genes and EBV early RNAs (EBER1, 2) [101, 105] . These genes include nuclear proteins EBNA1, 2, 3A, 3B and EBNA leader protein LP in addition to membrane proteins LMP1, LMP2A and 2B. In EBV latency III, activation of naïve B cells and transformation of B cells to proliferating blasts LMP1,2 and EBNA 1,2,3A-C and EBNA-LP are expressed. During the establishment of permanent infection of the host, EBV induce cells differentiation to memory cells with EBV viral expression reduced to EBNA1 to maintain the genome and LMP1,2A to prevent apoptosis to maintain growth of cell among latency II [107]Hudnall 2014) . Finally

the virus established a persistent latency I state with just EBNA1 expressed, to allow the EBV genome to be segregated to daughter cells after B cell division [98].

1.8.1 Cell mediated response to EBV

1.8.1.1 CD8 T Cell response to EBV lytic protein

The response of CD8+ T cell to EBV proteins expressed in lytic cycle shows a clear pattern of recognition, responses to Immediate early proteins are stronger than early and late cycle proteins [101, 108]. Similarly, testing CD8 T-cell clones specific for immediate early, early and late lytic protein epitopes against EBV LCLs (which contain a proportion of lytic cells) showed clear differences in recognition. CD8 T-cells specific for IE proteins recognised LCLs more efficiently than E with weak recognition of late lytic proteins[109]. As part of the global research studying the CD8 T-cell response to EBV, a study showed spontaneous CD8+ cell responses to BARF1 protein from patients with undifferentiated nasopharyngeal carcinoma [110].

1.8.1.2 CD8 T Cell response to EBV latency proteins

Turning to the latent EBV proteins, early studies showed EBV latent protein (EBNA3 A, B and C) expressed from recombinant vaccinia vectors were recognized by CD8+ cell [111, 112] restricted by certain HLA alleles such as A3 ,A11 and B7,8,and 44 [113]. Across all the latent proteins, the strongest CD8 responses were to different HLA I epitopes in the EBV latent proteins EBNA3A, 3B and 3C [114]. Other subdominant EBV proteins could occasionally elicit strong responses on some individuals carrying particular HLA alleles, such as epitopes from EBNA2 and EBNA-LP [115, 116]. Subsequent work on EBNA1, a key target given its expression in all EBV cancers, showed that an internal glycine alanine repeat domain (GAr) inhibited HLA class I presentation of EBNA1 antigen by the classical pathway [117].

GAr –deleted EBNA1 was processed and HLA I epitopes presented to CD8 T-cells [118]. However, despite its endogenous processing being inhibited, strong CD8 T-cell responses could be seen to EBNA1 in donors possessing certain HLA alleles such as HLA-B35.01 [119]; such responses being generated by cross presentation.

1.8.1.3 CD4 T cell response to lytic proteins

A recent study used nine MHC II tetramers representing a range of epitopes to identify human CD4+ T cell responses against EBV proteins during infectious mononucleosis. They found that EBV induces high frequency responses against the latent protein EBNA2 in addition to four lytic cycle proteins including BFRF1, BARF1, BMRF1 and BZLF1.In contrast, they found that in infectious mononucleosis patients the CD4+ T cell response against epitopes from EBNA1 were delayed [139]. Another study found that the CD4+ T cell response to the immediate early protein BZLF1 was higher than that against the early protein BMLF1 protein [140]. With regard to cell phenotype, a study detecting CD4+ memory T cell responses in healthy EBV carriers identified responses against both lytic and latent antigens, but the CD4+ T cells specific for lytic antigens expressed more CD45RA than those against the latent proteins, suggesting a later differentiated state [141]. Further studies have identified CD4+ T cell responses to 110 epitopes derived from different lytic and latent EBV proteins in blood donors. [142]. Importantly, EBV glycoprotein –specific T helper cells have been shown to inhibit proliferation and outgrowth of LCLs after primary B cell infection by EBV. The CD4+ T cells in this study were specific for EBV lytic glycoproteins including BALF4 (gp110), BZLF1 and BLLF1 (glycoprotein 350/220). Such a response may implicate their potential as direct effectors in therapy for disease

associated with EBV [143]. However CD4+ T cells also play a helper role, as they are important in antibody responses to EBV during infectious mononucleosis[144]. Furthermore, polyclonal CD4+ T cells generated by LCL-stimulation can prevent primary EBV outgrowth in B cells infected in vitro. These T cells comprised a pool of CD4+ T cells specific for EBV epitopes from a range of lytic proteins [145]. Patients with PTLD showed stable remission when infused with CD4+ T cells specific for a selected set of EBV epitope peptide, such as those derived from BNRF1 protein, suggesting that CD4+ T cells can have antitumor effects in vivo[145, 146]. This supports in vitro studies showing strong recognition of LCLs by cytotoxic CD4+ T cell clones to epitopes from all three stages of the lytic cycle even though only small fractions of EBV transformed B cell lines contain lytically infected cells .[139, 147]

1.8.1.4 CD4 T cell response to latency proteins

Several studies that have attempted to clarify the role of T helper 1 CD4+ T cells in defence against EBV have analysed the latent protein EBNA1, and showed that EBNA1 specific CD4+ T cells secreted IFN gamma [148, 149]. A study that determined the magnitude and frequency of Human CD4+ memory T cell response to pools of peptides derived from four EBV latent proteins in healthy EBV-positive donors assessed IFN gamma release. However, another study showed that some EBNA1 specific CD4 T cells secreted the Th2 cytokine, IL-4, whereas coincident responses to the EBNA3A protein secreted the Th1 cytokine IFN gamma[150]. Response to epitopes from EBNA1 and EBNA3C were reported to be stronger than those against LMP1 and LMP2[151]. In another study, CD4+ T cells were shown to recognize epitopes from the three latent proteins EBNA1,EBNA2 and EBNA 3C

antigens [148, 152]. Thus, EBV induces a broad spectrum of CD4+ T cell responses against multiple viral antigens in the majority of donors.

With regard to their therapeutic potential against human lymphoma, in vitro generated CD4+ T cell clones produced IFN gamma and had cytotoxic capacity against EBV transformed B cells, indicating a possible role in controlling the outgrowth of B cell malignancies [153]. EBNA1 specific CD4+ cells recognized MHC II (HLA-DP3) matched BL cells lines [154]. Furthermore, LMP1 and LMP2 specific CD4+ cytotoxic T cell recognized EBV transformed B cell lines leading to the production of Th1 cytokines and killing of the target cells by perforin mediated lysis. In addition, this study also showed that the cytotoxic CD4 cytotoxic specific for LMP1 and 2 epitopes could control LCL outgrowth, indicating their possible usefulness in therapies against LMP expressing tumours [155].

With regard to antigen processing for CD4+ T cell recognition, EBNA1 specific CD4+ T cell epitopes (SNP, VYG and PQC) that are displayed on the surface of infected cells were shown to gain access to the MHC II processing pathway via macroautophagy when EBNA1 was endogenously expressed [156]. Similarly, an early study analysising LCL recognition by CD4+ T cell specific for EBNA1 found that the presentation of epitopes derived from ENBA1 peptides was blocked upon addition of 3-methyladenine to inhibit autophagy [157]. However intercellular antigen transfer has been shown to play an important role in the presentation of the other EBV nuclear antigens targeted by CD4+ T cells. In this study, presented epitopes that derived from EBNA2 and ENBA3C were processed by intercellular antigen transfer without any apparent contribution from autophagy pathways. [158].

1.8.2 EBV associated Gastric cancer (EBVaGC) and EBV tumor Antigens

Epstein Barr virus (EBV) was the first virus associated with human malignancy. Multiple studies have shown EBV is involved in a number of different human cancers such as nasopharyngeal carcinoma (NPC) Hodgkin's lymphoma, lymphoproliferative disease and NK/T cell lymphoma. Throughout the world EBV is detected in about 10% of GC cases and around 80,000 new cases of viral-positive disease occur each year (assuming 10% of 800,000 total cases of gastric cancer) [120].

EBV latency genes play important roles in epithelial malignancies. The following genes are consistently detected: EBV nuclear antigen 1 (EBNA1), latent membrane protein 2 (LMP2) and BamH1 A rightward Forward -1 (BARF1). Additional RNA transcripts are also present, including the EBV early RNA (EBERs), Bam HI A rightward transcripts (BART) and BART miRNAs. In addition EBV early lytic genes such as BZLF1 and BFLF1 have been detected in EBVGC. The detection of these proteins suggests that a proportion of cells in the tumour are in lytic cycle. Regarding expression levels, the most abundant of the latent genes is EBER then BART, followed by LMP2A-B. Expression of EBNA1 is low raising the question of how viral genome is maintained in EBVGC [121].

EBNA1 is expressed in all EBV associated cancers and this gene is responsible for replication and persistence of viral episomes. However, until now there is little information about the specific role of EBNA1 in EBV associated gastric cancer. EBNA1 is considered the universal target in EBV associated cancers given its ubiquitous expression.

LMP2A in EBVGC cases have been reported in half of all cases compared with other EBV latent genes. These findings indicate that LMP2A expression plays important

roles in oncogene processes during EBV infection in Gastric epithelial cells. Recently, LMP2A was found to inhibit transformed growth factor b1 (TGF) induced cellular apoptosis in GC cell lines [122] .Moreover cellular survivin gene expression was unregulated through nuclear factor kb pathways in GC cell lines with LMP2A infection [123]. Furthermore, LMP2A induces the phosphorylation of STAT3 in EBVGC, activating DNA methyltransferase1 (DNMT1). This leads to promoter hypermethylation of tumor suppressor gene [124].

BARF1 has been detected in EBVGC by several groups [125]. BARF1 is thought to act as an antiapoptotic protein in EBVGC by increasing the Bcl-2 to Bax ratio [126]. Moreover, cyclin D1 is overexpressed when BARF1 is transfected into gastric epithelial cells. In addition BARF1 increased cell proliferation via upregulated NF-kB, cyclin D1 and decreased cell cycle inhibitor P21 expression [127]. Initial reports suggested that BARF1 is expressed in EBV carcinomas but rarely in lymphomas. More recent studies have reported that BARF1 is expressed in both EBV positive B cells and B lymphoma [128].

Although not encoding protein, the EBERs are involved in the maintenance of epithelial malignancy by a apoptosis resistance ,effect on cell proliferation, enhance cellular signaling and production of autocrine growth factors [129] . In EBVGC, the expression of insulin like growth factor-1 (IGF1) is induced by the EBERs. Recently EBERs were reported to suppress E-cadherin in a gastric cell line with cellular alteration miRNA expression in epithelial to mesenchymal transition (EMT)[130]. Moreover EBER upregulate Interlukin-6 (IL-6) expression in addition to downregulate cell cycle inhibitor p27 and p21 by activated regulator STATM in gastric carcinoma cell line [121].

1.8.3 Epstein-Barr virus BamH1-A Reading Frame-1 (BARF1) Oncogene as New Immunotherapy Target

1.8.3.1 BARF1 Gene and Structure

The EBV BARF1 gene encodes a 221 amino acid 31-33kDa protein containing a secretory sequence at the amino terminus. The 20 amino acid secretory sequence is cleaved and the remainder of the protein secreted into the intercellular environment [131]. BARF1 has multiple functions that not only induces malignant transformation in rodent fibroblasts but also enhancing the ability of certain EBV negative cells to bring about malignant formation. The N-terminus of the BARF1 genes contains about 54 amino acids that up regulated the Blc-2 protein that has anti-apoptotic activity [132]. These 54 amino acids are also the reason why BARF1 is able to form malignant transformations in a number of cells. Moreover, the BARF1 encoded protein that is usually secreted as a hexameric molecule possessing immune modulation properties. In addition, it is a homologue of c-fms and the colony stimulating factor 1 (hCSF-1) receptor and capable of binding CSF-1, in turn inhibiting interferon-alpha (IFNa) secretion from the mononuclear cells [133] . Although the immune modulating capabilities that BARF1 possesses allows EBV-positive cells to escape elimination by the host immune response, BARF1 is also a potential immune target. Several HLA-A 0201-restricted cytotoxic T lymphocyte (CTL) epitopes have been identified in BARF1[134].

The structure of the BARF1 gene is similar to some cellular molecules, for example the CD80 gene, from which the gene is thought to have originated from during evolution [135]. However, despite the close similarity, there is a difference in domain orientation and oligomerization between BARF1 and CD80. The interaction

between CSF-1 and CSF-1 receptor must be principally different from the binding between BARFI and hCSF-1[133]. The N-terminal domain and the C-terminal domain are the immunoglobulin like domains that make up the BARF1 protein[136]. These domains belong to different families; the N-terminal domain belongs to the variable domain subfamily whereas the C-terminal domain is related to the constant immunoglobulin.

Structurally, the unusual BARF1gene hexamerisation involves the contact of the N terminal that comes first and C terminal domain that comes second. The C-terminal however gets in contact through a surface extending to beta-sandwich of the immunoglobulin domain through the second particle. Contrarily, the N-terminal contact contains the immunoglobulin domains with an unusual relative orientation but usually with classical contact surface having dimer interactions of immunoglobulin domains sizes [136].

1.8.3.2 BARF1 in cancers- Gastric and nasopharyngeal cancers

The BARF1 gene was first identified in 1989 in NPC tumors[137]. BARF1 transcription was demonstrated for first time in NPC tissue from North African patients using RT-PCR [138]. Later, the BARF1 ORF was expressed and translated with high p31 protein in the most NPC biopsies [139]. Furthermore BARF1 transcript mRNA was detected in NPC patient among nasopharyngeal brushings containing high DNA EBV loads [140]. Another study that used epithelioid malignancies to study whether BARF1 is a lytic or latent gene found high expression of BARF1 in gastric carcinoma and NPC tissues in the absence of lytic gene expression [141].[142].

The BARF1 gene was found to be expressed in EBV+ve gastric carcinoma GC by Hausen et al [125]. Subsequent work showed that in EBV-GC, BARF1 gene

expression in the presence of abnormal p53 expression inhibited apoptosis[132]. A similar study demonstrated an anti apoptotic effect through Bcl-2[126]. A recent study showed increased cell proliferation of EBV- gastric carcinoma with secreted BARF1 leading to up-regulation of cyclin D1 and nuclear factor kappa B NF-kB [133]. The above studies all demonstrated BARF1 carcinoma expression occurred without lytic gene expression. BARF1 mRNA was detected in breast cancer tumours in two studies with lytic gene expression [143, 144]; this detection is presumably due to the presence of EBV-infected B cells in the tumour. BARF1 mRNA has been detected in Burkett lymphoma [145] , NK/T cell lymphoma [146] but this may be a result of lytic cycle rather than latency [142]

AIMS AND OBJECTIVES

1- Undertake a systematic investigation of T cell responses specific for EBV tumour antigens in healthy donors, to include: EBNA1, LMP1, LMP2 and BARF.1

2- Study the T cell response to the BARF1 oncogene, a potentially important target for immunotherapy:
   - Generate BARF1-specific T-cell clones to characterize epitopes
   - Explore potential for BARF1-specific T cells to be used for immunotherapy.
   - Study processing of BARF1 to determine the relative contributions of endogenous and exogenous antigen processing to BARF1 epitope presentation.

3- Characterize the phenotype and frequency of immune cells in gastric cancer patients' blood.

4- Characterize the phenotype and frequency of immune cells in gastric cancer patients' tumours.

5- Determine potential utility of T-cell based therapy for gastric cancer based on expansion of tumour infiltrating lymphocytes from tumour specimens. To include ability to recognize autologous tumour cells.

CHAPTER 2

MATERIALS AND METHODS

2.1 Tissue and cell culture

2.1.1 culture media and reagents

Standard Culture Media: RPMI 1640 media (Sigma) supplemented with 2 mM L glutamine (Gibco), 100 µg/ml streptomycin (Gibco) 100 IU/ml penicillin (Gibco), and 10% fetal bovine serum (FBS) (Biosera)

Monkey Leukocyte antigen-144 supernatant (MLA-144): Supernatant is derived from cultured MLA-144 cells line in RPMI 1640 + 10% FCS and 1% pen/strep then filtered by Millipore Steritop 0.22µm vacuum and stored at -20C^0.

T cell cloning media: standard culture media supplemented with 30% MLA144 supernatant, 1% human serum (TCS Biosciences) and 100U/ml Proleukin (IL2) (Novartis).

TIL media : RPMI, HEPES 25mM, 1% L-Glutamine (Gibco); 100 µg/ml streptomycin (Gibco); 100 IU/ml penicillin (Gibco); 1% Na Pyruvate (Gibco), 0.1% (50mM); 2β-mercaptoethanol (Sigma/Gibco), 10% human serum.

T cell media: AIM-V media (Fischer Scientific) 10% human serum 100 µg/ml streptomycin (Gibco) 100 IU/ml penicillin (Gibco). (Supplemeted with IL-7 and IL-15)

Freezing media: RPMI media, 20% FBS and 10% Dimethyl sulphoxide (DMSO) (Fischer Scientific).

Optimen (Gibco): serum free media for preparing cells for transfection

Epithelial cells media .DMEM (Gibco) or RPMI 1640 media (as appropriate for the cell line) supplemeted with 10% FCS + 100 µg/ml streptomycin (Gibco); 100 IU/ml penicillin (Gibco)

Monkey Leukocyte antigen-144 supernatant (MLA-144): Supernatant is derived from cultured MLA-144 cells line in RPMI 1640 + 10% FCS and 100 µg/ml streptomycin (Gibco) 100 IU/ml penicillin (Gibco) then filtered by Millipore Steritop 0.22µm vacuum and store in -20C^0.

Leucocytes Cone cells: Cones and Buffy coat cells were obtained from Birmingham National Blood Service. PBMCS were isolated and prepared as cell feeders as described below

2.2 CELL CULTURE:

2.2.1 Growing of Suspension cells:

Suspensions cells (*Table 3*) were grown in RPMI or DMEM + 10% FCS in 25cm^2 flask. Cells were spilt 1:2 and fed two times in week.

2.2.2 Growing Adherent cells

These cells (

Table 4) were grown in RPMI or DMEM + 10% FCS in 25 cm^2 flasks or 75 cm^2 flasks but some cells needed additional growth factors. Cells were spilt when the confluencyt was 70% or more . For spilting, the cells were washed two times with PBS then trypsinsed using TrypLE Express Enzyme (1X), phenol red (Gibco) for a few minutes in the incubator. Once detached, media was added to stop enzyme activity . The split ratio used to establish flasks of cells was dependent on the cell type.

2.2.3 EBV transformed Lymphoblastoid cell lines (LCLs)

LCLs cells were generated by transforming B cells with EBV virus. EBV supernatant 4ml (not fed for at least 3 days) from B95.8 virus producer lines was spin at 1500 rpm for 5 min to pellet cells then supernatant was then collected and filtered through using a 0.45um syringe filter. At the same times 5-10 $x10^6$ PBMCs were pelleted by centrifugation and supernatant removed. The B95.8 supernatant was combined with 500ul of FBS then added to PBMCs and incubated at 37C /5% CO2 overnight. The next day, PBMCs were centrifuged at 1300rpm for 5min and the supernatant was discarded. PBMCs were suspended in 2ml of CSA media (RPMI+10% FCS, 1ug/ml Cyclosporin A + 100 µg/ml streptomycin (Gibco) 100 IU/ml penicillin (Gibco)) and transferred to 24 well plate for 2 weeks until cells transformed into LCLs . These were maintained in LCL culture media and spilt as needed. Growing LCLs were transferred to 25cm flask when there were at least 4 thick wells of LCL cells.

2.2.4 CD4 T cell depletion

The required number of CD4 Dynabeads were washed, added to PBMCS in RPMI medium then incubated at 4C° for 30min with gentle rotation. The cells-bead mixture

was inserted into a magnet for 2 min and the supernatant then transferred to anew tube. This step was repeated to ensure robust CD4 depletion.

2.2.5 Cryopreservation of Cells

Cells were transferred to sterile cryovial tube, centrifuged and and suspended autologous plasma or medium RPMI -1640 with 20% Fetal Calf Serum (FCS) and 10% Dimethyl Sulfoxide (DMSO) (sigma). Cryovials were inserted into a controlled cooling device (Mr Frosty, Thermo) and place into a -80 freezer for 16 hours; this ensured a slow cooling rate of 1C per minute. Cells were transferred to liquid nitrogen for long term storage.

To revive cells, cryovials were thawed in 37C waterbath then cells were gently transferred to 15 ml tube containing 10ml warm standard medium. After 2min cells were washed by centrifugation at 850 rpm for 10 min, resuspention with standard medium then centrifuged again at 1300rpm for 5min.

2.3 Cloning EBV-specific T-cells

2.3.1 Reactivation of EBV peptide (BARF1) specific T-cells

The PBMCs were stimulated by adding of 5μM EBV epitope peptides or pepmixes then incubated at 37C 5%CO_2 for one hour. Subsequently the cells were washed in RPMI media to remove any peptides or alternatively cells were used directly without washing. The cells were cultured with AIM-V %10 human serum in a 24-well plate at $1x10^6$ cells/ml or a 96 well plate at $0.25x10^6$ cells / 200ul from 10 to 14 days in present of 10 ng/ml IL-7 and 0.5 ng/ml IL-5 in addition to 20 IU/ml IL-2 . Half of the media from each well was replaced with fresh media and cytokines on day 5 then every 2 days depending on media colour. Later, a part of the PBMCs were harvested

and re-stimulated for 4 hours with 5μM of the same pepmix or epitope peptide to be tested in a TNFa secreting assay to check T-cell specificity. .

2.3.2 T-cell sorting and cloning

Antigen-specific cells were sorted by FACS using an TNFa secretion assay after re-stimulation for 4 hours with 5μM of the same pepmix or epitope peptide used to establish the polyclonal culture in the presence of anti-TNF-APC antibody and TAPIO inhibitor of ADAM17. On the day of sorting, 96 well round plates were prepared by adding 100 ul per well of T cell media (RPMI + 30% MLA ,10% FCS, Human serum , 50 IU of IL_2 100IU/ml penicillin and 100μg/ml streptomycin and 1/1000 OKT3 antiCD3 antibody (ebioscience) and $4x10^5$ irradiated phytohemagglutinin-treated (10μg/ml) mixed buffy coat feeder cells (from at least two different donors). After TNFa antibody (APC) cultured, cells were stained with viability dye eFluor720 and CD3 BV421 then suspended in cold T cell media on ice. Cells were sorted by FACS to one cell per well using by the core facility at the University of Birmingham. Plates were incubated until next day then the media was topped up 100 ul gently with T cell media. Plate were then incubated for 2 weeks. Any wells icontaining growing cells were screened for response to specific peptide using IFNγ ELISA assay.

2.3.3 T cell Clone Expansion

BARF1-specific T cell clones were expanded from 96 well to 24 well plates in T cell media containing $1x10^6$ γ-irradiated (4000 rads) phytohemagglutinin-treated mixed allogeneic feeder cells (from three different donors) and $1X10^5$ peptide-pulsed γ-irradiated LCLs.

2.3.4 T cells clone Maintaining

To maintain T cells clones, clones were fed two times per week. T-cells were split into new wells when cells reached $1x10^6$ per ml. Every two weeks clones were stimulated by $1X10^5$ peptide-pulsed γ-irradiated LCLs and phytohemagglutinin-treated (10μg/ml) buffy coat cells from three allogeneic donors.

2.3.5 HLA restriction of T cells clones

To identify T cell clone HLA type, different LCL cells with known HLA types were stimulated with 5ug/ml specific peptides (or DMSO as control) for 1-2 hours in 37C incubator. The tubes were flicked every 20 minutes to resuspend cells. Then, cells were washed 4x with LCL media and resuspended in media. $5X10^4$ LCL cells in 100 ul were added to each well of a 96 well V bottom plates. T cell clone (3000 cells) were added to each well. T cell clones alone and LCL cells alone were also tested as controls. Cells were incubated overnight then 50 ul of supernatants were tested with IFNg ELISA assay.

2.3.6 Characterisation of T cell clones: peptide titration

Stock peptides at 5mg/ ml were diluted to 1/100 in LCL media to make 0.05 mg /ml which was then used to set up seven wells, diluting ten-fold. In 96 V bottom, well plates 20 ul of diluted peptide and DMSO as control were plated, then 80ul of $0.5 x10^6$ HLA matched LCL cells were added to wells to give 0.010 mg/ml (10uM) concertation in the first well, with lower concentrations in the remained. After 30 minutes – 1hours incubation 100 ul of 3x103 T cell clones were added to wells then incubated for overnight in 37C/CO2. Supernatants were tested with IFNg ELISA assay.

2.4 T cell functional assay

2.4.1 Tumour narcosis factor alpha (TNFa) secretion assay

Briefly, to determine the T cells response after stimulation as describe later, cells were cultured for 4-6 hours in present of TNFa antibody and TAPIO (Enzo) to ensure TNFa wsa not released from the surface of the cell producing the cytokine. After harvesting the cells and washing with PBS, cells were stained with cell surface antibodies then analysed by flow cytometry. Responding cells were identified by the presence of the APC-labelled TNFa-specific antibodies.

2.4.2 Enzyme linked immunospot (ELIspot) assay

Ethanol (35%) was added to a 96 well plate containing nitrocellulose at the bottom of each well (EMD Millipore) then the plate was washed immediately two times with filtered Phosphate-buffered saline (PBS). First antibody (1-D1K, Mabtech Vikdalsagen 50, Sweden) was added to the plate and incubated at 4C° for 24 hours or at room temperature for 4 hours. After washing the plate four times with filtered PBS, the plate was blocked with AIM-V medium (Gibco) containing 1% Bovine Serum Albumin (BSA) (sigma) for 1-2 hours at room temperature. The plate was then washed with filtered PBS four times and 50 ul of AIM-V medium was immediately added to each well of the plate to prevent the wells from drying out. Then 10 ul was added from (DMSO, Pepmix (JPT peptides) or peptides and Phytohemagglutinin (PHA) as positive control, the cells were added (50 ul) to wells. The plate was incubated for 24 hours in a 37C, 5% CO_2 incubator. The plate was washed PBS with 0.5% tween 20 (Sigma) eight times. Then the second antibody (7-B6-1-Biotin, Mabtech Vikdalsagen 50, Sweden) was added (50 ul) to each well of the plate and incubated for 2-4 h at room temperature. After washing, the Streptavidin-Alkaline Phosphatase (Mabtech

Vikdalsagen 50, Sweden) reagent was added to wach wels and incubated 1-2 hours at room temperature. The Plate was washed eight times with PBS /tween20 then four times with PBS to remove tween. Chromogen substrate (Bio-Rad Alkaline Phosphatase conjugate substrate Kit) was prepared and added to wells then incubated in dark until 60 min at room temperature. Plates were monitored and, if necessary, development was stopped once clear spots were visible. The plate was rinsed with tap water to stop colour development and the plate was left to dry before reading.

2.4.3 IFNγ ELISA

ELISA involved pre exposing cell lines to peptide or DMSO as a control for 1-2 hour then washing three times with standard media. Exposed cells and T cells were co-cultured overnight at 37°C 5% CO_2. The next day the IFNγ released into the supernatant by responding T-cells was measured using the IFNγ ELISA protocol (Thermo Scientific). First, primary IFNγ antibody was diluted in coating buffer and 50 µl was added to each well of a 96 well Maxisorp plate (Nunc). The plate was incubated at 4°C for 4 hours RT or overnight. Then, 200µl of blocking buffer was added to each well. The plate was washed with PBS/tween and 50µl of test supernatant or IFNγ standard were added. IFNγ standard was prepared by double dilutions from 20,000 pg/ml to 0pg/ml in RPMI. After incubation for at least two hour at room temperature, the pate was washed and 50 ul of diluted secondary antibody (biotin labelled IFNγ) was added to each well and incubated for one hour at room temperature. The plate was washed four times with PBS/ tween and 50µl of Extravidin (Sigma) was added to each well of the plate. After 30minutes at room temperature was washed and developed with 50µl of TMB (Life Technologies) To stop colour

development 50µl of 1M HCL was added to each well. Finally, plate was read on the Biorad iMark microplate reader at 450nm.

2.5 TIL and organoid co-cultured

2.5.1 Organoid growing medium:

- Wnt3A conditioned medium (50%) from Wnt3A-producing cells
- R-spondin conditioned medium (10%) from R-spondin-producing cells
- Noggin conditioned medium (10%) from Noggin-producing cells
- Advanced DMEM/F12 (Life Technologies) (30%),
  supplemented with 1x glutamax, 10mM HEPES, 1x Penstrep (all from life technologies), and primocin 1x (ant-pm-1, invivoGen)
- EGF 50ng/ml
- Nicotinamide 10mM
- B27 without vitamin A 1x (12587-010, Life Technologies)
- LY27632 (Rho kinase inhibitor) (Y0503, Sigma) 10µM
- A83-01 (TGF-β inhibitor) [2 µM] (2939, Tocris)
- Primocin 1x

Organoid and TIL culture media: 50% Organoid growing medium and 50% TIL cell media

2.5.2 Preparing organoid

For passaging organoids, matrigel was dissolved by pipetting then spin 300g for 5min at 4C. after remove the most of supernatant, the spheroids were broken by pipetting then trypsin added for 5min at 37C. Advanced DMEM/F12 supplementedwith 10% fetal bovine serum (FBS, gibco) was added to quench trypsin.

After centrifugation, spheroids were washed with medium lacking serum then seeded drop-wise on 6-well plate. The plate was incubated upside down for at least 15min at 37C. growing medium. Medium was replaced with fresh media every 2-3 days until the next passaging.

Organoids were prepared and seeded for TIL assay as follows. After passaging pellets were washed twice in cold PBS then incubated in matrigel dissolving solution (Corning, 354253) on ice for 1 hour. After washing with PBS, spheroids were incubated in 96 well pate in organoid growth medium overnight.

The next day, organoid media was replaced with TIL/organoid culture media. TIL cells ($3x10^5$) were added to organoid at 96 well plate. The response of TIL cells was measured using the TNFa TAPIOassay after 6 hours. Co-cultures were also left for 10 days then re-tested for antigen specificit as above. During the co-culture, aliquots of supernatant were collected 6 hours, 1day, ,7 days and 10 days after the start. These supernatants were saved at -20C for subsequent INFg ELISA.

2.6 Cell transduction and transfection

2.6.1 Retrovirus Production

To prepare cells for retrovirus transfection (Day 0) GP2-293 packing cells line were washed by PBS then cells were trypsinised and suspended at $4X10^5$cells /ml in DMEM 10% FCS without antibiotics. Cells were added to 75cm2 flasks and incubated at 37° C 5% CO_2 overnight. On day1, to transfect the packing cell line 24ug of PVSV-G plasmid (envelope plasmid) and 24ug of PQCXIN plasmid (containing gene of interest with flag marker or GFP, and no gene with GFP as control) were added to 1.8ml of optimem media. In a separate tube 80ul of lipofectamine 2000 was added to 1.8ml of optimem media and incubated at room temperature for 15 minutes. The DNA and

Lipofectamine were then mied together and incubated at room temperature for 30 minutes. During this time media was removed from GP2-293 cells then DNA transfection mixture was added to cells. Transfected cells were incubated at 37^0C for 5 hours. After that, 18ml of media (DMEM 10% FCS no antibiotics) was added and the cells incubated at 37C 5%CO_2 for approximately 64 hours.

On day 4, media was collected from the GP2-293 transfected cells and centrifuged at 2000rpm for 10 minutes. The supernatant was removed and filtered through a 0.45um filter to remove any cells. Then supernatant was transferred to Beckmann centrifuge tubes and centrifuged in a Beckmann centrifuge at 19,500rpm for 2hours at 4^0C with deceleration set at slow.

2.6.2 Retroviral Transduction of Suspension Cells using PQCXIN Vector

Cells were counted and $5X10^5$ added to four different 15ml tubes. After centrifugation, the supernatant was removed and the concentrated retrovirus-containing supernatant were added to the cells tubes. Polybrene (10ng/ml) was added to this supernatant and mixed. The cells were then incubated 30min at 370C centrifuge at 3200rpm with 32C for 2.5 hours to perform spinfection . infected cells were transfer to 24 well plate with medium to incubate for 72 hours in 37C 5% CO_2 incubator. G418 geneticin antibiotic was then added at half of the optimal concentration to select for transduced cells.

2.6.3 Retroviral Transduction of adherent cells using PQCXIN Vector

Cells were seeded in 6 well plate at about $4x10^5$cells the day before transduction to produce a 70% confluent monolayer. On the day of transduction, supernatants were removed from each well of cells and the cells infected with concentrated retrovirus-containing supernatant and incubated 37C 5%CO^2 overnight. The next day, each well

was topped ip with growth medium. The next day cells were transfer to 75 cm^2 flasks and selection with G418 performed using the antibiotic at half of the optimal concentration.

2.6.4 Selection G418 geneticin antibiotic – Killing carve

To determine the best concentration of G418 geneticin antibiotic to use for retrovirus selection, serial concentrations of G418 were added to the cells that would be used for transduction. After two weeks of treatment with antibiotic, the lowest concertation of antibiotic that can completely kill non-resistant cells was determined.

2.6.5 Transfection of Epithelial Cells: Lipofectamine 2000 Method

Cells were seeded in 6 well plates in RPMI or DMEM + 10% FCS without antibiotic. The next day, cells at 90% confluent were ready for transfection. For each transfection 5ug of plasmid DNA was diluted in 150 ul of optimem media and 10-12 ul of Lipofectamine was diluted in 150 optimem media and incubated for 10 minutes at room temperature. The Lipofectamine and DNA were mixed and incubated for 20-30 minutes at room temperature. While DNA+lipofectamine complexes were forming, growth media was removed from the cells then 350 ul of optimem media was added to the cells. The DNA+lipofectamine mixture was gently added to cells which were incubated at 37C 5% CO_2 for 4 hours. Medium with no antibiotic was then added to each well without removing the transfection mixture. Cells were harvested after 24 – 48 hours and use as targets in T cell recognition assays and molecular assays.

2.6.6 Transfection of Suspension cells: Electroporation

This method needed 5-10X10^6 cells per electroporation. Cells were spilt 1:3 the day before transfection to ensure they were in active growth phase. Media (20% FCS) was prepared and added to 6 well plate then incubated at 37C 5%CO_2 to be ready after

electroporating cells. Cells were washed with PBS and resuspended in 300 ul optimem medium. Plasmid DNA (10ug) was added to a labelled electroporation cuvette, then cells added gently to mix the cells with the DNA. Elecroporation was immediately performed at 240V and 975uf using a Biorad electroporator. Immediately, 1ml of 20%FCS containing media was added to the cuvette and the cells gently transferred from the cuvette to a well of a 6 well plate for 24 – 48 hours before further use.

2.7 MOLECULAR TECHNIQUES

2.7.1 BARF1 Plasmids

Luria Broth (LB) media: LB powder (Invitrogen) 20g/L was disolved in sterile distilled water (SDW). The mixture was autoclaved at 121C for 20 minutes at 15psi for sterilization

LB ager Plates: LB Ager powder (Invitrogen) 20g/L was dissolved in SDW. The mixture was autoclaved at 121C for 20 minutes at 15psi for sterilization. LB ager plates were prepared by cooling the LB agar in a 50°C waterbath . After adding antibiotic, LB agar was poured into plates, allowed to set, dried and then stored at 4°C until use.

Glycerol solution: Glycerol solution was prepared under sterile conditions by diluting 100 % glycerol in SDW. Diluted glycerol was then stored at 4C.

Antibiotic: Ampicillin powder (1000X stock was prepared at 100mg/ml in distilled water then stored at - 20ºC as aliquots.

Bacterial Strains: XL1-blue complement cells were sorted as aliquots in -80°C.

2.7.1.1 Transformation of bacteria to DNA plasmid

Competent cells (XL1-Blue) were slowly thawed on ice. 10 ng of plasmid DNA was prepared in a microcentrifuge tube then mixed with 50 ul of competent cells on ice for

30 minutes. After that, the tube was transferred to waterbath to heat shock for 45 seconds at 42°C and immediately transferred to ice. 950 ul of SOC media was added to cells tube then incubated with shaking (200 rpm) at 37C for 1 hour.

2.7.1.2 Bacteria culture

20ul of transformed bacteria cells were spread onto rewarmed LB agar plates containing appropriate antibiotics (usually Ampicillin at 100ug/ml). After leaving plates to dry at room temperature, the plates were inverted and incubated at 37C overnight.

The next day, individual colonies were transferred to 5 ml of LB media containing Ampicillin 100ng/ml then shaken at 37C for 6-8 hours 1ml of the culture was added to 100 ml of LB media with Ampicillin then incubated in shaker at 37C overnight. The 100ml of culture ws used to prepare plasmid DNA using commercially available Maxiprep kits. 500 ul of the culture was stored as a glycerol stock at -70C.

2.7.1.3 Bacterial Glycerol stock

For long term storage500 ul of overnight culture were mixed with 500ul of glycerol solution then frozen in -80 C freezers**.**

2.7.1.4 Purification of plasmid DNA

To purify large amount of pure plasmid DNA , 100ml of bacterial culture was processed using a Purelink Hipure plasmid Filter Maxiprep Kit (Invitrogen) as per the supplied protocol. The concentration of plasmid DNA pure was measured using a Nanodrop 1000 (Thermo Scientific).

2.7.1.5 DNA sequencing

10 ng of DNA and 3-10 pg of forward or reverse primer were prepared as a 10 ul reaction then sent to he functional genomics laboratory at Birmingham University for diDeoxy sequencing.

2.7.2 Detection of gene expression by qPCR

2.7.2.1 RNA extraction

Suspension and adherent cells were counted then 1-2 $X10^6$ cells were wshed with PBS and stored at -80C as a dry pellet. RNA was extracted using NucleoSpin RNA isolation kit (Macherey-Nagel) following the manufacturer's protocol. Isolated RNA was eluted in RNAse free water then quantified using a Nanodrop 1000 (Thermo Scientific). RNA was used immediately to make cDNA or frozen at -80C.

2.7.2.2 Synthesis of cDNA

Any contaminating DNA was removed from purified RNA extraction using DNA-free kit (Ambion). RNA was then reverse transcribed to cDNA using iscript reverse Transcription Supermix kit (Bio-Rad). The cDNA was frozen at 20C in DNase-free water until use

2.7.2.3 Determination of EBV Gene expression using PCR

cDNA was analysed using BARF1 and BZLF1 gene specific quantitative PCR assays and FAM/TAMRA-labelled probes. Glyceraldehyde-3-phosphate dehydrogenase (GAPDH) was used as endogenous control (Life Technologies).

2.7.3 Western Blot

2.7.3.1 Protein Quantification

At least $2x10^6$ cells were washed twice in ice-cold phosphate buffered saline (PBS) then put on ice. Cells were lysed by adding of 50µl Urea buffer (9M Urea, 5mM EGTA, 5mM EDTA, 2-4% CHAPS, 1%DTT); after that cells were disrupted by sonication for 20 seconds.

Protein concentration was determined via the Bio-Rad DDC Protein assay. Briefly, Urea buffer was used to diluted cell 5-fold. Then 5µl of Samples were added in duplicat to a 96 well plate in addition to 5µl protein standards (5, 2, 1, 0.5, 0.2 and

0.1mg/ml BSA to make up a stranded curve.) After that, 200 ul of WR mixture (50:1) from Reagents A and B were added to each well and incubated for 30 minutes at 37C. The plate was transferred to a plate reader to measure absorbance at 550nm then the protein concentration was calculated based on the BSA stranded curve. After adding Beta-mercaptoethanol (1ul in 20ul), Gel Sample Buffer (GSB) was used to dilute samples to 2-4mg/ml concentration then protein sample were denatured by heating at 100C for 5 minutes on a heat block.

2.7.3.2 Protein Electrophoresis and Membrane Transfer

Mini-PROTEAN Tetra BIORAD GEL was assembled into Mini Bio-Rad tank. Upper and lower chamber were filled with 1X running buffer from 10X stock (700ml for 2 gels; 1000ml for 4 gels. Then, 5ul of samples and molecular weight marker were loaded onto the gel, The gel was electrophoresed at 140V for 30min-1hour. The gel was then removed from cassettes and placed into a clean dish containing PBS-Tween solution. The gel was transfered to a PVDF membrane using Midi Trans-blot Turbo transfer system as per manufacturer's instructions. After transfer, membrane was placed in PBS-Tween. For ponceau staining, membrane was washed in dH2O then ponceau stain solution added so liquid was just covering membrane. After 30s the stain was removed using dH2O until bands were visible. Excess PVDF membrane was removed and MWt markers labelled onto the membrane. Ponceau stain was removed using PBS-Tween.

2.7.3.3 Membrane Blocking and Antibody Detection

After transfer, the membrane was blocked with 5% of milk in PBS-Tween for 1hour then the membrane washed with PBS-T. Primary antibody was diluted in blocking

buffer then sealed with the membrane in a plastic bag at RT for 2 hours or cold room overnight. After washing with PBS-T wash, the membrane was sealed with secondary antibody for 1 hour on rocker at RT then washed 5 times with PBS-T buffer. Membrane was covered for 60 second with ECL western blotting detection reagents (GE healthcare), rapped in Saran wrap and placed in an audoradiograph cassette, with CL Xposure X-ray film (Thermo Scientific). The exposed film was developed using a Kodak X OMAT 1000 film processor.

2.8 Healthy Donor and Gastric Cancer Patients Sample Processing

2.8.1 Donor samples

Blood was taken from healthy donors with informed consent. Heparinized and EDTA tubes were used as appropriate

2.8.2 Patient samples

All blood and tissue samples were collected with informed patient consent from Gastric cancer patients at Queen Elizabeth Hospital Birmingham. Blood was collected directly into one EDTA blood tube (4ml) and two heparin tubes (16ml total). All samples were transferred directly to the laboratory for immediate processing. Fresh tumor and normal tissue samples were provided by the pathology laboratory at the Queen Elizabeth Hospital Birmingham. Tissue was stored in serum free RPMI-1640 media for up to 24hr at 4C to allow informed consent to be verified prior to tissue being released for research.

2.8.3 EDTA blood

Plasma was separated from cells by centrifugation then aliquot and transferred to a -80C freezer for storage. The cells were then diluted with PBS and the equivalent of

1ml blood was lysed 1X RBC lysis buffer (10X RBC Lysis Buffer, ebioscience diluted to 1X with distilled water). After 10-15 mins incubation at room temperature the cells were washed two times with PBS buffer and the number of cells determined by counting using a haemocytometer.

2.8.4 Heparin Blood

Heparin blood was diluted 1:1 with RPMI 1640 (sigma) and layered onto Lymphoprep media. Following centrifugation at (1900 rpm for 30 mins) plasma was collected and frozen at -80C. Peripheral blood mononuclear cells (PBMC) were harvested from the top of the lymphoprep layer, washed and counted. Cells were frozen in 1: 10 autologous plasma or medium RPMI -1640 with 20% Fetal Calf Serum (FCS) and 10% Dimethyl Sulfoxide (DMSO) (sigma) then frozen for subsequent applications

2.8.5 Isolation of cells from Tissue using collagenase D digestion

Tumor tissue was cut into small fragments about 2-3 mm in size then put in 5ml of LCL media containing 1mg/ml collagenase D in a 15ml conical tube. Tissue was digested at 37 C for 1 hour with constant gentle mixing. The digested tissue was transferred into a gentelmacs tube and mechanical dissociated (GentleMACS Miltenyi Biotec) using program spleen 01.01. The cell mixture was passed through a 70µm filter and washed three times by centrifugation at 1800rpm for 5min. Cells were counted and frozen as described above

2.8.6 Isolation and expansion of Tumor infiltrating Lymphocytes (TIL) from tissue biopsy

Small biopsy specimens were cut into small fragments then placed into a single well of a 24 well tissue culture plate with TIL media comprising RPMI, 25mM HEPES, U/ml penicillin-streptomycin (Gibco), 1% L-Glutamine, 0.1% sodium pyruvate (Gibco), 0.1% β-mercaptothanol (Sigma) and 10% Human serum. High dose IL-2 (6000 IU/ml final concentration) was added to wells. Media was changed every 2/3

days and cells spilt if required. After 3-5 weeks cells were transferred to Gas Permeable flask G-Rex (Wilson Wolf, USA) with 6000IU/ml IL-2 every second day for TIL rapid expansion.

2.8.7 Tissue for EBV and RNA test

Two fragments of tumor tissue were frozen (-80C) in two separate tubes to allow i) EBV DNA to be measured by quantitative PCR and ii) RNA to be isolated from the tissue.

2.9 Flow cytometry

2.9.1 Cell surface staining

Cells were counted and added into FACS tubes., Cells were then washed by centrifugation at 1600rpm for 5mins with MACS buffer. The supernatant was decanted and the cells were then stained with a viability dye and antibodies (*Table 6*). After that, cells were incubated at 4^0C for at least 30 min and washed with MACS buffer. Cells were fixed for with IC Fixation Buffer (BD bioscience) for 30 min in at 4^0C then washed twice or run without fixation by suspending in MACS buffer. Sample were analysed on an LSR-II (BD biosciences). Data were analysed using FlowJo.

2.9.2 Intracellular staining

First, cells were stained with surface staining as described above. Then, cells were fixed with mixture of 1/10 (Fixation/Permeabilization Diluent and concentrated) (eBioscience) for 30mins at 4^0C. After that, 1/10 of Permeabilization Buffer (eBioscience) were added to cells and cells washed by centrifugation at 1900rpm for 5mins. Cells then were stained with intracellular markers antibodies (*Table 6*) for at

least 30min then washed again with perm buffer one time then with MACS buffer two times before analysis on an LSR-II flow cytometer.

2.9.3 Intracellular staining For Flag

Cells were counted and $2X10^5$ cells added to Eppendorf tubes. Cells were then washed 1x with MACS buffer. Cells were fixed with 200ul of 2%PFA-PBS and incubated in room temperature 20 min dark. Cells were washed by MACS buffer then washed 1X by Saponin buffer (PBS, 0.5% saponin, 5% FCS), suspended and incubated in Saponin buffer for 20 min in dark. Diluted FLAG Ab (sigma F3165) 1/5000 in Saponin buffer was added to cells (final concentration 1/10000) for 30 min at 37C then cells were washed with Saponin buffer. After that, 50 ul (1:50) secondary anti-Mouse IgG-PE (SEROTEC SRAR76) was added to tubes for 30 min at 37c . Cells were washed with Saponin buffer then washed by MACs buffer. Cells were suspended in MACs buffer and analysed by flow cytometry.

Table 1: EBV peptide pepmixes

pepmix	number of peptides	stock concertation	final concentration	source
EBNA1	158	25µg	5ng/ml	JPT
LMP1	94	25µg	5ng/ml	JPT
LMP2	122	25µg	5ng/ml	JPT
EBNA3A	234	25µg	5ng/ml	JPT
BARF1	53	25µg	5ng/ml	JPT

Table 2: Tumour Antigens peptide Pepmixes

pepmix	number of peptides	stock concertation	final concentration	source
NY-ESO-1	43	25µg	5ng/ml	JPT
MAGEA1	75	25µg	5ng/ml	JPT
MAGEA3	76	25µg	5ng/ml	JPT
MAGEA4	77	25µg	5ng/ml	JPT
CEA	173	25µg	5ng/ml	JPT
PSMA	185	25µg	5ng/ml	JPT

Table 3: Suspension cells lines

Name or code	Cell type	Source	EBV
MS5	lymphoblastoid cell lines (LCLs)	T cell group	EBV+
MS10	LCLs cells	T cell group	EBV+
MS13	LCLs cells	T cell group	EBV+
MS18	LCLs cells	T cell group	EBV+
MS-9	LCLs cells	T cell group	EBV+
MS-17	LCLs cells	T cell group	EBV+
MS-25	LCLs cells	T cell group	EBV+
MS-31	LCLs cells	T cell group	EBV+
AD	LCLs cells	Graham Lab	EBV+
MS	LCLs cells	Graham Lab	EBV+
MC	LCLs cells	Graham Lab	EBV+
HL	LCLs cells	Graham Lab	EBV+
GR	LCLs cells	Graham Lab	EBV+
JZ	LCLs cells	Graham Lab	EBV+
JB	LCLs cells	Graham Lab	EBV+
CSL	LCLs cells	Graham Lab	EBV+
CSD	LCLs cells	Graham Lab	EBV+
DDC	LCLs cells	Graham Lab	EBV+
NK	LCLs cells	Graham Lab	EBV+
OT	LCLs cells	Graham Lab	EBV+
GT	LCLs cells	Graham Lab	EBV+
DCC	LCLs cells	Graham Lab	EBV+
BJAB	Human Burkett lymphoma B cell	Graham Lab	EBV negative
Kem -BL	Human Burkett lymphoma B cell	B cell group	EBV+
SUDHL4	human B cell lymphoma	Alex D	EBV negative
SUDHL5	human B cell lymphoma	Alex D	EBV negative
HL	human B cell lymphoma	Alex D	EBV negative
SUDHL4-EBV	human B cell lymphoma	Alex D	EBV positive
SUDHL5-EBV	human B cell lymphoma	Alex D	EBV positive

Table 4: adherent cell clines

Name or code	CELL TYPE	SOURCE	EBV INFECTION
C666	Nasopharyngeal carcinoma cell line	Graham lab	EBV positive
NP460	Nasopharyngeal cell line	Graham lab	EBV negative
MKN1	Gastric carcinoma	Graham lab	EBV negative
MKN28	Gastric carcinoma	Graham lab	EBV negative
YCCEL	Gastric carcinoma	Graham lab	EBV positive/ negative
NUGC4	Gastric carcinoma	Graham lab	EBV negative
HEK293	Epithelial	Graham lab	EBV negative

Table 5: Generating new BARF1 plasmids

Construct	gene	Indicator	Sequence
Construct1	empty	3xHIS FLAG and mclover3 tag -Kozak sequence	
BARF1 Construct 2	full-length BARF1 (**secretory signal of BARF1**)		**MARFIAQLLL LASCVAAGQA** VTAFLGERVT LTSYWRRVSL GPEIEVSWFK LGPGEEQVLI GRMHHDVIFI EWPFRGFFDI HRSANTFFLV VTAANISHDG NYLCRMKLGE TEVTKQEHLS VVKPLTLSVH SERSQFPDFS VLTVTCTVNA FPHPHVQWLM PEGVEPAPTA ANGGVMKEKD GSLSVAVDLS LPKPWHLPVT CVGKNDKEEA HGVYVSGYLS Q
BARF1 Construct 3	**Delta Δ-secretory signal of BARF1**		VTAFLGERVT LTSYWRRVSL GPEIEVSWFK LGPGEEQVLI GRMHHDVIFI EWPFRGFFDI HRSANTFFLV VTAANISHDG NYLCRMKLGE TEVTKQEHLS VVKPLTLSVH SERSQFPDFS VLTVTCTVNA FPHPHVQWLM PEGVEPAPTA ANGGVMKEKD GSLSVAVDLS LPKPWHLPVT CVGKNDKEEA HGVYVSGYLS Q
BARF1 Construct 4	**Invariant chain (Ii)** targeted deltaΔ BARF1		
BARF1 Construct 5	**Invariant chain (Ii)** targeted minimal BARF1 region **TFF – ISH – QEH**		HRSAN**TFF**LV VTAAN**ISH**DG NYLCRMKLGE TEVTK**QEH**LS VVKPLTLSVH SERSQFPDFS
BARF1 Construct 6	**Invariant chain** targeted minimal EBNA1 region **SNP – VYG- PQC**		RRPFFHPVGE ADYFEYHQEG GRGQGG**SNP** KFENIAEG L RALLARSHV ERTTDEGTWV AGVF**VYG**GSK TSLYNLRRGT ALAI**PQC**RLT PLSRLPFGMA PGPGPQPGP

Table 6: Flow cytometer surface and intracellular markers antibodies

Antibody conjugated anti human	source	Clone
FITC – CD3	Biolegend	SK7
FITC – CD8	eBioscience	53-6-7
FITC – CD19	Biolegend	HIB19
FITC – CD56	eBioscience	MSK39
FITC-CD57	eBioscience	HCD56
APC-CY7- CD14	eBioscience	6ID3
APC-CY7- CD19	eBioscience	HIB19
BV510- CD4	Biolegend	RPA-T4
BV510- CD3	Biolegend	SK7
PerCP-Cy5.5-CD8	Biolegend	HIT8a
PerCP-Cy5.5- NK2GD	Biolegend	1D11
PerCP-Cy5.5-CD45 RA	Biolegend	H1I00
PerCP-Cy5.5- CD14	eBioscience	6ID3
PerCP-Cy5.5-CCR7	eBioscience	G04317
AF 700- CD8	Biolegend	SK1
AF 700- CD19	Biolegend	HIB19
AF-CD4	Biolegend	OKT4
PE- TCR γδ	eBioscience	B1
PE-CD8	Biolegend	SK1
PE-PD1	Biolegend	EH12.2H7
PE- DR	eBioscience	L243
PE-KI67	eBioscience	20Raji
PE- IFNγ	Biolegend	4S.B3
PE-CY7- CD16	eBioscience	eBioCB16
PE-CY7-CD4	eBioscience	RPA.TA
PE-CY7-TIM3	eBioscience	F38-2E2
PE-CY7-FOXP3	eBioscience	PCH101
PE-CY7-CD56	Biolegend	HCD56
PE-CY7-CD33	eBioscience	WH-53
BV421-CD3	Biolegend	SK7
BV421-CLTA4	Biolegend	BN13
BV421-CD127	Biolegend	A019DS
BV421-CD15	eBioscience	W6D3
BV421-CD38	Biolegend	HB-7
APC-CD56	eBioscience	CM55B
APC-CD56	Biolegend	HCD56
APC-TNFa	eBioscience	MAb11
APC-LAG3	eBioscience	3DS223H
APC-CD25	eBioscience	BC96
APC-CD11b	eBioscience	ICRF44
APC- IFNγ	eBioscience	4S-B3
APC-CD28	eBioscience	CD28.2
PE-CF594 - CD27	eBioscience	M-T271
PE-CF594 -CD57	eBioscience	NK1
PE-CF594 – CD39	eBioscience	TU66
PE-CY7 – 45RA	eBioscience	H1100

Table 7: EBV-LMP1 B95.8 peptides

Pool		LMP1 B95-8 sequence	Peptides code	position	Concentration 5mg/ml
1	1	MEHDLERGPPGPRRPPRGPP	M422-A2	1	5
	2	ERGPPGPRRPPRGPPLSSSL	M422-A3	6	5
	3	GPRRPPRGPPLSSSLGLALL	M422-A4	11	5
	4	PRGPPLSSSLGLALLLLLA	M422-A5	16	5
	5	LSSSLGLALLLLLLALIFWL	M422-A6	21	4.7
2	6	GLALLLLLALLFWLYIVMS	M422-A7	26	4.3
	7	LLLLALLFWLYIVMSDWTGG	M422-A8	31	5
	8	LLFWLYIVMSDWTGGALLVL	M422-B1	36	5
	9	YIVMSDWTGGALLVLYSFAL	M422-B2	41	4.3
	10	DWTGGALLVLYSFALMLIII	M422-B3	46	2.9
3	11	ALLVLYSFALMLIIIILIIF	M422-B4	51?	4
	12	YSFALMLIIIILIIFIFRRD	M422-B5	56	5
	13	MLIIIILIIFIFRRDLLCPL	M422-B6	61?	2
	14	ILIIFIFRRDLLCPLGALCI	M422-B7	66	5
	15	IFRRDLLCPLGALCILLLMI	M422-B8	71	5
4	16	LLCPLGALCILLLMITLLLI	M422-C1	76	3.6
	17	GALCILLLMITLLLIALWNL	M422-C2	81	5
	18	LLLMITLLLIALWNLHGQAL	M422-C3	86	5
	19	TLLLIALWNLHGQALFLGIV	M422-C4	91	5
	20	ALWNLHGQALFLGIVLFIFG	M422-C5	96	5
5	21	HGQALFLGIVLFIFGCLLVL	M422-C6	101	2.9
	22	FLGIVLFIFGCLLVLGIWIY	M422-C7	106	5
	23	LFIFGCLLVLGIWIYLLEML	M422-C8	111	5
	24	CLLVLGIWIYLLEMLWRLGA	M422-D1	116	5
	25	GIWIYLLEMLWRLGATIWQL	M422-D2	121	5
6	26	LLEMLWRLGATIWQLLAFFL	M422-D3	126	5
	27	WRLGATIWQLLAFFLAFFLD	M422-D4	131	5
	28	TIWQLLAFFLAFFLDLILLI	M422-D5	136	5
	29	LAFFLAFFLDLILLIIALYL	M422-D6	141	5
	30	AFFLDLILLIIALYLQQNWW	M423-A2	146	5
7	31	LILLIIALYLQQNWWTLLVD	M423-A3	151	5
	32	IALYLQQNWWTLLVDLLWLL	M423-A4	156	5
	33	QQNWWTLLVDLLWLLLFLAI	M423-A5	161	5
	34	TLLVDLLWLLLFLAILIWMY	M423-A6	166	4.7
	35	LLWLLLFLAILIWMYYHGQR	M423-A7	171	5
8	36	LIWMYYHGQRHSDEHHHDDS	M423-B1	181	5
	37	YHGQRHSDEHHHDDSLPHPQ	M423-B2	186	5
	38	HSDEHHHDDSLPHPQQATDD	M423-B3	191	5
	39	HHDDSLPHPQQATDDSGHES	M423-B4	196	5
	40	LPHPQQATDDSGHESDSNSN	M423-B5	201	5
9	41	QATDDSGHESDSNSNEGRHH	M423-B6	206	5
	42	SGHESDSNSNEGRHHLLVSG	M423-B7	211	5
	43	DSNSNEGRHHLLVSGAGDGP	M423-B8	216	5.1
	44	EGRHHLLVSGAGDGPPLCSQ	M423-C1	221	5

	45	LLVSGAGDGPPLCSQNLGAP	M423-C2	226	5
10	46	AGDGPPLCSQNLGAPGGGPD	M423-C3	231	5
	47	PLCSQNLGAPGGGPDNGPQD	M423-C4	236	5
	48	NLGAPGGGPDNGPQDPDNTD	M423-C5	241	5
	49	GGGPDNGPQDPDNTDDNGPQ	M423-C6	246	5
	50	NGPQDPDNTDDNGPQDPDNT	M423-C7	251	5
11	51	PDNTDDNGPQDPDNTDDNGP	M423-C8	256	5
	52	DNGPQDPDNTDDNGPHDPLP	M423-D1	261	5
	53	DPDNTDDNGPHDPLPQDPDN	M423-D2	266	5
	54	DDNGPHDPLPQDPDNTDDNG	M423-D3	271	5
	55	HDPLPQDPDNTDDNGPQDPD	M423-D4	276	5
12	56	QDPDNTDDNGPQDPDNTDDN	M423-D5	281	5
	57	TDDNGPQDPDNTDDNGPHDP	M423-D6	286	4.6
	58	PQDPDNTDDNGPHDPLPHSP	M423-D7	291	5
	59	NTDDNGPHDPLPHSPSDSAG	M423-D8	296	5
	60	GPHDPLPHSPSDSAGNDGGP	M423-E1	301	5
13	61	LPHSPSDSAGNDGGPPQLTE	M423-E2	306	5
	62	SDSAGNDGGPPQLTEEVENK	M425-B6	311	5
	63	NDGGPPQLTEEVENKGGDQG	M425-B7	316	5
	64	PQLTEEVENKGGDQGPPLMT	M425-B8	321	5
	65	EVENKGGDQGPPLMTDGGGG	M425-C1	326	5
14	66	GGDQGPPLMTDGGGGHSHDS	M425-C2	331	5
	67	PPLMTDGGGGHSHDSGHGGG	M425-C3	336	5
	68	DGGGGHSHDSGHGGGDPHLP	M425-C4	341	5
	69	HSHDSGHGGGDPHLPTLLLG	M425-C5	346	5
	70	GHGGGDPHLPTLLLGSSGSG	M425-C6	351	5
15	71	DPHLPTLLLGSSGSGGDDDD	M425-C7	356	5
	72	TLLLGSSGSGGDDDDPHGPV	M425-C8	361	5
	73	SSGSGGDDDDPHGPVQLSYY	M425-B5	366	5

Table 8: LMP2 B95.8 peptides

#	LMP2 sequence	Peptides code	Position	Concentration 5 mg/ml
1	MGSLEMVPMGAGPPSPGGDP	M371-A1	1	3.2
2	MVPMGAGPPSPGGDPDGYDG	M371-A2	6	5
3	AGPPSPGGDPDGYDGGNNSQ	M371-A3	11	5
4	PGGDPDGYDGGNNSQYPSAS	M371-A4	16	5.5
5	DGYDGGNNSQYPSASGSSGN	M371-A5	21	6.4
6	GNNSQYPSASGSSGNTPTPP	M371-A6	26	3.5
7	YPSASGSSGNTPTPPNDEER	M394-A2	31	5
8	GSSGNTPTPPNDEERESNEE	M394-A3	36	5
9	TPTPPNDEERESNEEPPPPY	M394-A4	41	5
10	NDEERESNEEPPPPYEDPYW	M394-A5	46	5
11	RESNEEPPPPYEDYWGNGD	M371-B3	50	5
12	EPPPPYEDPYWGNGDRHSDY	M371-B4	55	5
13	YEDPYWGNGDRHSDYQPLGT	M371-B5	60	5
14	WGNGDRHSDYQPLGTQDQSL	M371-B6	65	44.3
15	RHSDYQPLGTQDQSLYLGLQ	M371-B7	70	5.05
16	QPLGTQDQSLYLGLQHDGND	M371-B8	75	5
17	QDQSLYLGLQHDGNDGLPPP	M371-C1	80	4.5
18	LGLQHDGNDGLPPPPYSPRD	M394-A6	86	2.7
19	DGNDGLPPPPYSPRDDSSQH	M394-A7	91	5
20	LPPPPYSPRDDSSQHIYEEA	M394-A8	96	5
21	PPYSPRDDSSQHIYEEAGRG	M371-C5	99	5.05
22	RDDSSQHIYEEAGRGSMNPV	M371-C6	104	1
23	QHIYEEAGRGSMNPVCLPVI	M371-C7	109	5
24	EAGRGSMNPVCLPVIVAPYL	M371-C8	114	7.2
25	SMNPVCLPVIVAPYLFWLAA	M371-D1	119	5
26	CLPVIVAPYLFWLAAIAASC	M371-D2	124	5
27	VAPYLFWLAAIAASCFTASV	M371-D3	129	5
28	FWLAAIAASCFTASVSTVVT	M371-D4	134	9.4
29	IAASCFTASVSTVVTATGLA	M371-D5	139	7.8
30	FTASVSTVVTATGLALSLLL	M371-D6	144	5
31	STVVTATGLALSLLLLAAVA	M371-D7	149	9.3
32	ATGLALSLLLLAAVASSYAA	M371-D8	154	7.5
33	LSLLLLAAVASSYAAAQRKL	M371-E1	158	5.05
34	LAAVASSYAAAQRKLLTPVT	M371-E2	164	6.7
35	SSYAAAQRKLLTPVTVLTAV	M371-E3	169	7.2
37	AQRKLLTPVTVLTAVVTFFA	M381-E4	176	6.7
38	LTPVTVLTAVVTFFAICLTW	M371-E5	179	5
39	VLTAVVTFFAICLTWRIEDP	M371-E6	184	4
40	VTFFAICLTWRIEDPPFNSL	M371-E7	189	49
41	ICLTWRIEDPPFNSLLFALL	M372-A1	194	67.4
42	RIEDPPFNSLLFALLAAAGG	M372-A2	199	5
43	PFNSLLFALLAAAGGLQGIY	M372-A3	204	5
44	LFALLAAAGGLQGIYVLVML	M372-A4	209	5
45	AAAGGLQGIYVLVMLVLLIL	M372-A5	214	1.5
47	LQGIYVLVMLVLLILAYRRR	M372-A6	219	4.5

48	VLVMLVLLILAYRRRWRRLT	M372-A7	224	5
49	VLLILAYRRRWRRLTVCGGI	M372-A8	229	5
50	AYRRRWRRLTVCGGIMFLAC	M372-B1	234	37
51	WRRLTVCGGIMFLACVLVLI	M372-B2	239	3.5
52	VCGGIMFLACVLVLIVDAVL	M372-B3	244	3.3
53	MFLACVLVLIVDAVLQLSPL	M372-B4	249	5
54	VLVLIVDAVLQLSPLLGAVT	M372-B5	254	5
55	VDAVLQLSPLLGAVTVVSMT	M372-B6	259	5
56	QLSPLLGAVTVVSMTLLLLA	M372-B7	264	5
57	LGAVTVVSMTLLLLAFVLWL	M372-B8	269	5
58	VVSMTLLLLAFVLWLSSPGG	M372-C1	274	5
59	LLLLAFVLWLSSPGGLGTLG	M372-C2	279	5
60	FVLWLSSPGGLGTLGAALLT	M372-C3	284	5
61	SSPGGLGTLGAALLTLAAAL	M372-C4	289	5
62	LGTLGAALLTLAAALALLAS	M372-C5	294	5
63	AALLTLAAALALLASLILGT	M372-C6	299	5
64	LAAALALLASLILGTLNLTT	M372-C7	304	5
65	ALLASLILGTLNLTTMFLLM	M372-C8	309	5
66	LILGTLNLTTMFLLMLLWTL	M372-D1	314	5
67	LNLTTMFLLMLLWTLVVLLI	M372-D2	319	5
68	MFLLMLLWTLVVLLICSSCS	M372-D3	324	5
69	LLWTLVVLLICSSCSSCPLS	M372-D4	329	5
70	VVLLICSSCSSCPLSKILLA	M372-D5	334	5
71	CSSCSSCPLSKILLARLFLY	M372-D6	339	5
72	SCPLSKILLARLFLYALALL	m372-D7	344	5
73	KILLARLFLYALALLLLASA	M372-D8	349	2.6
74	RLFLYALALLLLASALIAGG	M372-E1	354	2
75	ALALLLLASALIAGGSILQT	M372-E2	359	5
76	LLASALIAGGSILQTNFKSL	M372-E3	364	5
77	LIAGGSILQTNFKSLSSTEF	M372-E4	369	5
78	SILQTNFKSLSSTEFIPNLF	M372-E5	374	5
79	NFKSLSSTEFIPNLFCMLLL	M372-E6	379	5
80	SSTEFIPNLFCMLLLIVAGI	M372-E7	384	5
81	IPNLFCMLLLIVAGILFILA	M372-E8	389	5
82	CMLLLIVAGILFILAILTEW	M372-F1	394	1.4
83	IVAGILFILAILTEWGSGNR	M372-F2	399	5
84	LFILAILTEWGSGNRTYGPV	M372-F3	404	5
85	ILTEWGSGNRTYGPVFMCLG	M372-F4	409	5
86	GSGNRTYGPVFMCLGGLLTM	M372-F5	414	5
87	TYGPVFMCLGGLLTMVAGAV	M372F6	419	5
88	FMCLGGLLTMVAGAVWLTVM	M372-F7	424	5
89	GLLTMVAGAVMLTVMSNTLL	M372-F8	429	5
90	VAGAVWLTVMSNTLLSAWIL	M373-A2	434	5
91	WLTVMSNTLLSAWILTAGFL	M372-A3	439	5
92	SNTLLSAWILTAGFLIFLIG	M373-A4	444	5
93	SAWILTAGFLIFLIGFALFG	M373-A5	449	5
94	TAGFLIFLIGFALFGVIRCC	M373-A6	454	4.7
95	IFLIGFALFGVIRCCRYCCY	M373-A7	459	5
96	FALFGVIRCCRYCCYYCLTL	M373-A8	464	5

97	VIRCCRYCCYYCLTLESEER	M373-B1	469	5
98	RYCCYYCLTLESEERPPTPY	M499-A8	474	5
99	YYCLTLESEERPPTPYRNTV	M394-A1	476	5

CHAPTER 3

SYSTEMATIC INVESTIGATION OF T CELLS RESPONSES AGAINST EBV TUMOUR ANTIGENS IN HEALTHY DONORS

3.1 Introduction

EBV infects almost 95% of people worldwide and is associated with almost 200,000 cases of lymphoid and epithelial cancer each year. These include almost all cases of nasopharyngeal carcinoma, about 10% of gastric carcinoma (GC) cases and several types of lymphoma that express EBV antigens[120, 147].These antigens are principally EBNA1 and LMP2. Two other antigens, LMP1 and BARF1 are also expressed in some cases of EBV-associated cancer[148]. While the T-cell response to these different antigens has previously been measured, each study has focused only one or two of these antigens. Furthermore, the different groups have used different techniques and some have examined only CD8 T-cells or have used epitope prediction algorithms focusing on only a narrow subset of HLA alleles [149]. Thus, the current model of immune hierarchy could be biased. Understanding this hierarchy in healthy people would help inform the development of effective immunotherapies.

To address this problem, I conducted a systematic analysis of the immune response to the four key EBV tumor antigens in healthy donors. Twenty-five healthy donors were evaluated, using antigen pepmixes to identity the T cells response to each of the four EBV antigens (EBNA1, LMP1, LMP2 and BARF1) in an individual in a single assay. Pepmixes are overlapping pools of 15mer peptides that span the entire protein sequence; thus, they can stimulate any responses present in an individual regardless of their HLA type.

An ex vivo interferon-gamma ELIspot was used, as this method is the most sensitive technique for measuring ex vivo responses. In brief, $0.5x10^6$ PBMCs from each donor were stimulated by each pepmix in duplicate of triplicate wells. This cell number was the maximum that can be used in such assays and was chosen to maximise assay

sensitivity. DMSO was used as negative control and PHA as a positive control. The mean number of spots in the DMSO wells was subtracted from the mean number of spots in each pepmix well to calculate the frequency of the pepmix-specific T-cell response as a continuous variable – the mean adjusted reading expressed per million PBMC. An antigen-specifc response was scored as being present if the mean number of spots in the pepmix wells was ≥2-times and ≥10 more spots than the mean of the DMSO negative control.

3.2 T cell response to EBV tumour antigens

As shown in Figure 1 , across all 25 donors studied, the hierarchy of the T-cell response size to EBV antigens was: EBNA1 > LMP2 > LMP1 > BARF1. The mean size of the responses (expressed per 10^6 PBMC) were: EBNA1 78 (91SD), LMP2 63 (66SD), LMP1 31(44 SD) and BARF1 10 (15SD). The median size of each response was: EBNA1, 45; LMP2, 43; LMP1, 20 and BARF1, 2.

Regarding the number of donors scored as having a response, LMP2 was the highest with 9/25 (36 %) donors having a response, followed by EBNA1 6/25 (24%), LMP1 5/25 (20%) and BARF1 2/25 (8%). Looking at the size of response in those donors scored as having a response. Result showed that the highest T cells responses to LMP1 (129) and (198) were correlated to EBNA1 (127) and (173) response.

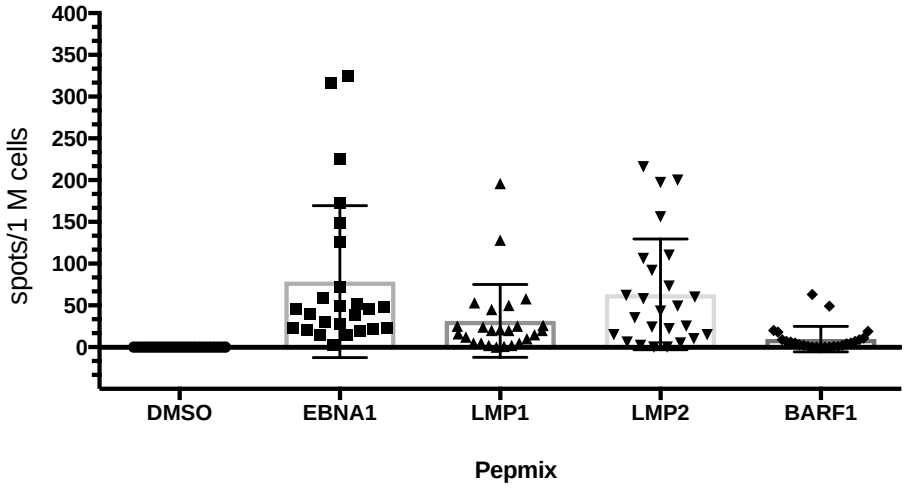

	MEAN	MEDIAN	Range	STD.P	STD.S	VAR.P	VAR.S
DMSO	0	0	0	0	0	0	0
EBNA1	78	45	322	89	91	7958	8290
LMP1	31	20	196	43	44	1835	1911
LMP2	63	43	216	65	66	4221	4397
BARF1	10	5	63	15	15	230	240

Figure 1 : Investigation of T cell response in healthy donors against EBV tumour antigens.

PBMCs from 25 healthy donors were stimulated by four EBV pepmixes: EBNA1, LMP1, LMP2 and BARF1. The responses of T cells which released IFNγ were measured by IFNγ ELISpot assays, DMSO was used as negative control and PHA was also included as positive control. The mean spot number of each donors negative control was subtracted from the pepmix stimulated test wells. Each bar represents the mean +/- SD of spot number, after subtraction of the background DMSO response for each individual.

While T cell responses to BARF1 were rare, I found weak BARF1 responses (63 per 10^6 PBMC) in a subject who also had an LMP2 response (110 per 10^6 PBMC) and an EBNA1 response (317 per 10^6 PBMC) response. A second donors also had a response to BARF1 I also found a response to BARF1 (49 per 10^6 PBMC) with LMP2 (92), LMP1 (128) AND EBNA1 (126) responses also present in that individual.

Interestingly, I found that the highest responses to LMP1 (196 per 10^6 PBMC) and LMP2 (216 per 10^6 PBMC) were from the same subject – donor D2; this donor also had an EBNA1 response (173 per 10^6 PBMC). Given that LMP1 is typically a poor T-cell target, I selected this donor for further analysis.

3.3 Analysis of the LMP1 specific T cell response.

To further characterise the LMP1 T-cell response in donor D2, I retested PBMCs using smaller pools of LMP1 peptides. First, 73 LMP1 20 mer peptides were used to prepare 15 pools, each containing 5 peptides as shown in (chapter 2) . Then, $0.5x10^6$ PBMCs were tested in ex vivo ELIspot assays as described above, using by LMP1 pepmix or the above peptide pools in duplicate or triplicate wells for each pool. As shown in Figure 2 I found LMP1 peptide specific T cell responses with pool numbers 3, 4, 5, 6 and 7.

To identify the specific individual peptide from each pool, I retested PBMCs from donor D2 with 24 separate peptides. As shown in Figure 3 A, LMP1 peptides A3 and A4 stimulated interferon-gamma production. To know the type of LMP1 peptide specific T cell response, CD4 T cells were depleted from PBMCs then the cells (either undepleted or CD4 depleted) were tested with peptides A3 and A4. The results Figure 3**.** showed that the T cells responses did not decrease upon CD4 depletion, indeed they

increased when CD4 cells were depleted cell indicating that the T-cell response was CD8 mediated. As shown inTable 9, both LMP1 peptides A3 and A4 contain the sequence YLQ, a previously defined LMP1 epitope.

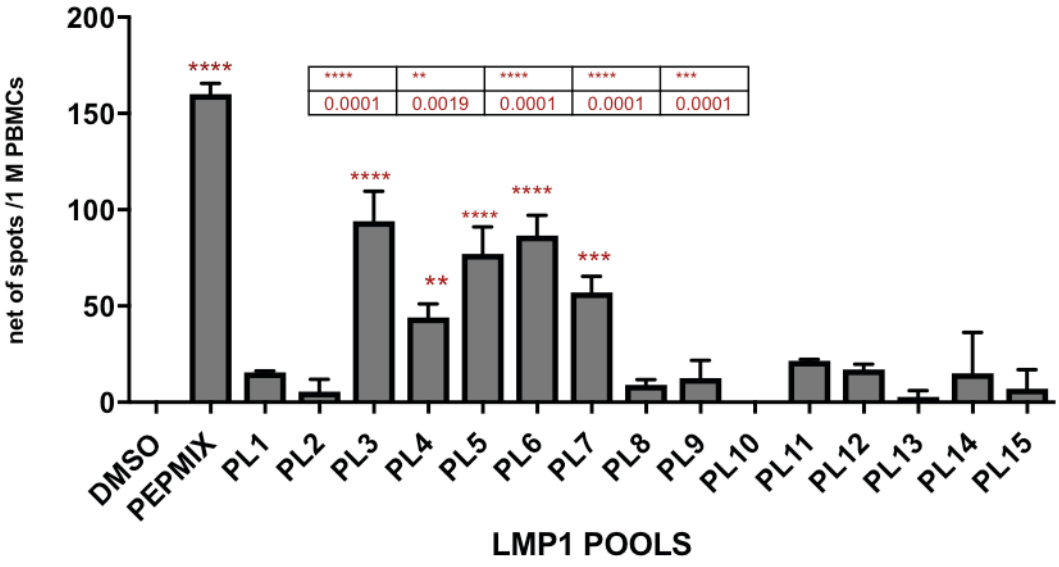

Figure 2 : T cell response to LMP1 peptide pools

PBMCs from donor D2 were stimulated by pepmix or 15 pools of LMP1 peptides prepared from 73 LMP1 20 mer peptides in an ex vivo IFNg ELIspot assay. Results show the mean of cells secreting IFNg per million PBMC after subtracting the negative control (DMSO) value.

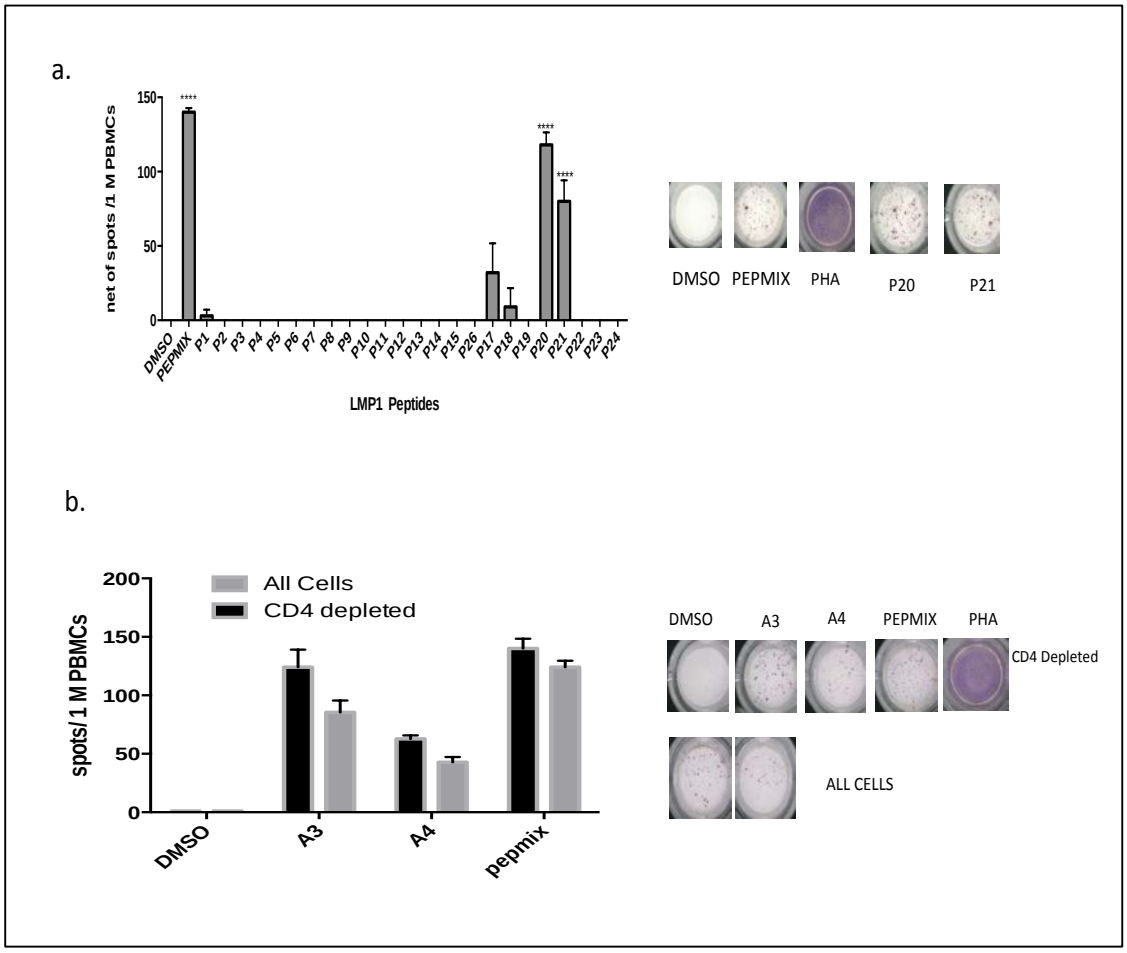

Figure 3 ***identified LMP1 specific- CD8 T cell response.***

(a) Identification of LMP1 T cell responses in donor D2 using ex vivo IFN-g ELIspot and LMP1 pepmix or 24 individual LMP1 peptides (20 mer). DMSO was used as a negative control and PHA as a postive control. (b) The LMP1 peptide specific response was further characterised by stimulated CD4 depleted cells with LMP1 peptides (A3) or (A4) or pepmix .

3.4 Identified New LMP2 specific- CD8 and CD4 T cell response.

Due to the strength of the LMP2 T-cell response in donor D2, which was much higher than all other donors, I also characterised this response. The same approach as used to test the LMP1 response was used. First, 20 pools of LMP2 peptides were prepared from 98 individual peptides, each pool containing 5 peptides as shown in **(**chapter 2) . Then, $0.5x10^6$ PBMCs were stimulated by LMP2 pepmix or each of the peptides pools in duplicate or triplicate wells for each pool. As shown in Figure 4 A**.** after subtracting the DMSO negative control I found significant LMP2 peptide specific T cell responses were stimulated by pool numbers 11, 12, 14 , 15, 18 and 19.

To identify the specific individual peptides stimulating T-cell activity, 30 individual peptides from these six pools were used to stimulate PBMCs from donor D2; cells were also stimulated with pepmix as a control with DMSO and PHA serving as negative and positive controls respectively. As shown in Figure 4b, LMP2 peptide specific T cell responses were stimulated by peptides 9 ,14 , 22, 26 and 27. To identify the type of LMP2 peptide specific T cell response, CD4 T cells were depleted from PBMCs cells then the undepleted and CD4 depleted cells were tested with peptides C7 and A3 (Figure 4**c)**. The results show that T cell response induced by peptide C7 decreased upon CD4 depletion indicating this response was a CD4 T-cell response. In contrast, the response induced by peptide A3 increased upon CD4 depletion showing this response was mediated by CD8 T-cells.

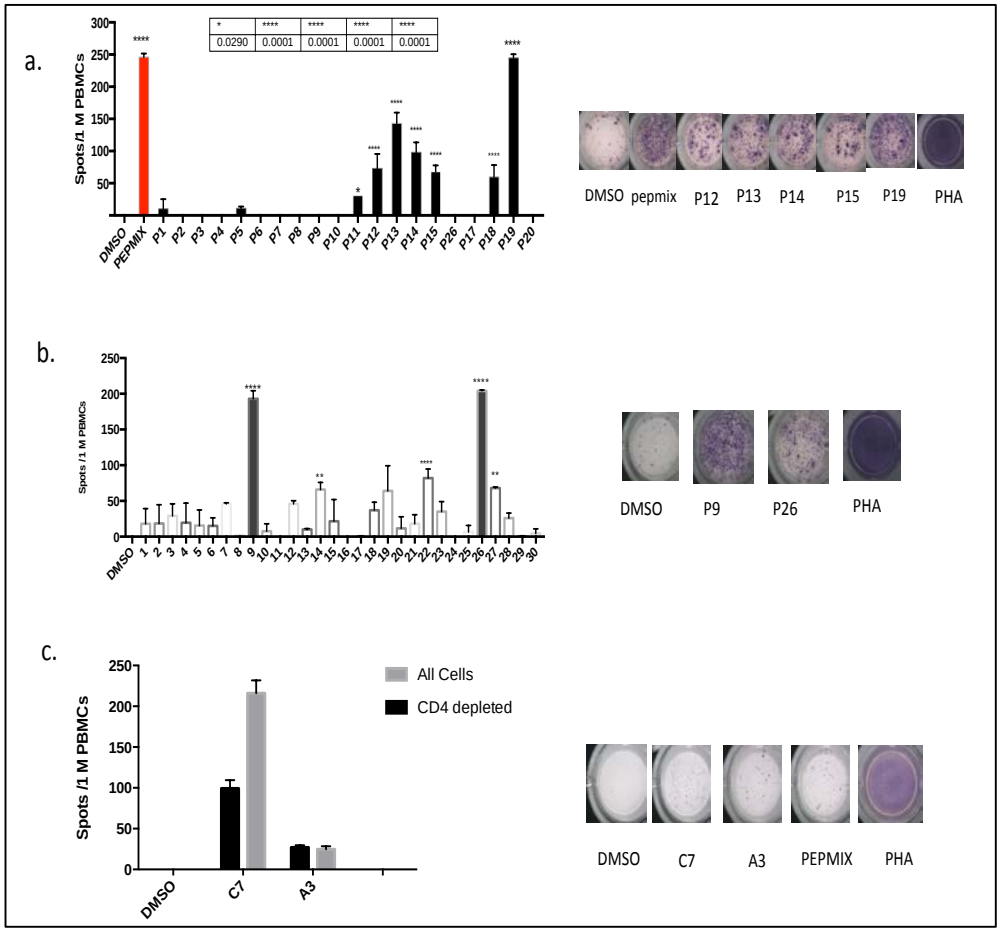

Figure 4 : Identified New LMP2 specific- CD8 and CD4 T cell response.

(a) PBMCs were stimulated by pepmix and 20 pools of LMP2 peptides were prepared from 98 individual peptides to recognize T cell response using IFNg ELIspot assay(b) T cells response to 30 individual LMP2 peptides from responded pools, PHA used as positive control and DMSO as negative control. (c) Recognition of T cells type response to LMP2 peptides with CD4 depletion. When peptide (9) C7 is CD4 response and peptide (26) A3 is CD8 T cell response

Table 9 : **summary of LMP1 and LMP2 –specific CD4 and CD8 response**

antigen	B95.8 sequence	position	phenotype
LMP1	LILLIIALYLQQNWWTLLVD	151	CD8
LMP1	IALYLQQNWWTLLVDLLWLL	156	CD8
LMP2 (C7)	LAAALALLASLILGTLNLTT	304	CD4
LMP2 (A3)	WLTVMSNTLLSAWILTAGFL	439	CD8

Position: the number of the first amino acid in the peptide sequence in the B95.8 strain of EBV

3.5 Identified new novel LMP2A specific CD8 T cells clones.

While studying LMP2 T-cell responses in donor D2, a co-worker produced LMP2-specific T-cell clones to an unknown, presumably novel, T-cell epitope. I was able to use these clones in my experiments to study this T-cell response. In total, seven CD4 and CD8 T cell clones specific for LMP2A were studied. Autologous LCL cells were stimulated with 20 pools of LMP2 peptides then cultured with T cell clones overnight. T-cell activity was determined by measuring INFγ in the cell supernatant by ELISA (data not shown). Having identified the relevant pools, I tested individual peptides to identify the specific peptide. I found five T cell clones were specific for two LMP2 peptides (FLY) and (TYG) which had previously been studied and were already known (data not shown).

Interestingly, I found two new T cell clones which were specific for LMP2. Using flow cytometry I determined that these were both CD8+ T-cell clones (data not shown). As shown in Figure 5a ELISA results show that LMP2 pool specific T cell clone 50 responded to pool 6 when compared to relevant controls: T clones alone, LCL alone and T+LCL without peptide. CD8 T cell clone 50 specifically recognized the individual LMP2 peptides (P4) and (P5) within pool 6 (Figure 5b). The result in Figure 6 shows data from CD8 T cell clone 71. This clone was found to be specific to individual peptides (P4) and (P5) from LMP2 peptide pool 26. These data show both clones recognize epitopes that have never been described. These interesting findings need more research to characterize the clone further, but this was not performed in my project.

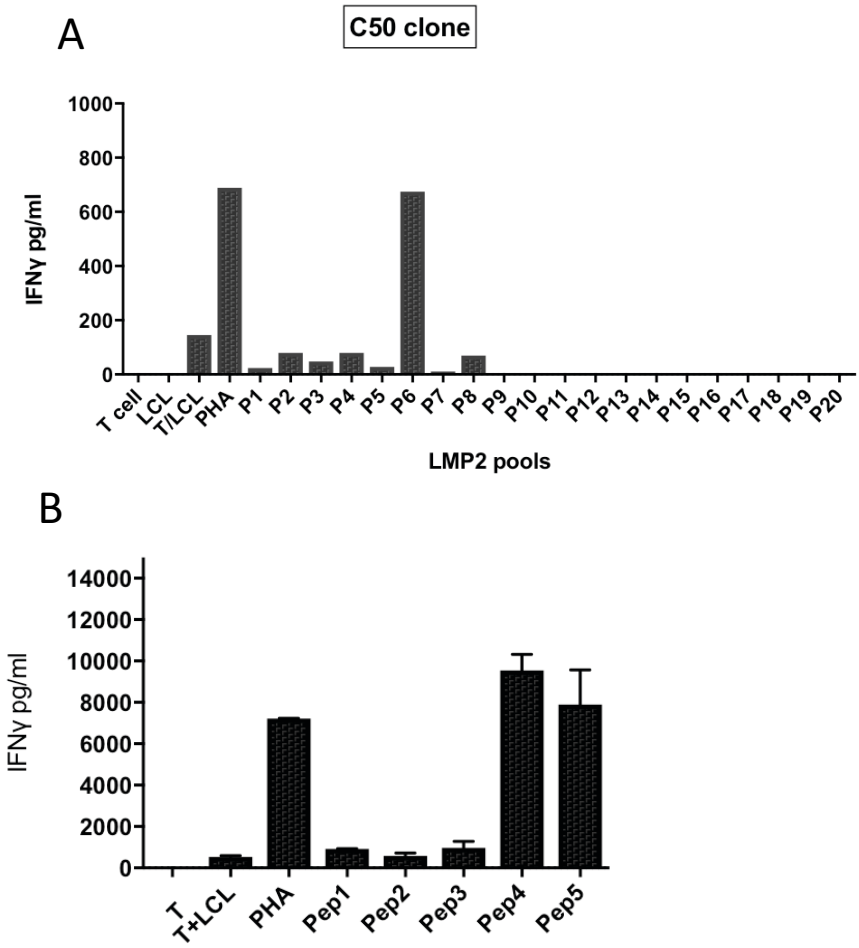

	peptide	B95.8 sequence	position
Pool 6	1	CLPVIVAPYLFWLAAIAASC	124
	2	VAPYLFWLAAIAASCFTASV	129
	3	FWLAAIAASCFTASVSTVVT	134
	4	IAASCFTASVSTVVTATGLA	139
	5	FTASVSTVVTATGLALSLLL	144

Figure 5 New LMP2 specific- CD8 T cell response (clone 50).

T cell clones specific for LMP2A were cultured with autologous LCL after pulsing with LMP2 peptide pools or individual peptides to identify which of these peptides was reasonable for T cell response. Released INFγ was detected by ELISA. (A) T cell clone (CD50) responds to pool 6, which include five peptides (B) CD8+ clone CD50 responded to pep 4 (IAA)and pep5 (FTA) LMP2 peptides.

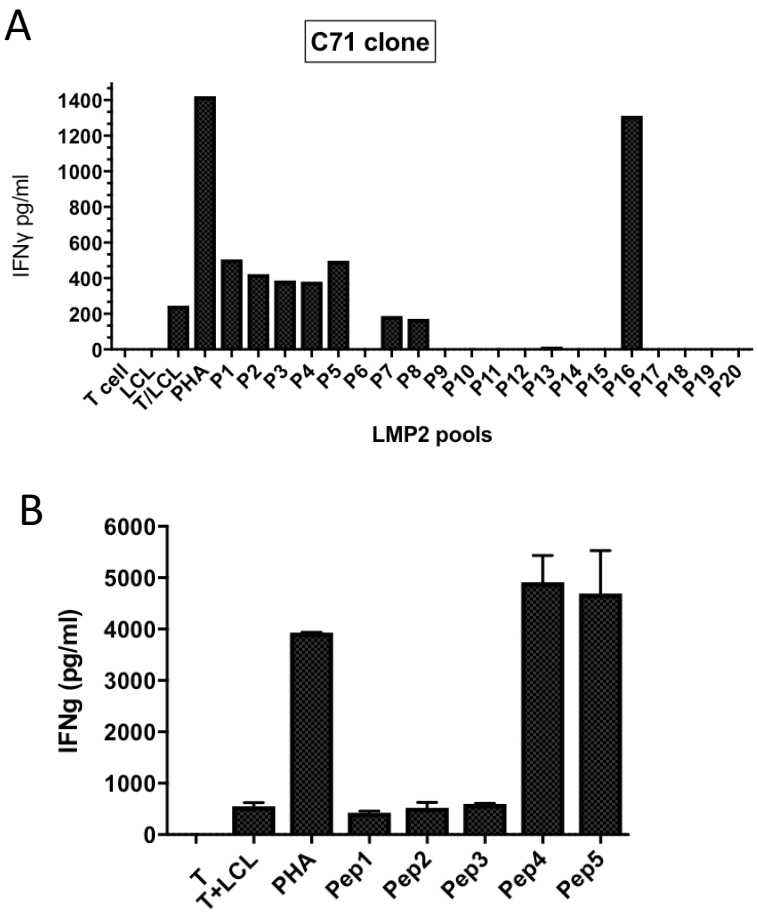

	peptide	B95.8 sequence	position
	1	LLASALIAGGSILQTNFKSL	364
	2	LIAGGSILQTNFKSLSSTEF	369
Pool 16	3	SILQTNFKSLSSTEFIPNLF	374
	4	NFKSLSSTEFIPNLFCMLLL	379
	5	SSTEFIPNLFCMLLLIVAGI	384

Figure 6 New LMP2 specific- CD8 and T cell response (clone 71).

T cell clones specific for LMP2A were cultured with autologous LCL after pulsing with LMP2 peptide pools or individual peptides to identify which of these peptides was reasonable for T cell response. Released INFγ was detected by ELISA. (A) T cell clone (CD71) responds to pool 6, which include five peptides (B) CD8+ clone CD50 responded to pep 4 (NFK)and pep5 (SST) LMP2 peptides.

3.6 Novel response of BARF1 specific CD4+ T cell clones as new immunotherapy target

As shown above, in ex vivo ELispot assays I found weak T cell responses to BARF1 pepmix antigen in 3 of 25 heathy donors. BARF1 plays an important role in EBV disorders as an oncogene and there is limited information about the immune to this antigen. Therefore, I decided to further study the T cell response against BARF1.

3.6.1 Selection of T cell response to BARF1 antigen using new TNFa assay.

It is possible that ex vivo ELIspot assays may miss antigen-specific responses that either: i) secrete other cytokines or ii) consist of central memory responses that do not produce cytokines in short term assays. I therefore tested 11 donors for BARF1 T-cell responses using cultured assays with flow cytometry as the assay readout.

Briefly, after isolating PBMCs from a donor, I exposed cells to BARF1 pepmix and cultured them in T cell media with IL-7 and IL-15 cytokines for 10 days. Cells were fed on day 3 and day 7 with fresh media and cytokines. At day 10, a part of the culture was re-stimulated with pepmix in the presence of anti-TNFa-APC antibody and TAPI-0 for 4-6hours. After staining with phenotype-specific antibodies (anti-C3, anti CD4, anti-CD8) T cells that produced TNFa were detected by flow cytometry. Remaining cells in the culture plate were re-stimulated with pepmix and cytokines for 10 days more, and T cell responses were detected (now on day 20) as described.

The results in Figure 7**a** show results of one and two stimulations with BARF1 premix. In general I found BARF1 specific T cell responses after one stimulation and these increased in size after a second stimulation as shown in Figure 7b.

In total, 36 patients were tested in either an ex vivo assay or a cultured assay as described above. I selected 5 healthy donors that appeared to have a BARF1 response in the above assays for further study.

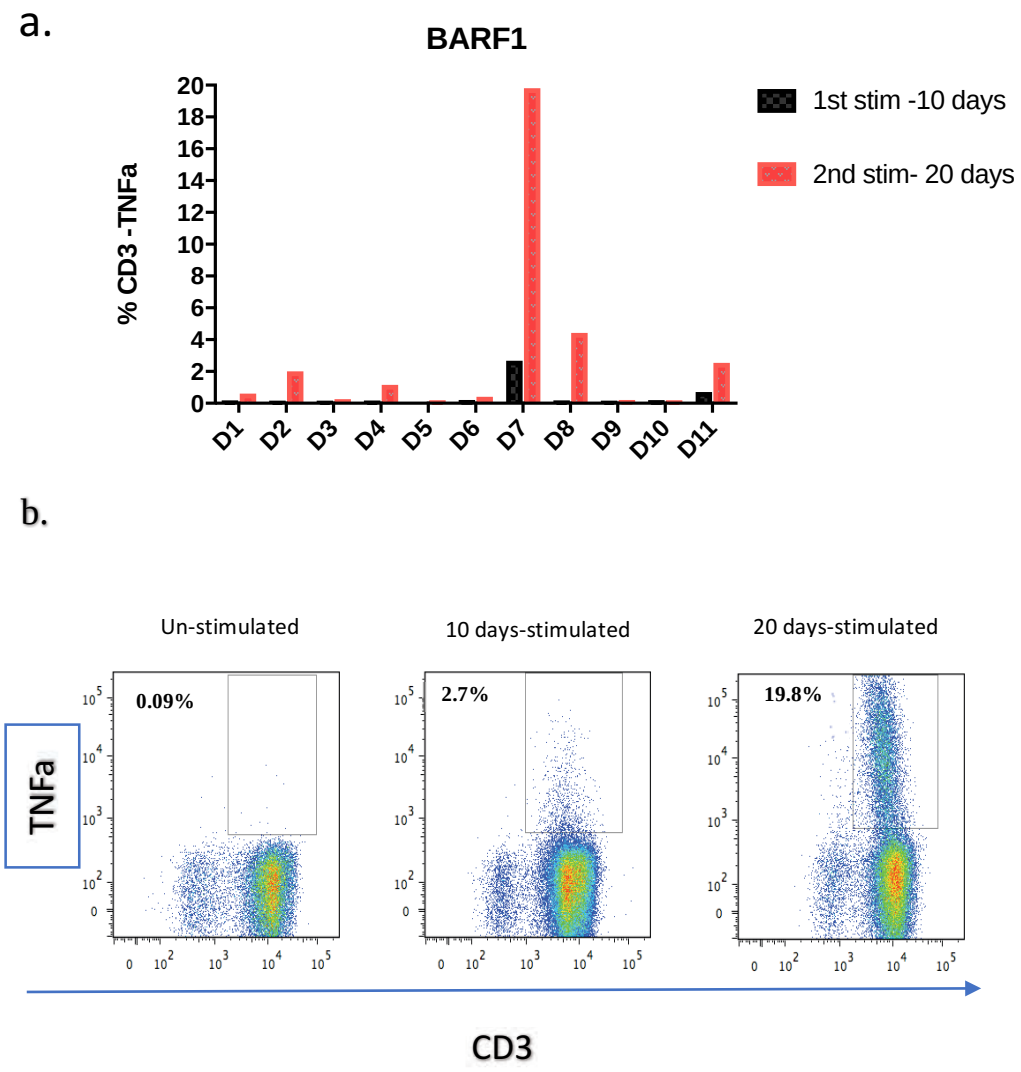

Figure 7 Identification of T cell response to BARF1 antigen using new TNFa assay.

PBMCs from 11 healthy donors were tested in cultured assays with BARF1 pepmix. Cells were cultured for 10 days then part of the culture was stimulated for 4-6 hours with BARF1 pepmix in the presence of TNFa antibody and TAPI-0 . Cells were counter stained for CD3, CD4, CD8 and analysed by flow cytometry. Remaining cells in culture plate were re-stimulated with pepmix and cytokines for 10 days more and the T cell response to BARF1 was again measured as before. The results obtained for one donor are shown. Un-stimulated is the results of culturing cells for 10days without any pepmix. The results obtained after culturing cells with BARF1 pepmix for 10 or 20 days are also shown.

3.6.2 Production of BARF1-specific and T-cell clone

Fresh PBMCs from 5 healthy subjects were cultured with BARF1 pepmix to reactivate specific epitope T cells for 10 days as discussed above. Then, cells were re-stimulated and cultured for 4-6 hours in present of TNFa antibody and cells were stained with viability and CD3 staining then suspended in cold T cell media. Responding cells were isolated using the TNFa capture assay with positive cells sorted by FACS at one cell per well into 96 well plates containing T cell media (irradiated PHA -treated mix cones, anti- CD3 and IL-2). T-cells were grown for two weeks and growing cultures were tested for specificity.

3.6.3 Donor 2: Characterization of 3 New BARF1-specific and CD4 T-cell clones: HLA-B*5101

3.6.3.1 Determination of T cell clone specificity

I screened 35 growing microcultures from donor 2 to determine whether they were specific for BARF1 peptide. I co-cultured the expanded T cells with autologous LCL pre-exposed to BARF1 pepmix cells DMSO. The next day I measured IFNγ in the culture supernatant by ELISA assay. As shown in Figure 8, three of the growing microcultures (4,5and 6) produced IFNγ in response to BARF1-exposed LCL but not to unmanipulated LCL. These T cell clones were expanded with irradiated stimulated autologous LCL and PHA- treated allogeneic mixed cells.

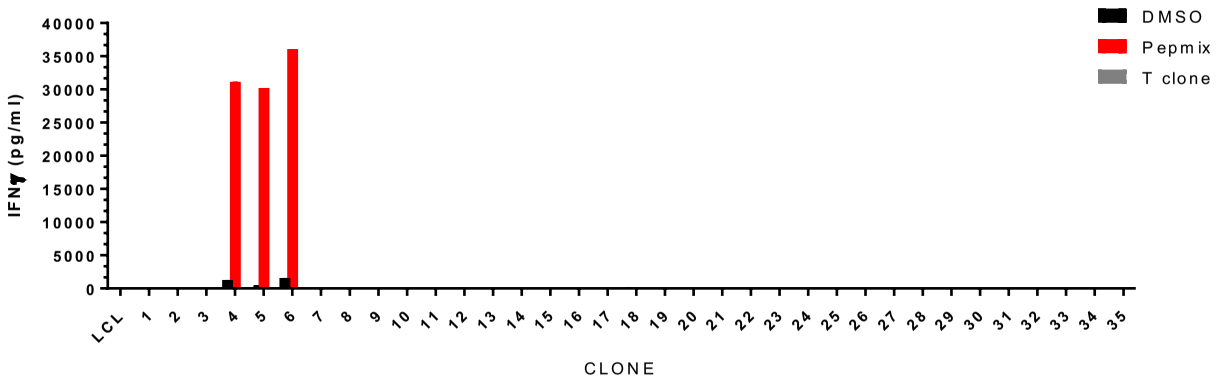

Figure 8 : Determining T cell clone specificity

To identify specificity of growing T cell clones, T cells were cultured with autologous LCL either unmanipluated or pre-exposed to BARF1 pepmix followed by IFNγ detection by ELISA. Three clones were specific to BARF1 pepmix while the other cell cultures were not specific. For each culture two negative control were included, T-cells alone (grey bars) and T cell with DMSO-pulsed LCL (black bars) , LCL without T cells was also tested (left first column)

3.6.3.2 Mapping BARF1 T-cell epitopes using BARF1-specific T-cell clones.

Autologous LCL cells were separately pulsed with 21 individual peptides then incubated with T cell clones (C4, C5, and C6). T cell clone responses were detected by ELISA. As shown in Figure 9 all clones responded to exposed – LCL with BARF1 peptide nine (9). Flow cytometry showed all three clones were CD4 positive (data not shown).

3.6.3.3 Avidity of T cell clones

Having identified the cognate 20mer peptide it was possible to determine the avidity of the T cell clones in titration assays. Because the initial BARF1 peptide library consisted of 20mers overlapping by 10 amino acids, I designed and had synthesised additional peptides overlapping these peptides by 5 amino acids to allow finer identification of the optimal epitope peptide for each clone. The sequences of the additional peptides (called peptide A and peptide B) are shown in Figure 10.

Data from the titration experiments is also shown in in Figure 10. Each clone was tested against the individual peptides in the range 10^{-5} to 10^{-11} M and DMSO control. In this assay, the functional avidity is the peptide concentration that required to causes half (50%) of the maximal IFNg released by T cell activation. T cell clones recognized peptide 9 and B but no response was obtained with peptide A. All three clones (4,5 and 6) recognized pep B slightly more than pep9. Peptide B (TFF , aa 87-105) was therefore selected as the optimal epitope peptide sequence. T cell clone avidity to this peptide varied, ranging from 181nM with clone 5 then 1460 nM with clone 4 and 5.

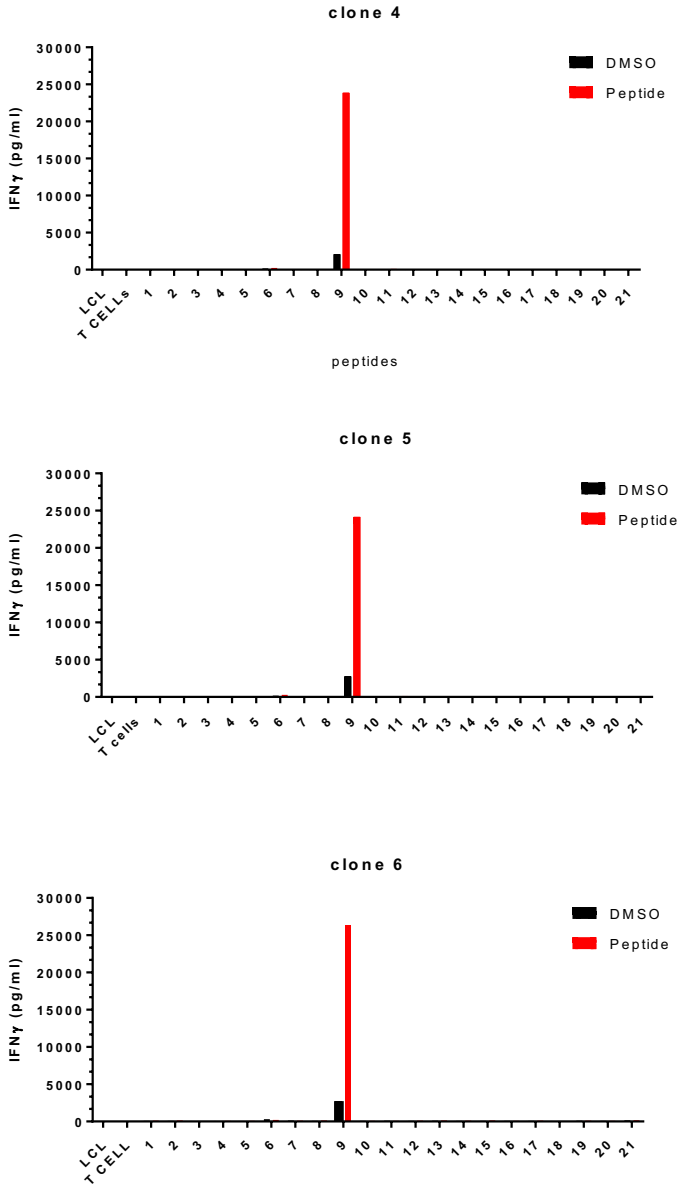

Figure 9 :Identified T cell clone response to target individual peptide

Autologous LCL were pulsed with 21 individual peptides then incubated with T cell clones (C4, C4, and C6). T cell clone responses were detected by ELISA. All clones responded to the 20 mer BARF1 peptide nine (aa 90-110).

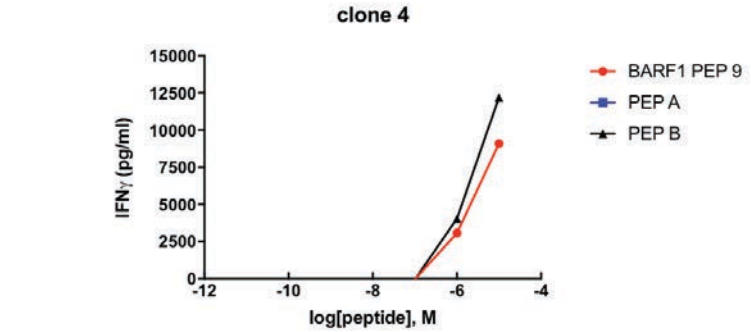

	BARF1 PEP 9	PEP B
LogIC50	-5.829	-5.846

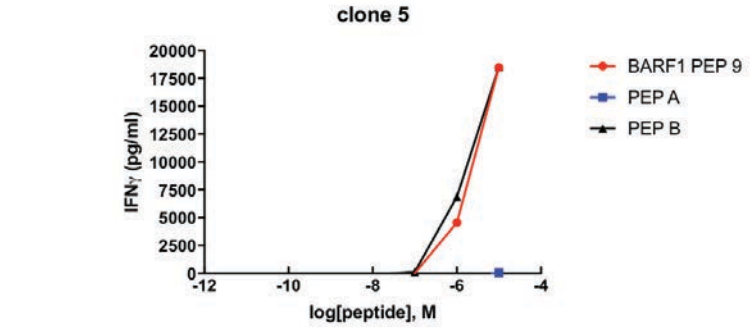

	BARF1 PEP 9	PEP B
LogIC50	-5.701	-5.849

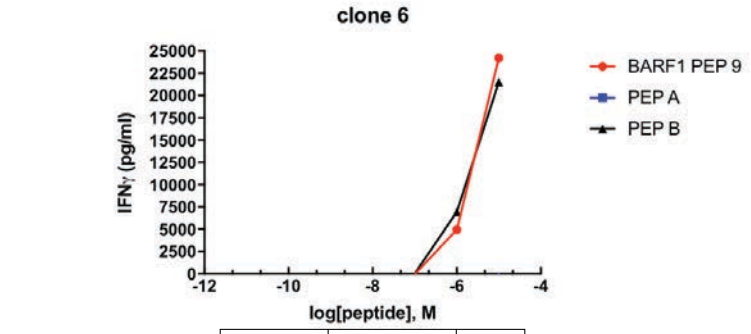

	BARF1 PEP 9	PEP B
LogIC50	-5.695	-5.835

Pep 8	EWPFRGFFDIHRSANTFFLV	71-90aa
Pep A	GFFDIHRSANTFFLVVTAAN	76-95aa
Pep 9	HRSANTFFLVVTAANISHDG	81-100aa
Pep B	TFFLVVTAANISHDGNYLCR	86-115aa

Figure 10: T cell clone avidity

BARF1- specific CD4 T-cell clones 4, 5 and 6 were tested with LCL pulsed with individual peptides in the range of 10^{-5} to 10^{-11} M and DMSO control. In this assay, the functional avidity is the peptide concentration that causes half (50%) maximal IFNg release by T cells.

3.6.3.4 T cell clone HLA restriction

To determine the class II HLA restriction of the T cell clones I made a panel of LCL cells that include the autologous LCL and different allogeneic LCLs which were partially HLA matched to the original donor as shown Table 10 . LCLs were exposed to BARF1 peptide then cultured with T cell clones before testing the supernatant by ELISA to measure IFNg release. Figure 11 shows all T cell clones responded to autologous LCL, DR51 positive (LCLs 3 and 4) but not to any other LCLs. Therefore all T cell clones (4, 5, and 6) were DR-51 HLA restricted.

Table 10 : Panel of LCL cell lines used for HLA restriction of BARF1-specific CD4 T-cell clones

LCL		DR				DQ	
1	Autologous	9	15	51	53	6	9
2	DR-53	4		53		7	9
3	DR-51	12	16	51	52a	5	7
4	DR51 -15	15	17	51	52a	2	6
5	DQ-6	13	17		52a	2	6

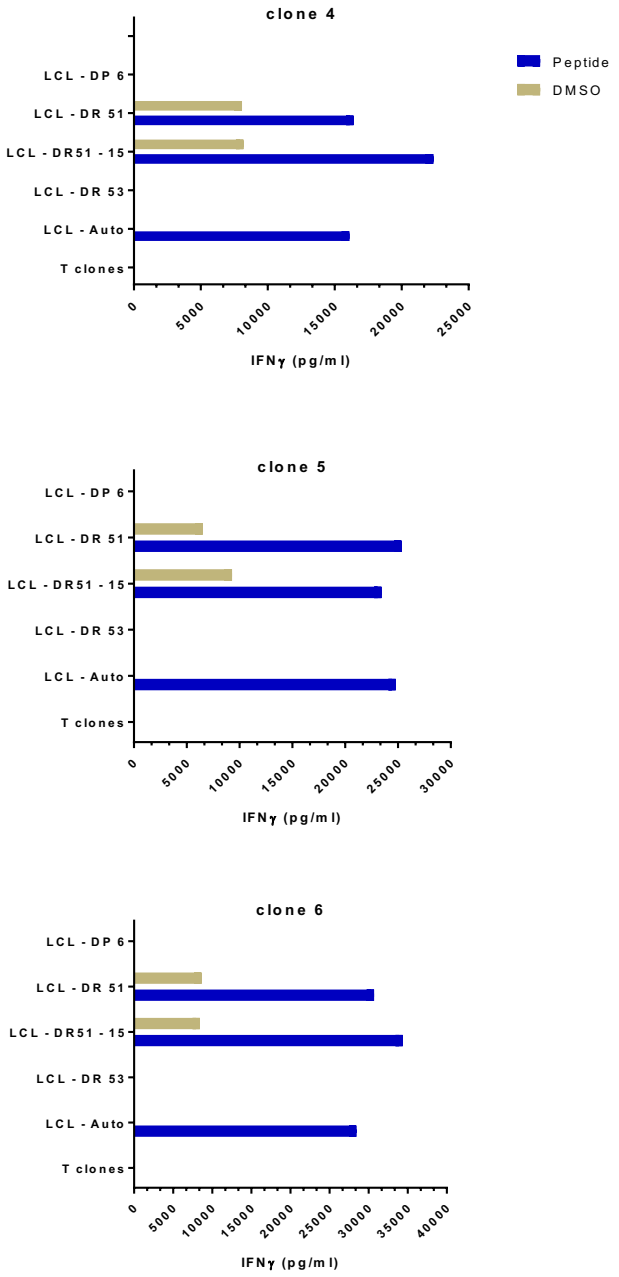

Figure 11 :T cell clone HLA restriction

A panel of LCL cells that include the autologous LCL and different cell lines partially HLA class II matched to the original donor were exposed to the BARF1 epitope peptide. LCLs were then cultured with T cell clones (4 , 5, and 6) and interferon gamma release measured by ELISA. All T cell clones were responsive (IFNg released) to autologous LCL, DR51 matched LCLs but not to other LCLs. T cell clones (4, 5, and 6) were thereforeDR-51 HLA restricted.

3.6.3.5 Efficiency of T cell clone response to LCL cells lines.

The data shown in Figure 11 clearly showed that BARF1 T-cell clones C4, C5, C6 produced interferon-gamma when exposed to unmanipulated HLA-matched LCLs. In other words, LCLs that had not been exposed to synthetic peptides. To quantify this recognition T cell clones were cultured with a range of matched LCL (DR-51) that were unmanipulated or, to set a benchmark of maximum interferon-gamma production, were pre-exposed to synthetic peptide. T-cell activity was determined by IFNg ELISA. Different number of T cell clones were added per well (3000 or 1000 T cell clones). The efficacy of T clones response to unmanipulated LCL was expressed as a percentage of maximal response to the same LCLs exposed to epitope peptide.

Figure 12 shows a range of efficacies with T cell clones and LCL cells line. In general, I found that the percentage of efficacy with clone 6 was the highest then clone 5 and then clone 4 with LCL1 (63 %,53% and 52%), LCL2 (23%,30% and 8%) and LCL3 (35%, 25% and 16%) respectively.

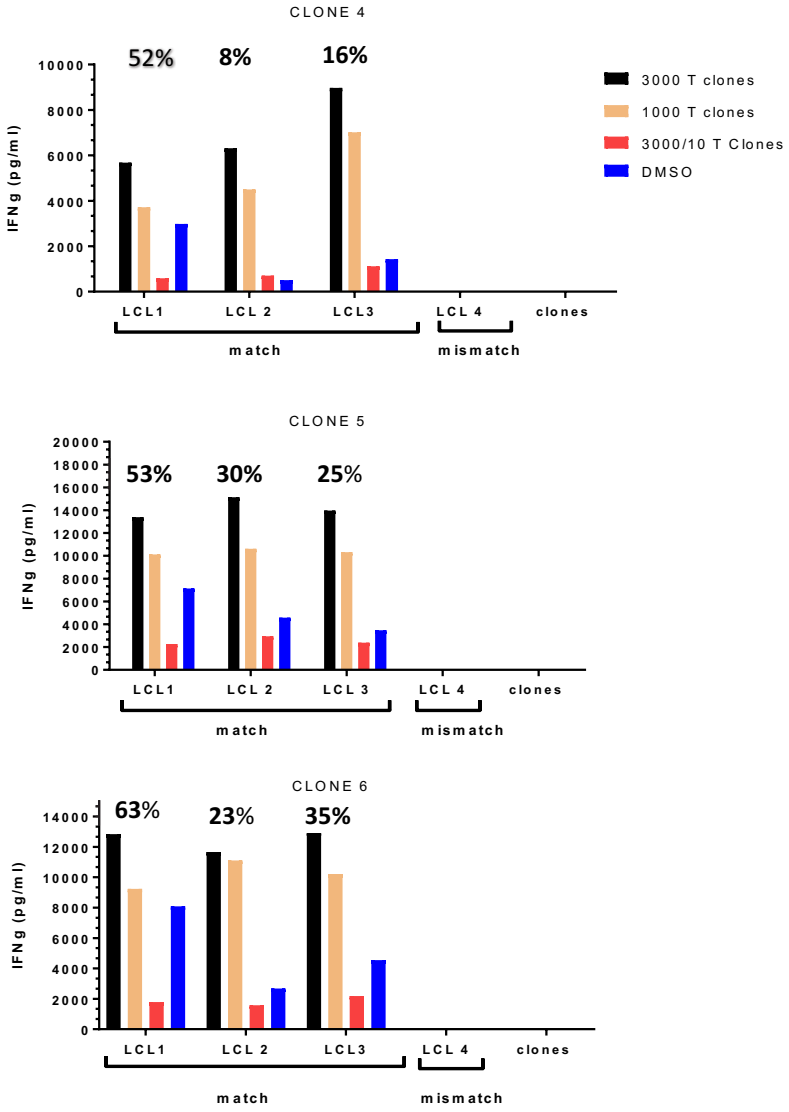

Figure 12 :Efficiency of T cell clone response to LCL:

T cell clones were cultured with a range of matched LCL (DR-51) that were unmanipulated or exposed with epitope peptide. T-cell activity was measured by IFNg ELISA. Different number of T cell clones were added per well (3000, 1000 T cell clones) The efficacy of T clones response to unmanipulated LCL was expressed as a percentage of maximal response to the same LCLs exposed to epitope peptide. Note that HLA-mismatched LCLs were never recognised by the T-cells.

3.6.3.6 Expression of BARF1 and BZLF1 gene in targeted LCL cell lines

The three BARF1-specific CD4+ T cell clones were clearly capable of recognising B cells line transformed with the EBV (B95.8) strain, although the efficiency of recognition varied for the different LCLs. Given that BARF1 has been reported to be expressed when EBV enters lytic cycle, I undertook a series of experiments to determine the level of BARF1 gene expression in the LCLs. I also measured the expression of the BZLF1 gene, which induces LCLs to enter lytic cycle. This was performed to determine if recognition correlated with lytic cycle activity in the culture, to begin to examine whether BARF1 was likely to be expressed in lytic cycle or, potentiall, could be expressed as a latent cycle protein

I made cDNA from RNA that was collected twice at different times (A) and (B) from a range of LCL cell lines. BZLF1 knockout (K/O) LCLs incapable of entering lytic cycle were included as controls to explore if BARF1 was expressed in the absence of lytic cycle. RNA expression was detected by qPCR assay. As shown in Figure 13 , expression of BARF1and BZLF1 were detected in LCL lines (A1-A4) and (B1-B4) but no detectable expression was seen with BZLF1 K/O cells. This transcript analysis suggests that BARF1 is expressed only in the presence of BZLF1 suggesting it is a lytic cycle transcript in LCLs.

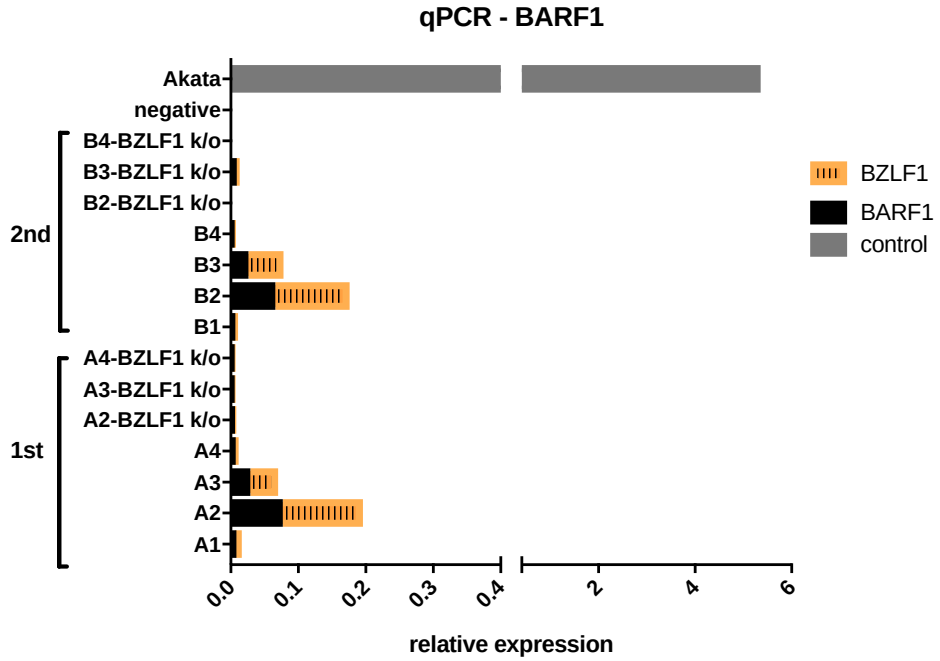

Figure 13 :Detection of BARF1 and BZLF1 gene expression in LCLs:

To measure the expression of BARF1 and BZLF1 genes in LCLs cDNA was made from RNA that was collected twice at different times (A) and (B) from the same range of LCL cell lines. The LCLs include BZLF1 knockout K/O cells lines. EBV positive Akata cells was used as positive control and DNAse free water as negative control.

3.6.4 Donor 2: Characterization of 6 new novel BARF1-specific CD4 T-cell clones

3.6.4.1 T cell specificity

T-cell clones from growing microcultures were tested as described earlier. I screened 13 cultures for their specificity towards BARF1 pepmix. As show in Figure 14 **a**, seven expanded T-cell clones produced IFNγ in response to BARF1-pepmix loaded LCL. To identify the specific BARF1 peptide that each clone recognised, autologous LCL was loaded with one of four different peptide pools each containing 5 peptides table. These LCLs were then co-cultured with each of the seven expanded T cell clones and INfg release measured. The result shows that T cell clone C1 responded to pool 1, T cell clones C2, C4, C7, C10 and C12 responded to pool 3 and T clone 12 responded to pool 2 peptides as shown in Figure 14b. To detect specific individual epitope peptides, responding T cell clones were cultured with autologous LCL exposed to each of the 5 individual peptides within the relevant pool. I found six novel T cell clones to 3 different BARF1 epitopes as shown in Figure 14**c.** Clone 1 responded to peptides 3 and 4 from pool 1, clones 2 , 4, 7 and 10 responded to peptide 2 from pool3 and clone 12 responded to pep5 from pool2 and pep1 from pool3 which overlap.

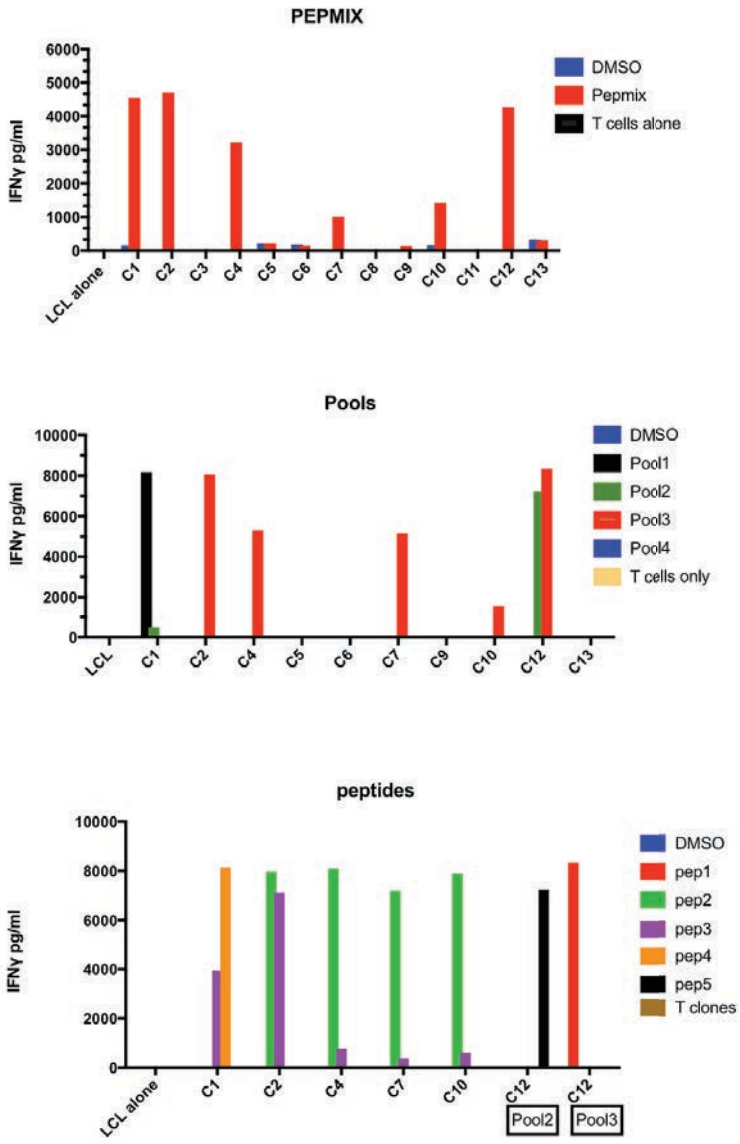

Figure 14 T cell specificity:

First, 13 expanded cultures were tested to know their specificity towards BARF1 peptide. Expanded T cells were cultured with autologous LCL cells pre-exposed to BARF1 pepmix or DMSO. The next day IFNγ was measured by ELISA assay(A) . To identify specific peptides generating each response, autologous LCL was exposed to four pools each containing 5 peptides per pool. These LCL cells were cultured with each of the 7 expanded T cells and INfg release detected (b) . After that, to detect specific individual epitope peptides T cell clones were exposed to autologous LCL exposed to each of the 5 individual peptides within the apporiate pool (c).

3.6.4.2 Avidity of T cell clone response:

As performed for clones from donor 1 (3.6.3.3), I performed a series of experiments to characterise the clones in more detail. I designed and had synthesised additional 20mer peptides to allow more precise identification of the relevant epitope peptide. These new peptides (called A1, A3, A3, A4, A5, A6, A7) are described in Table 11 Each clone was tested with individual peptides using peptide concentrations within the range 10^{-5} to 10^{-11} M and DMSO as a control. In this assay, the functional avidity is the peptide concentration that required to cause half (50%) maximal IFNg released by T cell activation. Results in Figure 15 show that the functional avidity of specific T cell clone1 to designed peptides A2 (GER) (41nM) was lower than the response to P4 (82nM) and A3 (357 nM). I therefore identified the epitope peptide for clone 1 as GER. As shown in Figure 15 the functional avidity of specific T cell clone 12 was 62nM with P4 (VTA), 887nM with P1 (NYL) and 268nM with A5 (ISH) . Moreover, the result in Figure 16 shows the high avidity of T cell clones (2,7 and 10) with P2 (TEV) (20 nM , 74nM and 34nM) compared to the avidity with A7 (QEH) peptide**.**

Table 11: optimal BARF1 peptides for T cell avidity.

clone		BARF1 peptide (P) and Designed peptide (A)	POSTION
CLONE 1	P2	LASCVAAGQAVTAFLGERVT	11-30aa
	A1	AAGQAVTAFLGERVTLTSYW	16-35aa
	P3	VTAFLGERVTLTSYWRRVSL	21-40aa
	A2	GERVTLTSYWRRVSLGPEIE	26-45aa
	P4	LTSYWRRVSLGPEIEVSWFK	31-50aa
	A3	RRVSLGPEIEVSWFKLGPGE	36-55aa
CLONE 2-7-10	P1	NYLCRMKLGETEVTKQEHLS	101-120aa
	A6	MKLGETEVTKQEHLSVVKPL	106-125aa
	P2	TEVTKQEHLSVVKPLTLSVH	111-130aa
	A7	QEHLSVVKPLTLSVHSERSQ	116-135aa
	P3	VVKPLTLSVHSERSQFPDFS	121-140aa
	A8	TLSVHSERSQFPDFSVLTVT	126-145aa
CLONE 12	Pool2 -P4	HRSANTFFLVVTAANISHDG	81-100aa
	A4	TFFLVVTAANISHDGNYLCR	86-105 aa
	Pool2 -P5	VTAANISHDGNYLCRMKLGE	19-110 aa
	A5	ISHDGNYLCRMKLGETEVTK	96-115 aa
	pool3 -P1	NYLCRMKLGETEVTKQEHLS	101-120 aa
	A6	MKLGETEVTKQEHLSVVKPL	106-125 aa

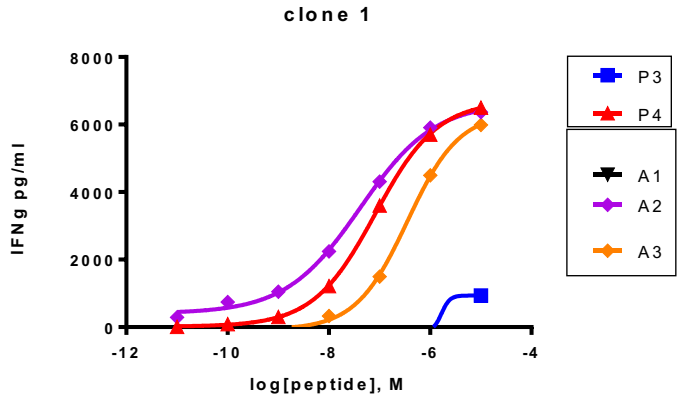

	P3	P4	A1	A2	A3
LogIC50	~ -5.776	-7.082		-7.382	-6.447

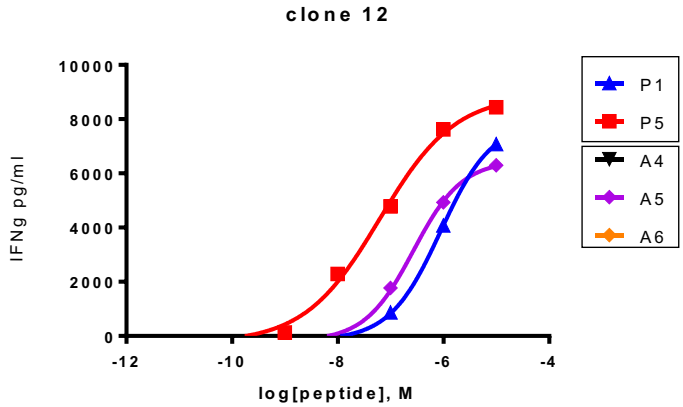

	P5	P1	A4	A5
LogIC50	-7.206	-6.052		-6.571

Figure 15 :T cell clone avidity

Each clone was tested with LCL exposed to individual peptides from the epitope regions, for clone (1) peptide 3 (21-40 aa) and Peptide 4 (31-50 aa) (20mers overlapping by 10 aa) were identified as optimal. Additional 20mer peptides A1 (16-35 aa), A2 (26-45 aa**)** and A3 (36-55 aa**),** were designed from peptide P3, P4 and their neighbour P2 and P5 from pool 1 of BARF1 gene to cover the entire region of BARF1 which may contain the epitope (all peptides now overlapping by 15aa rather than the original 10aa). For clone **12** two specific peptides from pool 2, peptide P5 (91-110 aa) and from pool3, peptide P1 (101-120 aa) were used to design three additional peptides: A4 (86-105 aa), A5 (96-115 aa) A6 (106-125 aa) so all peptides in this region now overlapped by 15aa. Each clone was tested with LCL and the relevant peptides at concentrations ranging 10^{-5} to 10^{-11} M, with DMSO alone used as a negative control. in this assay, the functional avidity is the peptide concentration that causes half maximal (50%) IFNg release by each clone.

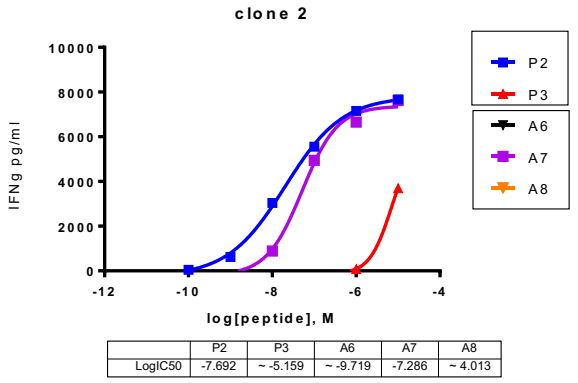

	P2	P3	A6	A7	A8
LogIC50	-7.692	~ -5.159	~ -9.719	-7.286	~ 4.013

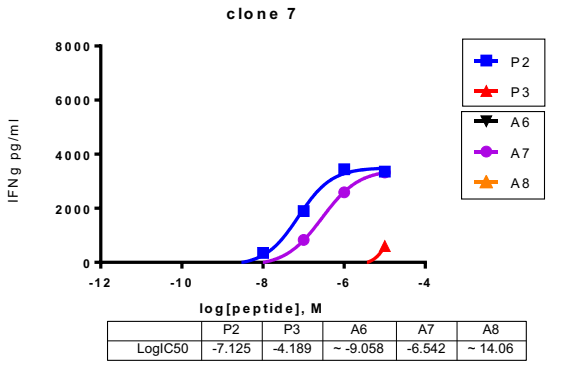

	P2	P3	A6	A7	A8
LogIC50	-7.125	-4.189	~ -9.058	-6.542	~ 14.06

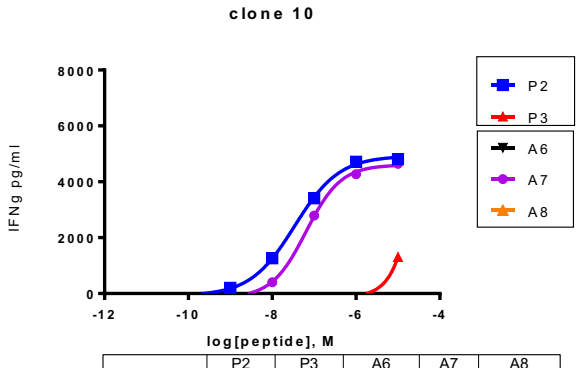

	P2	P3	A6	A7	A8
LogIC50	-7.462	-3.606	~ 14.32	-7.19	~ -42.78

Figure 16:T cell clone avidity

Each clone was tested with LCL exposed to individual peptides from the epitope regions, for clone 2,7 an10, peptide P2 (111-130 aa) and peptide P3 (121-140 aa) (20mers overlapping by 10 aa) were identified as optimal. Additional 20mer peptides A6 (106- 125 aa), A7 (116-135 aa) and A8 (126-145aa)**),** were designed from peptide P2 and P and their neighbours the BARF1 gene to cover the entire region of BARF1 which may contain the epitope (all peptides now overlapping by 15aa rather than the original 10aa). Each clone with LCL and the relevant peptides at concentrations ranging 10^{-5} to 10^{-11} M with DMSO as a negative control. in this assay, the functional avidity is the peptide concentration that causes half maximal (50%) IFNg release by each clone.

3.6.4.3 T cell clone HLA Restriction

To know the relevant HLA restriction allele for each T-cell clone, T-cells were first stained with CD4 and CD8 antibodies. Flow cytometry showed that all clones were CD4 positive (data not shown). To identify the class II HLA restriction of the T cell clones I designed a panel of LCL cells that include the autologous LCL and different cell lines which were partially HLA class II matched to the autologous donor as shown Table 12. These LCLs were exposed with each clones BARF1 epitope peptide then cultured with T cell clones overnight then IFN-g was tested by ELISA. Figure 17 shows the results of this series of experiments. I found that all clones responded to the autologous cell line (LCL2). Clone 1 responded to LCL4 (DR-53 matched to autologous) while clones 2, 4 and 7 responded to LCL 5 (DP-2 matched to autologous. Clone 12 responded to LCL6 (DR-13 matched to autologous). No clone responded to the LCL that was mismatched at all HLA class II alleles.

Table 12 : panel of LCL cell lines used for T cell restriction

	DR				DQ		DP	
LCL1	17			52a				
LCL2	4	13	53	52c	3	6	2	4
LCL3	4	7			2	4	4	
LCL4	9	15	51	53	6	9		
LCL5	103	11		52b	4	7	2	4
LCL6	13	15	51	52C	6			

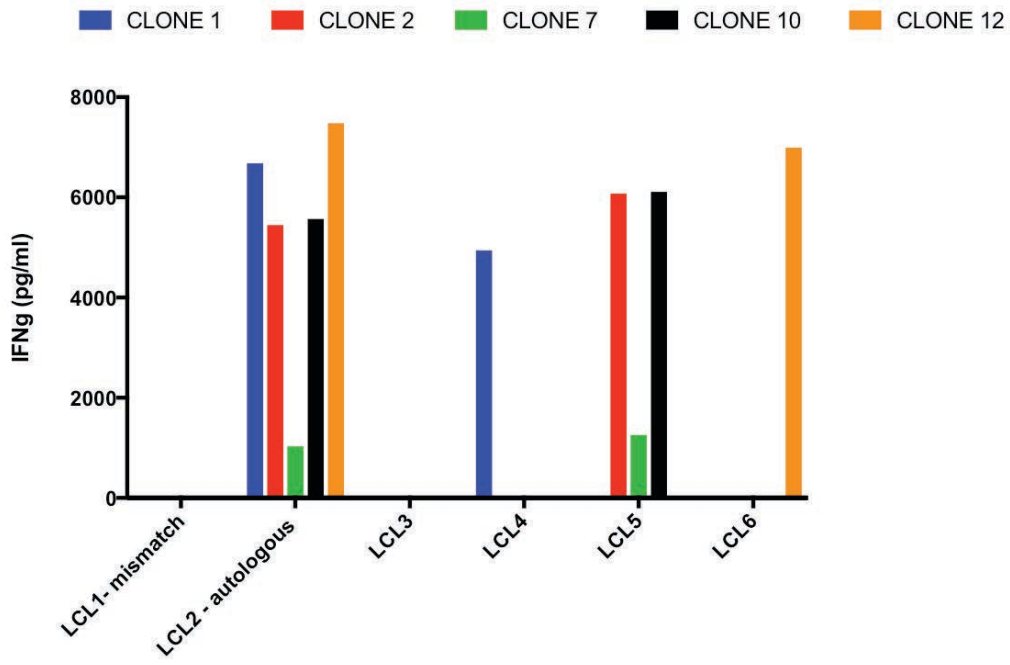

Figure 17:T cell clone HLA Restriction

A panel of LCL cells that include the autologous LCL (LCL2) a mismatch (LCL1) and different cell lines overnight partially class II matched to the autologous donor were exposed to relevant BARF1 epitope peptides. The various LCLs were then cultured with T cell clones (1, 2, 7,10 and 12) then tested for IFN-g release by ELISA. All T cell clones responded (IFNg released) to autologous LCL. Clone 1 responded to LCL4 (DR-53 matched) while clones 2, 4 and 7 responded to LCL 5 (DP-2 matched) and clone 12 responded to LCL6 (DR-13 matched).

3.6.5 Donor 3: Characterization of four novel BARF1-specific CD4 T-cell clones: DRB1*0301

3.6.5.1 T cell specificity

I sorted BARF1-specific T-cells from donor 3 into 390 wells of a 96 well plate as described earlier. Five growing T cell cultures were obtained after two weeks of expansion. These were tested as described earlier to identify their specificity towards BARF1 pepmix. T cells were cultured with autologous LCL pre-exposed to BARF1 pepmix or DMSO and IFNγ released by T-cells detected by ELISA. As shown in Figure 18**a**, 4 T cell cultures produced IFNγ in specific response to BARF1 -exposed LCL while there were no responses with remaining cells cultures because they were not specific to BARF1 pepmix or exhausted T-cells. To identify specific peptides, autologous LCL was exposed to four pools of BARF1 peptides each pool containing 5 peptides. LCL cells were then cultured with each of the 4 expanded T cell clones and IFN-g release detected by ELISA. The result shows that T cell clones 1, 2, 3, and 5) responded to pool 4 as shown in Figure 18b. To detect specific individual epitope peptides these four were then tested with autologous LCL exposed to each of the 5 individual peptides in pool 4. As shown in Figure 18 **c,** all clones (1 ,2, 3 and 5) responded to peptide 4 (pool 1).

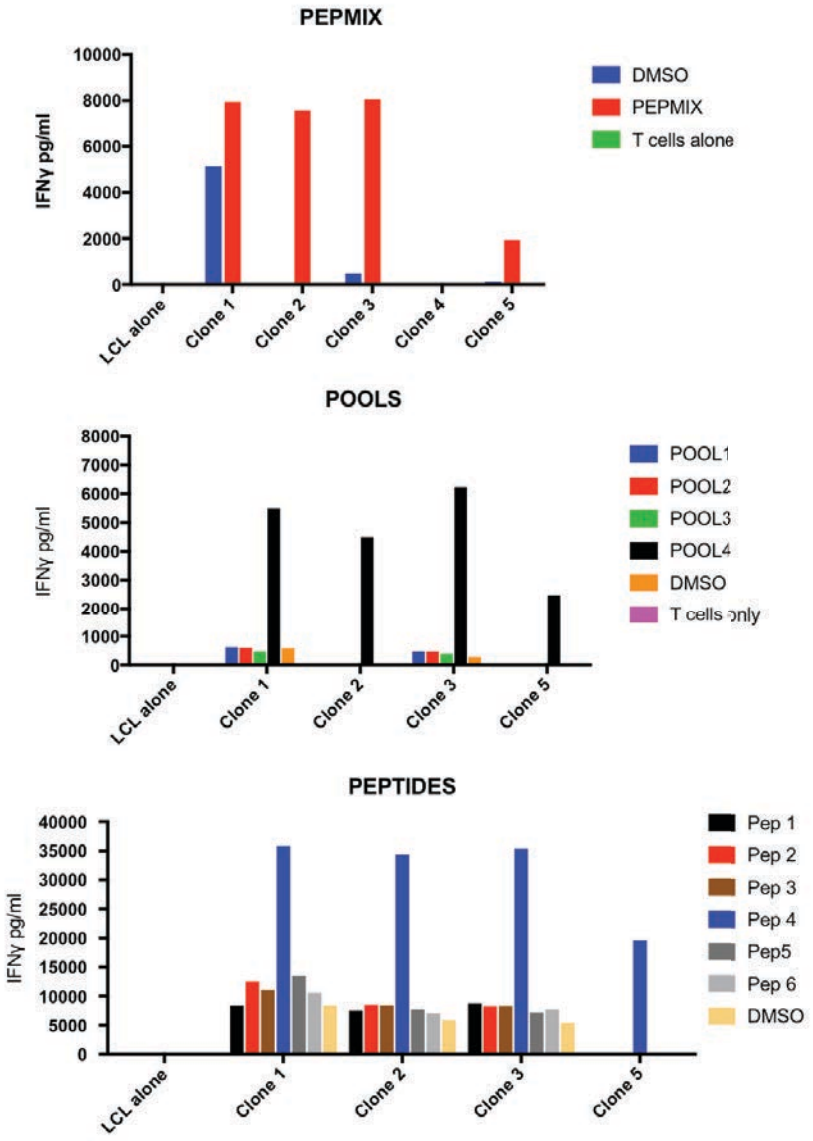

Figure 18: T cell specificity:

All five of the growing T-cell cultures were tested to know their specificity towards BARF1 peptide. Expanded T cells were cultured with LCL pre-exposed to BARF1 pepmix or DMSO then IFNγ was detected by ELISA assay(A). To identify specific peptides responsible for the response, autologous LCL was exposed to four pools each containing 5 peptides from BARF1. LCL cells were cultured with the 5 clones and INfg release detected (b) . To detect specific individual epitope peptides, T cell clones were cultured with LCL exposed to each of the peptides within pool4 or DMSO as a negative control.

3.6.5.2 Avidity of T cell clone response:

The peptides in pool 4 were 20mers overlapping by 15aa. To identify each clones optimal peptide I first designed and synthesized additional peptides so that the peptides in this region of BARF1 overlapped by 15a. These peptides were used in titration assays as previously described. The results show that no clones responded to peptide B2 but all T cell clones responded to peptides P4 and B1. as shown in Figure 19 comparing these two peptides, in three cases the T-cell clones responded better to peptide P4 compared to B1. Clone 1 (15nM P4, 44nM G1), clone 3 (9.5 nM P4, 41 nM B1, clone 2 (106 nM P4, 113nM G1.. Clone 5 was the highest affinity clone and its response to the two peptides was essentially the same (1.8uM P4, 1.4uM G1). Together these resuls indicate that P4 (GSL) represented the optimal epitope peptide.

3.6.5.3 T cell clone HLA Restriction

Flow cytometry of T cell clone cells stained with CD4 and CD8 antibodies determined that all clones were CD4 positive (data not shown). To identify the class II HLA restriction of the T cell clones, I designed a panel of LCL cells that included the autologous LCL and different LCLs partially class II allele matched to the autologous donor as shown Table 13. The LCLs were exposed to the BARF1 GSL peptide, cultured with T cell clones overnight and the supernatant tested by IFN-g ELISA assay. As shown in Figure 20 all clones responded to the autologous LCL (LCL) and LCL 2 (DR-17 and DR52a matched) but not LCL3 (DR52a matched). This result indicates that the GSL epitope is presented to CD4 T-cells by DR-17.

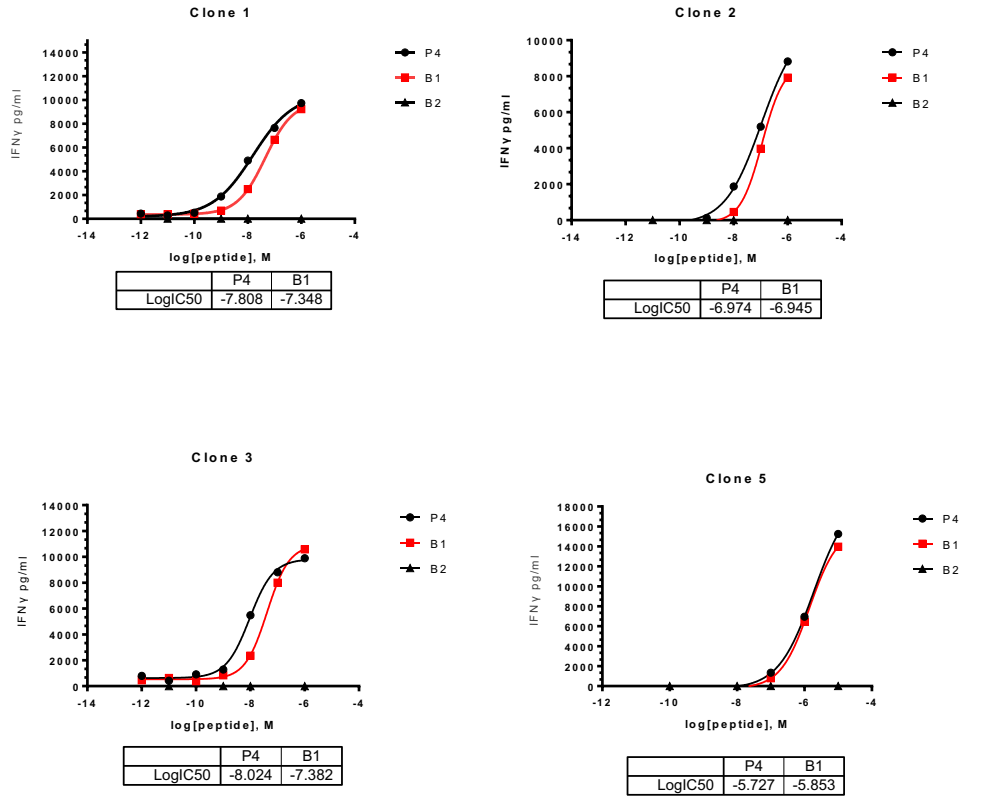

	P4	B1
LogIC50	-7.808	-7.348

	P4	B1
LogIC50	-6.974	-6.945

	P4	B1
LogIC50	-8.024	-7.382

	P4	B1
LogIC50	-5.727	-5.853

P3	ANGGVMKEKDGSLSVAVDLS	171-190aa
B1	MKEKDGSLSVAVDLSLPKPW	176-195aa
P4	GSLSVAVDLSLPKPWHLPVT	181-200aa
B2	AVDLSLPKPWHLPVTCVGKN	186-105aa

Figure 19 :T cell clone avidity (donor 3):

Each clone was tested with LCL exposed to individual peptides from the epitope regions, for clone 1,2 and 5, peptide P4 (181-200 aa (20mers overlapping by 10 aa) were identified as optimal. Additional 20mer peptides B1 (176-195 aa), peptide B2 (186-105 aa), were designed from peptide P3, P4 and their neighbours the BARF1 gene to cover the entire region of BARF1 which may contain the epitope (all peptides now overlapping by 15aa rather than the original 10aa). Each clone with LCL and the relevant peptides at concentrations ranging 10^{-5} to 10^{-11} M with DMSO as a negative control. in this assay, the functional avidity is the peptide concentration that causes half maximal (50%) IFNg release by each clone.

Table 13 : Panel of LCL cell lines for T cell restriction

	DR				DQ	
LCL1 AUTO	17	15	51	52a	2	6
LCL2	17			52a		
LCL3	13			52a	2	6
LCL4	4	16	51	53	5	8
LCL5	4	7	53		2	4
LCL8	4	15	51	53		

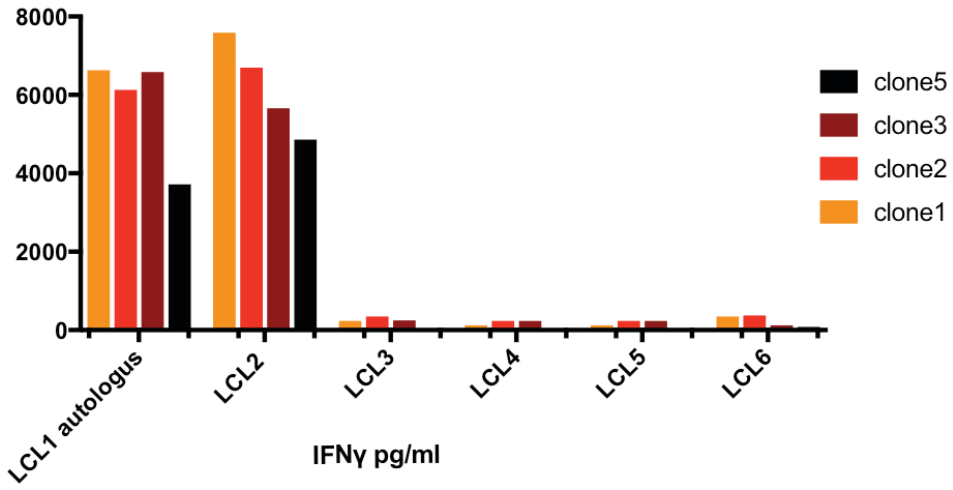

Figure 20 :T cell clone HLA Restriction

A panel of LCL cells that included the autologous LCL and different lines which were partially class II allele matched to the autologous line were exposed to the GSL epitope peptide. The LCLs were then cultured with T cell clones (1, 2, 3 and 5) overnight and the supernatants tested by ELISA. All T cell clones responded to autologous LCL and LCL 2 (DR-17 DR52a matched) but not LCL3 (DR52a matched).

3.6.6 Donor 4: Characterization of four novel BARF1-specific CD4 T-cell clones: HLA-DRB1*0103

3.6.6.1 T cell specificity

Following FACS based cloning, sixteen expanding T cell microcultures were generated. These were tested for BARF1 specificity by culturing them overnight with autologous LCL cells exposed to BARF1 pepmix or DMSO. The following day, IFNγ in the supernatant was measured by ELISA. As shown in Figure 21a, eight of the growing T cell microcultures produced IFNγ in response to BARF1. To identify the relevant epitope peptides, autologous LCL was exposed to four pools of BARF1 peptides each containing 5 peptides per pool then cultured with each of the eight T cells microcultures. INfg release was detected by ELISA. As shown in Figure 21b the result shows that T cell clones (C1, 2, 6 and 8) responded to pool 3. To detect specific individual epitope peptides these T cell clones were cultured with autologous LCL exposed to each of the five individual peptides from the pool. As shown Figure 21c, T cell clones (1, 2, 6 and 8) responded to peptide 2.

3.6.6.2 Avidity of T cell clone response:

Because the 20mer peptides used in pools and individual to identify peptide 2 overlapped each other by 10aa, I designed and had synthesised additional peptides to provide a set of 20mer peptides spanning the region of interest and overlapping by 15aa. These peptides were used in a titration assay to identify the optimal epitope peptide that the clones recognized (Figure 22). The result shows that all T cell clones responded to peptides P2 and A7 , low avidity was found with clones ; clone 1 (722nM and 4.8uM) clone 2 (970nM and 348nM) , clone 6 (443nM) and clone 8 (2m4nM and 122nM) as shown P2 (TEV) epitope compare to B7(QEH) epitope .

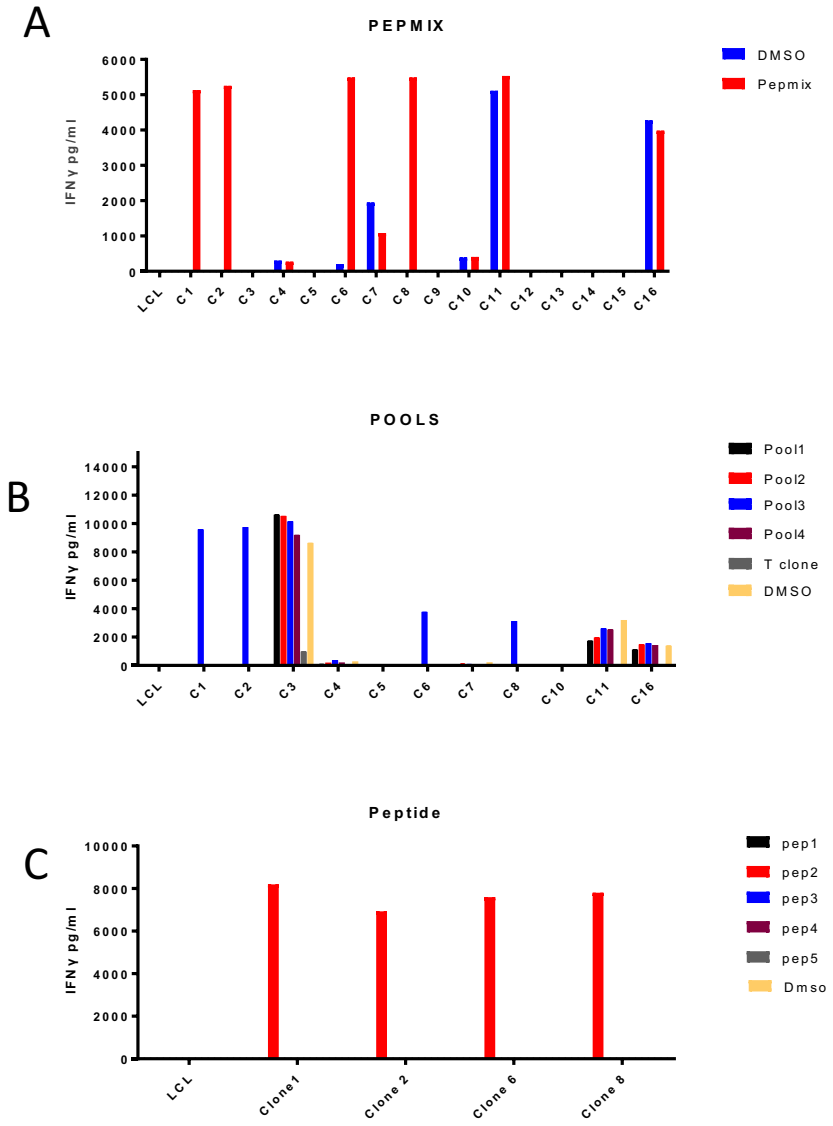

Figure 21: T cell specificity:

sixteen growing T-cell cultures were tested to know their specificity towards BARF1 pepmix. Expanded T cells were cultured with autologous LCL cells exposed to BARF1 pepmix or DMSO and the following day IFNγ was measured by ELISA assay(A). To identify the region of BARF1 recognised by the T-cells, autologous LCL was exposed to four pools containing 5 BARF1 peptides per pool and used to stimulate each T-cell clone that had responded to pepmix in the earlier experiment (b). After that (c), to detect specific individual epitope peptides T cell clones that responded to the pools were co-cultured with autologous LCL exposed to each of the 5 individual peptides from the relevant pools. IFN-g release was measured by ELISA.

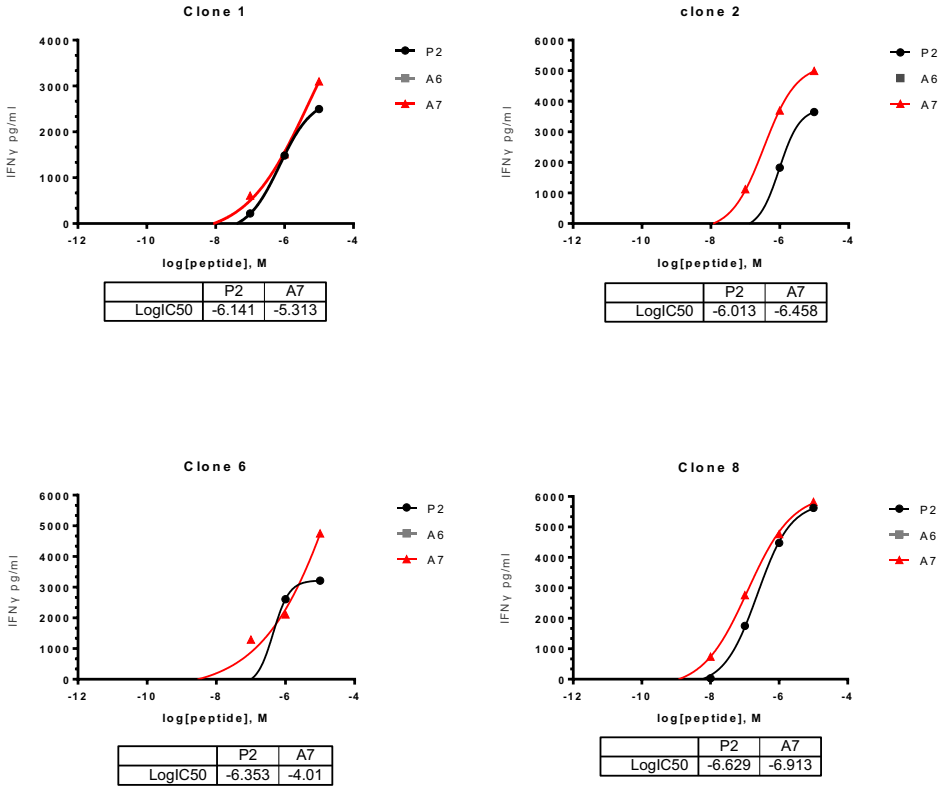

	P2	A7
LogIC50	-6.141	-5.313

	P2	A7
LogIC50	-6.013	-6.458

	P2	A7
LogIC50	-6.353	-4.01

	P2	A7
LogIC50	-6.629	-6.913

P3	NYLCRMKLGETEVTKQEHLS	101-120aa
A6	MKLGETEVTKQEHLSVVKPL	106-125aa
P2	TEVTKQEHLSVVKPLTLSVH	111-130aa
A7	QEHLSVVKPLTLSVHSERSQ	116-135aa

Figure 22: T cell clone avidity (Donor 4) :

Each clone was tested with LCL exposed to individual peptides from the epitope regions, for clone 1,2 an5, peptide P2 (111-130 aa) (20mers overlapping by 10 aa) were identified as optimal. Additional 20mer peptides peptide A6 (106-125 aa), peptide A7 (116-135 aa**),** were designed from peptide P1, P2 and their neighbours the BARF1 gene to cover the entire region of BARF1 which may contain the epitope (all peptides now overlapping by 15aa rather than the original 10aa). Each clone with LCL and the relevant peptides at concentrations ranging 10^{-5} to 10^{-11} M with DMSO as a negative control. in this assay, the functional avidity is the peptide concentration that causes half maximal (50%) IFNg release by each clone.

3.6.6.3 T cell clone HLA Restriction

To know the relevant HLA restriction allele for each T-cell clone, T-cells were first stained with CD4 and CD8 antibodies. Flow cytometry showed that all clones were CD4 positive (data not shown). To identify the HLA restriction of the T cell clones, I used a panel of LCL cells that include the autologous LCL and different cell lines partially class II matched to the autologous donor as shown Table 14 . These LCLs were exposed to the BARF1 epitope peptide then cultured with the T cell clones overnight; the next day IFN-g in the supernatant was measured by ELISA. Figure 23 shows all clones responded to the autologous LCL (LCL1) and LCL 4 (DR-103 matched) demonstrating that this epitope was a DR-103 restricted CD4 T cell response. The T-cell clones could not be

3.6.7 Donor 5: Characterization of novel BARF1-specific and CD4 T-cell clones:

3.6.7.1 T cells specificity

Following FACS cloning, twenty growing T-cell microcultures were obtained. These were tested for specificity by culturing them overnight with autologous LCL pre-exposed to BARF1 pepmix or DMSO. The following day, IFNγ release by the T-cells was measured by ELISA. As show in Figure 24 a, 16 T-cell microcultures produced IFNγ in response to BARF1 pepmix. To identify the specific peptides reasonable, autologous LCL was exposed to four pools of peptides each containing 5 BARF1 peptides per pool. The LCL cells were cultured with each of the 16 T cell clones and INfg in the supernatant measured the following day. The result shows that T cell clone (C1, 2, 4 ,6,7,8,10,11,12,13,14,16 , 17 and 20) responded to pool 3 as shown in Figure 24b. To determine which of the five peptide in pool 3 was recognised by the T-cells,

I then exposed autologous LCL to each peptide from pool 3 individually then co-cultured these with each of the clones, testing IFN-g release the following day. As shown IN Figure 24**c**, T cell clones (2, 4, 6 and 10, 11, 13, 16, 17, 19, and 20) responded to peptide 5 from pool 3. This peptide is a new BARF1 epitope peptide. These T cell clones were not studied further and additional experiments would be needed to identify the optimal epitope peptide and HLA restriction.

Table 14 : Panel of LCL cell lines for T cell restriction

	DR				DQ	
LCL1	103	15	51		6	7
LCL2	17			52a		
LCL3	4	15	51	53		
LCL4	103	7	53		2	7
LCL5	12	16	51	52a	5	7
LCL6	13	17		52a	2	6
LCL7	4	16	51	53	5	8

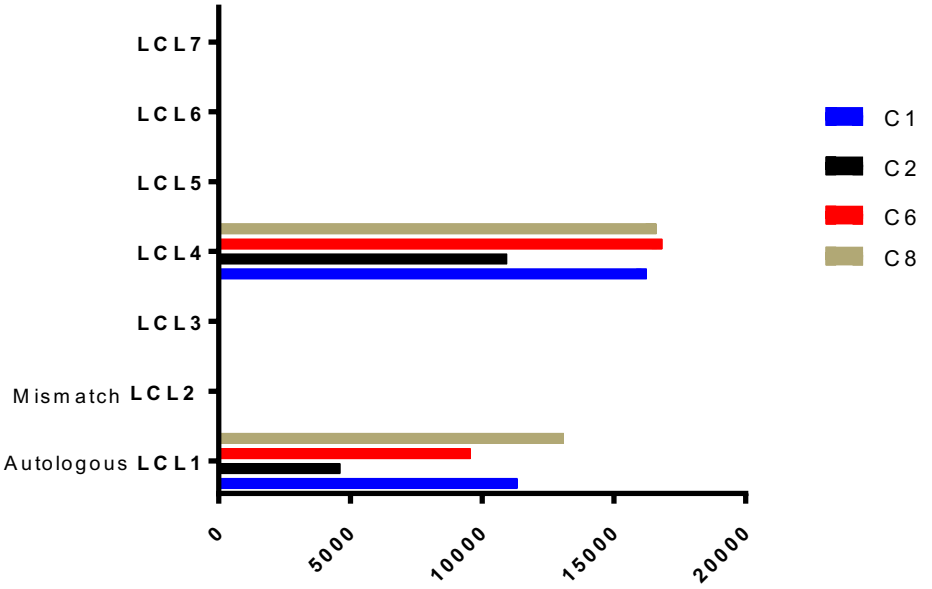

Figure 23 : T cell clone HLA restriction

A panel of LCL cells that include the autologous LCL and different partially class II matched LCLs were exposed to BARF1 epitope peptide then cultured with T cell clones (1, 2,6 and 8). IFN-g release by T-cells was determined by ELISA. All T cell clones responded to LCL1, the autologous LCL, and LCL4 (DR-103 matched) but not to the other LCLs. . All four clones (1, 2,6 and 8) are therefore restricted by DR103.

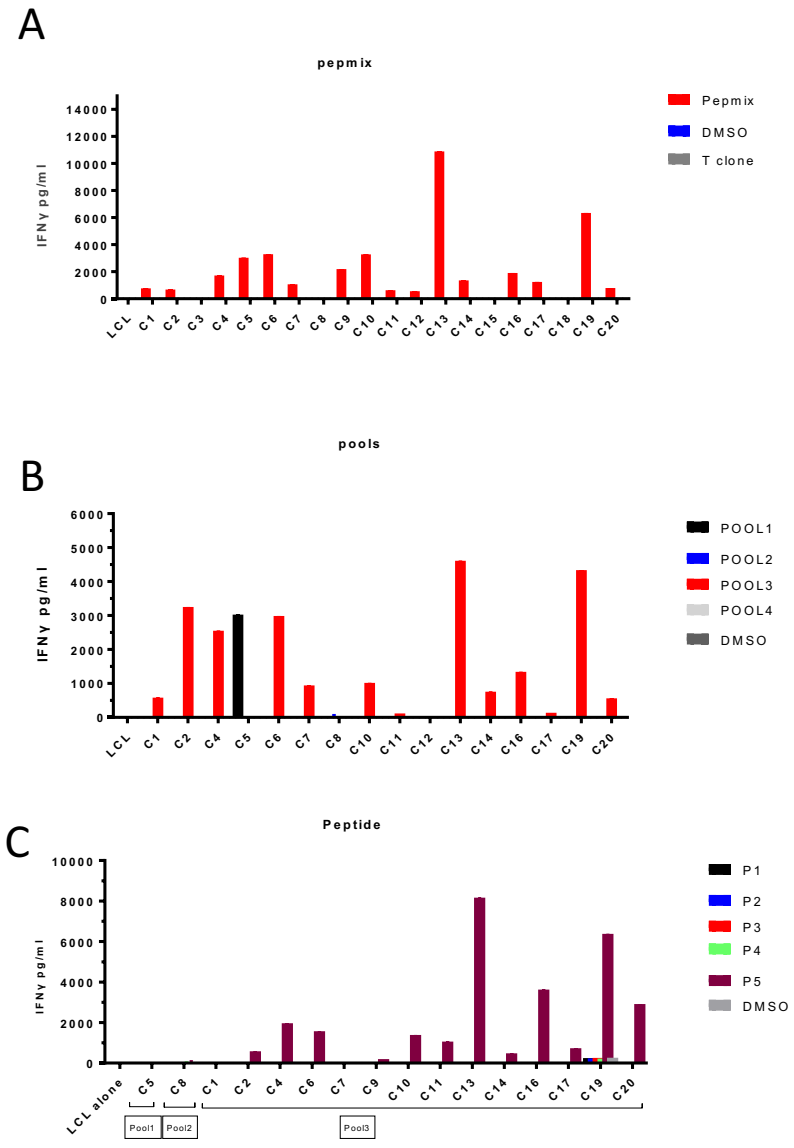

Figure 24 : T cell specificity

Twenty T cell microcultures generated from from donor 5 were tested to know their specificity towards BARF1 epitope peptide. T cells were cultured with autologous LCL pre-exposed to BARF1 pepmix or DMSO as a negative control. The next day, IFNγ release by T-cells was measured by ELISA (A). To identify the specific peptide reasonable for the response, autologous LCL was exposed to four pools of peptide each containing 5 peptides per pool (b) and IFN-g release by T-cells measured the next day. To detect the individual peptide from the pool, the autologous LCL was exposed to the individual epitope peptides, washed and used to stimulate T-cells. IFN-g release by T-cells was measured the following day by ELISA (c).

3.7 BARF1 (TFF) – specific T-cell clone responses to naturally expressed and presented target epitope

In the above experiments, I found that some BARF1-specific T cell clones made IFN-g when cultured with the autologous unmanipulated (i.e. not exposed to synthetic peptide) LCL but not to HLA-mismatched LCL. Examples can be seen for clones in Figures (Figure 12). Closer examination of this phenomenon for clones established from donor 1, testing LCLs by qPCR, suggested that BARF1 and BZLF1 genes were expressed by the LCLs recognised by the T-cells. Such data suggested that T-cells may be able to recognise biological levels of BARF1 proteins and I investigated this further using two different types of target cell. First, I used HLA-matched LCLs from three donors. The LCLs were established using either the B95.8 virus or, for comparison, an engineered B95.8 virus that lacked the BZLF1 gene (BZLF1 K/O) essential for EBV entry into lytic cycle. Therefore, I could study whether BARF1 recognition required a proportion of the LCLs within the culture to enter lytic cycle, or whether cells that were entirely latent could be recognised. Second, I also tested the EBV positive NPC cell line C666, which I made HLA matched to BARF1-specific DR51-restricted T-cell clones from donor 1 by transducing HLA-DR51 (data not shown). The aim was to investigate if an EBV+ve epithelial tumour cell line could potentially be recognised by BARF1-specific CD4 T-cells.

HLA -matched cell lines (LCL and c666) were exposed to the BARF1 TFF epitope peptide or an equivalent amount of the DMSO solvent used to dissolve the peptide, washed well and then incubated with three T cell clones (C4, C5, C6) from donor 1 that were all specific to the TFF epitope. The T-cell responses to the target cells were measured after overnight culture using IFNg ELISA. The results shown in Figure 25

suggested that the T cell clones recognized naturally expressed BARF1 in C666 and LCL cells (cells treated with DMSO solvent only).

Recognition of LCLs treated only with DMSO was consistently highest for clone 6, the most avid of the three clones in peptide titration assays). This clone also produced IFN-g when exposed to LCLs that lacked the BZLF1 gene, although this was always lower than the corresponding B95.8 LCL in which a proportion of cells were in lytic cycle. This result suggests that BARF1 may be expressed at low level in latent cycle in LCLs. Interestingly, clone 6 also recognised DR51 transduced C666 cells that were treated only with DMSO. Importantly, no IFN-g was produced by any of the clones incubated with the HLA-mismatched control LCL (data not shown) or the C666 cell line that had not been transduced with DR51 (referred to as mismatch in Figure 25) that were included as controls in the experiment.

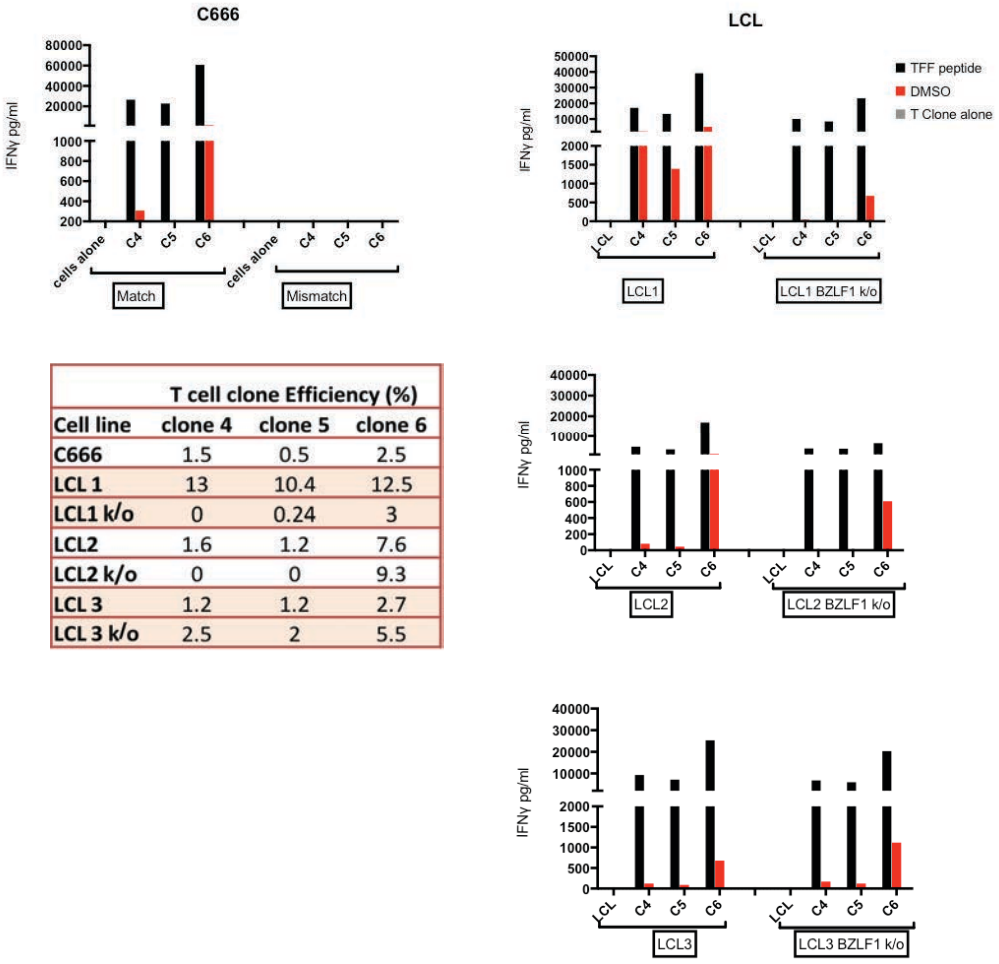

	T cell clone Efficiency (%)		
Cell line	**clone 4**	**clone 5**	**clone 6**
C666	1.5	0.5	2.5
LCL 1	13	10.4	12.5
LCL1 k/o	0	0.24	3
LCL2	1.6	1.2	7.6
LCL2 k/o	0	0	9.3
LCL 3	1.2	1.2	2.7
LCL 3 k/o	2.5	2	5.5

Figure 25 BARF1 (TFF) – specific T-cell clone responses to LCL and C666 cells loaded with epitope peptide or DMSO solvent alone. Target cells were LCLs from three donors, transformed with B95.8 EBV or the same virus lacking BZLF1 (BZLF1 k/o) or C666 cells either transduced with HLA-DR51 (match) or untransduced (mismatch). Target cells were either loaded with epitope peptide or the same amount of DMSO solvent, washed and used as targets for three different T-cell clones from donor 1 specific for the BARF1 epitope TFF. After incubation overnight, the amount of IFN-g produced by T-cells was measured by ELISA. Percentage efficiency of recognition was calculated by dividing the amount of IFN-g produced by cells treated with DMSO by the amount of IFN-g produced by the dame cells loaded with epitope peptide then multiplying by 100. A representative result from three independent experiments is shown.

3.8 Identification of BARF1 Antigen Transfer with epithelial and B cell lymphoma cells

BARF1 is a secreted protein that can be detected in culture media and in sera from NPC patients [150]. It is therefore possible that recognition of cells by BARF1-specific T-cells may be due to the uptake of BARF1 from the surrounding media. An alternative endogenous route may also be possible, since secreted proteins such as the CMV gb protein have been reported to access the HLA class processing pathway during secretion [151]. Either pathway could be therapeutically relevant for CD4 control of EBV-infected cells within a tumour. Endogenous access would mean that it is the BARF1-expressing cells themselves that are directly targeted by CD4 T-cells. Exogenous access would mean that a small number of cells in lytic cycle producing and secreting BARF1 would sensitise neighbouring cells, of which many would be in latent cycle or indeed EBV negative cells in the vicinity, for T-cell attack.

I investigated if BARF1 was present in the cell supernatant and could be taken up by cells and presented to T-cell clones. To produce a source of antigen, I cultured a range of EBV+ve and EBV-ve cells in serum-free AIM-V medium for three days then collected and concentrated the supernatant. Concentrated supernatants (S/N) were obtained from EBV+ve cells (B95.8 LCLs, BZLF1 k/o LCLs cells, C666 NPC epithelial cells) and as a control an EBV negative cell line (NP460 an epithelial line). Three different groups of cells, DR51-positive therefore HLA matched to the DR51 restricted T-cell clones, were exposed to the concentrated supernatants for 24-48 hours and then tested with T-cells. The first group consisted of epithelial cells lines including two EBV+ve epithelial tumour cell lines (c666 – an NPC cell line and YCCEL – a gastric carcinoma cell line) and two EBV-ve epithelial tumour cell clines (MKN1 and MKN28, both gastric carcinoma). Although genetically these lines were DR51

positive, it was important to confirm that they expressed functional HLA class II molecules and these were displayed on the cell surface for recognition by T-cells. Previous work in the laboratory had showed that the DR51 transduced C666 was indeed HLA positive, both using T-cell clones (see Figure 25) and by flow cytometry (data not shown). To check the gastric lines, cells were treated with a range of IFNg concentration (0-500 ug/ml) for 3 days then surface stained with MHC class II –PE antibody and analysed by flow cytometry. As shown in Figure 26 MNK1 and YCCL1 were strongly HLA class II positive, even in the absence of IFN-g treatment, and this level of expression did not increase with IFN-g. Interestingly, the MNK28 cell line consisted of cells with a wide range of different HLA class II levels, with some cells appearing to lack HLA class II whereas other cells were strongly HLA-class II positive. Again, IFN-g treatment did not alter MHC-II expression. The three gastric cell lines were transduced with the same DR51 expressing retrovirus vector used previously to make C666 HLA-matched to the DR51-restricted BARF1-specific T-cell clones. A stably transduced cell line was then established using G418 selection.

The second group of cells were five B cell lymphoma cell line. Two lines were EBV positive (SUDHL5++ and Kem) and three were EBV negative (HT, SUDHL4 and SUDHL5, the negative counterpart to SUDHL5++) Four of these five lines had previously been transduced with HLA-DR51, I generated the DR51-positive variant of Kem for use in the transfer experiments as described above. Kem was an important cell lines as it has previously been shown to uptake EBNA3C from conditioned supernatant and present epitopes to EBNA3C-specific CD4 T-cell clones [152].

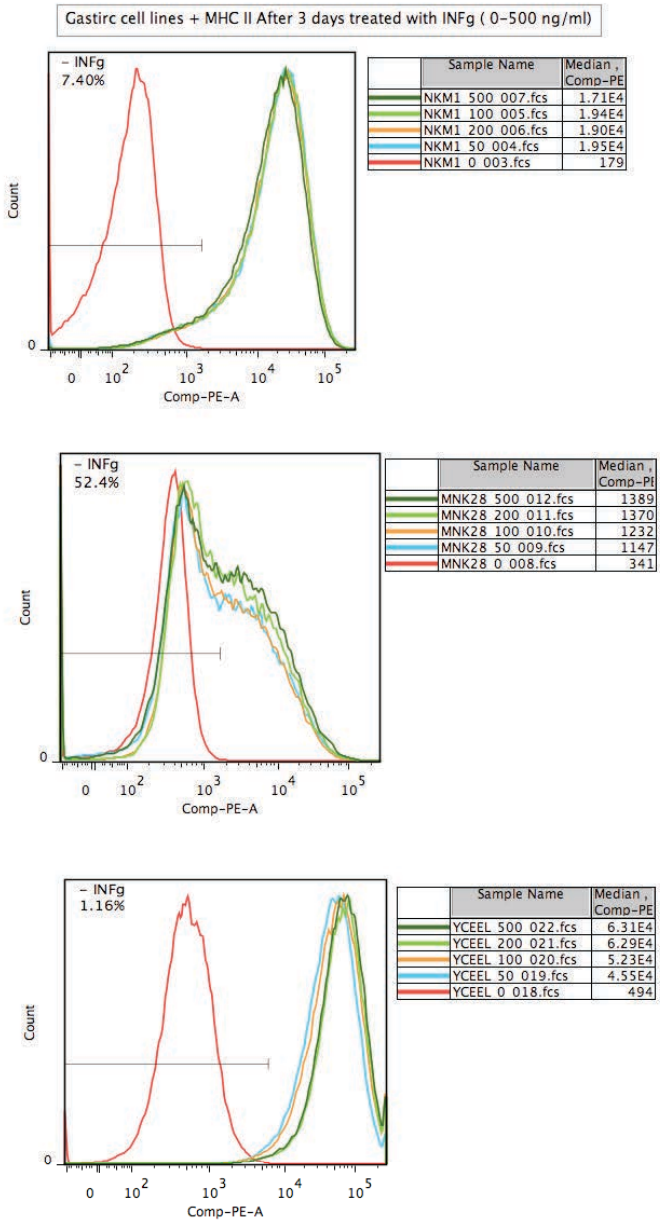

Figure 26 : Expression of MHC II in gastric cell lines

Gastric cell line were treated with a range of IFNg concentration (0-500 ug/ml) for 3 days then stained with MHC class II –PE antibody to determine the surface levels of these cells to MHC II and level of expression.

The third group of cells were HLA matched LCL cell lines which were used as controls for the assay. These cells were exposed to BARF1 TFF peptide or DMSO and included in the assay to confirm correct functioning of the T-cells.

Each experiment tested these different cell lines either unmanipulated or, for the negative control, the same cell type exposed to concentrated supernatant prepared from the EBV-ve NP460 cell line. The latter was used as the baseline for each assay. Cells were also exposed to concentrated supernatant prepared from the EBV+ve B95.8 LCL or the EBV+ve C666 cell line. After 36 hours, the cells were washed and incubated overnight with T-cells to detect if exposure to concentrated supernatant resulted in an increase in the level of cell surface BARF1 epitope peptides. I used T-cell clone 6 from donor 2 as this was the highest avidity clone specific for the DR51-restricted epitope TFF and, based on its ability to recognise EBV+ve BARFV1+ve LCLs, it appeared able to detect epitopes generated from BARF1 protein.

The results from exposing the four epithelial cell lines to different concentrated supernatants is shown in Figure 27a. As seen previously (figure 25) the T-cell clone produced IFN-g when co-cultured with DR51-transduced EBV and BARF1 positive C666 cells. As expected, incubating these cells with concentrated supernatant from EBV+ve NPC460 cells did not alter this recognition but recognition increased significantly after the C666 cells had been incubated with concentrated supernatant from the EBV+ve LCL or C666 cell lines. In contrast, the gastric carcinoma cells were not recognised and only a small increase observed for YCCEL cells treated with concentrated supernatant from the LCL (the same supernatant that yielded the largest increase when applied to C666 cells.

Figure 28a, shows the results obtained after exposing three different lymphoma cell lines to the same supernatants. Exposing these cells to concentrated supernatant from the LCL of C666 significantly increased T-cell recognition for 3/3 or 2/3 cell lines respectively. An experiment of the same design was performed using LCLs from two donors, transformed with either B95.8 or a BZLF1 ko EBV, either untreated or treated with the two different concentrated supernatants. The recognition of unmanipulated LCLs by the T-cell clone was higher in these experiments, making it harder to detect a supernatant-induced increase in recognition, but again the LCL supernatant significantly increased recognition of the four LCLs, with the C666 supernatant producing smaller increases that were significant for two of the four LCLs. cell lines

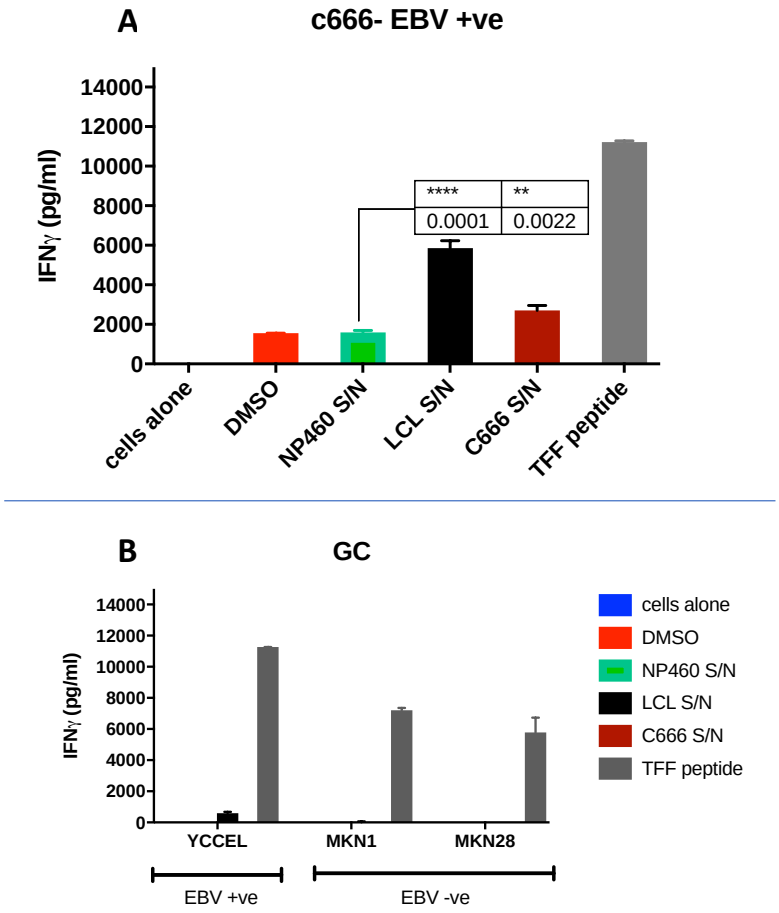

Figure 27 :BARF1 antigen transfer with epithelial cell line

Concentrated supernatant (S/N) prepared from cultured BZLF1 k/o LCL cells (EBV positive) , C666 ,NPC epithelial cells (EBV positive) and NP40 , NPC epithelial (EBV negative) were used to target transduced (DR-51) epithelial cells line include three Gastric cell lines YCCEL which known as EBV positive, MNK1 and MNK28 as EBV negative cell lines, and C666 cell lines EBV positive. After 24-48 hours incubation with , BARF1 (TFF) – specific T clone (clone 6) were added to all cell lines to recognize of expressed BARF1 epitope, the response was detected by ELISA IFNg assay. however, the mean value of recognition (IFNg released) was calculated by compare to mean of control which is NP460 s/n EBV –ve . Target cells were also exposed with TFF peptide or DMSO as controls.

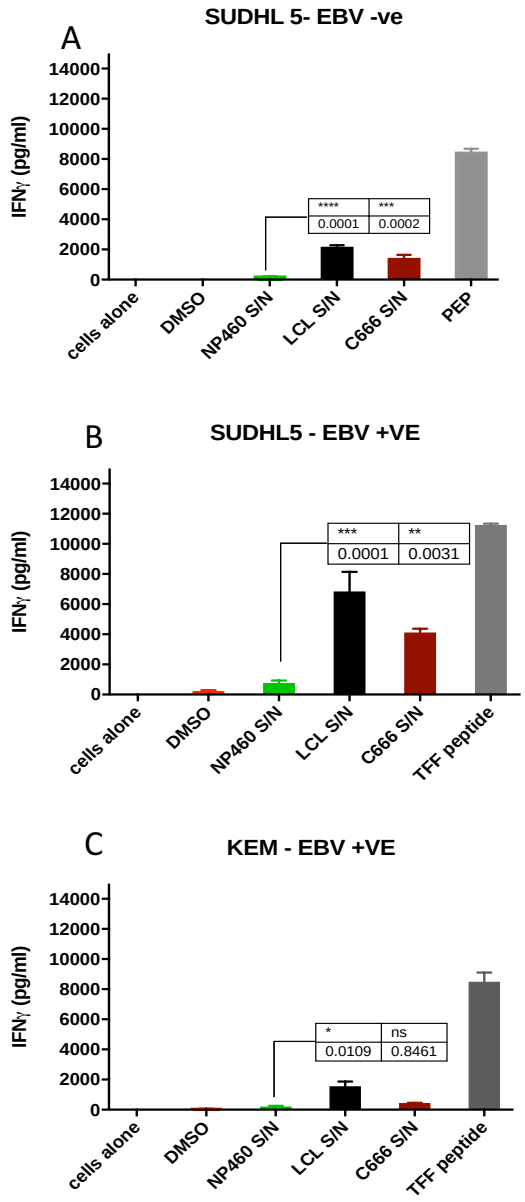

Figure 28 :BARF1 antigen transfer with B cell lymphoma lines

Concentrated supernatant (S/N)prepared from cultured BZLF1 k/o LCL cells (EBV positive) , C666 ,NPC epithelial cells (EBV positive) and NP40 , NPC epithelial (EBV negative) were used to target transduced (DR-51) B cell lymphoma cells line include Diffuse Large B Cell Lymphoma Cell Lines, SUDHL5, EBV negative and SUDHL5++ as EBV positive , And EBV positive transduced (DR-51) Burket lymphoma (Kem) . After 24-48 hours incubation with , BARF1 (TFF) – specific T clone (clone 6) were added to all cell lines to recognize of expressed BARF1 epitope, the response was detected by ELISA IFNg assay. however, the mean value of recognition (IFNg released) was calculated by compare to mean of control which is NP460 s/n EBV –ve . Target cells were also exposed with TFF peptide or DMSO as controls.

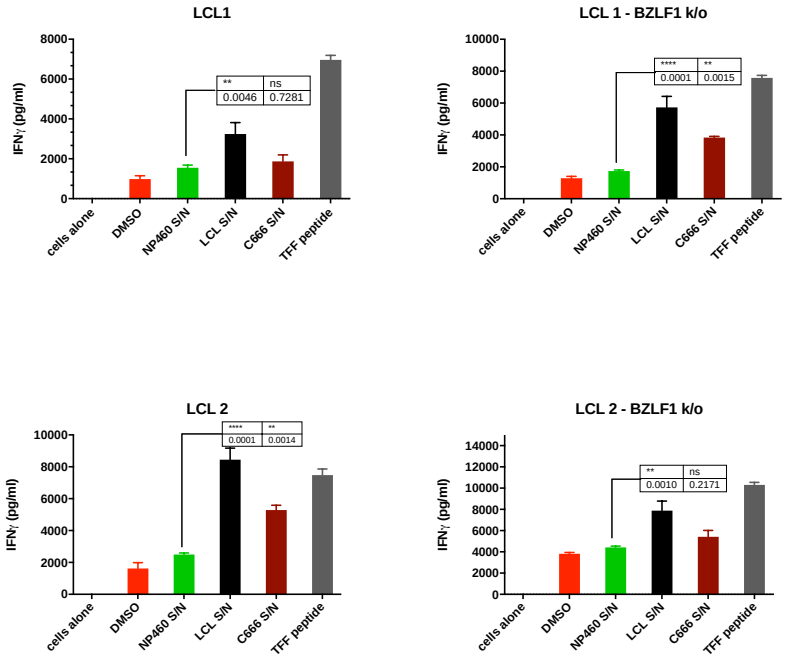

Figure 29: BARF1 antigen transfer with LCL cell line

Concentrated supernatant (S/N) prepared from cultured BZLF1 k/o LCL cells (EBV positive), C666, NPC epithelial cells (EBV positive) and NP40, NPC epithelial (EBV negative) were used to target two different LCL cell lines include BZLF1 k/o cells . After 24-48 hours' incubation with, BARF1 (TFF) – specific T clone (clone 6) were added to all cell lines to recognize of expressed BARF1 epitope, the response was detected by ELISA IFNg assay. however, the mean value of recognition (IFNg released) was calculated by compare to mean of control which is NP460 s/n EBV –ve . Target cells were also exposed with TFF peptide or DMSO as controls.

3.9 Study the recognition of endogenously expressed BARF1

To study whether endogenously expressed BARF1 could potentially be recognized by CD4 T-cells, I transfected YCCEL cells with pcDNA based expression plasmid containing the full length BARF1 gene (kindly provided by Dr. Jaimin Zuo, University of Birmingham). The cells were co-transfected with a GFP expressing plasmid to measure transfection efficiency. I selected YCCL1 cells for these experiments because its lack of detectable background recognition from the T-cell should make the assay more sensitive.

As show in Figure 30a YCCL1 cells clearly expressed GFP 48 hours after transfection. These cells were co-cultured with the BARF1 TFF epitope specific clone 6 overnight, then IFN-g in the supernatant was measured by ELISA. As shown in Figure 30b. there was no recognition of the transfected cells, although cells that were pulsed with peptide strongly stimulated the T-cells. To confirm BARF1 was expressed from the plasmid, I first sequenced the plasmid to confirm it was correct (data not shown). I then performed western blotting of cell extracts from the transfected cells using a BARF1 specific antibody (provided by Prof. Jaap Middeldorp, University of Amsterdam). Because BARF1 is rapidly secreted, complicating its detection. I incubated some of the transfected cell with brefeldin A to block secretion. The blot in in Figure 30b shows a band of the predicted size of BARF1 in the transfected cells which increased in intensity in the brefeldin A treated cells confirming BARF1 expression.

This result suggested that the lack of background recognition of YCCL1 by the T-cell clone may mean that the cell processes and presents the BARF1 epitope from protein

poorly. This hypothesis is supported by the low recognition achieved after exposing the cells to concentrated supernatants which dramatically enhance the recognition of other cell types. I therefore decided to test endogenous BARF1 expression in other cell types. There was insufficient BARF1 antibody available to biochemically confirm BARF1 expression in other experiments I used newly produced plasmids provided by my supervisor, Dr Graham Taylor (University of Birmingham). These new plasmids expressed full length BARF1 or derivatives of BARF1 lacking the secretory sequence or regions of BARF1 (BARF1 delta). These two BARF1 sequences were also fused to the first 80 amino acids of the invariant chain protein which redirects proteins into the endolysosomal system[153]. These constructs expressed BARF1 as an amino-terminal fusion to mClover3, a bright green fluorescent protein, allow BARF1 expression to be readily detected in cells. Also provided by my supervisor was a positive control plasmid, which expressed a short region of EBNA1 containing a DR51-restricted epitope (SNP) fused to the invariant chain targeting sequence and mClover3. This is the same restriction allele as seen by the BARF1 specific TFF clone 6, allowing the same panel of cells to be tested in T-cell assays using a well-characterized EBNA1-specific CD4 clone (Taylor et al. PNAS). Details of the constructs are provided in (table 5 method) .

I used BARF1-expressing plasmids to transfect different EBV-negative cells that were HLA DR51 positive and therefore matched to the TFF T-cell clones. The cells used included the GC cell line YCCEL, which was previously not recognized after transfection with pCDNA-BARF1, two other GC lines, MKN1 and MKN28, and the B cell line SUDHL-5.

GC cell lines were transfected with plasmid DNA using lipofectamine 2000 while B cell lines were transfected by electroporation. After 48 hours, transfected cells were tested by fluorescent microscopy and flow cytometry as shown in Figure 31 to detect mClover3 and confirm transfection. Cells transfected with the delta-BARF1 construct consistently had lower levels of fluorescence than other constructs, even compared with the full length BARF1 construct that was the same as the delta BARF1 construct apart from the additional secretory sequence present at the N-terminus of full-length BARF1.

Cells transfected with the different constructs were tested in T-cell assays using the BARF1-specific CD4 T-cell clone TFF and the EBNA1-specific CD4 T-cell clone SNP (both restricted by DR51). (GSL presented by DR17 and TFF presented by DR51) with the EBNA1-aspecific CD4 T-cell clone SNPc51 used to detect epitope presentation from the positive control plasmid. After overnight incubation, the supernatant was tested for interferon-gamma by ELISA. As shown in Figure 32, the results show that there was no recognition by the two BARF1 clones (specific for epitopes TFF and GSL) to the three transfected GC cell lines with BARF1 constructs even in present of Invariant chain (In) as we expected. In another hand, EBNA1 SNP – specific clone was responded to minimal EBNA1 construct which contain four overlap EBNA1 epitopes with chain (In) used as positive control.

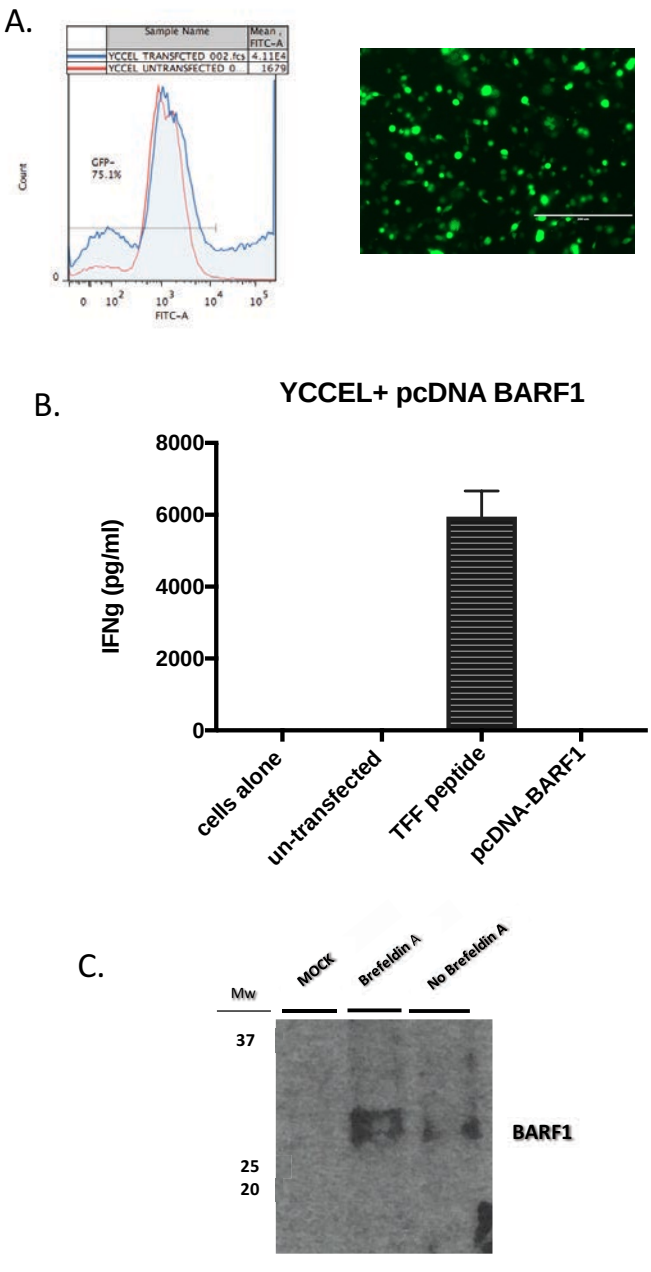

Figure 30 : expression of BARF1 epitope from transfected YCCEL and effect of Brefeldin A in BARF1 presentation

(a) YCEEL cells line was transfected with GFP-pcDNA plasmid (Full BARF gene). (b) cells were targeted by BARF1 TFF- CD4 T cell clone 6 to recognize response using IFNg ELISA . (c) transfected YCCEL with or without Brefeldin A were assayed using w.blot assay .

MKN28

A.

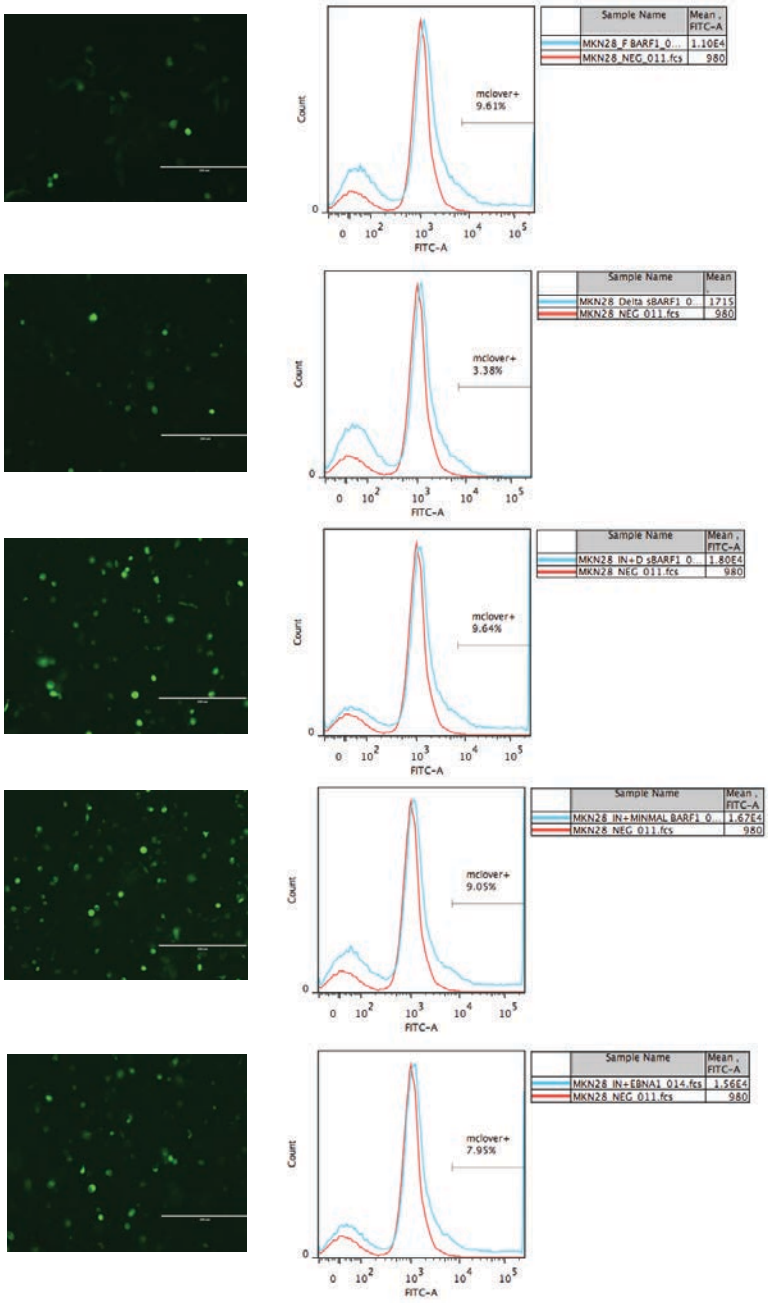
Sample Name
Mean , FITC-A
MKN28_F BARF1_0...
1.10E4
MKN28_NEG_011.fcs
980
mclover+
9.61%
Count
FITC-A
Sample Name
Mean
MKN28_Delta sBARF1_0...
1715
MKN28_NEG_011.fcs
980
mclover+
3.38%
Count
FITC-A
Sample Name
Mean , FITC-A
MKN28_IN+D sBARF1_0...
1.80E4
MKN28_NEG_011.fcs
980
mclover+
9.64%
Count
FITC-A
Sample Name
Mean , FITC-A
MKN28_IN+MINMAL BARF1_0...
1.67E4
MKN28_NEG_011.fcs
980
mclover+
9.05%
Count
FITC-A
Sample Name
Mean , FITC-A
MKN28_IN+EBNA1_014.fcs
1.56E4
MKN28_NEG_011.fcs
980
mclover+
7.95%
Count
FITC-A

MKN1

B.

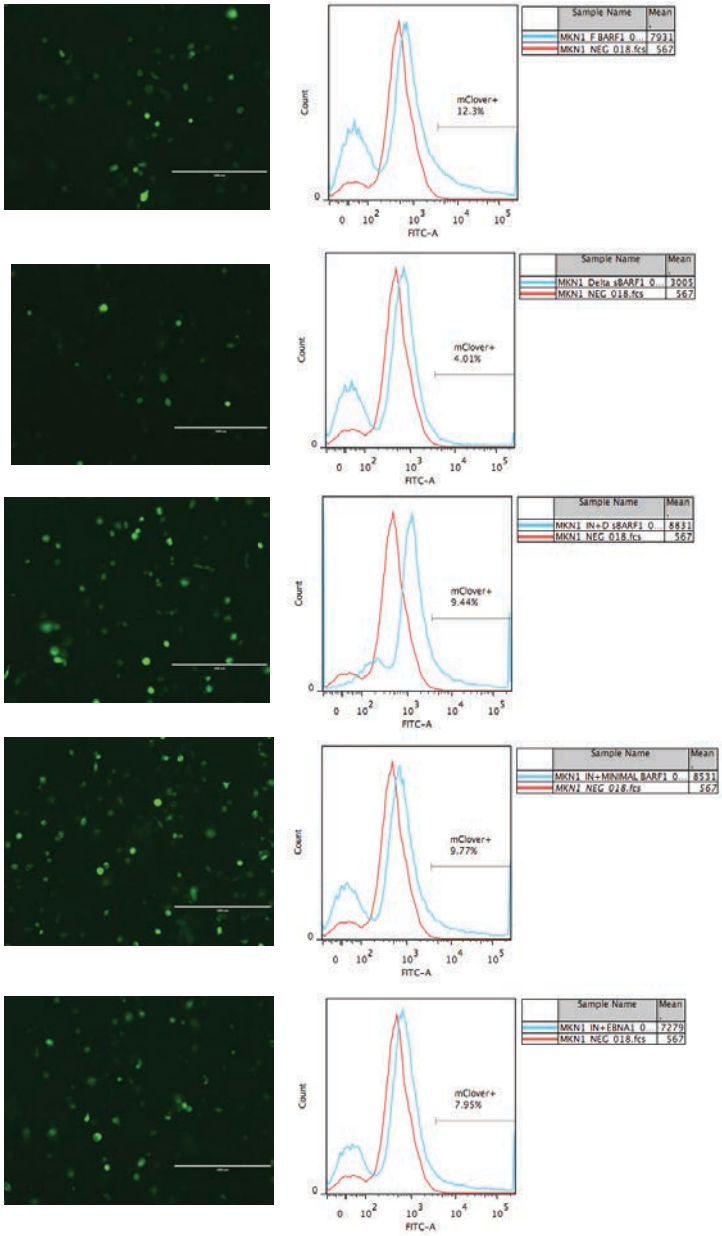
Sample Name
Mean
MKN1_F BARF1_0...
7931
MKN1_NEG_018.fcs
567
mClover+
12.3%
Count
FITC-A
MKN1_Delta sBARF1_0...
3005
MKN1_NEG_018.fcs
567
mClover+
4.01%
MKN1_IN+D sBARF1_0...
8831
MKN1_NEG_018.fcs
567
mClover+
9.44%
MKN1_IN+MINIMAL BARF1_0...
8531
MKN1_NEG_018.fcs
567
mClover+
9.77%
MKN1_IN+EBNA1_0...
7279
MKN1_NEG_018.fcs
567
mClover+
7.95%

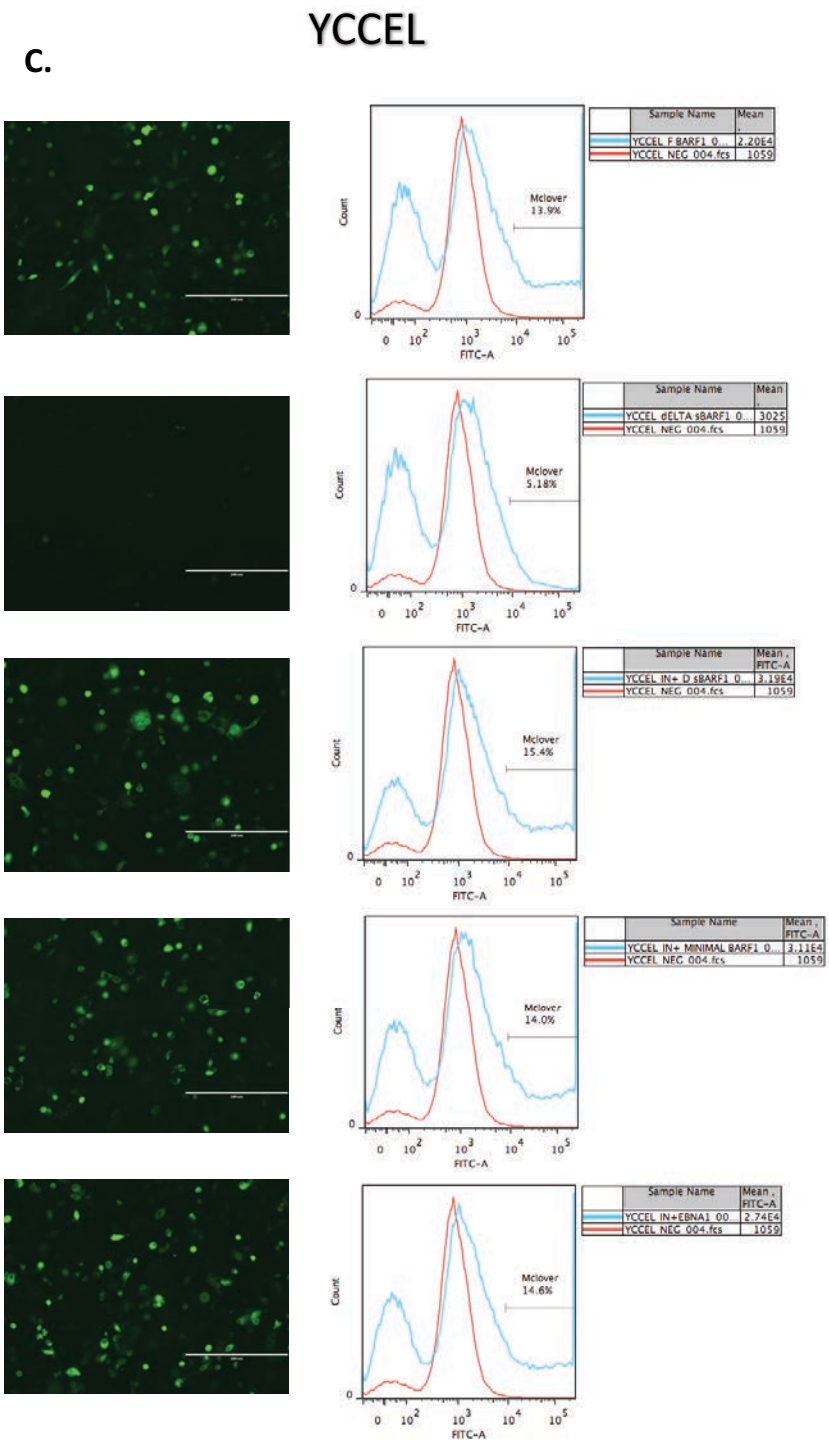

Figure 31 : transfected Gastric cell lines with new BARF1 constructs

GC cell lines MKN28 (A) MKN1(B) YCCEL(C) were transfected with six new constructs contain green fluorescent protein mClover . After transfection cell were checked by fluorescent microscope and flow cytometer to detect level of Mclover .

In the same study, with B cell lines we found different results as shown in Figure 33, BARF1-TFF clone 6 clearly recognized targeted transfected B cell with two BARF1 plasmids which contain Full BARF1 gene and Minimal BARF1 – invariant chain, where recognition level was found increased in present of (In) chain. However, no response was detected from BARF1 –GSL clone compare to high recognition from EBNA1-SNP clone to minimal EBNA1 plasmid.

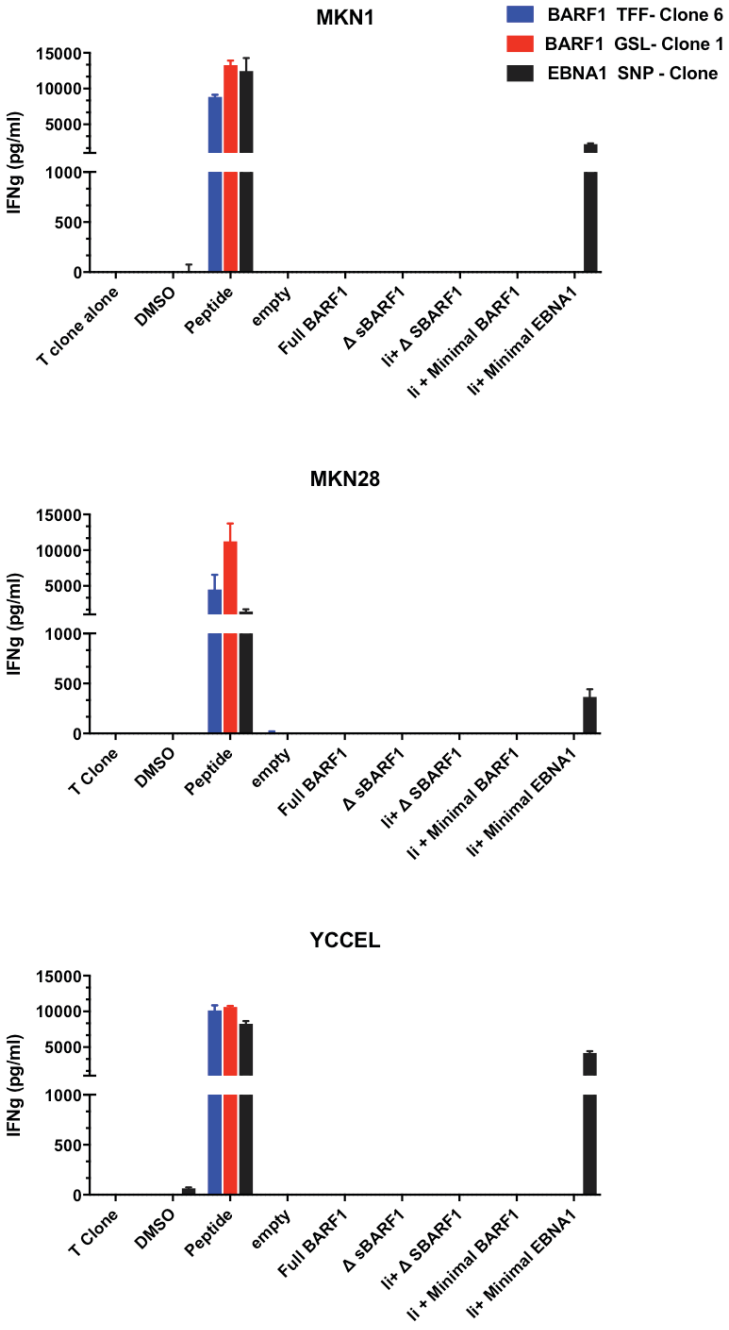

Figure 32 : recognition of BARF1 antigen using new generated constructs on epithelial cells.

Gastric cell lines were transfected with six new generated BARF1 constructs as show in (chapter 2) using lipofecamine 2000 method. These cells were targeted by BARF1 (GSL) -specific clone (DR-17), BARF1 (TFF) and EBNA1 (SNP) (DR-51) to detect recognition by IFNg ELISA assay.

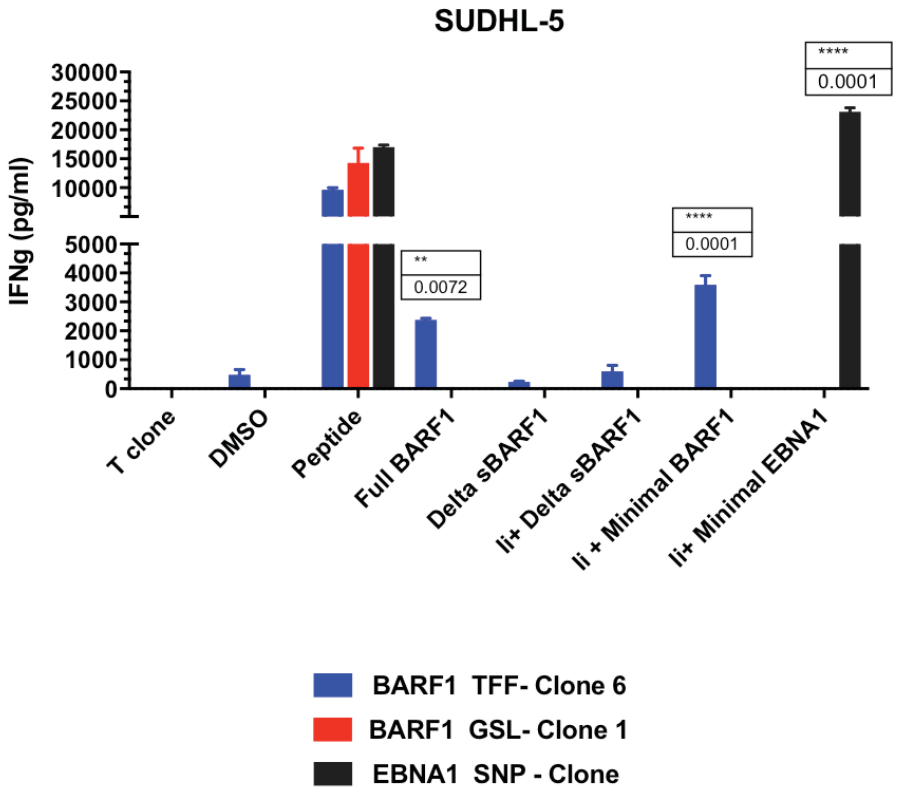

Figure 33 : Study recognition of BARF1 antigen using new generated constructs on B cell lines.

SUDHL-5 cell line was transfected with six new generated BARF1 constructs as show in. These cells were targeted by BARF1 (GSL) -specific clone (DR-17), BARF1 (TFF) and EBNA1 (SNP) (DR-51) to detect recognition by IFNg ELISA assay.

3.10 T cell receptor cloning

Taken together, the results showing TFF clone 6 recognises: i) unmanipulated C666 cells, ii) C666, SUDHL5 and Kem cells exposed to concentrated supernatant from EBV+ve cells, iii) SUDHL5 cells expressing BARF1 protein from plasmids suggests that further work exploring BARF1 as a CD4 target is warranted. Given that DR51 is a common allele in the human population an effective T-cell response to this peptide could be therapeutically relevant for the treatment of EBV+ve cancers.

I therefore undertook a final set of experiments to obtain the TCR sequence from clone 6, capable of recognising native BARF1. To further study the T-cell response to this epitope I also sought to obtain the TCR sequence from the other two clones generated from the same donor that were specific for the same epitope but had lower avidity in titration assays.

To obtain the TCR sequence I isolated RNA from all three TFF specific CD4 T-cell clones (C4, C5 and C6) and amplified the TCR alpha and beta chains by rt-PCR. Amplified DNA from three clones was then analysed by agarose gel electrophoresis. As shown in Figure 34, DNA products of the predicted size were generated. The DNA ws cut from the gel, purified and the TCR alpha and beta chains for all three clones were sequenced. Analysis of the sequence data using the IMGT website (http://www.imgt.org/) showed all three clones had the same TCR beta chain usage (TRBV3-1*01 which is V-beta 9). To confirm this result, the three T-cell clones were stained with Vbeta.9 -PE antibody with Vbeta.8 – FITC antibody used as a control. PBMCs were also stained with these antibodies as additional controls to confirm the antibodies were functional. The flow cytometer results, shown in Figure 35, confirmed that all three clones were TCR V-beta 9.

Alignment of the TCR sequences for all three clones showed that not only were they the same v beta type, there were in fact identical at the nucleotide level. Therefore the clones appear have identical TCR sequences although there were clear biological differences between the three in terms of their avidity and ability to recognise EBV+ve cells, differences that were reproducible across multiple independent experiments.

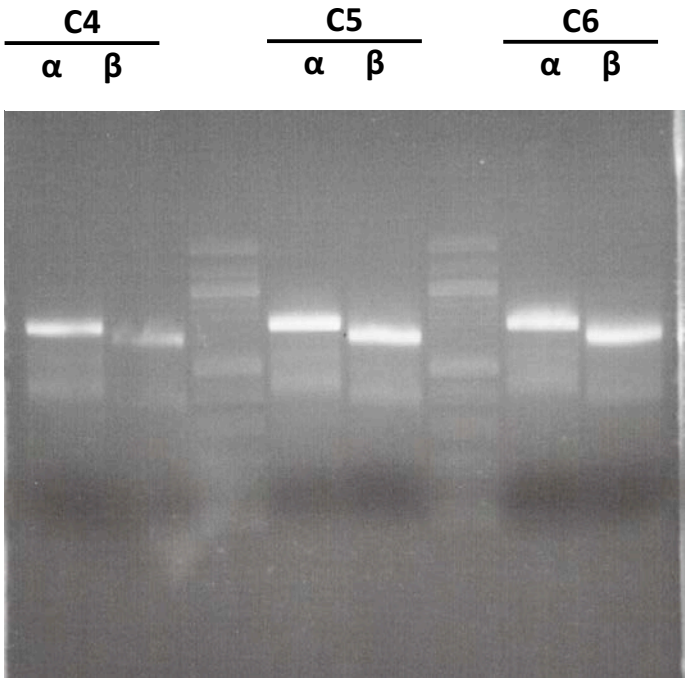

Figure 34: RT-PCR amplification of TCR alpha and beta chains

TCR alpha and beta chains were amplified using specific primers and SMART RACE cDNA Amplification. Amplified DNA from three clones was then analysed by agarose gel electrophoresis to identify amplification products.

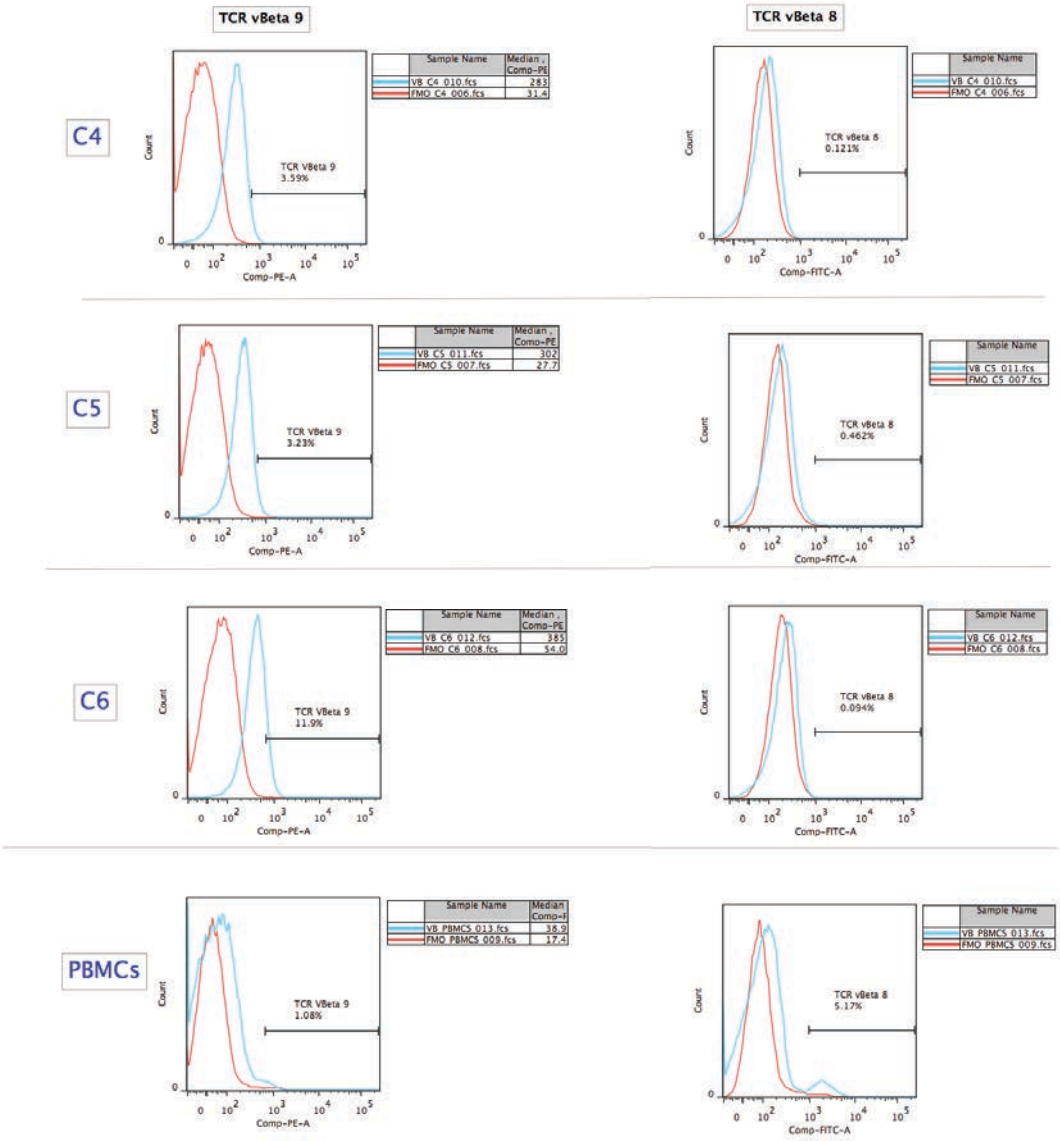

Figure 35 : Flow cytometry analysis of TCR beta chains.

TFF-specific CD4+ T-cell clones (C4, C5 and C6) were stained with V-beta.9 -PE and Vbeta.8 – FITC antibodies. PBMCs were also stained as a positive control. All three clones were clearly positive for TCR- beta 9.

3.11 Summary and Discussion

Epstein–Barr virus (EBV) has been implicated in several lymphoid and epithelial cancers [120, 147]. These tumours express EBV antigens, principally EBNA1 and LMP2. Two other antigens, LMP1 and BARF1 are also expressed in some cases of EBV-associated cancer [148]. Understanding the T cell response to these tumor antigens is very important for immune therapy. However, the T-cell response to these tumor antigens has previously been measured individually by different groups using different strategies and techniques. More importantly, some of these studies have examined only CD8 T-cells or have used epitope prediction algorithms focusing on only a subset of HLA alleles [149]. Thus, the current model of immune hierarchy could be biased.

I therefore conducted a systematic analysis of the immune response to the four key EBV tumor antigens in twenty-five healthy donors. My work has identified that in terms of the highest T cell response to EBV antigens (the mean adjusted reading in ex vivo ELIspot assays), the pattern of immunodominance was EBNA1> LMP2> LMP1 >BARF1. Based on the number of donors having an immune response, LMP2 was the highest of these four antigens. A potential limitation of my work is that I measured the total T-cell response to each antigen, not further breaking it down into CD8 or CD4 subsets. However, the broad aim of my work was to examine the total magnitude of the antigen-specific response in an unbiased way.

Interestingly, I found that the strongest response to LMP1 and LMP2 occurred in the same donor (who also had a high response to the EBNA1 antigen). I decided to characterize T cell responses for both latent membrane antigens in this healthy subject. I identified an LMP1 specific- CD8 T cell response after screening seventy-three

LMP1 peptides that was the already-defined YLQ epitope. Previous experience from others in the research group is that this response is weak, the strength of the YLQ response is therefore novel. More interestingly, testing with ninety-eight LMP2 peptides identified novel CD4 and CD8 T-cell responses against LMP2 antigen. Additional experiments assayed seven uncharacterized CD4 and CD8 T cell clones specific for LMP2A pepmix. Five T cells clones were specific to two LMP2 peptides (FLY) and (TYG) which had previously been studied [154, 155] but the other two T cell clones are specific for novel epitopes. These results clearly show that additional T-cell reactivity against LMP2 exists and that further screening and characterization of these key therapeutic antigens is required.

The T cell response to BARF1 antigen in ex vivo assays was weak in the healthy donors I studied. It remains to be seen if stronger resposnes exist in patients with EBV carcinomas which express BARF1. Nevertheless, because the main function of BARF1 during EBV infection is anti- apoptosis it is important to consider this gene as a potential immunotherapy target.

The TNFa assay was used to measure T cell responses against BARF1 antigen after culture. This assay can confirm a weak ex vivo response from is indeed real but also importantly allows FACS cloning of the T-cells. Using this method I succeeded in confirming that weak BARF1 T cell responses in ex vivo assays were real, based on the greater strength of these assays after the first and second stimulations. BARF1-specific T-cells from 5 healthy subjects were FACS sorted and cloned to classify specific T cell response. Interestingly, I identified several novel BARF1 – specific CD4 T cell clones; HLA-DR51 restricted BARF1 (TFF) –specific T cell clones, HLA-DR-53 restricted (GER), HLA-DP-2 restricted (TEV). Moreover, HLA-DR17

restricted (GSL), HLA-DR-103 restricted (TEV) specific T cell clone response. To confirm these clones were indeed specific for these peptides, and not cross reactive low avidity responses, I measured the functional avidity of these T cell clones against a range of peptide concentration. Avidity varied from clone to clone**.** With high T cell avidity determined as (<1nM peptide) , moderate avidity (1nM – 100 nM) and low avidity (> 100nM) [156, 157] the avidity of BARF1 TFF- specific clones was low(>100 nM) with three T clones but other clones were high (16-53%). Some of the high avidity T cell clones appeared able to respond to naturally presented epitope on LCLs. Using a panel of HLA – matched LCL that include the epithelial NPC c666 cell line that expresses BARF1, I demonstrated that multiple T clones recognized naturally presented epitopes from these cell line. Because BARF1 is highly secreted from NPC cells and latently LCL [150] I then analyzed whether intracellular transfer of BARF1 protein occurred, asking if supernatant from these cells was able to sensitize B cells and epithelial cells to CD4 T cell recognition. Using concentrated supernatant prepared from LCL and C666 as BARF1 positive, and supernatant prepared from the NP460 cells as a BARF1 negative control, I show that BARF1 was transfered from LCL B cell to epithelial cell (c666) more than epithelial to B cell. ,

The important step in development of TCR-based T cell immunotherapy is selection of target T cell epitope. Given that DR51 is a common HLA allele in the population, and that BARF1 (TFF) specific CD4 T-cells restricted by DR51 could recognize EBV-positive cells, I decided to examine this response in more detail. Reprogramming of T-cell specificity, by transducing them with a new T cell receptor, is a rapidly developing area of cancer therapy, including for EBV cancers [147, 158, 159] [160]. I PCR amplified the TCRα/β genes and obtained the TCR sequences. Interestingly,

all three clones had the same TCR sequence, despite having different avidities in T-cell assays. It is likely that other factors in the T-cells that contribute to T-cell binding to target cells, T-cell activation or T-cell effector function account for these differences. Understanding these factors would help to improve T-cell immunotherapy, and the clones I generated could assist in this goal.

I generated new BARF1-expressing DNA constructs to further study T-cell recognition of BARF1 antigen as shown in Table 5 (chapter 2). I found no recognition by BARF1- specific T clones (TFF) and (GSL) to all three transfected GC cell lines (YCCEL, MKN1 and MKN28) with BARF1 constructs even when expressed as an Invariant chain fusion. These epithelial cells were also not recognised after incubation with BARF1-containing cell supernatants. Interestingly, the B cell (SUDHL-5) transfected with the minimal BARF1-il- plasmid was recognized by the TFF-specific T clone.

To further investigate these different results, I transfected YCCEL cells with GFP-pcDNA plasmid (Full BARF1 gene), but no response has seen from T cell clone. At the same time, I treated some of the transfected YCCEL with Brefeldin A (BFA) to stop BARF1 secretion. After that, BARF1 protein was detected by monoclonal BARF1 antibody. I suggest BARF1 is secreted through the classical pathway when block protein passage at specific stage with BFA via secretory pathway as shown in previous report [161] . These finding suggest that BARF1 protein is highly secreted in epithelial cells more than B cells, so T cells may not recognise the expressed antigen.

CHAPTER 4: RESULTS

INVOLVEMENT AND FUNCTIONAL OF IMMUNE CELLS IN PATIENT BLOOD WITH GASTRIC CANCER: FEATURES OF ANTIGEN -SPECIFIC T CELL RESPONSE TO EBV AND TUMOUR ANTIGENS.

4.1 Introduction

The fourth most common cause of cancer-related death in the world is Gastric Cancer[33]. In 1990 EBV was linked to Gastric carcinoma (GC) by polymerase chain reaction and in situ hybridization (ISH) of EBV encoded small RNA (EBER) [162]. Throughout the EBV is detected in about 10% of GC cases , 80,000 cases of EBV+ve disease occur each year[120]. Subsequent studies have provided further information about EBV associated GC including: posttranscptional regulation by cellular, epigenetic abnormalities, role of latent and lytic EBV gene, alteration of genome and EBV micro RNA[163]. EBV latency genes play important roles in EBVGC. Expression of the following genes is consistently detected: EBNA1, LMP2 [164].Additional RNA transcripts are also present, including the EBV early RNA (EBERs), Bam HI A rightward transcripts (BARTs) miRNA[165]. In addition, EBV early lytic genes such as BZLF1 and BFLF1 have been detected in EBVGC, which may be a result of some of the EBV+ve cells entering lytic cycle[166]. Regarding levels of the latent gene transcripts, the most abundant are the EBERs, then BARTs, then LMP2A-B. Expression of EBNA1 appears to be low [121].

However, it is unclear what the status of EBV-specific immunity is in GCa patients. My project seeks to develop better understanding of how best to harness EBV-specific immunity to develop immunotherapy for patients with EBV-associated gastric cancer by measuring T-cell immunity to the EBNA1, LMP1, LMP2 and BARF1 antigens that are expressed in the malignant cells of GCa. Immunity to EBNA3A, which is not expressed in the malignant cells, serves as a control. T-cell immunity to EBV antigens measured in patients with EBV-positive and EBV-negative disease provides an interesting comparison to explore if the former lack immunity to the virally-encoded

antigens within their tumour. Comparison to healthy donors of a similar age allows for general defects in T-cell immunity in gastric cancer patients in general to be assessed.

There are several known tumors associated antigens in of gastric cancer. Antibody responses to some of these have been detected in the blood of such patients; it is currently unknown what the status of T-cell immunity to these antigens is [73, 167, 168]. Therefore, I investigated T cell responses to cellular tumour antigens including CEA, MUCIN1, MAGEA1, MAGEA3, MAGE4 and NY_ESO-1 which have been detected in gastric cancer [73, 169-171]

Cancer patients often show perturbations of immune cells in the blood, suggesting that the disease has wider systemic effects on immunity[172]. However, its remains unclear the prognostic significance of immune cells in peripheral blood of patients with advanced GC. To determine if this is also the case for gastric cancer patients I investigated the frequency and phenotype of immune cells in peripheral blood from GC patients including effectors and suppressor immune cells. Gastric cancer cells also produce a range of immunomodulatory cytokines including: IL-1, IL-6, IL-8, TNFa, Transforming growth factor β (TGFβ) and monocyte chemoattractant protein (MCP)-1 with higher levels of some of these detected in plasma from patients [173] [174, 175]. In the present study, I therefore examined systemic cytokine levels in plasma from GC patients, with healthy donors as controls, to gain a more detailed picture of systemic immunity in gastric cancer.

4.2 Detection of antigen-specific T-cells in blood from healthy donors and gastric cancer patients using a cultured immune assay.

4.2.1 EBV tumour antigen-specific T cell response

To study the level of T cell recognition to EBV antigens in gastric patients' blood, PBMCs from patients (n=12) or control healthy donors (n=10) were stimulated with five latent EBV tumour antigen pepmixs (EBNA1, LMP1, LMP2, BARF1 and EBNA3A) using a T-cell culture assay I developed. After ten days, cells were incubated with TNFa-specific antibody in the presence of TAPI0 inhibitor for 4-6 hours. Cells were then surface stained for phenotypic markers and analysed by flow cytometry. Example results from a single patient are shown in **Figure** 36 – left hand side panels. The results from all donors tested are presented in **Figure 37**. The size of the T-cell response to each antigen varied from person to person, but there were no statistically significant differences in response size between gastric cancer patients and healthy donors.

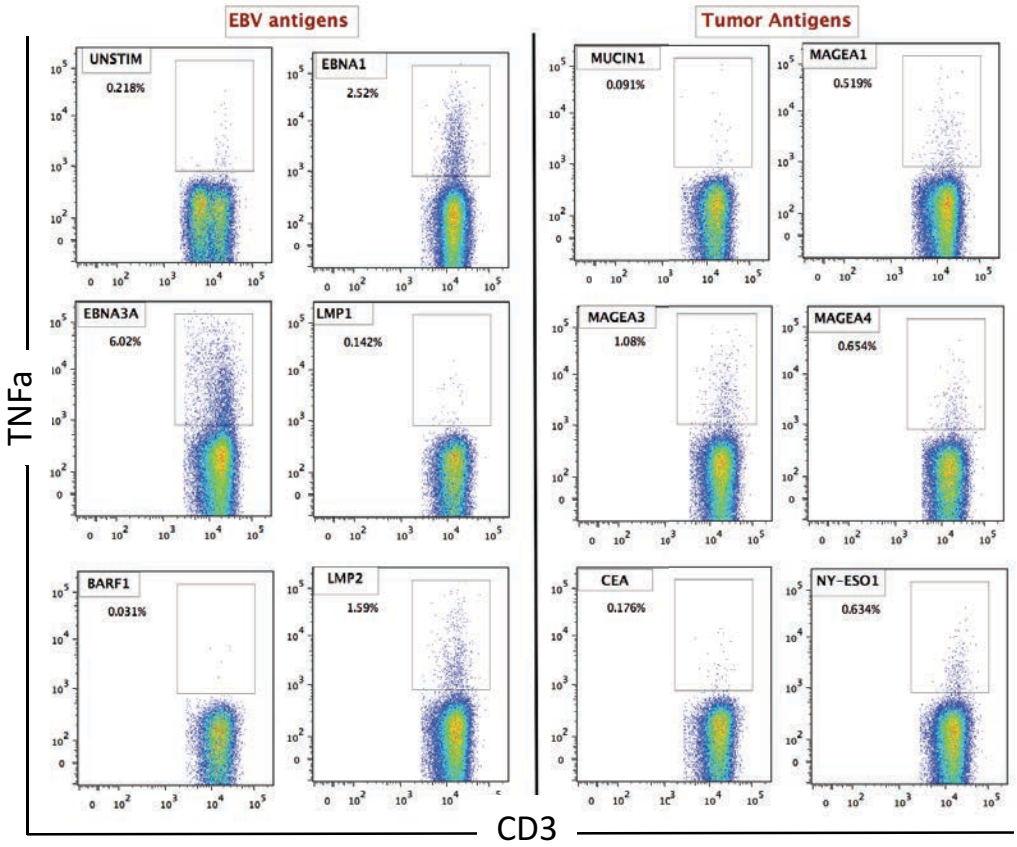

Figure 36 ; **: gating for detection of T cell response to EBV and Tumor antigens:**

Percentage of T cell response was detected after cultured T cell – TNFa assay. Response of T cell was gated as CD3+ TNFa+ . Unstimulated PBMCs were used as negative control. (left groups) are stimulated PBMCs with EBV pepmixes and (Right group) are stimulated PBMCs with Tumor associated antigens pepmixes.

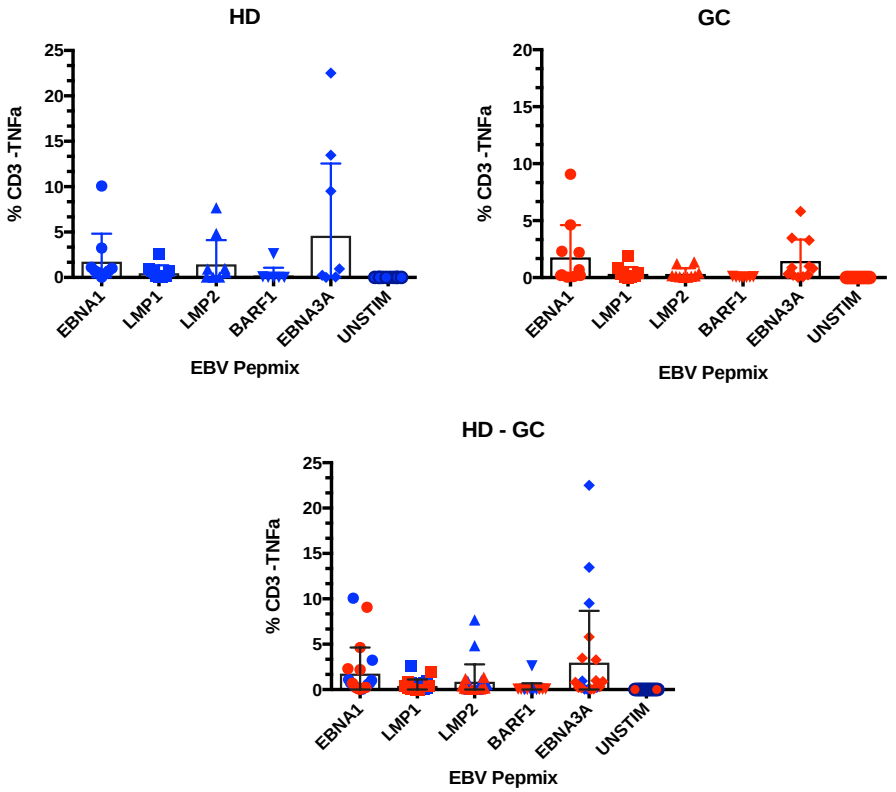

Healthy Donor - HD							
	Mean	Median	Range	STD.P	STD.S	VAR.P	VAR.S
EBNA1	1.74	0.73	10.59	2.93	3.09	8.59	9.55
LMP1	0.48	0.15	3.16	0.82	0.87	0.68	0.76
LMP2	1.45	0.30	8.30	2.53	2.67	6.40	7.11
BARF1	0.18	0.00	3.24	0.83	0.88	0.69	0.77
EBNA3A	4.60	0.14	23.13	7.54	7.95	56.84	63.15

Gastric Cancer Patient - GC							
	Mean	Median	Range	STD.P	STD.S	VAR.P	VAR.S
EBNA1	1.78	0.24	9.16	2.69	2.83	7.26	7.99
LMP1	0.33	0.09	1.99	0.56	0.59	0.31	0.34
LMP2	0.33	0.13	1.47	0.47	0.50	0.22	0.25
BARF1	0.01	0.03	0.30	0.07	0.08	0.01	0.01
EBNA3A	1.46	0.80	5.78	1.80	1.88	3.23	3.55

Figure 37 : : EBV tumour antigens specific T cell response in HD and GC

Isolated PBMCs from Healthy Donors (n=10) and gastric cancer patient (n=12) were stimulated with five latent EBV tumour antigen EBNA1, LMP1, LMP2, BARF1 and EBNA3A pepmixs using newly development T cell culture assay. After ten days, cells were cultured with TNFa antibody in present of TAPIO inhibitor then TNFa-T cell response percentage were measured by flow cytometer after surface staining. T cell recognition to EBV pepmix, gated as (CD3+ TNFa+), is shown, with unstimulated PBMCs used as negative control.

4.2.2 Tumour associated antigen specific T cell response

In this study, I have selected several tumour antigens for study: NY-ESO-1, MUCIN1, MAGEA1, MAGEA3, MAGEA4 and CEA based on prior evidence of expression in gastric cancer or detection of specific antibodies in patients. T-cell responses to these antigens were measured by the cultured assay using appropriate pepmixes. Isolated PBMCs from Gastric cancer patient (n=12) or Healthy Donors (n=10) were stimulated and cultured with these pepmixes then T cell response was detected by TNFa cultured assay. A typical result is shown In Figure 1 – right hand side panels. Across the study cohort, I detected T-cell responses to all six of these antigens. The results from all donors tested are presented in **Figure 37**. The size of the T-cell response to each antigen varied from person to person but there were several key differences between healthy donors and patients. The mean value of the T cell response in patients specific for MAGEA1, MAGEA4, and NY-ESO-1 were significantly higher than T-cell responses in healthy donors ($p<0.05$ Mann-Whitney U test). Two other interesting observations are apparent from the data. First, some of the healthy donors has detectable T-cell responses to the tumour antigens although for 5/6 antigens the mean size of the detected response was lower than for patients. Second, while patients lacked a detectable T-cell response to CEA, five healthy donors had T-cell responses to this protein.

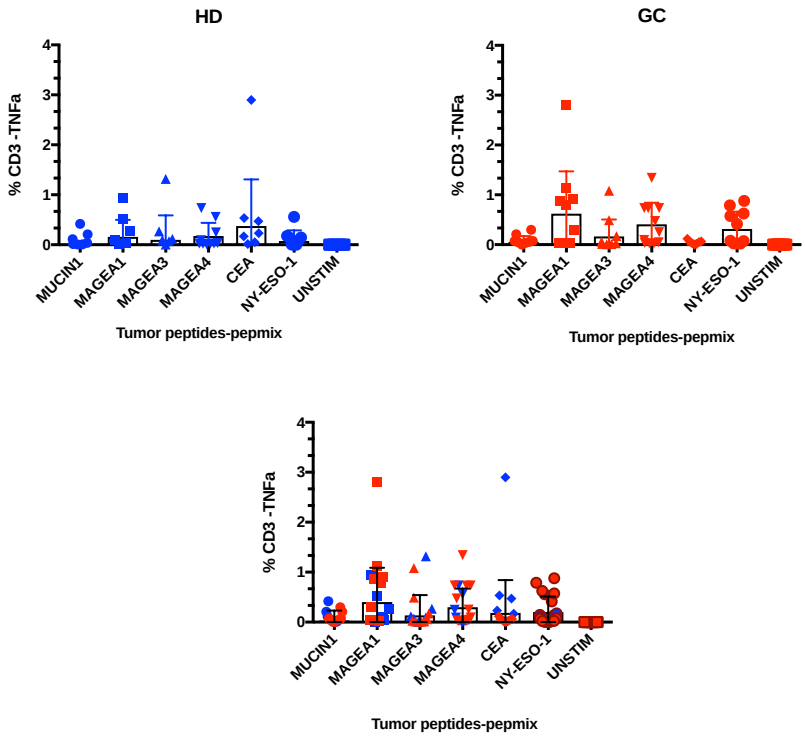

Healthy Donor - HD							
	Mean	Median	Range	STD.P	STD.S	VAR.P	VAR.S
MUCIN1	0.01	0.01	1.07	0.26	0.28	0.07	0.08
MAGEA1	0.16	0.02	1.16	0.32	0.34	0.10	0.12
MAGEA3	0.10	0.04	1.94	0.47	0.49	0.22	0.24
MAGEA4	0.18	0.03	0.73	0.25	0.26	0.06	0.07
CEA	0.38	0.11	3.41	0.89	0.93	0.78	0.87
NY-ESO-1	0.08	0.05	0.80	0.20	0.21	0.04	0.04

Gastric Cancer Patient - GC							
	Mean	Median	Range	STD.P	STD.S	VAR.P	VAR.S
MUCIN1	0.05	0.05	0.43	0.11	0.12	0.01	0.01
MAGEA1	0.62	0.30	2.89	0.81	0.85	0.66	0.73
MAGEA3	0.17	0.01	1.10	0.37	0.40	0.14	0.16
MAGEA4	0.40	0.25	1.32	0.41	0.43	0.17	0.19
CEA	0.01	0.02	0.25	0.06	0.07	0.00	0.00
NY-ESO-1	0.31	0.08	0.92	0.33	0.35	0.11	0.12

Figure 38 : Tumour associated antigens specific T cell response HD and GC
Isolated PBMCs from Healthy Donors (n=10) Gastric cancer patient (n=12) were stimulated with tumour antigen pepmixes; NY-ESO-1, MUCIN1, MAGEA1, MAGEA3, MAGEA4 and CEA using newly development T cell culture assay. After ten days, cells were culture with TNFa antibody in present of TAPIO inhibitor then TNFa-T cell response percentage were measured by flow cytometer after surface staining. T cell recognition to EBV pepmix gated as (CD3+ TNFa+), is reported, with unstimulated PBMCs used as negative control .

4.3 Immunophenotyping immune cells in blood from gastric cancer patients and healthy donors.

To investigate if there were differences in the frequency and/or properties of immune cells between gastric cancer patients and healthy donors I used five separate flow cytometry panels to stain PBMCs or whole blood collected from gastric patients (n=12) and healthy donors (n=10).

4.3.1 Classification of lymphocytes subsets in GC patients

Antibody panel 1 was designed to detect key lymphocyte subsets including: CD4 and CD8 T-cells, B-cells, NK cells and gamma/delta T-cells. The gating strategy used and an example of the quality of the flow cytometry data is shown in **Figure 39**. Overall results from all GC patients and donors analysed are presented in **Figure 40**. The relative frequencies of CD4 and CD8 T-cells are presented in Figure 5A, median percentage of GC vs HD, CD4 (44 to 49) and CD8 (31to 44). There was no significant difference in the frequency of CD4 and CD8 T-cells nor was there a difference in the CD4:CD8 ratio between GC patients (median 1.2) and healthy donors (1.8). However, 5/12 (42%) gastric cancer patients had a CD4:CD8 ratio of less than 1.0 whereas only 1/10 (10%) of patients had a ratio of less than 1.0.

Figure 40b show the frequency of CD19-positive B cells. The percentage of B cells in the lymphocyte population was significantly higher in HD than GC (p=0.0109; median values were 7.7% vs 3.8 %). The frequency of gamma/delta T-cells is shown in **Figure 40c**. The mean percentage of gamma delta (γδ) T cells in CD3-positive lymphocytes was higher in gastric cancer patients (median GC 1.9% vs 1.4% in healthy donors) but this difference was not statistically significant. The frequency of different subsets of NK cells, including NKT cells, is shown in **Figure 41**.. The median

percentage of CD3+ CD56+ NKT cells was significantly higher in gastric cancer patients compared to healthy donors median GC 6% vs 1.8% in healthy donors). There were no significant differences in the frequency of other NK cell

types.

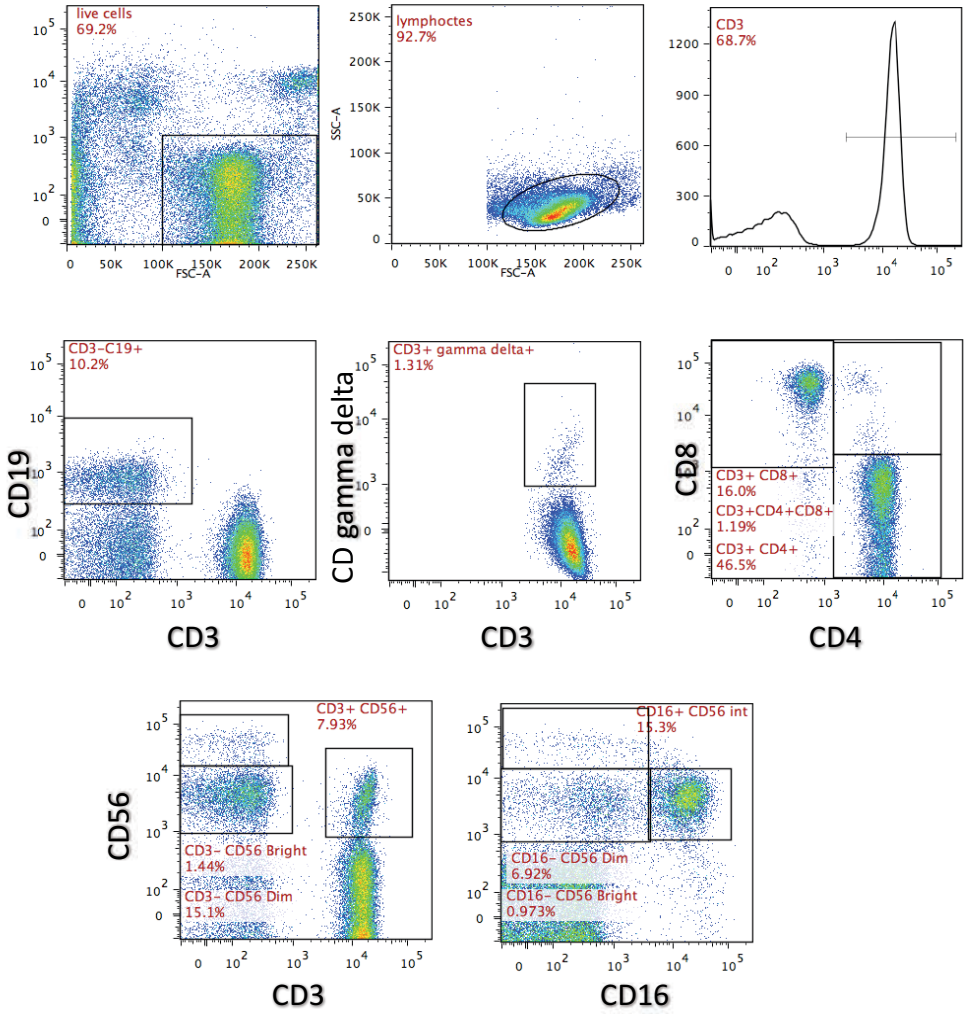

Figure 39 : classification of lymphocyte subsets using flow cytometry
A panel of antibodies were used to classify lymphocytes into T cells (CD4 , CD8 and gamma delta subsets) , B cell (CD19) and NK and TNK cells (CD56 , CD16) populations

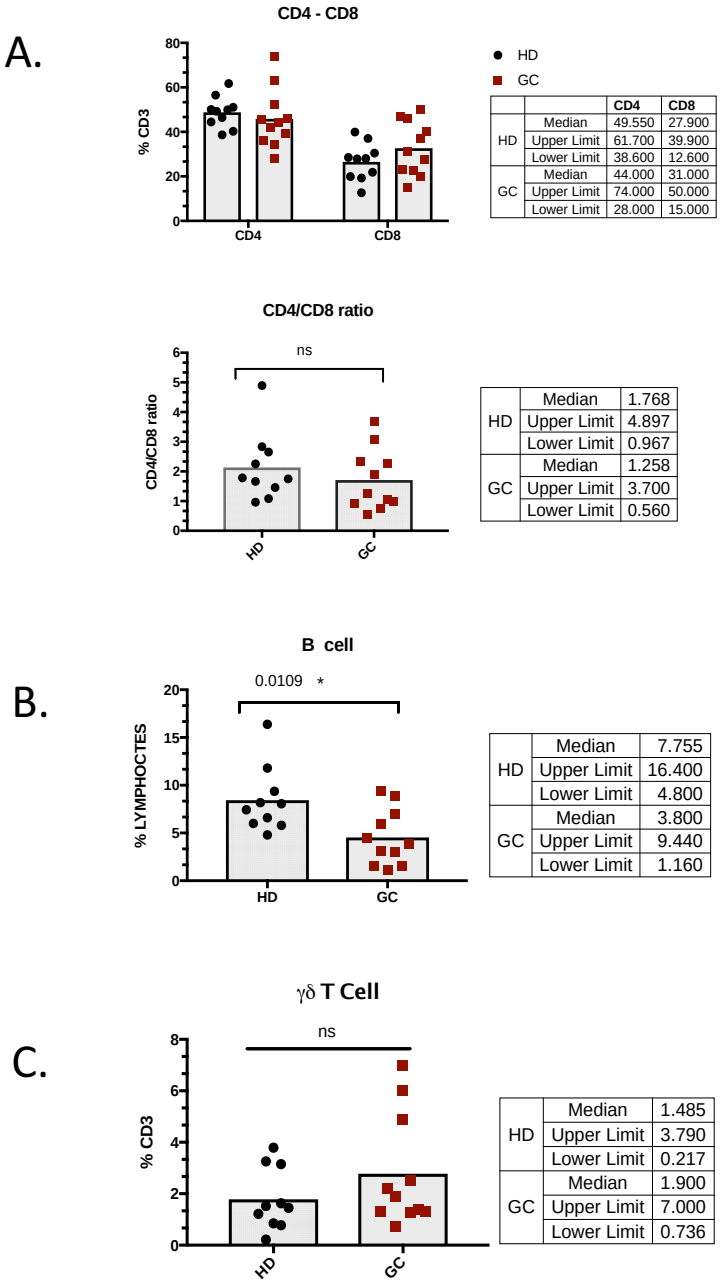

		CD4	CD8
HD	Median	49.550	27.900
	Upper Limit	61.700	39.900
	Lower Limit	38.600	12.600
GC	Median	44.000	31.000
	Upper Limit	74.000	50.000
	Lower Limit	28.000	15.000

HD	Median	1.768
	Upper Limit	4.897
	Lower Limit	0.967
GC	Median	1.258
	Upper Limit	3.700
	Lower Limit	0.560

HD	Median	7.755
	Upper Limit	16.400
	Lower Limit	4.800
GC	Median	3.800
	Upper Limit	9.440
	Lower Limit	1.160

HD	Median	1.485
	Upper Limit	3.790
	Lower Limit	0.217
GC	Median	1.900
	Upper Limit	7.000
	Lower Limit	0.736

Figure 40 : Comparison of lymphocytes subsets between GC and HD
Isolated PBMCs from Healthy Donors (n=10) Gastric cancer patient (n=12) were stained using a panel of antibodies marker for lymphocytes populations. A. percentages of CD4 , CD8 and the ration of CD4/CD8 . B. percentage of B cell (CD19) in lymphocytes population. C. percentage of gamma delta T cell in CD3 population. Bars (grey) is the mean value, the table show that median and Range value (Upper and lower limit)

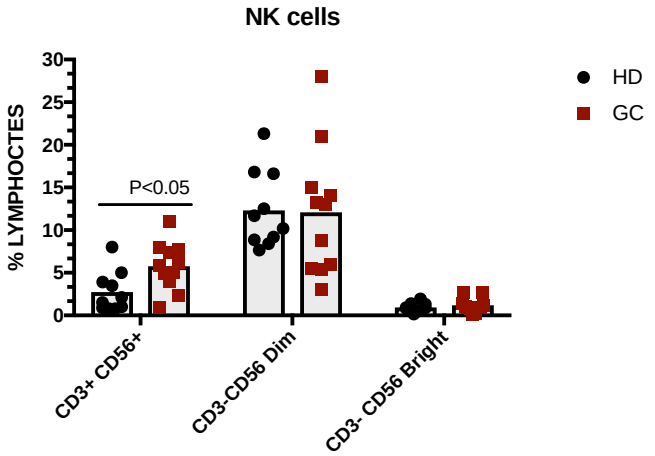

	HD			GC		
	Median	Upper Limit	Lower Limit	Median	Upper Limit	Lower Limit
CD3+ CD56+	1.820	8.000	0.775	5.900	11.000	0.880
CD3-CD56 Dim	10.950	21.300	7.670	13.000	28.000	3.000
CD3- CD56 Bright	0.869	1.930	0.172	0.993	2.720	0.167

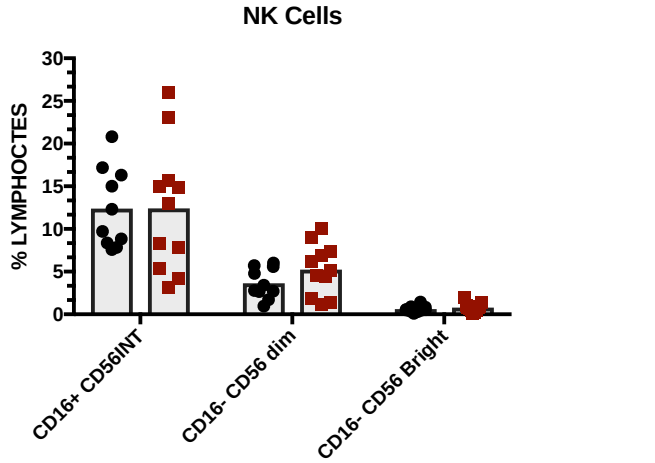

	HD			GC		
	Median	Upper Limit	Lower Limit	Median	Upper Limit	Lower Limit
CD16+ CD56INT	11.010	20.800	7.600	13.000	26.000	3.190
CD16- CD56 dim	3.105	6.000	0.971	5.150	10.000	1.150
CD16- CD56 Bright	0.525	1.430	0.123	0.770	2.000	0.092

Figure 41 : Comparison of lymphocytes (NK cells) between GC and HD

Isolated PBMCs from Healthy Donors (n=10) Gastric cancer patient (n=12) were stained using a panel of antibodies marker for lymphocytes populations. Top figure, show NKT cell and NK cells. Bottom figure, show subtype of NK cells. Bars (grey) is the mean value, the table show that median and Range value (Upper and lower limit)

4.3.2 The distribution of Effector and Memory CD8+ and CD4+ T cell subsets in GC patients.

Panel 2 was designed to study the phenotype of CD4 and CD8 T-cells using six markers including: CCR7, CD27, CD28, CD45RA, CD38 and HLA-DR. The gating strategy and an example of the quality of the staining is shown in **Figure *42***. It was not possible to specifically gate on the CD3+ CD8+ T-cells, therefore they are defined here as CD3+CD4- cells. Comparison with other panels showed this was a valid means to identify the CD8 T-cell subset (data not shown). The phenotype of the bulk CD3-positive population as well as the CD3+CD8+ T-cells and CD3+ CD4+ T-cells are presented in Figure 8. As shown in **Figure 43a,** results show that the percentage of markers on total CD3 when the bars clarify the mean of percentage values. comparison between HD vs GC, I found that the median of percentage (%) value as; CCR7 (25% vs 14%), CD27 (84 vs 78), CD45RA (64vs 61), CD28 (87 vs 81), CD38 (52 vs 53) and HLA-DR (7.5 vs 15). Second, memory and effectors CD4 and CD8 T cells were identified based on expression of CD27 or CCR7 and CD45RA, the results are defined as naive T cells (Naïve: CD45RA+CD27+) or (CD4RA+ CCR7+), central memory T cells CM; (CD45RA−CD27+) or(CD45RA-CCR7+), effector memory T cells: EM (CD45RA−CD27-) or(CD45RA-CCR7-) and terminally differentiated effector memory cells re-expressing CD45RA (CD45RA+CD27-) or (CD45RA+ CCR7-) subsets of CD8+ and CD4 T cells, in HD and GC patients.

Figure 43b, results show that CD45RA CD27 subpopulation of CD8 and CD4 T cells in HD vs GC, the median with CD8; Naïve (46 vs 43), CM (16 vs 13), EM (5 vs 6) and TEMRA (39 vs 30) while CD4 Naïve (50 vs 41), CM (33 vs 48), EM (10 vs 7.4) and TEMRA (1.6 to 1) . However the results in **Figure 43c** show that (CD45RA CCR7) CD8 and CD4 T cells when the median of CD8 population naïve (21 vs 12), CM (1.4 vs 1.3) , EM (20 vs 18) and TEMRA (60 vs 62) while CD4 naïve (38 vs 28) , CM (11 vs 7) , EM (35 vs 45) and TEMRA(7 vs 15) .I found no significant difference between HD and GC in naïve and memory cells in addition to CD27 and CD28 populations as shown in **Figure 43d**, with CD4 and CD8 T cell.

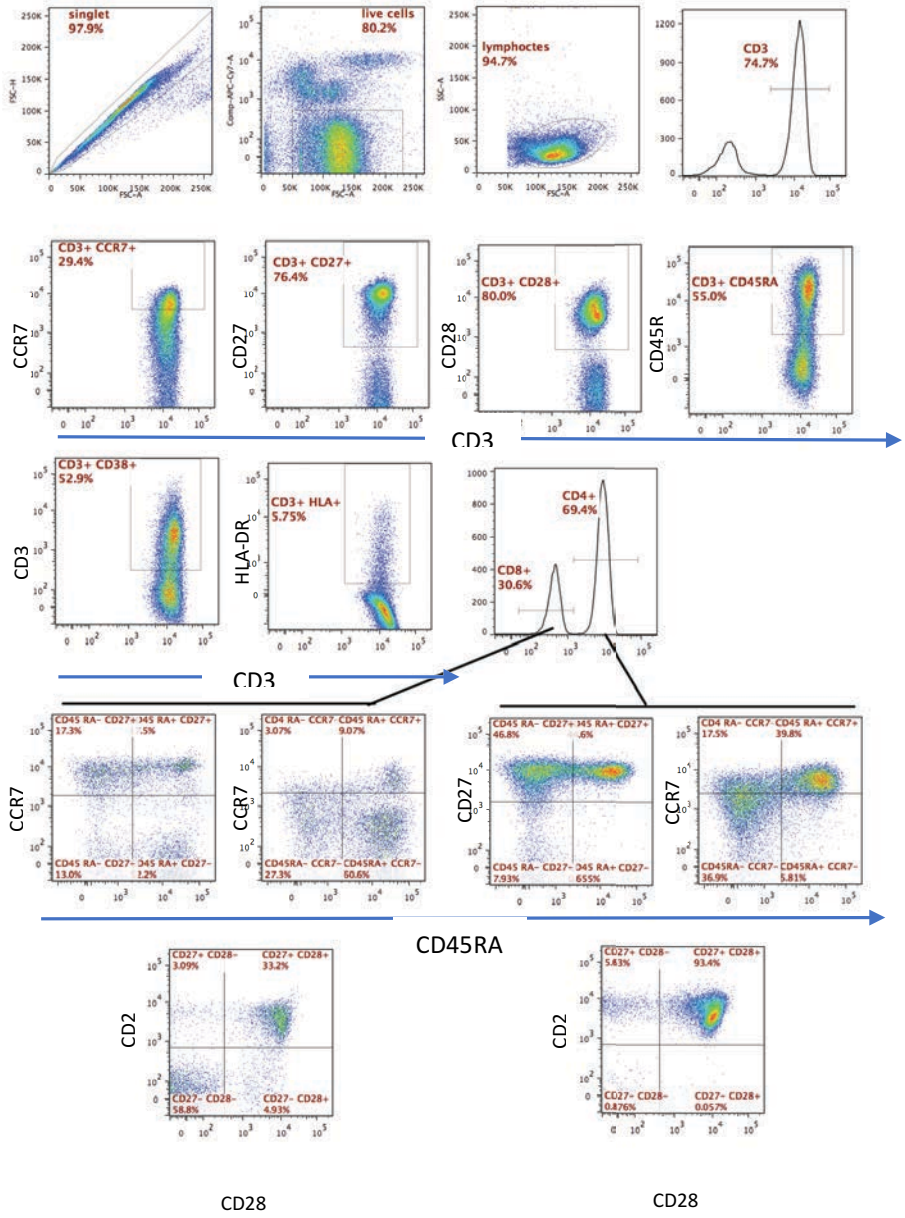

Figure 42 : classification of CD4 and CD8 T cell in GC : activation and differentiation markers.

After gated live cells (CD14- CD19-), the function of CD4 and CD8 T subsets were classified by six markers include CCR7, CD27, CD28, CD45RA, CD38 and HLA-DR on total of CD3 T cell. Next, memory and effectors CD4 and CD8 T cell were classified as naïve (Naïve: CD45RA+CD27+) or (CD4RA+ CCR7+), CM; (CD45RA−CD27+), or (CD45RA-CCR7), EM (CD45RA−CD27-) or (CD45RA-CCR7-) and TEMRA (CD45RA+CD27-) or (CD45RA+ CCR7-) . This gating strategy were determined depend on three controls; 1) unstained cells control, 2) control for viability, CD3, CD4 T cell ,3) FMO control; CCR7, CD45RA .

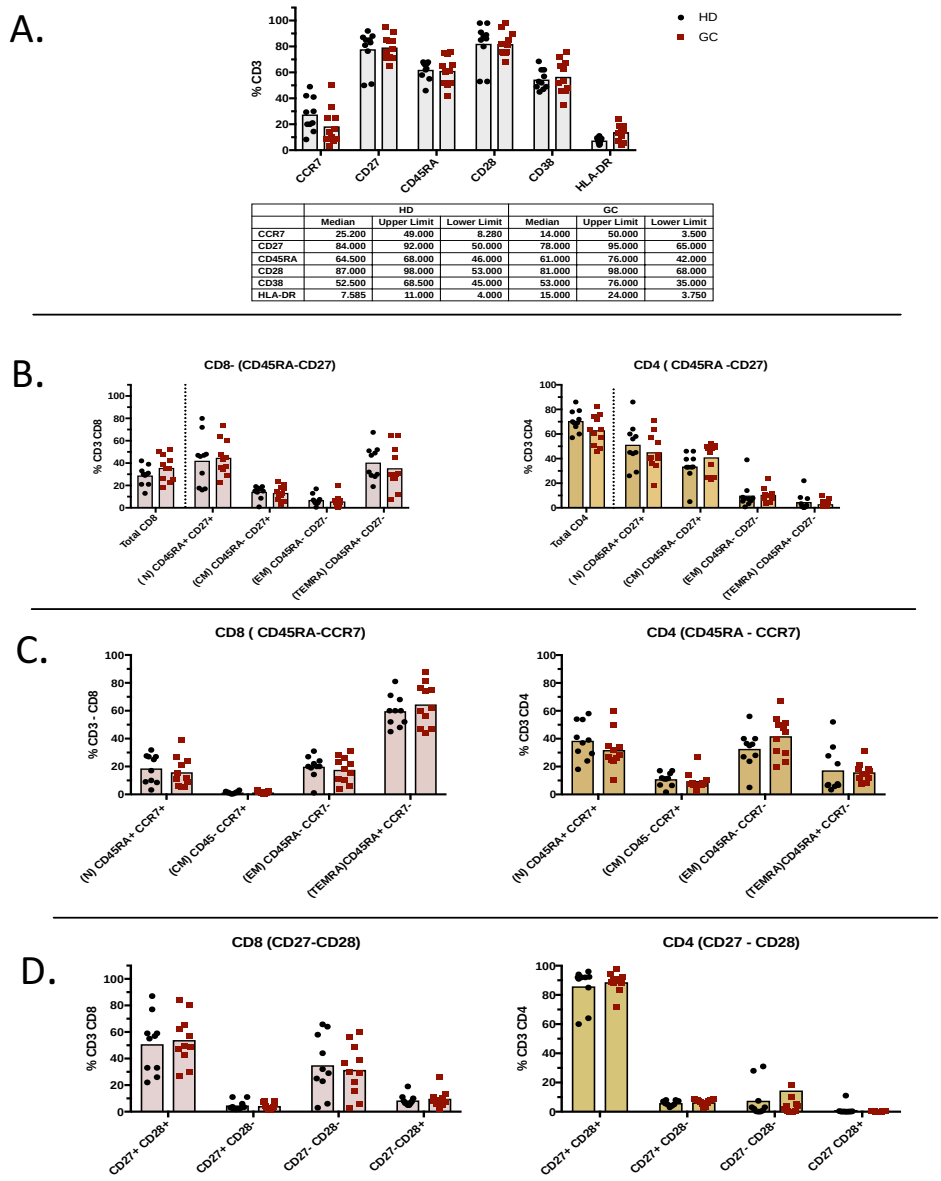

	HD			GC		
	Median	Upper Limit	Lower Limit	Median	Upper Limit	Lower Limit
CCR7	25.200	49.000	8.280	14.000	50.000	3.500
CD27	84.000	92.000	50.000	78.000	95.000	65.000
CD45RA	64.500	68.000	46.000	61.000	76.000	42.000
CD28	87.000	98.000	53.000	81.000	98.000	68.000
CD38	52.500	68.500	45.000	53.000	76.000	35.000
HLA-DR	7.585	11.000	4.000	15.000	24.000	3.750

Figure 43 : The distribution of Effector and Memory CD8+ and CD4+ T cell subsets in GC

PBMCs from GC and HD were stained with T cell activation and differentiation on markers. The function of CD4 and CD8 T subsets were classified by six markers include CCR7, CD27, CD28, CD45RA, CD38 and HLA-DR on total of CD3 T cell (A). Next, (B and C) memory and effectors CD4 and CD8 T cell were classified as naïve (Naïve: CD45RA+CD27+) or (CD4RA+ CCR7+), CM; (CD45RA−CD27+) , or (CD45RA-CCR7) , EM (CD45RA−CD27-) or (CD45RA-CCR7-) and TEMRA (CD45RA+CD27-) or (CD45RA+ CCR7-). (D) classification of CD27 CD28 expression on CD4 and CD8 T cell. (Bars) are mean of percentage values. All data were analysed statistically using U test (Mann-Whitney test), ($P < 0.05$) significantly different.

4.3.3 Augmentation of immune checkpoint inhibitor receptors in GC patients

Panel three was designed to analyze expression of immune checkpoint inhibitors on immune cells in the blood of patients with gastric cancer or healthy controls. Four immune checkpoints, selected on the basis of therapies targeting them being already in the clinic or well advanced in clinical trials, were studied: PD1, TIM3, LAG3 and CTLA4. The expression of CD57 was also measured to determine whether there was a difference in the activation status of the T-cells, given that activation increases checkpoint receptor expression on T-cells; an increased in the expression of CD57 has been reported in blood of GC patients[176].The gating strategy and an example of the quality of the staining is provided in Figure 44. The gates were positioned using FMO controls.

My results (Figure 45) show that there was no difference in the activation status of CD8+ CD57+ T-cells between GC patients and HD controls (p=0.69). Examination of PD1 and TIM3 showed there was no significant difference between GC patients and HD controls (% median 10 vs 12 , p=0.81 and 0.673 vs 0.258 p=0.06 respectively) although two patients has markedly higher frequencies of TIM-3 positive CD8 T-cells. Interestingly, gastric cancer patients have significantly higher frequencies of LAG-3 positive CD8 T-cells and CTLA4 positive T-cells than healthy donors (p=0.015 and p=0.001 respectively). Although these differences were significant, it should be noted that the number of positive cells was always low. With the exception of one patient, who had 5% of CD8 T-cells positive for LAG3, the frequency of LAG3 or CTLA4 positive T-cells was always below 3%.

The results for CD4+ T-cells are shown in Figure 46. As observed for the CD8+ T-cells, there was no significant difference in expression of CD57 (% median 12.4 vs 6.86, p= 0.08640 or PD1 (% median 8 vs 9.13, p= 0.465) on CD4 T-cells from patients vs healthy donors. Like CD8+ T-cells, the frequency of CTLA4-positive CD4+ T-cells was higher in patients compared to healthy donors (%median 2,11 vs 0.35 p=0.0002). In contrast to the CD8 T-cells, patients had no difference in the frequency of LAG3-positive CD4+ T-cells but did have a higher frequency of TIM3 positive CD4+ T-cells (1.86 vs 0.594, p=0.0098).

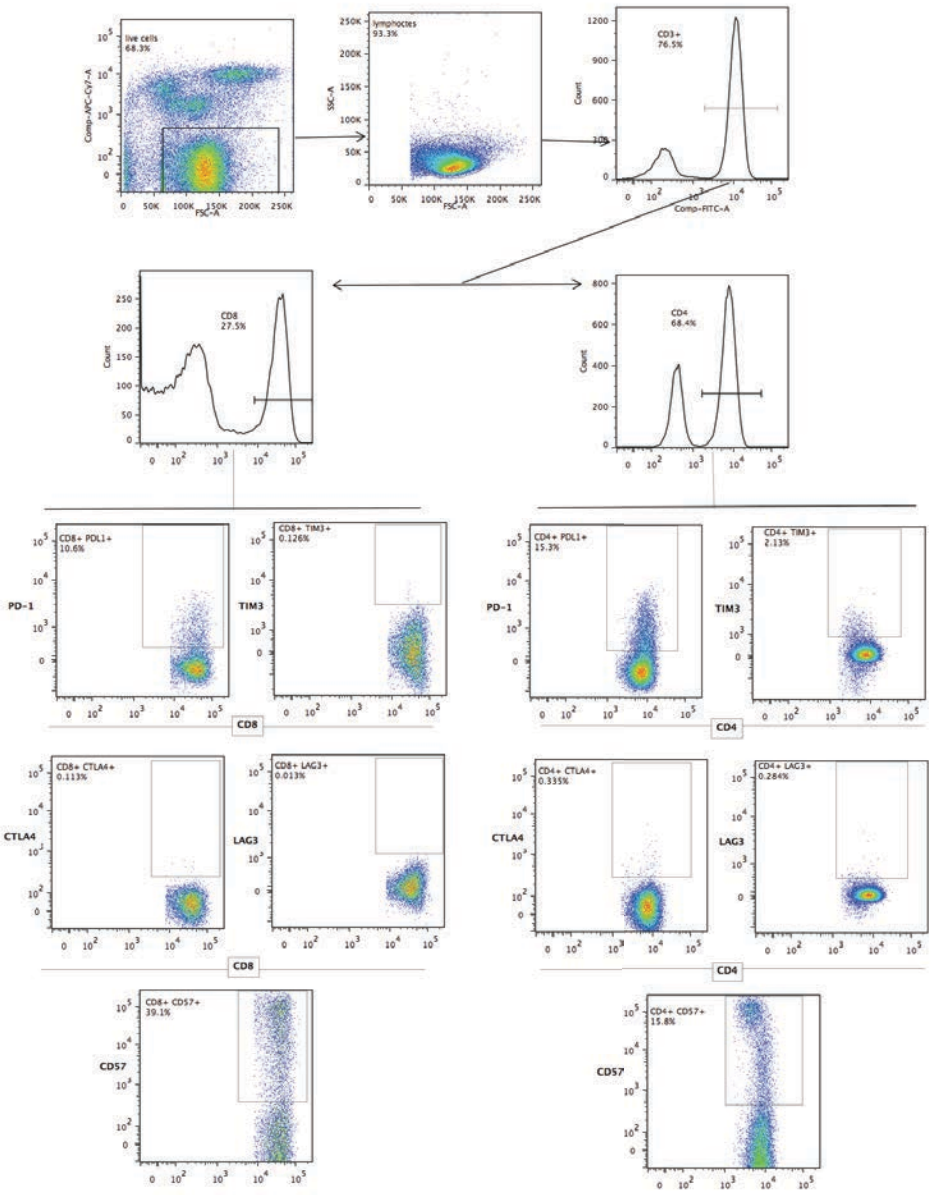

Figure 44 : **Flow cytometry gating for Immune checkpoint receptors**

Immune checkpoint inhibitor markers include PD1, TIM3, LAG3 and CTLA4 were gated on CD4 and CD8 T cells. This gating strategy depended on two controls, unstinted cells and FMO control.

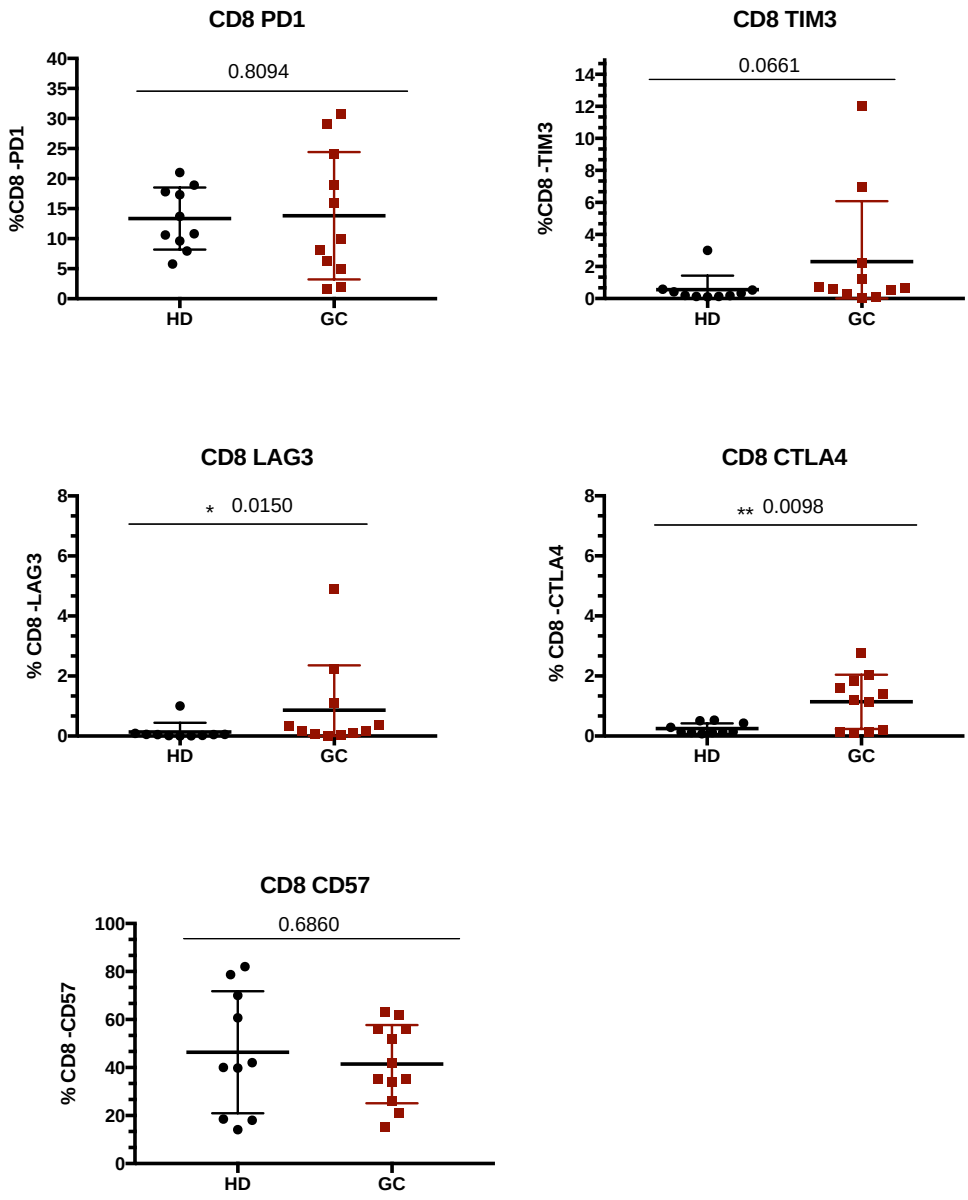

Figure 45 : Expression of immune checkpoint inhibitor receptors on CD8+ T cell

Immune checkpoint inhibitor receptors induced PD1, TIM3, LAG3 and CTLA4 were analysed in GC patients' blood to identify the level of expression compare to healthy subjects. Using flow cytometer, the percentage of expression was detected for every receptor on CD8+ cells population as show in figures above that represent the mean of percentage to compare between GC and HD. data were analysed statistically using U test (Mann-Whitney test), ($P < 0.05$) significantly different

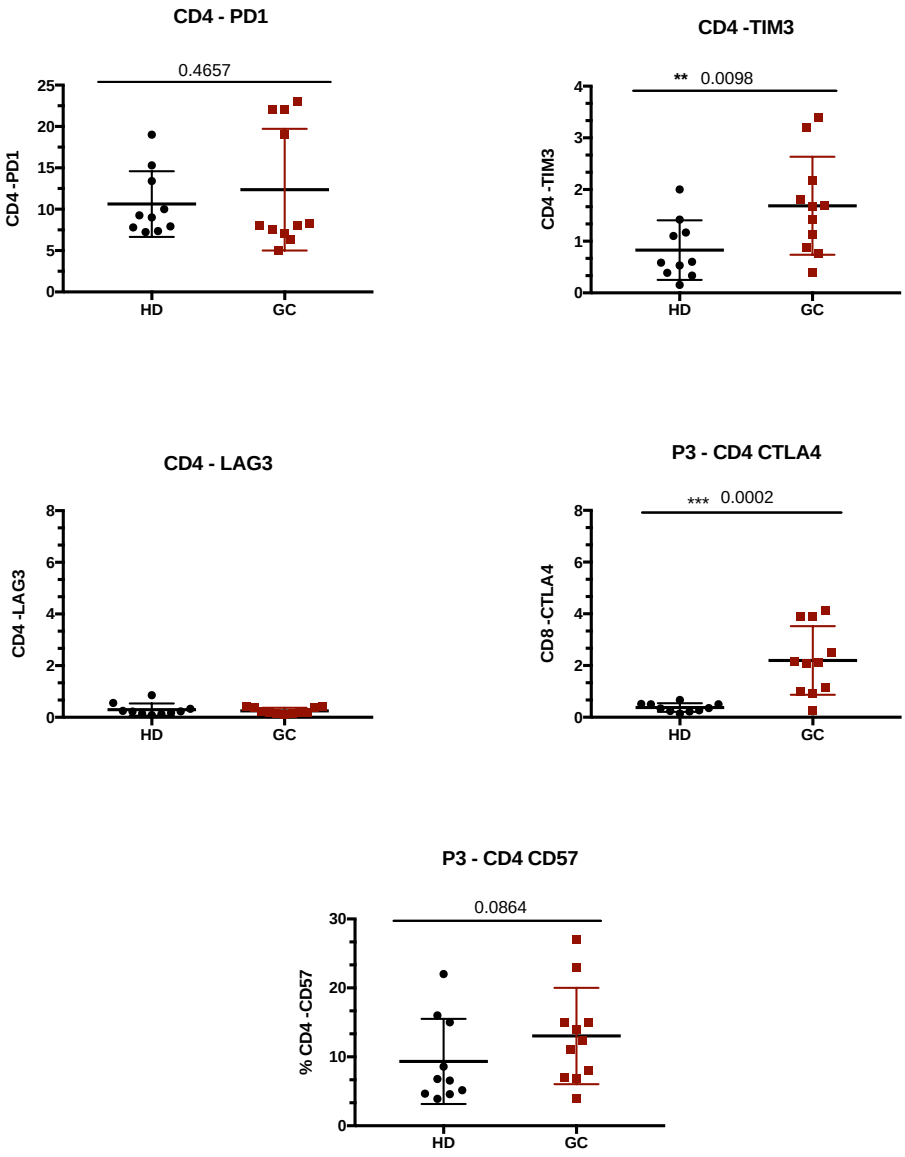

Figure 46: Expression of immune checkpoint inhibitor receptors on CD4+ T cells

Immune checkpoint inhibitor receptors including PD1, TIM3, LAG3 and CTLA4 were analysed in GC patients' blood to identify the level of expression compare to healthy subjects. Using flow cytometery the percentage of expression was detected for every receptor on the CD4+ cell population as show in figures above that represent the mean of percentage to compare between GC and HD. data were analysed statistically using U test (Mann- Whitney test), ($P < 0.05$) significantly different

4.3.4 Analysis of potentially immunosuppressive cells in gastric cancer patients blood

4.3.4.1 The frequency and phenotype of regulatory T cells in GC blood.

Panel four was designed to analyze expression of regulatory T cells in the blood of patients with gastric cancer or healthy controls. The gating strategy is showen in Figure 47a. the frequency of CD25+ CD127- T-reg in CD4 T-cells were found to be significantly higher in GC patients compare to HD controls (mean % ± SEM GC vs HD) 7.89±1.2 vs 3.8 ±0.2 , P= 0.0071.A new strategy to identify regulatory T-cells has recently been described, which uses FoxP3 and CD39 to better identify suppressive T-reg cells . Using this approach, I found, overall, that gastric cancer patients had a significantly higher frequency of FoxP3+CD39+ cells compared to healthy donors (41.26% ± 8.112 vs 17.68% ± 3.063, P=0.02) as show in ***Figure 47***b. Closer examination of the data showed that the gastric cancer patients divided into two groups. Seven patients had a high frequency of FoxP3+ CD39+ cells whereas five patients had lower numbers of FoxP3 CD39+ cells comparable to the frequency measured in healthy donors.

Assessment of another T-reg phenotypic marker, CD45RA, showed that T-regs from gastric cancer patients had a lower frequency of CD45RA negative T-regs (27.17 % ± 3.291 vs 38.9% ± 5.71 p=0.0419) with four patients having particularly low frequencies of CD45RA-positive cells. In contrast, there was no significant difference in the percentage of T-reg that expressed Ki67 (GC 11%± 1 vs HD 9.8%±0.6 , p=0.221).

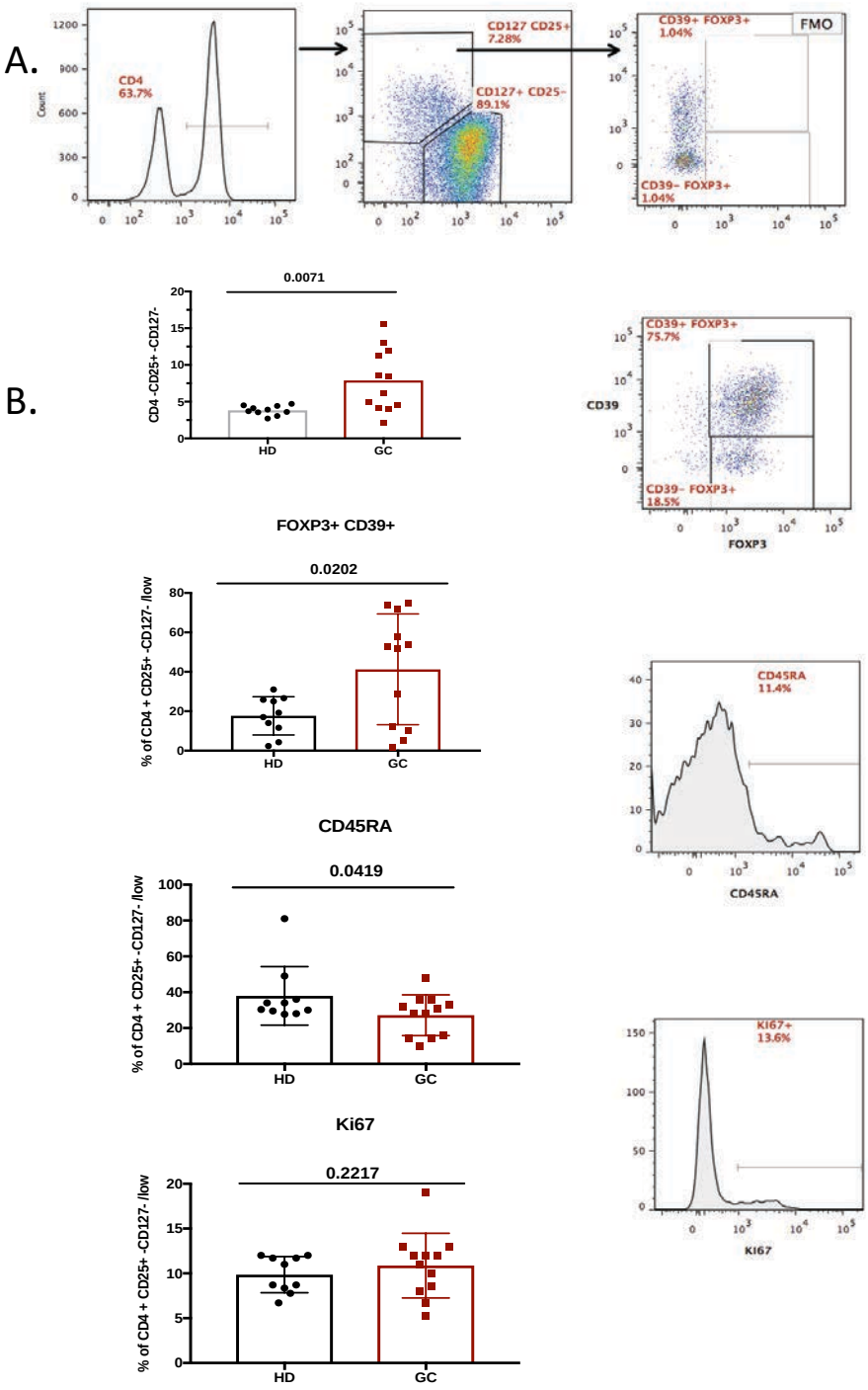

Figure 47,: Monitoring regulatory T cells in GC blood

To examine Treg cells, PBMCs from patients and healthy donors were stained with a panel of surface (viability, CD3, CD4, CD25, CD127, CD39 and CD45RA) and intracellular (FOXP3 and Ki67) markers. (A). T reg were gated as (CD4+ CD25+ CD127-/low FOXP3+ and CD39 +) and T cell non-regulatory cells as (CD4+ CD25- CD127+) based on FMO and unstained cell controls. (B) Treg Cells expressing Foxp3 were determined in HD and GC, and expression of CD45RA and Ki67 in CD25+ CD127-low subpopulation.

4.3.4.2 The frequency and phenotype of Myeloid-derived suppressor cells (MDSCs) in whole blood and PBMCs from gastric cancer patients.

Because granulocytes are lost from PBMC preparations, I analysed fresh EDTA blood from 10 healthy donors and 12 patients to analyse these cells. Whole blood was treated with RBC lysis buffer and leukocytes stained for MDSC surface markers. The gating strategy is shown in Figure 48a, Myeloid M-MDSC cells were detected as Lin-, HLA-DR-, CD33+, CD11b+, CD14+ cells and Granulocytes G – MDSCs as Lin-HLA DR-, CD33+, CD11b+, CD15+ cells. The absolute numbers of cells were calculated using count beads as number of cells/100µl of whole blood. As shown in Figure 48b the median percentage of M-MDSCs in GC blood was not significantly higher than in healthy donors (p=0.1699) but two patients had markedly higher frequencies of these cells, which were three times higher than the rest of the patients. The same results were seen for absolute numbers of M-MDSCS cells. In 100 ul of blood there were 223± 75 cells in gastric patients vs 150± 22 in healthy donors, a difference that was not significant (p= 0.4813) Figure 48c. The two patients who had higher frequencies of M-MDSCs also had higher absolute numbers of these cells. There was no significant difference in the absolute number of G – MDSCS between patients and healthy donors (P=0.431) Figure 48d.

It is well documented that cancer patients may have elevated frequencies of low density granulocytes that co-purify with PBMCs[177]. I therefore also measured M-MDSCs and G MDSCs in PBMCs. I gated M-MDSCs as shown in Figure 49a. The results showed an increased frequency of M-MDSCs in some patients as show in Figure 49b but no significant (P=0.285) differences were seen relative to HD controls. Interestingly, as shown in ***Figure 49***c, G-MDSCs were found significantly greater in patients (P=0.0440) than healthy subjects

A.

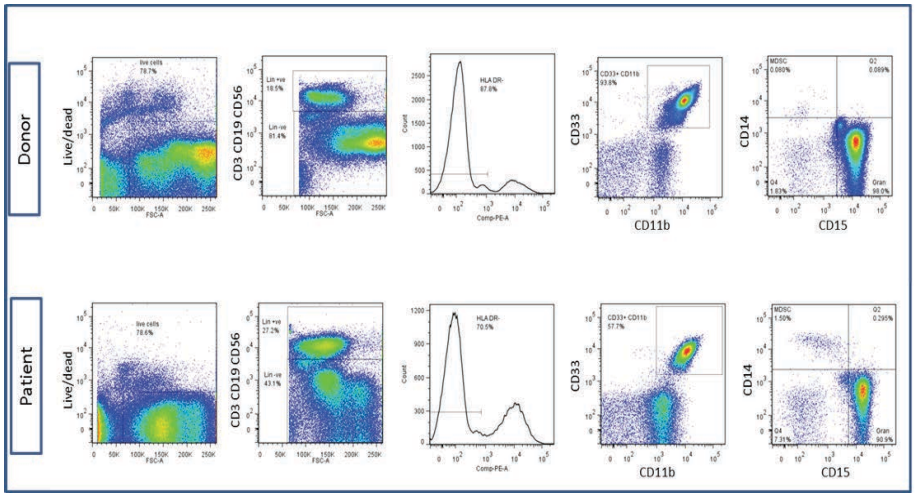

B.

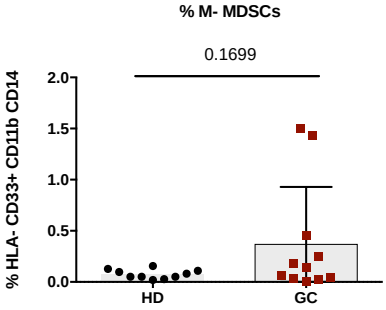

C.

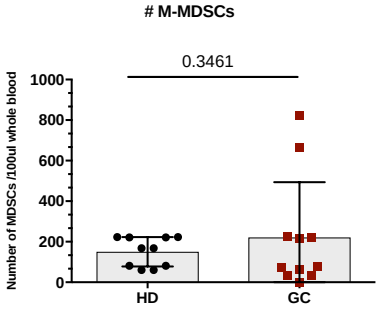

D.

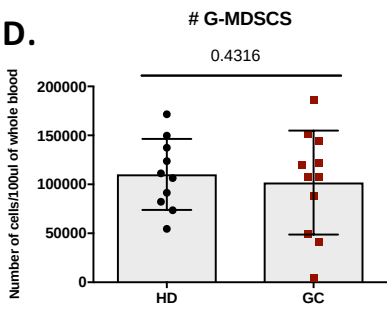

Figure 48 : gating strategy and monitoring of MDSCs cells in Fresh Whole blood

Total cells were analysed after red blood cell lysis of 500µl fresh EDTA blood. MDSC are defined as: singlet, live, CD3-, CD19-, CD56- , HLA DR -, CD33+CD11b+, CD14+) for M-MDSCs and) HLA DR-, CD33+, CD11b+, CD15+). A. Gating strategy for MDSCs. B. the percentage of M-MDSCS. C. the absolute number of M-MDSCs. D. the absolute number of G-MDSCs

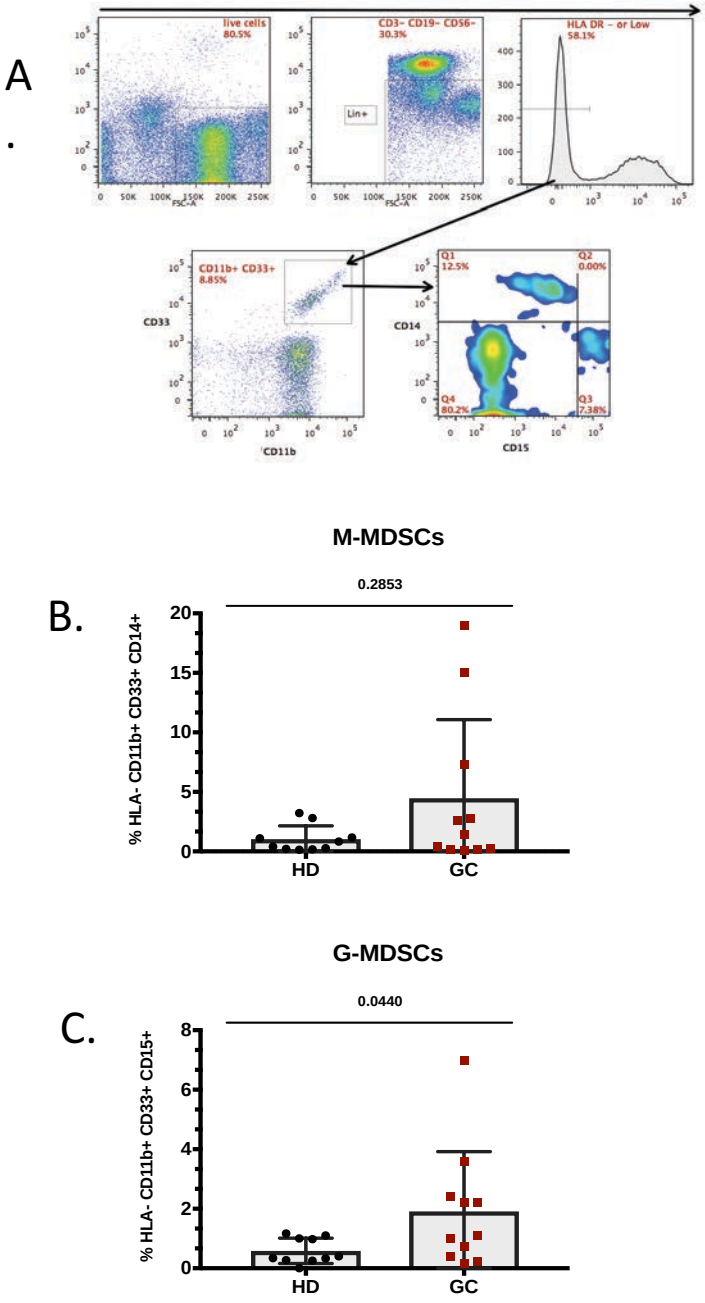

Figure 49 : gating strategy and monitoring of M-MDSCs in PBMCs

A. Gating strategy for M-MDSCs (singlet, live, CD3-, CD19-, CD56-, HLA DR -, CD33+CD11b+, CD14+ or CD15 for G-MDSCs.
B. The frequency of M-MDSCs in HD and GC PBMCs cells
C. the frequency of G-MDSCs in HD and GC PBMCs cells

4.4 Summary and Discussion

The fourth most common cause of cancer-related death in the world is Gastric Cancer[33]. Throughout EBV is detected in about 10% of GC cases and around 80,000 new cases

It is currently unclear what the status of EBV-specific immunity is in GCa patients. My study sought to understand how best to harness EBV-specific immunity to develop immunotherapy for patients with EBV-associated cancer by measuring T-cell immunity to the EBNA1, LMP1, LMP2 and BARF1 antigens that are expressed in the malignant cells of GCa. Immunity to EBV antigens measured in patients with EBV-positive and EBV-negative disease would have been desirable, but EBV testing of patients is not currently performed. Furthermore, the number of patients was too low to allow a meaningful subgroup analysis to be performed.

Generally, I found that there were no significant differences in T cell response to EBV antigens between donors and patients according on the mean value of T cell response. My results also showed the size of T responses in healthy donor (HD) was higher than patients (GC) except EBNA1, where the response was slightly higher in patients. Like HD the T cell response was found the higher with EBNA1 and EBNA3A in GC patients.

I have succeeded through this study in determining the T response in the blood to EBV antigens using a newly developed TNFa culture assay. However, these results may not reflect the full response of T cell to EBV tumour antigens in gastric cancer patients, I need to study more patients, especially as I have had difficulty in obtaining sufficient blood from the patients recruited to this study.

There are several known tumor associated antigens in the case of gastric cancer. Immune responses to most of these antigens have previously been detected in blood as humoral responses [73, 167, 168]. It is unclear what the status of tumour antigens - specific immunity is in GC. So, in this study I have investigated T cell response to cellular tumour antigens including CEA, MUCIN1, MAGEA1, MAGEA3, MAGE4 and NY-ESO-1 antigens which were found expressed in gastric cancer patients. My study is the first to compare the T response between these tumor antigens in GC patients' blood as well as comparing the response to HD blood. My results show that T cells from patients and donors responded to tumour antigens with variation of recognition. While the T response level was low, I have seen s differences between the mean value in GC and HD with some antigens. I found that T cell responses in GC patients to MAGEA1, MAGEA4, and NY-ESO-1 were more than HD. Interestingly, significant T cell response to MAGEA1 with GC patients compare to healthy subjects. Unlike donors, patient's T cells did not recognize CEA antigens as I expected. So, from this preliminary finding an important future question to address is why T cell did not response to CEA with the patients, especially as this antigen is the most elevated antigen in stomach cancer, as described by previous studies analysisng serum and Tissue[167, 178]. However, CEA-specific T cell response were generated after vaccinated colorectal cancer patient with CEA-loaded dendritic cells [179] Howevr, CEA signalling were found supresses the activation of human T cells[180]. In human gastric cancer, NY-ESO-1 was defined as being a taret of CD8 T cells that were negatively regulated by TIM3 and PD1[181]. Where correlation with antibody response CD4 T cell response to NY-ESO-1 in cancer patients[182] and specific cytotoxic CD4+ T cells in melanoma patients. Moreover , MAGE-A3 and MAGE-A4

were naturally detected by specific CD4+ T cell in neck cancer patients[183] .while spontaneous CD8 T cell response to MAGEA3 antigens in melanoma patients[184].

The immune system plays an important role in the pathogenesis and progression of gastric cancer[65, 66]. CD4+ and CD8+ T cells play a central role in the antitumor immune responses as main types of lymphocytes in cell mediated immunity. in the peripheral blood, the frequency of CD4+ and CD8+ T cells and the CD4+/CD8+ ratio was reported changes due to reduced percentage of CD4+ T in patients with different of cancers[185]. However, other studies have found normal ratio in other cancers. In my study, I found increased mean percentage of CD8 T-cells in PBMCs of GC Patients compared to healthy subjects. I also found that the mean of the CD4/CD8 ratio was lower in GC patients compared to HD but the difference was not significant.

I found that the percentage of B cells CD19+ in the lymphocytes is significantly different between GC patients and HD control with the results showing decreased B cells in the former. Recently, B cells have been reported to be present at lower levels in cancer patients with different type of cancers include GC [67] but also lung and breast cancers [186]. Moreover, in this study I also studied the incidence of gamma delta T cells in GC patients and HD control. I found that the mean of percentage gamma delta (γδ)T cells in CD3 population was increased in GC patients but was not significant t. Previously, in the peripheral blood the proportion of γδ T cells in GC patients was found to be higher in compared to healthy controls[68] this may explain the role of γδ T cells as antitumor to gastric cancer.

Immune checkpoint inhibitor receptors include PD1, TIM3, LAG3 and CTLA4 were analysed in GC patients. I measured the expression of inhibitory receptors on CD4+ and CD8+ T cells in PBMCs from GC and HD. In this study, the expression of LAG3 and CTLA4 was significantly increased in GC on CD8 T cells where the mean of TIM-3 was found more in GC, No significant differences were seen with PD1 and CD57 expression. For the CD4 population, expression of TIM3 and CTLA4 were found significantly evaluated in GC patients. I also found that the mean of PD1 and CD57 was higher in GC patients. However, PD-1 were found expressed on CD4+ and CD8+ T cells from GC patients was significant higher than that from healthy controls in PBMCS [65] and increased in PD1 , TIM3+ CD8 [187]. The frequency of CD4+ and CD8+ LAG3 cells were reported increased in blood of GC patients[188]. CD57 T Lymphocytes is considered correlated in prognosis in cancers[189, 190], moreover, in the peripheral blood of patients with advanced GC prognostic value of CD57 T lymphocytes have been reported[176].

Immune suppressor cells include T reg and MDSCs play an important role in cancer immunity. For that, it's important to identify the status of these cells in GC patient peripheral blood. I found that significant increase of Treg cells in GC patients in compared to HD. Moreover, CD45RA expression was found low in patients which reflect effector activator Treg cells in blood of patients. To identify the status of activation of T reg, I studied the expression of Ki67 and found it was slightly increased in GC patients but not significantly differences. However, there is little information about the frequency of T reg cells in peripheral blood with GC patients in compare to other types of cancers. In early study, increased T reg cells in PBMCs from GC

patients were reported but using surface markers for CD4 CD25 population[191]. Subsequent studies show accumulated T reg cells in patient blood[192, 193].

I have studied the frequency of MDSCs in whole fresh blood and PBMCs. I found that the frequency of M- MDSCs in Whole blood was elevated in some GC patients but not all according to the percentage or absolute number of cells. we also found no significant differences have seen with G –MDSCS number cells. in PBMCs, the results found that increased in the frequency of M-MDSCs in some of patients but no significant differences have seen compared to HD controls. But interestingly, G-MDCSs were significantly greater in gastric patients in this study. Recently these cells have been reported evaluated in PBMCs from cancer patients[177] [194]. Previously, MDSCs were reported elevated in GC patients as (CD33+ CD11b+) population[195].

CHAPTER 5: RESULTS

5 THE FUNCTION AND PHENOTYPE OF IMMUNE CELLS WITHIN GASTRIC TUMOURS

5.1 Introduction

The tumor microenvironment complex [15] comprising of malignant cells but also many other components including cancer parenchyma cells, mesenchyme cells, fibroblast, blood, and lymph vessels. Other components are tumor-infiltrating immune cells, cytokines, chemokine, cancer cells, stromal tissue and extracellular matrix[196].

The lymphocytes are found within the tumor and tumor stroma[197]. They can be isolated and expanded in the laboratory to generate tumour infiltrating lymphocyte (TIL) preparations. When these are administered to the original patients, they can re-infiltrate tumors to initiate tumor lysis. Most TILs are T lymphocytes[69]. In vitro, therapeutic tumor infiltrating lymphocytes are usually isolated from tissues and cultured with cytokines, such as interleukin 2[70]. In fact, TILs are considered a form of adoptive immunotherapy. Moreover, TIL dynamically change during tumor progression and in response to antitumor therapy.

In the tumor microenvironment, immune cells play important roles in tumorigenesis and tumor control[15]. Multiple types of immune cells are involved in tumor control including cytotoxic T lymphocytes, which can recognize tumour antigens expressed by cancer cells and kill those cells[198], and NK cells which can kill cancer cells in various cancer models[199, 200].. As well as direct killing of cancer cells, activated cytotoxic T lymphocytes and NK cells secrete cytokines including TNFa and IFN-γ that have anti-tumour effects [201].

On the other hand, the immune microenvironment plays a role in promoting tumor progression. The recruitment of MDSC and T reg cells contributes to immunosuppression in tumor microenvironment[202, 203]. Recently, MDCSs have been reported to be present in several cancers tissues such as breast cancer, pancreatic adenocarcinoma and glioblastoma[204-206]. Moreover, MDCS secrete immunosuppressive cytokines like TGF-β and IL-10 and induce T reg cells [202]. Furthermore, accumulation of T reg cells and tumor derived factors such as TGF-b and IL-10 within TME were reported with different cancers[207, 208]. Inhibitory immune checkpoint molecules are also upregulated, such as PD-

1, TIM-3, CTLA-4 and LAG-3 that limit T cell activation and proliferation during immune response to cancer cells [209, 210] .

Clinical trials of TIL therapy have been established with some cancers. In metastatic melanoma patients TIL infusion reduced tumours in half of cases [211]. Moreover, TIL therapy has been investigated in clinical trials to treat colorectal cancer, cervical cancer, breast cancer and ovarian cancer with reports of improved patient outcomes [69, 212, 213].

A study investigating the prognostic impact of immune cells in gastric cancer found that low density of immune cells correlated withthe presence of regional metastasis and poor prognosis [214]. A small number of studies have also reported the clinical prognostic impact of density of immune cells in the subset of patients with EBV disease [215] and these show similar results to the wider group containing all gastric cancers[216] .

Based on the above, In this study I have investigated the phenotype of immune cells in the tumor microenvironment of gastric cancer patients. I have measured the presence of T-cell specific for EBV-encoded tumour antigens and cellular tumour associated antigens. I also have investigated the phenotype of immune cells within the gastric cancer microenvironment cells, and in some cases compared these to the same cells in the blood of the same patient. Finally, I have studied whether it is possible to generate TIL cells from gastric tumours to assess the potential for TIL-based therapy of gastric cancer.

5.2 Isolation of Tumor infiltrating lymphocytes cells from gastric cancer tissue

To obtain TIL cells from the tumor microenvironment, tissues were processed using two protocols. The first was digestion of the tissue by collagenase D and dissociation. The second was to culture tumour tissue in TIL medium, allowing immune cells to exit the tissue. Following isolation of the immune cells they were expanded as described to generate TILs. **Table *15*** presents the results obtained from 14 gastric cancer tumours using these two methods and the number of TIL after in vitro expansion.

Table 15: Generation of Tumor infiltrating lymphocytes cells from GC patient tissue

	weight of whole tissue (gram)		Number of digestion TIL ($X10^6$)		Number of culture expanded TIL ($X10^6$)
patient	tumor	Non- tumor	Tumor	non-tumor	tumor
P2	0.9	-	4	-	-
P3	0.8	1.1	2.3	5	-
P4	0.7	0.9	2.8	3	-
P5	0.8	1	3.5	-	-
P13	0.5	-	2	-	200
P14	0.8	1.2	3.7	4	250
P15	0.7	0.9	2.9	3	200
P16	0.8	1	2.5	3.1	190
P17	0.7	1.1	3	3.6	250
P18	0.9	1.2	2.6	3.2	220
P19	0.7	0.9	2.5	3.4	290
P20	0.5	0.8	2.6	2.9	180
P21	0.6	0.8	2.2	3.8	200
P22	0.4	-	-	-	190

Note: three (2-3mm) pieces of tissue were cultured, two pieces were used for DNA extraction where remaining tissue were digested with collagenase.

5.3 Study of antigen-specific T-cells in Tumour infiltrated lymphocytes from gastric cancer tumour tissue using a cultured immune assay.

5.3.1 EBV tumour antigen-specific T cell response from TIL cells

To identify the level of T cell recognition to EBV antigens in gastric cancer patients, immune cells from patients (n=9) were stimulated with five latent EBV tumour antigen pepmixes (EBNA1, LMP1, LMP2, BARF1 and EBNA3A) using a T-cell culture assay I developed. The antigen-specific T-cell response was measured after 6 hours or after ten days of culture. Results from a single patient is shown in *Figure 50*.

T-cell responses against EBV antigens were observed in many patients with gastric cancer. A representative cultured TNFa response within 6 hours is shown in *Figure 51*a, Overall, T-cell responses to EBNA3A and LMP2 were detected in 33% (3/9), to EBNA1 were 22% (2/29) of patients with TIL cells. No response was detected to the LMP1 and BARF1 antigens. The results also showed that the frequency of EBV antigen-specific CD8+ T cells was greater than antigen-specific CD4+ T cells as show on figure 2a. Next, the size of the T cell responses were measured after ten days culture in vitro. The results show changes in the level of response to antigens as shown in *Figure 51*b. EBNA1 – specific T responses were detected in 44% (4/9), with same number of patients EBNA3A specific response were detected. Specifically, T cell responses to LMP1 and LMP2 were detected in one patient. No BARF1-specific responses were detected.

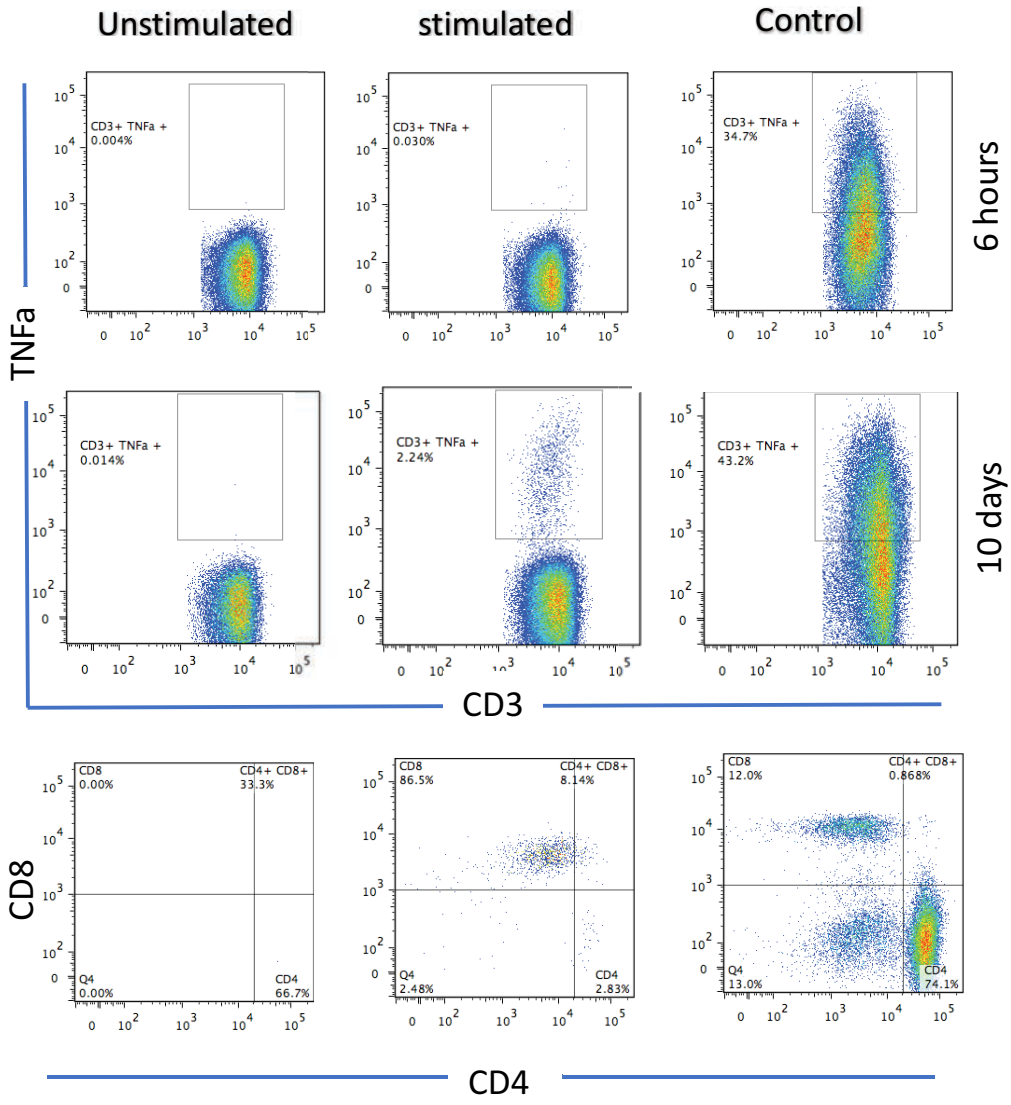

Figure 50: measuring antigens specific – T cells response on TIL cells

Expanded tumor TILs from patients were stimulated by EBV or tumor antigens pepmixes . After cultured part of cells for 6 hours with TNFa antibody, cells were stained with other surface marker then analysis. Remaining cells were cultured for 10 day then cells were re-stimulated for 6 hours as above before analysis by flow cytometer. The T cells response gated as CD3+ TNFa+ then classified to CD4 or CD8. Unstimulated TILs were used as negative control, TILs and anti-CD3 antibody were used as postive control.

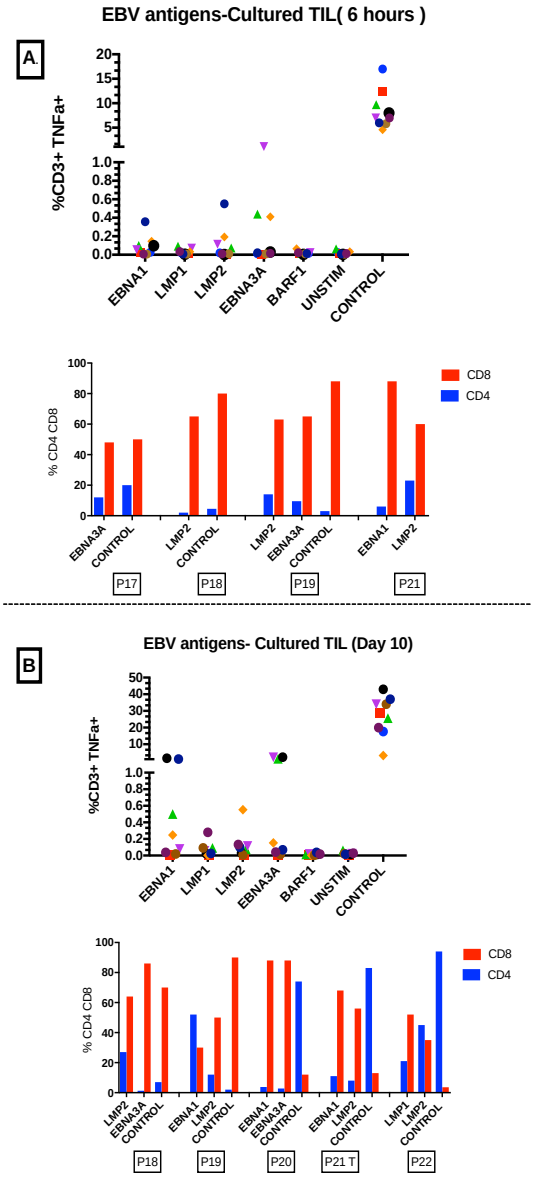

Figure 51 :EBV tumour antigen specific T cell responses ex vivo or after 10 day in vitro culture.

Cells from gastric cancer patient tumours (n=9) were stimulated with five latent EBV tumour antigens pepmixes using a newly development T cell culture assay. Cells were tested for antigen specificity after 6hours or after 10days of culture by flow cytometry. The CD3+ TNFa+ T cells responding to antigen were then classified as CD4 or CD8. Unstimulated TILs were used as negative control, TILs treated with anti-CD3 antibody were used as postive control.

In general, no significant differences were observed in this study but, interestingly, T cell responses were found decrease to antigen and increased to other after cultured assay with some patient's TIL cells. The frequency of EBV antigens -specific CD8+ T cells was greater than antigens-specific CD4+ T cells except three control TIL cells when the frequency of CD4 cells were found higher that CD8 Cells.

5.3.2 Tumor associated antigen-specific T cell response from TIL cells

In this study, several tumour antigens including: NY-ESO-1, MUCIN1, MAGEA1, MAGEA3, MAGEA4, CEA and PSMA were selected based on prior evidence of expression in gastric cancer or detection of specific antibodies in patients. T-cell responses to these antigens were measured by the cultured assay using appropriate pepmixes. Isolated TIL cells from tumour tissue of GC patients (n=9) were stimulated and cultured with these pepmixes then T cell response was detected by developed TNFa cultured assay after six hours and ten days culture. A typical result is shown In *Figure 52*. Across the study cohort, after six hours of culture (figure A), I detected T-cell responses to PSMA antigens in three patients but the level of was low and not significantly different when compare to unstimulated control cells. No T cell for other antigens was detected. As shown in figure A, PSAM –specific CD8 T cell response found greater than CD4 response. After ten day cultured *Figure 52*b, results found low level of MUCIN1 – specific CD8 T cell response with one patients but none was been seen for the other antigens.

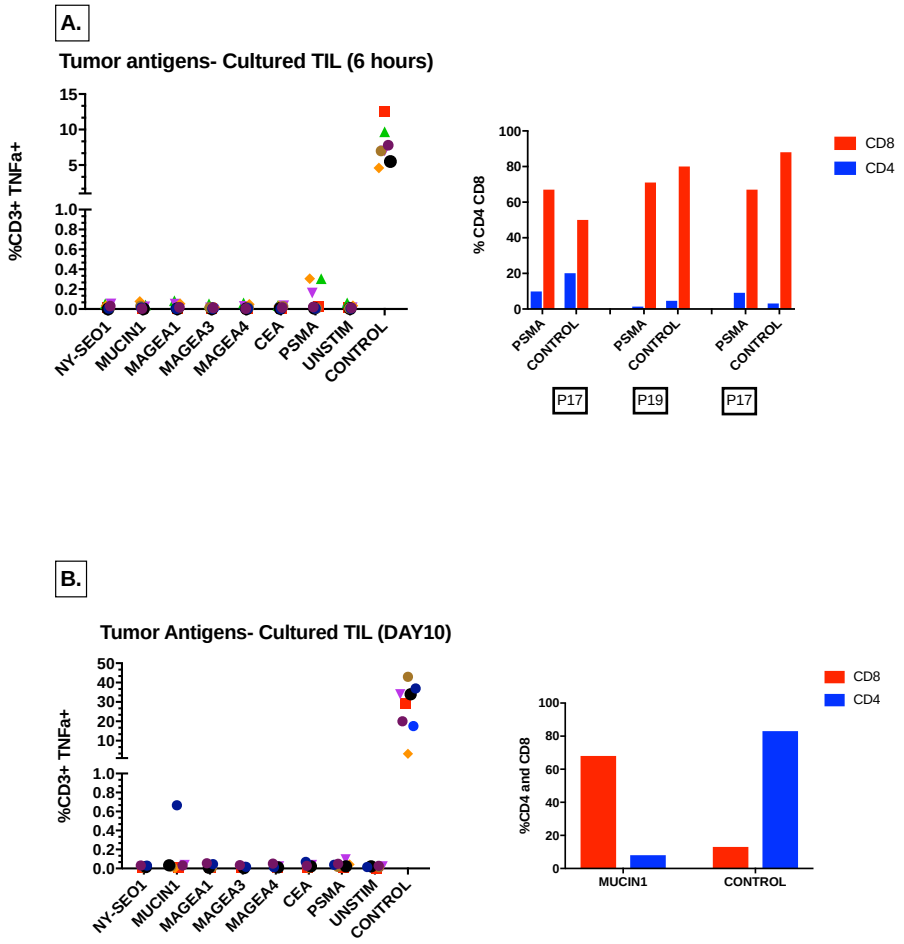

Figure 52:tumour associated antigens specific T cell response on TILs from tumour tissue

Immune cells from patients (n=9) were stimulated with seven tumour associated antigens pepmixs using newly development T cell culture assay. After cultured part of cells for 6 hours with TNFa antibody, cells were stained with other surface marker then analysed by flow cytometry. Remaining cells were cultured for 10 day then cells were re-stimulated for 6 hours as above before analysis by flow cytometer. The T cells responding to antigen were gated as CD3+ TNFa+ then classified to CD4 or CD8. Unstimulated TILs were used as negative control, TILs and anti-CD3 antibody were used as postive control.

5.4 Studying the immune cells in gastric cancer patients ex vivo.

In this part of the study I investigated the frequency and properties of immune cells in Tumor and Non-tumor tissue from gastric cancer patients. I used five separate flow cytometry panels to stain cells isolated from the tissues of gastric cancer patients.

5.4.1 Classification of lymphocyte subsets in Tissue of GC patients.

5.4.1.1 Comparing infiltrating lymphocytes between Tumor and Non-Tumor Tissue.

The frequency of lymphocyte subsets including: CD4 and CD8 T-cells, B-cells, NK cells and gamma/delta T-cells were measured in tumor and non tumor tissue of GC patients. The results were measured using flow cytometry as described in the previous results chapter. The relative frequencies of CD4 and CD8 T-cells are presented in *Figure 53*a, the percentage of % median in Tumour vs Non-tumour tissue, CD4 (60 vs 22) and CD8 (28 to 51). There was a significant difference in the frequency of CD4 (p=0.0015) and CD8 T-cells (p= 0.014) with CD4 increased and CD8 decreased in tumour tissue compared to non-tumour tissue. The results show a significan difference in the CD4:CD8 ratio (P= 0.023) between Tumour (median 2.4) and non-tumour (0.4). However, 100% of non-tumour had a CD4:CD8 ratio of less than 1.0 whereas only 28% of tumour sample had a ratio of less than 1.0. as shown in figure 4a**.**

*Figure 53*b shows the frequency of CD19-positive B cells. The percentage of B cells in the lymphocyte population was not significantly different between tumor and non-tumor. The frequency of gamma/delta T-cells is shown in *Figure 53*c. The mean percentage of gamma delta (γδ) T cells in the CD3 + lymphocyte population was higher in 5/7 tumor tissues; this difference was statistically significant compared to non-tumor tissue (P=0.0256).

The frequency of different subsets of NK cells, including NKT cells, is shown in. *Figure 54* . The median percentage of CD3+ CD56+ NKT cells in tumor tissue (3.5) compared to non-Tumor (0.6) was significantly higher (p=0.0199). Moreover, the results showed a significant difference (P= 0006) in the frequency of CD16- CD56dim NK cell which were increased in tumor tissue as shown in *Figure 54*.

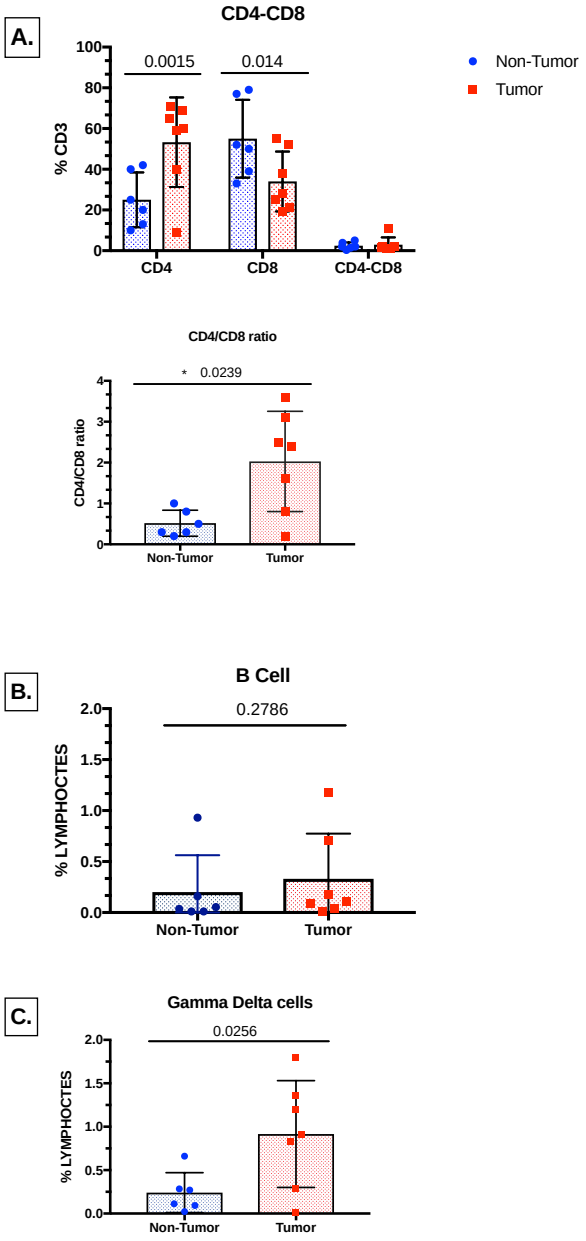

Figure 53:Classification of lymphocytes subsets on TILs from tumor and non-tumor fresh tissue

Isolated TILs from fresh tumor and non-tumor tissue were stained using a panel of antibodies to identify major lymphocyte populations. A. Percentages of CD4 and CD8 and the ratio of CD4/CD8 on CD3 cells . B. Percentage of B cell (CD19) in lymphocytes population. C. Percentage of gamma delta T cell on CD3 population. All data were analysed statistically using (Mann- Whitney test) , ($P < 0.05$) significantly different.

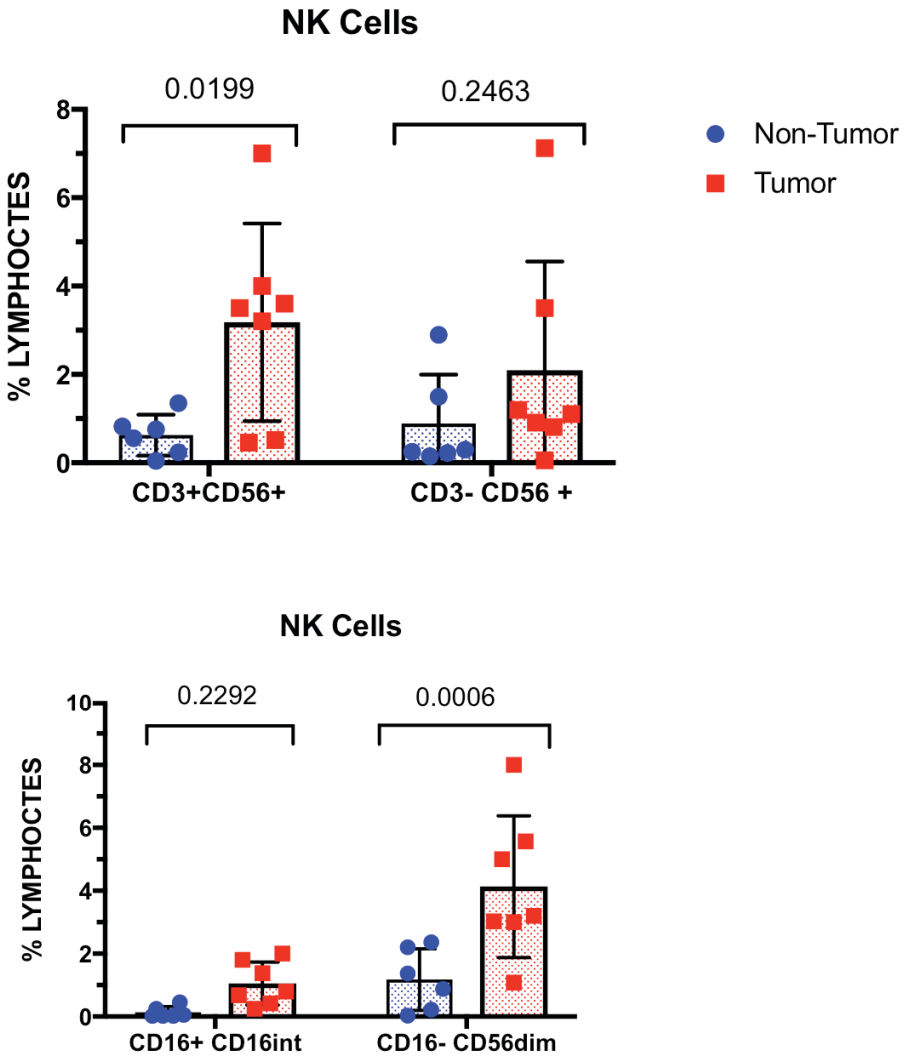

Figure 54: Comparison of NK cells on TILs from fresh tumor and non-tumor tissue

TIL cells were stained using a panel of antibodies to detect different NK cells populations. Top figure, show CD3+ /- CD56 population include NKT cell and NK cells . Bottom figure, show subtype of NK cells subpopulation. (Mann- Whitney test) , $P < 0.05$ significantly different

5.4.1.2 Analysing the status of lymphocyte subsets between fresh digested TIL and cultured TIL cells from tumour tissue.

Production of large numbers of Tumor Infiltrating Lymphocytes is necessary for adoptive T-cell immunotherapy. The phenotype of TIL cells produced by ex vivo culture (the time when they would be used to treat patients) is clearly important. to begin optimizing the production of TIL from gastric cancer tumours, I used flow cytometry to study the immunological status of lymphocytes isolated immediately after tissue dissociation (dTIL) and the same cells after expansion in culture (eTIL)..

First, the frequency of lymphocytes subsets was analyzed to compare between dTIL and eTIL. The relative frequencies of CD4 and CD8 T-cells are presented in *Figure 55*a. There was no significant difference in the frequency of CD4 and CD8 T-cells nor was there a difference in the CD4:CD8 ratio between eTIL (median 2.33) and dTIL (2.4).as shown in *Figure 55*b. Furthermore, the percentage of B cells in the lymphocyte population was significantly lower in eTIL than dTIL (p=0.0312) as shown in figure c. The frequency of gamma/delta T-cells is shown in *Figure 55*c. The mean percentage of gamma delta (γδ) T cells in CD3-positive lymphocytes was lower in expanded TIL , this difference was significant (P= 0.0181) compare to digested fresh TIL. The frequency of different subsets of NK cells, including NKT cells, is shown in *Figure 56*. The percentage of CD3+ CD56+ NKT cells was significantly higher in expanded TIL compared to Fresh dTIL . There were no significant differences in the frequency of other NK cell types.

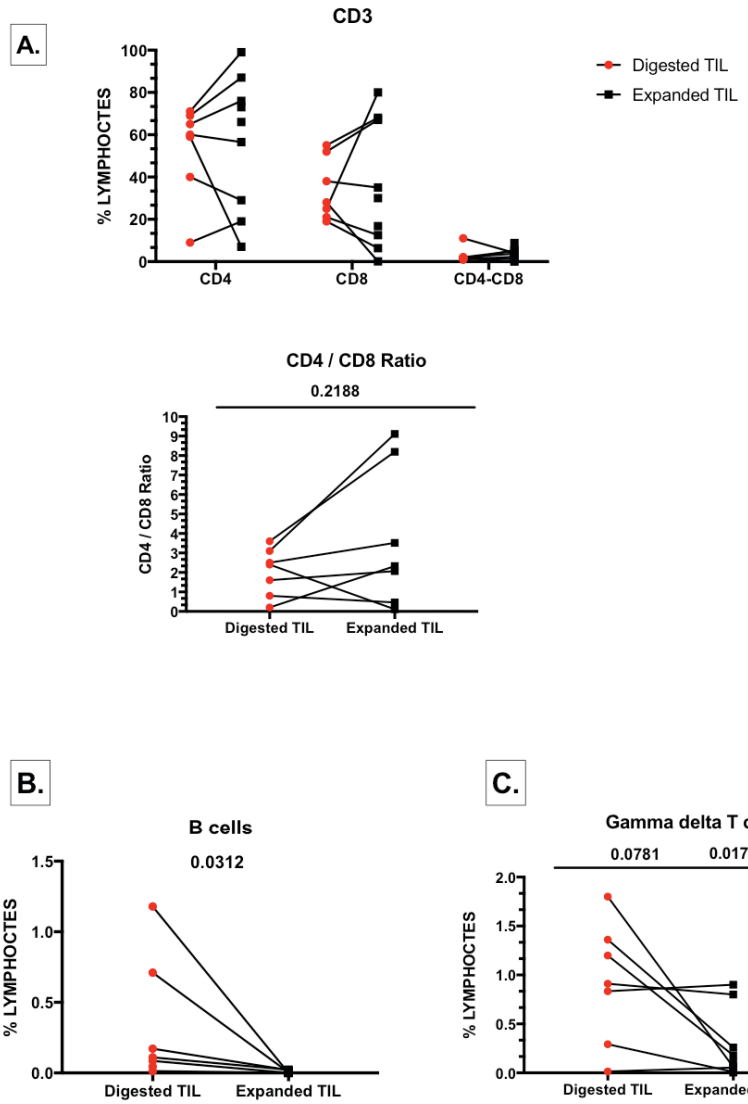

Figure 55: Analysing the status of lymphocytes subsets between lymphocytes freshly isolated from tumour tissue and after in vitro expansion.

Expanded TILs and lymphocytes from digested tissue (digested TIL) were stained using a panel of antibodies to measure lymphocyte subsets.. A. the frequency of CD4 and CD8 and the ratio of CD4/CD8 on CD3 cells . B. the frequency of B cell (CD19) in lymphocytes population. C. the frequency of gamma delta T cell on CD3 population. All data were analyzed statistical ($P < 0.05$) significantly different.

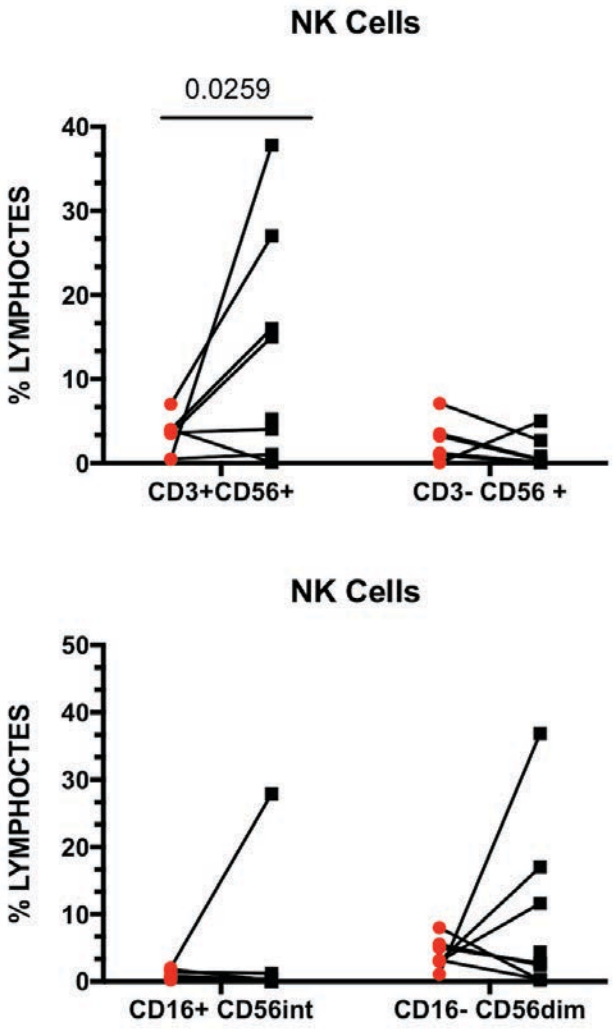

Figure 56: Comparison of NK cells on TILs from fresh digested and cultured tumor tissue

Eexpanded TILs and fresh TILs cells were stained using a panel of antibodies marker for NK cells populations. Top figure, show CD3+ /- CD56+ population include NKT cell and NK cells. Bottom figure, show subtype of NK cells subpopulation

5.5 The distribution of Effector and Memory CD8+ and CD4+ T cell subsets in Tissue of GC patients.

To measure the status of effector and memory cells in Isolated TIL cell from Tumour and non-tumour tissues in addition to comparing between fresh digested TIL to Expanded culture TIL I designed a flow cytometry antibody panel to study the phenotype of CD4 and CD8 T-cells. Six markers were used: CCR7, CD27, CD28, CD45RA, CD38 and HLA-DR. The gating strategy used is described in the previous chapter.

5.5.1 Effector and Memory isolated TIL cells from Tumour and non-tumour Tissue

The phenotype of the bulk CD3-positive population as well as the CD3+CD8+ T-cells and CD3+ CD4+ T-cells are presented in *Figure 57*a. In comparison between TIL from tumour and non-tumor in the bulk of CD3 population, the median percentage of CD28 and HLA-DR expression were significantly increased on T-cells from tumour tissue compared to non-tumour (67 vs 46, P=0.0150 and 64 vs 29 respectively). The frequency of CD27 on T-cells was increased in tumour (55 vs 47) whereas CD45RA was deceased in tumor (34 vs 50) in comparison to non-tumour although these differences was not significant. The was no differences in CCR7 and CD38 expression.

The frequency of the CD8+ T-cell population is presented in *Figure 57*b. Using CD45RA and CD27 to sub divide CD8 T cells, the results show the frequency of TEMRA (CD45RA- CD27-) and EM (CD45 CD27) were increased in non- tumor tissue whereas the frequency of Naïve and Effector memory were higher in tumor tissue.

These results indicated that significant differences in naïve (p=0.0099), CM (p= 0.0011) and TEMRA (p= 0.0005) existed between tumor and non-tumor tissue. However, according to CD8 (CD45RA CCR7), the results showed that EM and TEMRA were significantly increased in tumor tissue (p=0.0113) and both naïve and CM were decreased (p=0.0021) compared to non-tumor.

The frequency of CD4+ T-cells is presented in *Figure 57*c. According to CD45RA CD27 staining in both Tissue and non-tumor tissue groups TEMRA cells were increased but there were no significant differences between groups. However, with CD45RA and CCR7 staining most of the cells were TEMRA in tumor and non- tumor tissues with no significant differences

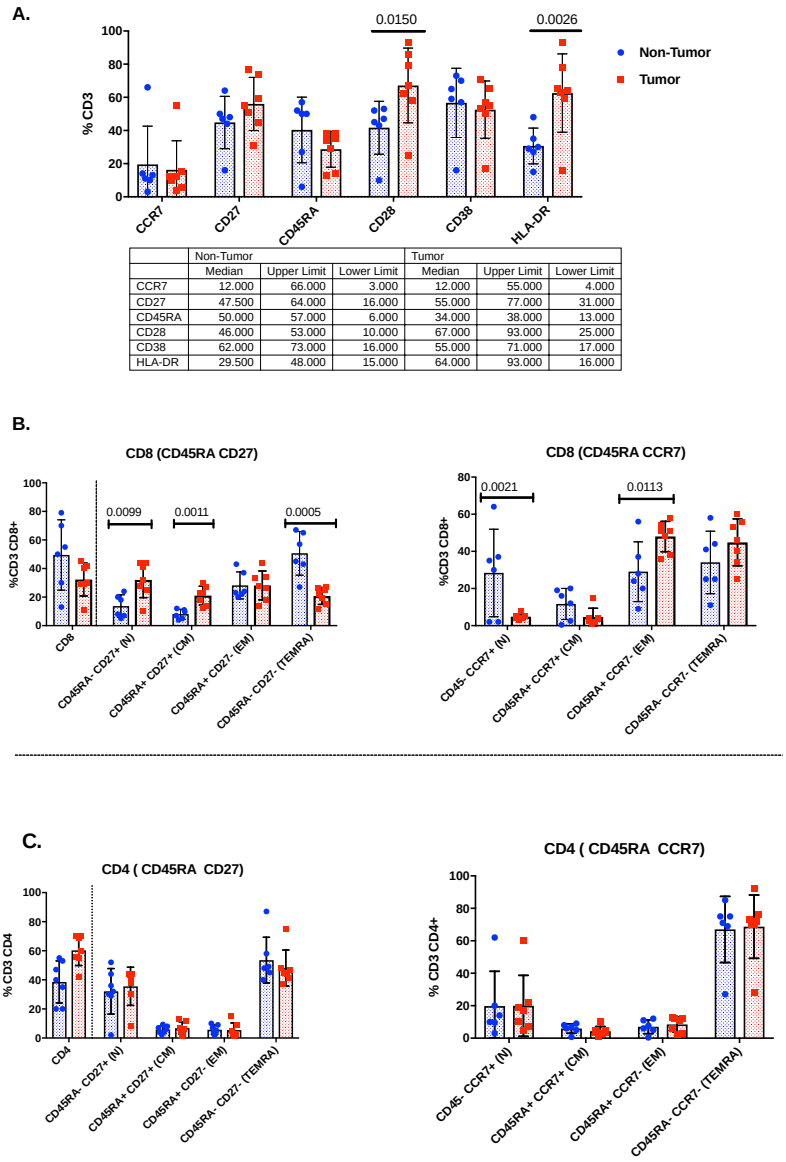

	Non-Tumor			Tumor		
	Median	Upper Limit	Lower Limit	Median	Upper Limit	Lower Limit
CCR7	12.000	66.000	3.000	12.000	55.000	4.000
CD27	47.500	64.000	16.000	55.000	77.000	31.000
CD45RA	50.000	57.000	6.000	34.000	38.000	13.000
CD28	46.000	53.000	10.000	67.000	93.000	25.000
CD38	62.000	73.000	16.000	55.000	71.000	17.000
HLA-DR	29.500	48.000	15.000	64.000	93.000	16.000

Figure 57: **distribution of Effector and Memory CD8+ and CD4+ TIL cell subsets in tumor and non-tumor tissue.**

Freshly Isolated TILs from fresh tumor and non-tumor tissues were stained with T cell activation and differentiation markers. The function of CD4 and CD8 T subsets were classified by six markers include CCR7, CD27, CD28, CD45RA, CD38 and HLA-DR on total of CD3 T cell (A) . Next , (B and C) memory and effectors CD4 and CD8 T cell were classified as naïve (Naïve: CD45RA+CD27+) or (CD4RA+ CCR7+), CM ; (CD45RA−CD27+) , or (CD45RA-CCR7) , EM (CD45RA−CD27-) or (CD45RA-CCR7-) and TEMRA (CD45RA+CD27-) or (CD45RA+ CCR7-).

5.5.2 The status of effector and memory cells subsets between Fresh digested TIL and Cultured TIL cells from Tumour tissue.

In this study, I also compared the phenotype of lymphocytes from freshly digested tumour tissue and the same cells after expansion in vitro to generate TIL. The relative frequencies of the CD3+ population are show in *Figure 58*a. The results show significant increases of CD45RA (p=0.0022) and CD38 (p= 0.05) expression in expanded TIL compare to dTIL with. Also, the results show significant decreases in the frequency of CD27 (p=0.024) and CCR7 (p= 0.011) with expanded TIL.

As shown in *Figure 58*b, based on the expression of CD8 (CD45RA CD27) populations, the frequency of central memory CM (CD45RA + CD27+) is the largest population in eTIL which was significantly higher (p= 0.021) than dTIL which had Naïve and EM cells in the same level. However, with CD8 (CD45RA CCR7) the highest frequency of EM (CD45RA + CCR7-) was in eTIL (p= 0.006) where TEMRA were significantly (0.0189) increased compared to dTIL cells. Examining CD4 T-cells as show in *Figure 58*c the frequency of TEMRA were greater in both but more in expanded TIL than dTIL in CD4 (CD45RA CD27) populations. The frequency of EM was higher (p= 0.0008) with eTIL whereas TEMRA was higher with dTIL cells in CD4 (CD4RA CCR7) populations.

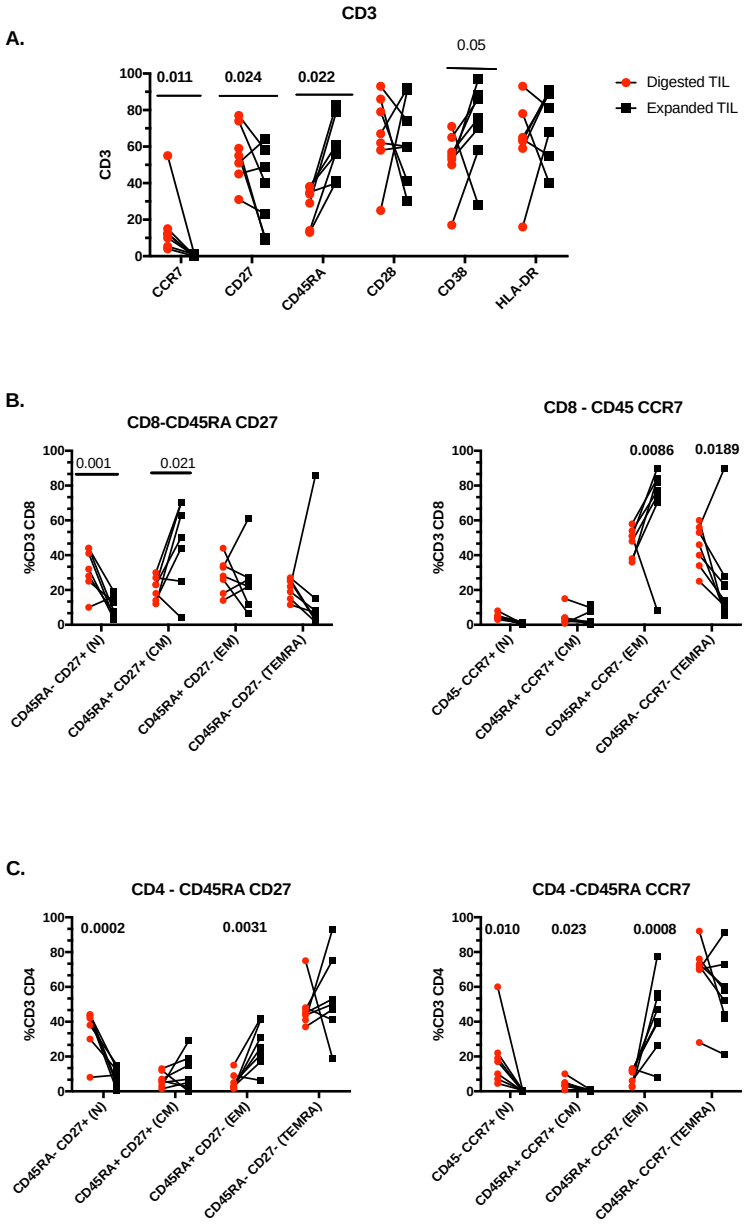

Figure 58:the status of effector and memory cells subsets between Fresh digested TIL and Cultured TIL cells from Tumour tissue.

Expanded TILs and fresh TILs from tumour tissue were stained with T cell activation and differentiation markers. The function of CD4 and CD8 T subsets were classified by six markers include CCR7, CD27, CD28, CD45RA, CD38 and HLA-DR on total of CD3 T cell (A) . Next, (B and C) memory and effectors CD4 and CD8 T cell were classified as naïve (Naïve: CD45RA+CD27+) or(CD4RA+ CCR7+), CM ; (CD45RA−CD27+) , or (CD45RA-CCR7) , EM (CD45RA−CD27-) or (CD45RA-CCR7-) and TEMRA (CD45RA+CD27-) or (CD45RA+ CCR7-).

5.6 Role of immune checkpoint inhibitor receptors in tissue of GC patients

To analyze expression of immune checkpoint inhibitors on immune cells in tumor and non-tumor from GC patientsI used the flow cytometry panel described in the earlier chapter. Four immune checkpoints, selected based on therapies targeting them being already in the clinic or well advanced in clinical trials, were studied: PD1, TIM3, LAG3 and CTLA4.

5.6.1 Status of immune checkpoint inhibitor receptors in tumor and non-tumor tissue of GC patients

The frequency of CD8 cells expressing the different receptors is shown in *Figure 59.* Examination of PD1 and TIM3 showed there was no significant difference between tumor and non tumor (% median 65 vs 60, p=0.602 and p=0.06 respectively) although one patient had markedly higher frequencies of TIM-3 positive CD8 T-cells. Regarding LAG3 there was no significant difference between tumor and non tumor (p= 0.403) although two patients has markedly higher frequencies of LAG3 in tumor tissue. The results showed increased expression of CD57 on cells from tumor tissue in 5/12 patients (p=0.0787). Interestingly, non-tumor tissues had significantly higher (p= 0.0264) frequencies of CTLA4 positive cells than tumor. The expression of inhibitor receptors on CD4 is presented in *Figure 60,* with the results showing that the percentage median of PD1 expression was higher (%70) in tumor tissue than non-tumor tissue (60%), but not significantly different(p=0.198).. There were no significant differences with TIM3 (P=0.3757), CTLA4 (P=0.9408) , LAG3 (p= 0.3907) or CD57 (P=0.3775) but the results also that one patient had increased cells with these receptors in non-tumor tissue

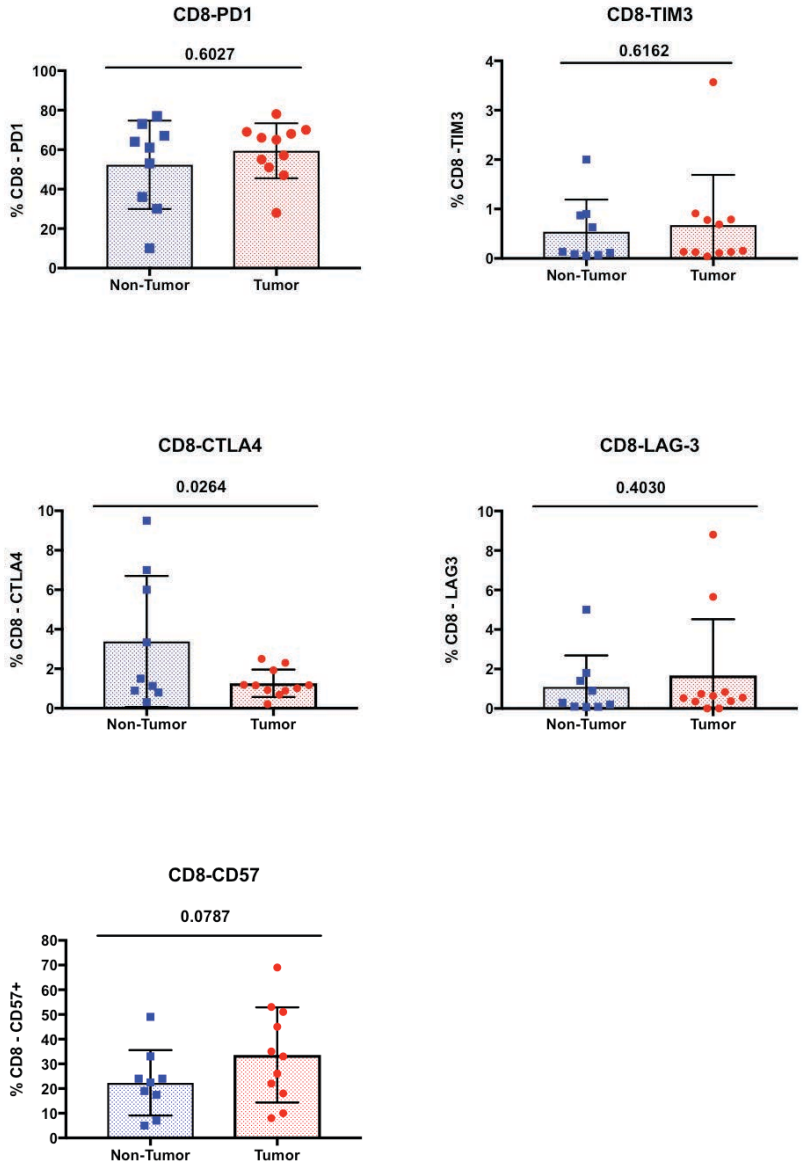

Figure 59: Expression of immune checkpoint inhibitor receptors on CD8+ cells isolated from tumor and non-tumor tissues

Immune checkpoint inhibitor receptors induced PD1, TIM3, LAG3 and CTLA4 in addition to CD57 were analyzed on CD+ lymphocytes isolated from tumor and non-tumor. Using flow cytometry, the frequency of expression was detected for every receptor on CD8+ T cell population. The figures represent the mean of percentage of for each group. data were analyzed statistically using Mann- Whitney test, with ($P < 0.05$) significantly different

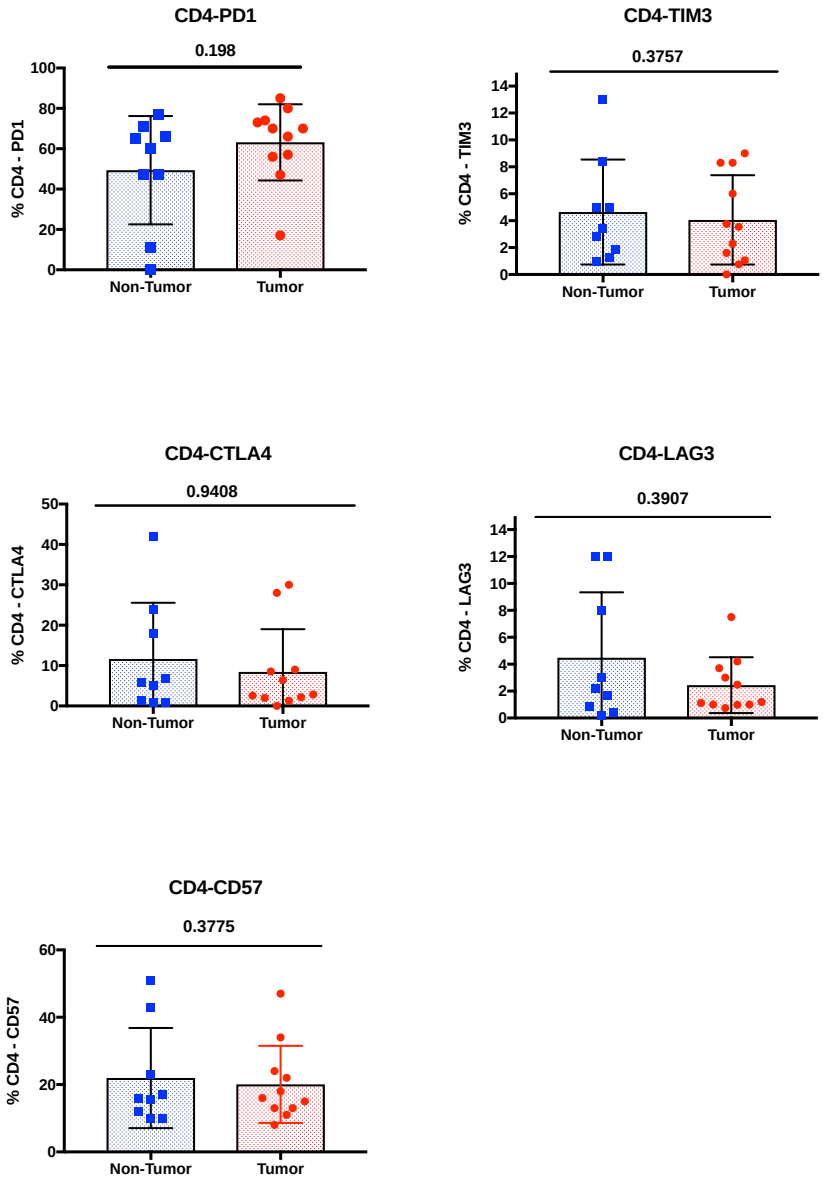

Figure 60: Expression of immune checkpoint inhibitor receptors on CD4+ TILs between tumor and non-tumor tissues

Immune checkpoint inhibitor receptors PD1, TIM3, LAG3 and CTLA4 in addition to CD57 were analyzed on cells isolated from tumor and non-tumor tissue. Using flow cytometry, the frequency of expression was detected for every receptor on the CD4+ T-cell population. The figures represent the mean of frequency for each group. data were analyzed statistically using Mann- Whitney test, with ($P < 0.05$) significantly different.

5.6.2 Understanding the expression of immune checkpoint receptors between fresh digested TIL and expanded culture TIL from tumor tissue.

Before useing in vitro expanded TIL cells in functional studies or as immunotherapy, it's important to know their expression of immune checkpoint inhibitors receptors which can limit tumour-specific immune responses in vivo. These receptors are upregulated following activation of immune cells and it is therefore possible that TILs may express one or more of them after expansion in vitro. In this study, I have measured the expression of immune checkpoint inhibitors receptors in fresh digested and expanded culture TIL from the same GC patients to identify the differences in expression resulting from in vitro expansion.

As show in *Figure 61,* for CD+ T-cells there was a significant decrease in PD1-expression after TIL expansion (p=0.0002) but no differences for CLTA4 and CD57 expression. Interestingly, the expression of LAG3 was significantly greater with expanded TIL cells (p=0.007).

However, for CD4+ T-cells there was significantly decreases in the expression of PD1, CLTA4 and CD57 (p= 0.0391, p= 0.0078 and p= 0.0039 respectively) after TIL expansion. Unexpected, I found significate increased in LAG3 (p=0.0078) with expanded TIL cells. the frequency of TIM3 – CD4+ cells show that no significant differences (p=0.4668) have been noted.

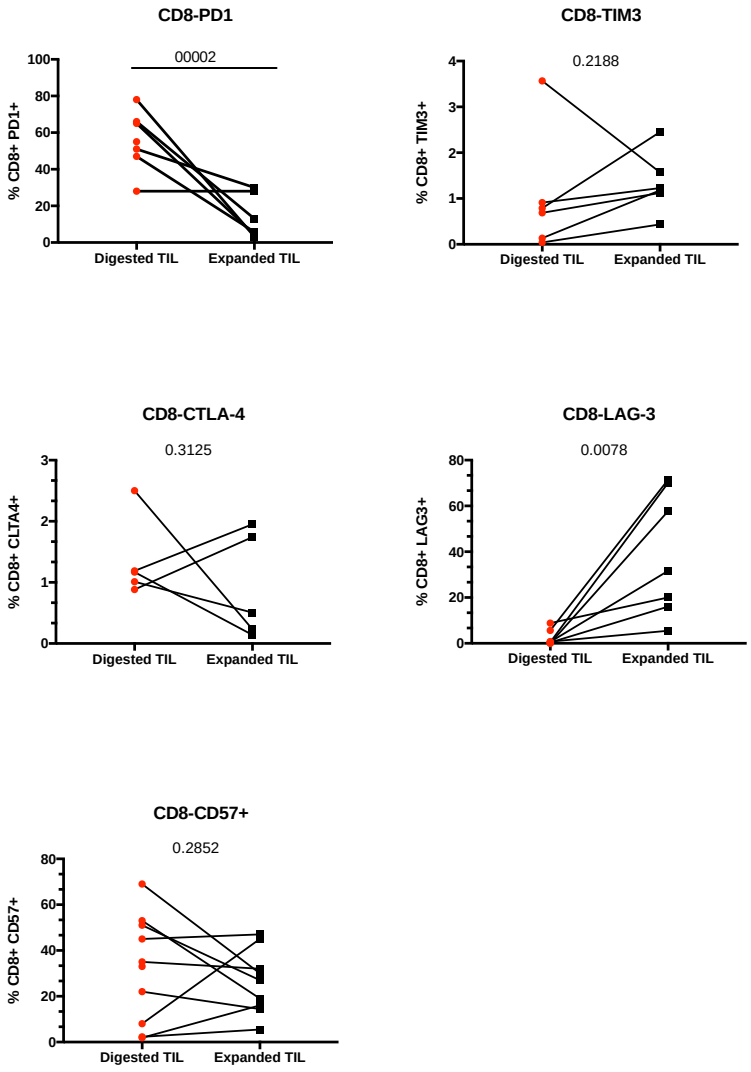

Figure 61: Understanding the expression of immune checkpoint inhibitors receptors on CD8 cells from tissue and after in vitro expansion.

Immune checkpoint inhibitor receptors induced PD1, TIM3, LAG3 and CTLA4 in addition to CD57 were analyzed on TILs to identify expression between freshly isolated cells and expanded culture TILs. Using flow cytometer, the frequency of CD8+cells expressing each receptor was measured. The figures represent the mean of percentage of for each group. data were analyzed statistically using paired test, ($P < 0.05$) significantly different.

5.7 Analysis of potentially immunosuppressive cells in tissue of gastric cancer patients

5.7.1 The frequency and phenotype of regulatory T cells in tumour and non-tumour tissue

The frequency of CD25+ CD127- T-reg in the CD4 T-cell population was significantly higher in tumour tissue compared to non-tumour (% median: 8 to 1, p= 0.0047) as show in *Figure 62*a. using FoxP3 and CD39 to identify suppressive T-reg cells . I found, overall, that tumour tissue had a significantly higher frequency of FoxP3+CD39+ cells compared to non-tumour (% median: 47 to 1 P=0.0012) as show in *Figure 62*b. Assessment of another T-reg phenotypic marker, CD45RA, showed that T-regs from tumour tissue had a higher frequency of CD45RA expression (median:6.8 to 0.8, p=0.0717) with four patients. Moreover, there was significant difference (median; 5.4 to 0.7, P=0.002) in the percentage of T-reg that expressed Ki67 in tumour tissue in compared to non-tumour tissue.

5.7.2 The frequency and phenotype of regulatory T cells in fresh digested TIL and expanded culture TIL from tumor tissue

Comparing expanded cultured TIL and the freshly isolated lymphocytes from the same patient, I found that the frequency of CD25+ CD127- T-reg in CD4 T-cells was significantly decreased in expanded TIL (p= 0.0156) as show in *Figure 63*a.. The results also show that expanded TIL had a significantly decreased frequency of Treg (FoxP3+CD39+) cells compared to fresh lymphocytes (P=0.0312) as shown in *Figure 63*b. According to the results in *Figure 63*c there were differences between expanded TIL and fresh lymphocytes in the expression of CD45RA which was decreased (p=0.0781) in expanded TIL cells. In contrast, there was significantly increased (p= 0.0078) percentage of T-reg that expressed Ki67 in expanded TIL cells as shown in *Figure 63*d

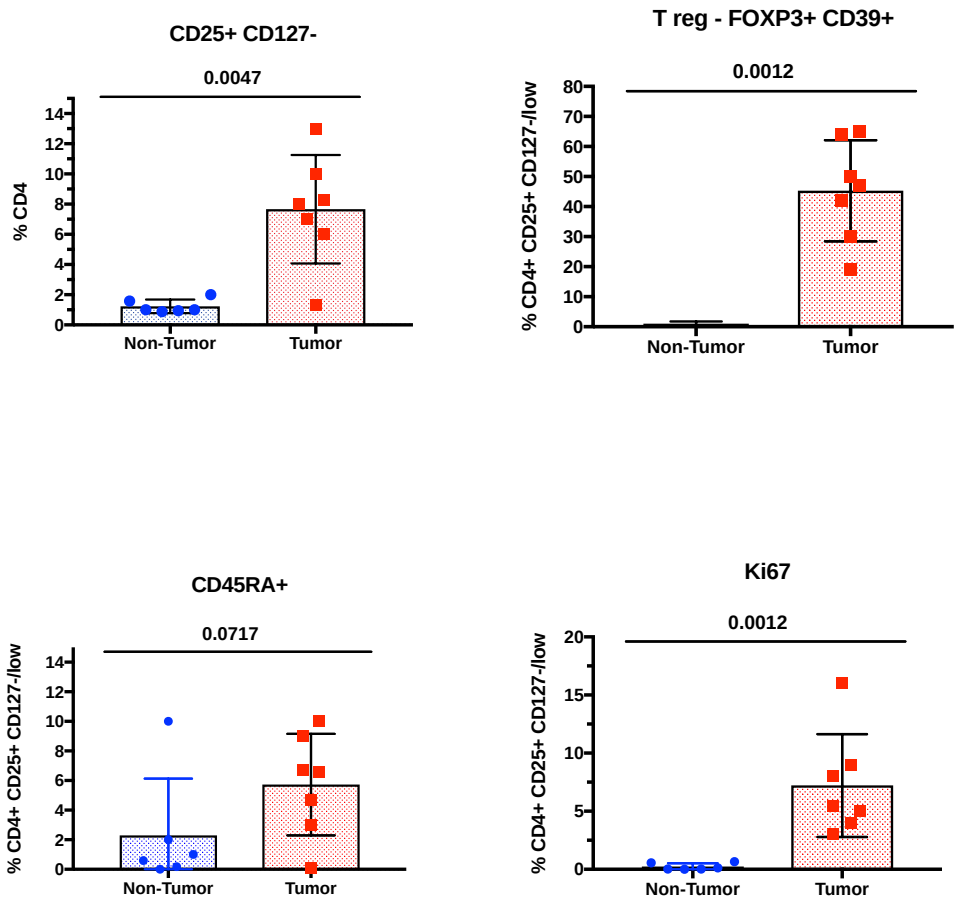

Figure 62: The frequency and phenotype of regulatory T cells in tumour and non-tumour tissue

To identify and phenotype Treg cells in tumor and non-tumor tissue, isolated TILs were stained with a panel of T reg surface marker (CD3 , CD4 , CD25 , CD127 , CD39 and CD45RA) and intracellular (FOXP3 and Ki67) markers. T reg were gated as (CD4+ CD25+ CD127-/low FOXP3+ and CD39 +) based on FMO and unstained cell controls .

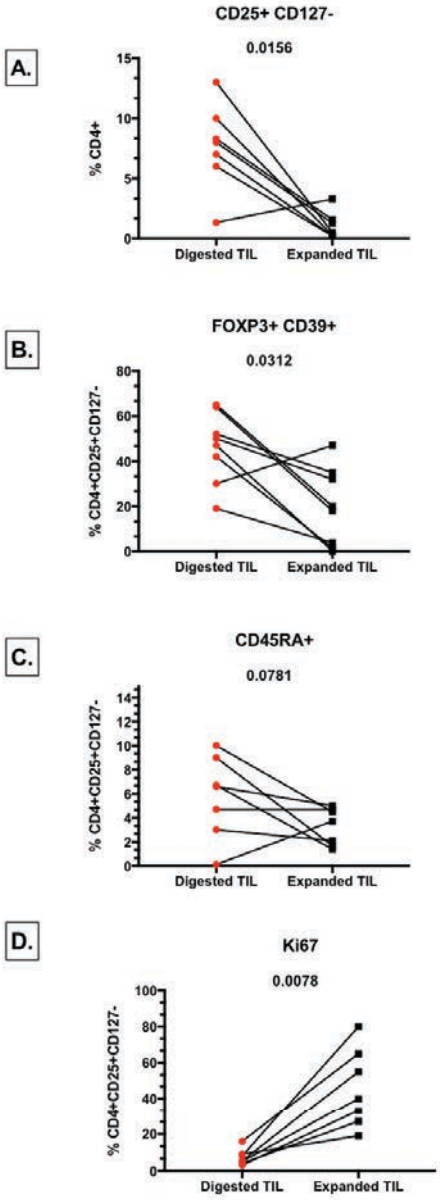

Figure 63: The frequency and phenotype of regulatory T cells between fresh digested and expanded culture TIL cells.

To identify and phenotype Treg cells in tumor and non-tumor tissue, isolated TILs were stained with a panel of T reg surface marker (CD3 , CD4 , CD25 , CD127 , CD39 and CD45RA) and intracellular (FOXP3 and Ki67) markers. T reg were gated as (CD4+ CD25+ CD127-/low FOXP3+ and CD39 +) based on FMO and unstained cell controls .

5.7.3 Myeloid-derived suppressor cells (MDSCs) in tumor and non-tumor tissue

Myeloid M-MDSC cells were detected as Lin-, HLA-DR-, CD33+, CD11b+, CD14+ cells and Granulocyte G – MDSCs as Lin-HLA DR-, CD33+, CD11b+, CD15+ cells as described in an earlier results chapter. The median percentage of myeloid M-MDSCs in GC tumour tissue was not significantly higher than in non-tumor ($p=0.0962$) but three patients had markedly higher frequencies of these cells, which were three times higher than the rest of the patients as show in *Figure 64*a. According to the median percentage of granulocytes G-MDSCs there were no differences ($p=0.1888$) in tumour tissue (85%) compared to (74%) non-tumour tissue as shown in *Figure 64*b.

5.7.4 The expression of Myeloid-derived suppressor cells (MDSCs) between fresh digested TIL and expanded culture TIL.

Comparing the expression of MDSCs between fresh Isolated lymphocytes and expanded culture TILs I found significant decreased M- MDSCs in expanded TIL ($p=0.0156$). As shown in *Figure 64*c, in all patients no expression of MDSCs was detected after expandsion of TIL cells. however, no G-MDSCs have been detected with all patients with expanded TILs.

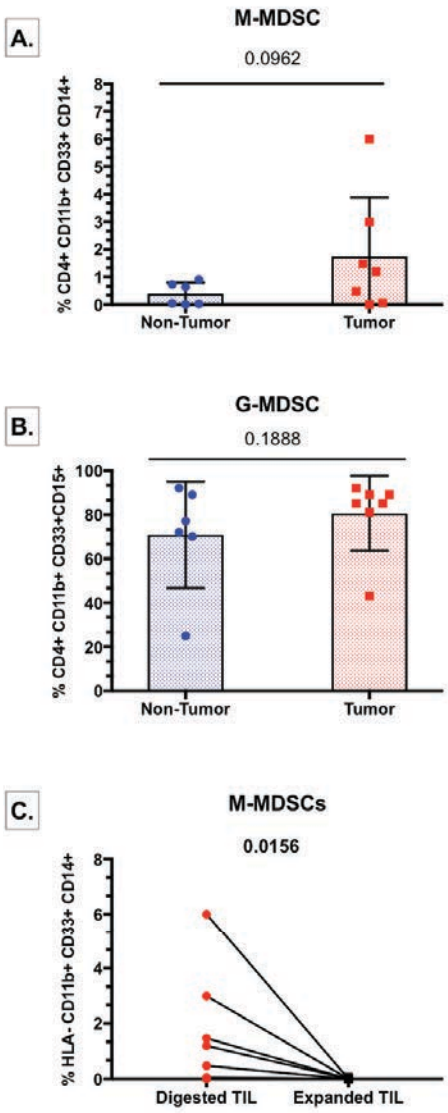

Figure 64: The frequency of MDSCs on lymphocytess from tumour or non-tumour tissue and expanded cultured TILs.

Cells were stained with antibodies and analysed by flow cytometry. MDSCs were defined as: live, (CD3- ,CD19- ,CD56-) , (HLA DR - CD33+CD11b+) CD14+ for M-MDSCs and CD15+ for G-MDSCs . A. The frequency M-MDSCS between tumour and non-tumor tissue. B. the frequency of G-MDSCs between tumor and non-tumor tissue. C. The frequency of M-MDSCs between expanded culture TILs and fresh isolated TIL cells.

5.8 The expression of immune checkpoint inhibitor receptors on immune cells in peripheral blood and the tumor microenvironment of GC patients.

To compare the expression of immune checkpoint inhibitor receptors on CD4 and CD8 cells in blood and isolated lymphocytes from fresh tumor tissue, three patients were studied. Cells from blood and tissue were analysed using flow cytometry as described earlier. On CD8 T cells, as presented in *Figure 65*, the frequency of PD1+ was significantly (P= 0.0002) higher on cells from tissue compared to peripheral blood . The expression of TIM3+ on CD8 T cells was significantly higher (P= 0.0398) on cells in tissue. CLTA4 and LAG-3 expression were higher on CD cells from tissue but not significantly (P= 0.0591, P= 0.1015 respectively). As shown. CD57+ CD8+ T cells were lower (P= 0.0659) in tissue in compare to peripheral blood.

The expression of immune checkpoint inhibitor receptors in CD4 T cells is presented in Figure 66. The results show that the frequency of PD1+, TIM-3+ and LAG3 on CD4 T cells were significantly higher in tissues than blood (P= 0.0045, P=0.0386 and P=0.0436 respectively) . The results also show there were no significant differences in the expression CTLA-4 (P=0.1603).

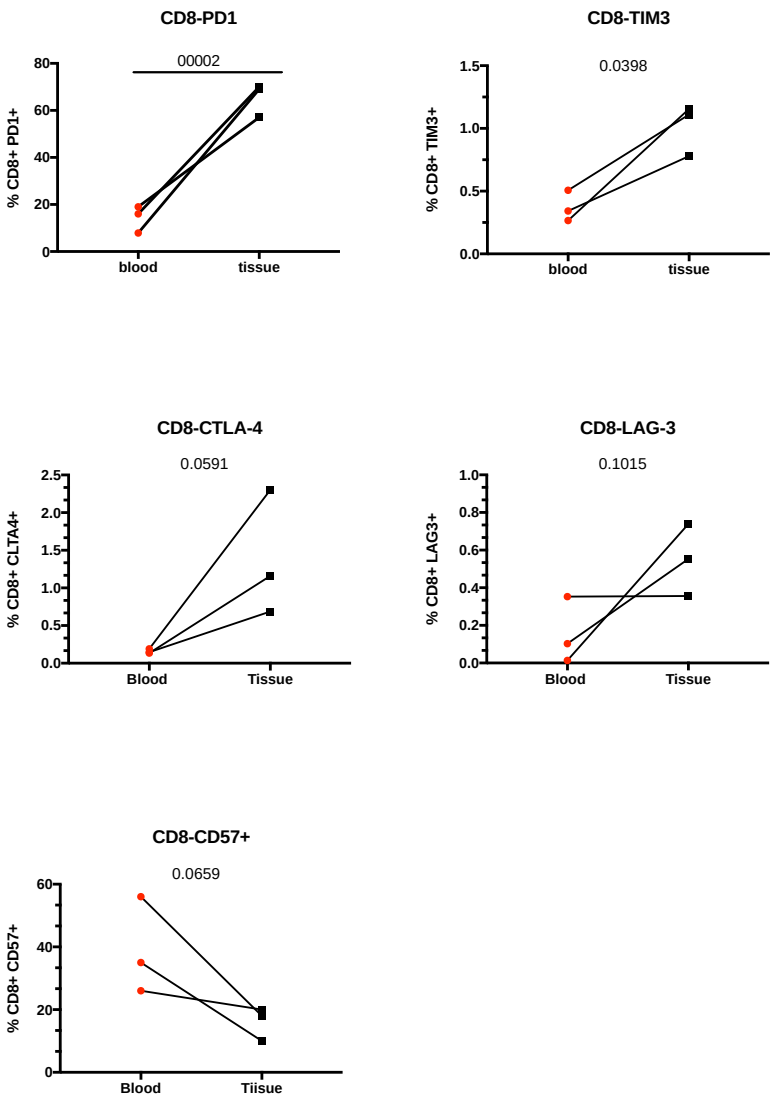

Figure 65: The expression of immune checkpoint inhibitor receptors on CD8 T cell between peripheral blood and tumor microenvironment in GC patients.

The frequency of immune checkpoint on CD8 T cells from PBMCs were compared to matched TIL cells frequency on CD8 T cell from tumor tissue of patients.

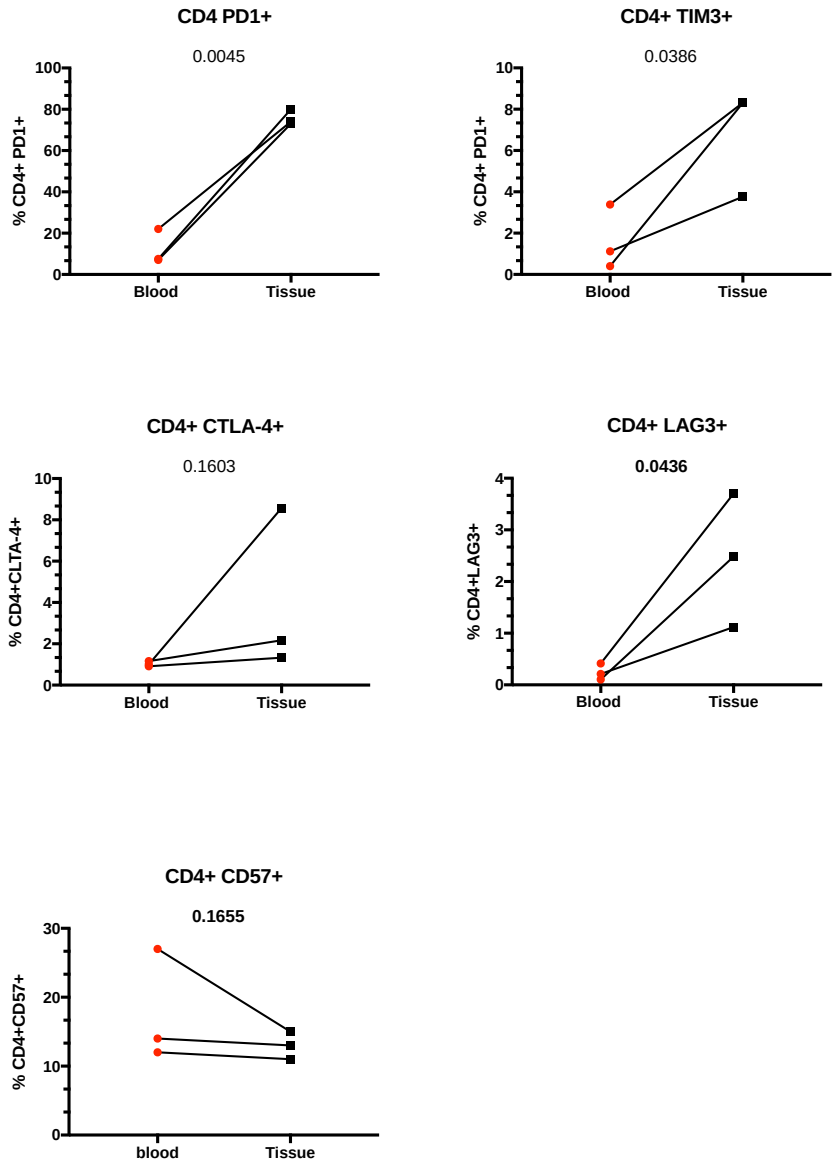

Figure 66: The expression of immune checkpoint inhibitor receptors on CD4 T cell between peripheral blood and tumor microenvironment in GC patients.

The frequency of immune checkpoint on CD4 T cells from PBMCs were compared to matched TIL cells frequency on CD4 T cell from tumor tissue of patients.

5.9 Summary and Discussion

The immune microenvironment of tumors is critically important, and can be used to determine prognosis, and inform the use of appropriate immunotherapies, such as immune checkpoint blockade. Tumor-infiltrating lymphocytes are considered a demonstration of the host immune response against tumor cells, and studies have already studied the potential of TIL cells as prognostic parameter for different human malignancies. My study has successfully isolated TIL cells from tissue of gastric cancer patients by digestion or culturing tissue in cytokine-containing medium then expanding the intratumoural immune cells to prepare high number of TILs cells. However, few studies have investigated the prognostic influence of TIL cells in gastric cancer. Nevertheless, a limited number of molecular and histological studies have reported the clinical prognostic impact of density of TIL cells in EBVaGC patients[215] EBVaGC patients and TIL cells have shown great outcomes in compare to typical gastric cancer[216] .The presence of EBV antigen specific T-cells in tumors is encouraging for these of EBV-specific T cells as treatment for the 10% of cases positive for the virus, although additional work would be needed to determine if virus-positive cases contain virus-sepecific T-cells.

Considering the specificity of the EBV-specific cells in GC, I found CD8 T cells specific for EBNA1, EBNA3A, LMP2 and LMP1 but no responses to BARF1 Further studies are necessary to detect the expression of EBV antigens in these patients.

In Gastric cancer patients, immune response to tumour associated antigen have been reported in blood [217] but no studies have investigated the immune response in the tumour microenvironment. In my study, several tumour antigens include: NY-ESO-1, MUCIN1, MAGEA1, MAGEA3, MAGEA4, CEA and PSMA were selected based on

prior evidence of expression in gastric cancer[218, 219] or detection of specific antibodies in serum of patients[73, 220]. In addition, during my project (previous chapter) I have investigated the specific T cell response in PBMCs cells from GC patients, the results showed that significant T cell response to some of these antigens or low response in compare to healthy subjects. In my study, TIL cells responses to these antigens were measured by the cultured assay using appropriate pepmixes. I observed low PSMA – specific CD8 T cell responses in three of nine patients after short ex vivo stimulation of TIL cells but no response was found to the other antigens. No specific responses were detected after 10 days of in vitro culture except a MUCIN1 – specific CD8 T cell response in one of nine patients. These finding indicate that tumours infrequently contain T-cells specific for these classical tumour associated antigens .

To know how immunotherapy could potential be used to treat gastric cancer, it is important to first characterize the phenotype and subset distribution of the immune cells in the tumour. In this study, I succeeded in isolating lymphocytes from digested patient's tissues and expanding these cells to high numbers in vitro. This allowed me to measure changes in TIL cells during culture as well as defining the identity and phenotype of the cells in the tumour. Such information would be valuable for the future development of TIL therapy to treat gastric cancer patients. My results strongly support the case for developing TIL therapy to treat this disease which, at present, has very poor prognosis.

However, the exact role of TIL immune cells in GC is less clear. The another aim of my study was to determine the prognostic significance by compare the function and phenotype of tumor and non-tumor TIL cells, in addition to compare between fresh

isolated and cultured expanded TIL cells for every patient. The results comparing of TIL lymphocytes subsets between fresh Tumor and Non-Tumor Tissue show that significant high CD4/CD8 ratio with isolated TILs from tumor to non-tumor tissues. whereas no significantly differences existed between fresh and culture expanded TILs. However, each T cells subset CD4 and CD8 paly role in antitumor response in different cancers[221], while cytotoxic T cell are main effectors immune cells of antitumor response , CD4 T cells are important to maintain and induce CD8 T cells response and can also act as anti-tumour effectors [222] .

The distribution of effector and memory CD8+ and CD4+ T cell subsets in tissue of GC patients was studied to allow me to be understanding the status of lymphocytes in tumour and non-tumour tissues in addition to comparing these to expanded TIL. Using six markers (CCR7, CD27, CD28, CD45RA, CD38 and HLA-DR) my results show that in comparison between TIL from tumour and non-tumor in the bulk of CD3 population, CD28 and HLA-DR expression were significantly increased in tumour tissue compared to non-tumour whereas CD45RA was deceased in tumour. On the hand, with expanded TILs the expression of CD45RA and CD38 increased while the expression CD27 and CCR7 were decreased on the CD3 population.

Analysing CD45RA+ CD27+ on CD8 T cells, a larger proportion of lymphocytes in tumour were TEMRA cells whereas CD45+ CCR7+ showed increase EM and TEMRA cells in tumor tissue compared to non-tumor. For CD4 T-cells high TEMRA cells were found in tumor and non-tumor tissue. However, after expansion EM of CD4 and CD8 T cell were increase for TILs.

My results showed no change in the frequency of B cells between tumour and non-tumour TILs but B cells were significantly lower in expanded TIL compard to freshly

isolated TILs. The role that tumour infiltrating B cells play in tumour progression is largely unknown, although high frequencies of B cells have been reported to be present for multiple different cancers including breast, colon, lung, prostate and melanoma [223-225].

My study found that gamma delta (γδ) T cells in CD3 + lymphocytes was statistically higher in tumor tissue than non-tumor tissue. The frequency of gamma delta cells was lower in expanded TILs in comparison to fresh isolated TILs. In recent years, a number of studies have been reported that γδ T cells have pro-tumour activity in cancer development[226, 227] moreover, in the cancer microenvironment, γδ T cells produce IL-17 that can promote tumour growth and induce angiogenesis in some cancers include gastric cancer[228]. In later stages of cancer, γδ T cells could exert antitumor effects by interacting with other lymphocytes [229] and exhibiting cytotoxicity against solid tumour[230]

NK cells potentially have the ability to destroy cancer cells. A number of studies have reported correlations between patient prognosis and the number of infiltrating NK cells in breast cancer [231] and the prognostic value of NK and NK-T cells in lung cancer and colorectal carcinoma [232] and gastric cancer[233]. However, nothing is known about the status of NK cells infiltrating gastric cancer. My study has found a significant increase in NK-T cells in tumor compared to non-tumor tissues but no difference in the NK cell population. In addition ($CD56^{Dim}$ $CD16^{-}$) NK were in identified cells in tumour TIL cells. However, I found that NK-T cells frequency was increased after in vitro culture but no significant differences occurred for NK cells. .

In cancers, the immune checkpoints play a crucial role in limiting and preventing anti-tumour T cell response through multiple mechanisms. They lead to reduced

proliferative and cytotoxic capacity [234]. Antibodies that inhibit these immune checkpoints, such as CTLA-4 specific antibodies (ipilimumab and tremelimumab) and PD1 specific antibodies (pembrolizumab and nivolumab) have now become firmly established as as anticancer agents [235, 236].

My study therefore investigated the expression of four immune checkpoints on lymphocytes isolated from tumor and non-tumor tissue, and expanded TILs. I also studied the expression of these receptors on lymphocytes in peripheral blood and tumor tissue of the same patients. However, my study showed on CD8+ T cells that there were not significant changes in expression of PD1, TIM3 and LAG3 between isolated lymphocytes from tumor and non-tumor tissues but the expression of CTLA4 was significantly lower on tumor compared to non-tumor CD T-cells.

Expression of PD1 on CD T-cells was decreased on expanded TILs but LAG3 was ; increased; the other inhbitors were unchanged. The frequency of immune checkpoint inhibitors on CD4+ T cells was not significantly different for lymphocytes from tumor and non-tumor tissue and was lower after in vitro expansion to generate TILs. The upregulation of LAG-3 expression in expanded TILs strongly suggests expression of this receptor is regulated differently.

Interestingly, my study also found that the expression of immune checkpoints was upregulated on both CD4 and CD8 T cells in tumor tissue in comparison to the expression on immune cells in patient's peripheral blood. An increase of PD1 has been documented by a previous study[65]. My results extend this work considerably by implicating TIM-3 , CLTA4 and LAG-3 as potential immune evasion mechanims in gastric cancer. Single agent anti-PD1 may therefore not be sufficient to initiate robust

tumour specific immunity. My data provide a strong basis for rational selection of immunotherapy combinations in this disease setting.

Regulatory T cells and MDCSs are important components of the tumour microenvironment [237]. A previous study has reported high frequencies of Treg and MDSC cells in blood of gastric cancer patients[238]. In my study, I have extended our understanding of gastric cancer by examing the frequency of such cells in the tumour itself. I also explored the frequencies of these cells in expanded TIL cells to ensure that such preparations did not contain suppressive cells. Interestingly, I found that the frequency of T reg CD4 T cells was significantly higher in tumor than non-tumor tissues. Moreover, the T regs in tumour tissue were antigen experienced (CD45RA) and had recently proliferated as determined by (KI67). Importantly, after in vitro culture the frequency of T reg cells significantly decreased in TILs. These results point to a role for T-reg in the tumour microenvironment.

The frequency of monocytes-MDSCs and granulocyte- MDSCs were greater in some tumour tissuea in compare to non-tumour tissues from the same patient. Expanded TIL cells showed downregulation of M-MDSCs.

Overall, my results provide new insights into gastric cancer immunology and new leads for future investigation, both scientifically but also for immunotherapy development.

CHAPTER 6: RESULTS

The functional assessment of Tumour infiltration lymphocytes with Three-Dimensional Organoid Derived from Gastric Cancer Patients tissue.

6.1 Introduction

An organoid is three-dimensions organ produced in vitro, that shows realistic micro-anatomy. Organoids are formed from one or more cells from embryonic stem cells, tissue and pluripotent stem cells. These cells can develop into a 3D organ by self-organizing in specific culture medium and extracellular matrix hydrogel, Matrigel or collagen [239]. Organoids have been generated from cerebral, thyroid, hepatic, pancreatic, lung, kidney, cardiac and gastrointestinal organs [240]. Through research studies organoids were found to be excellent tools to discover basic biological processes, in addition to providing an opportunity to generate cellular models of human cancers to understated the causes of cancers and develope possible treatments [241]. For example, the Clevers group used rectal biopsies to generated intestinal organoids for modal cystic fibrosis[242]. Gastric organoids were derived and generated from pluripotent stem cells in three-dimensional culture conditions by the temporal manipulation of BMP, retinoic acid, WNT, FGF and EGF signaling pathways[243]. Furthermore, organoids have been formed from LGR5 expressing gastric adult stem cells[244]. Moreover, Gastric organoids have been involved as model of the study of cancer [245, 246].

However, organoids models as cells co-cultivation demonstrated interplay functional between stromal fibroblasts and tumor, identifying the pathways of activated gene that involved in inflammation, hypoxia and epithelial-to-mesenchymal-transition[247]. Little information is known about the relationship between immune cells and tumor cells in a 3D environment. Some studies have used organoid + immune cell co-culture such as lymphocytes and TAM cells, but these have so far been used to study their influence on gene regulation and tumor cell proliferation[248, 249].

The interaction between TIL cells and matched gastric tumor organoids have not been established. This study is therefore the first attempt to study the interaction and crosstalk between the immune response and 3D organoids in gastric cancer patients. For that, surgical tissues from GC patients have been shared between and Dr. Claire Shannon-Lowe's laboratory (University of Birmingham) and myself. As described in the previous chapter, I succeeded in isolating TIL cells from tumor and non-tumor tissues and studied the status of the immune cells after expansion. Staff in Dr Shannon-Lowe's laboratory have been studying how to generate 3D organoids from tumor and non-tumor tissues. In my study, I have studied TILs in ex vivo and cultured experiments. The logical extension of this work was to study TIL cells against organoids generated from the same patient by Dr Shannon-Lowe's team.

6.2 Evaluation of rapid immune responses to 3D cultured gastric organoid.

In this study, autologous TIL cells were cultured with 3D spheroid or early differentiated organoid to detect the response of immune cells. TNFa responses were measured after six hours. The cultures were also maintained for ten days to allow low abundance TILs specific for the organoids to expand; TILs were then re-tested against fresh organoids to detect such responses. TILs were also stained with fluorescent antibodies to distinguish T cells and NK cells population and also to measure the expression of PD1, CD57 and CD107a as degranulation marker. Figure 67 shows microscopy images of spheroids and early differentiated organoids in addition to co-cultures between TIL cells and organoid cells in culture plates.

6.2.1 Patient 22: the response of Tumor TIL cells to Tumor and non-tumor derived organoid cells.

In this patient, TIL cells were cultured and expanded from tumor tissue as described in the previous chapter. For functional study, tumor TIL (T TIL) cells were cultured with matched tumor and non-tumor organoids then the response was detected as described above. As presented in ***Figure 68***, three immune cell populations were gated separately to discover the response and status of immune cells after interaction between TIL and organoid cells. The populations were T cells (CD3+ CD56-), NK cells (CD3- CD56+) and NK-T cells (CD3+ CD56+). Three controls were used in this experiment, unstained TIL cells for gating, TIL alone as negative control and TIL cells with anti-CD3 antibody as positive control.

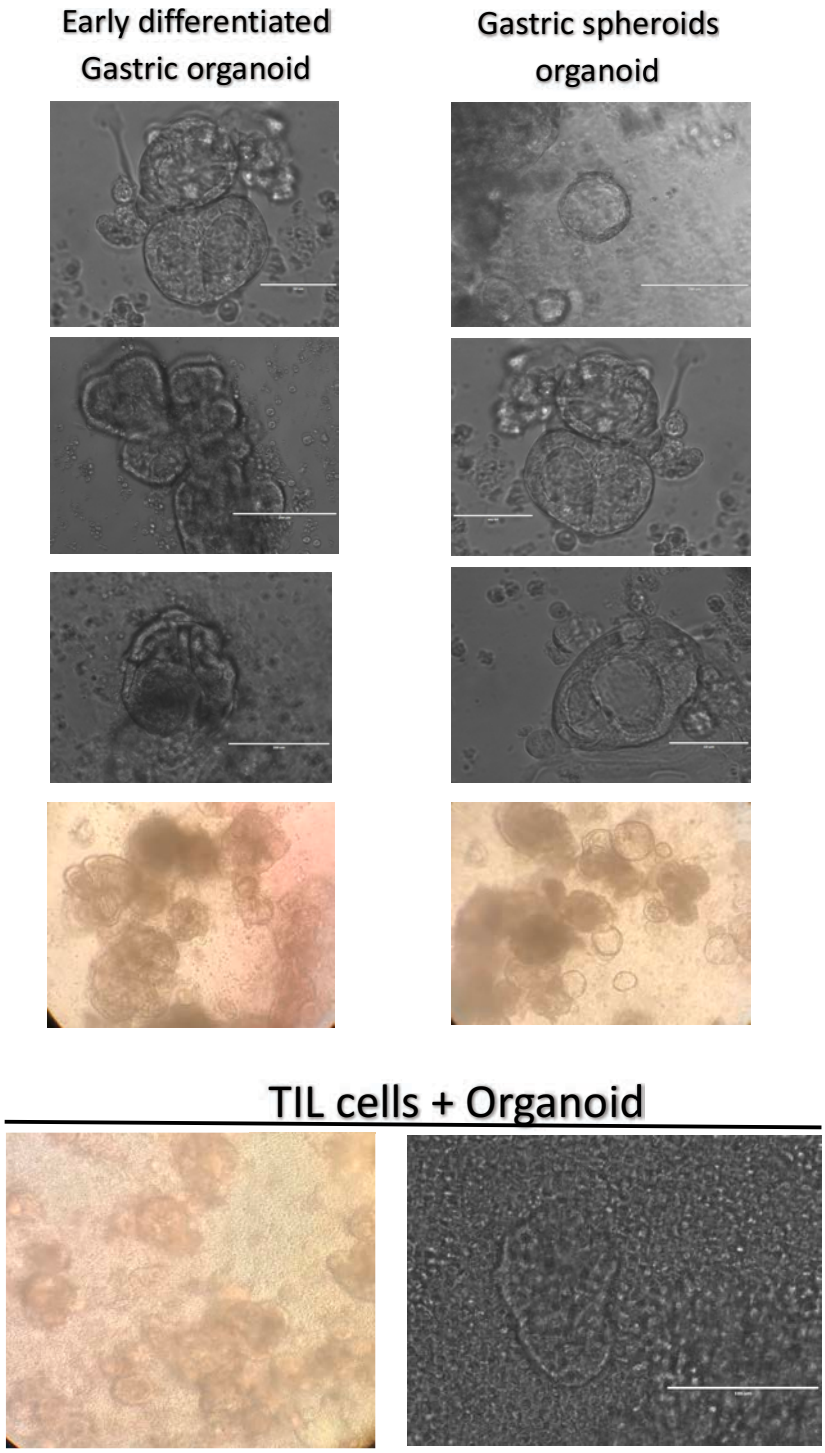

Figure 67 : Imaging of cultured 3D organoid

Organoid were seeded after removing Matrigel in culture plate the day before test, with organoid medium contain inhibitor and growing reagents. TIL cells were co-cultured with a mixture of spheroid and early differentiated organoids in 50/50 of TIL and organoid medium.

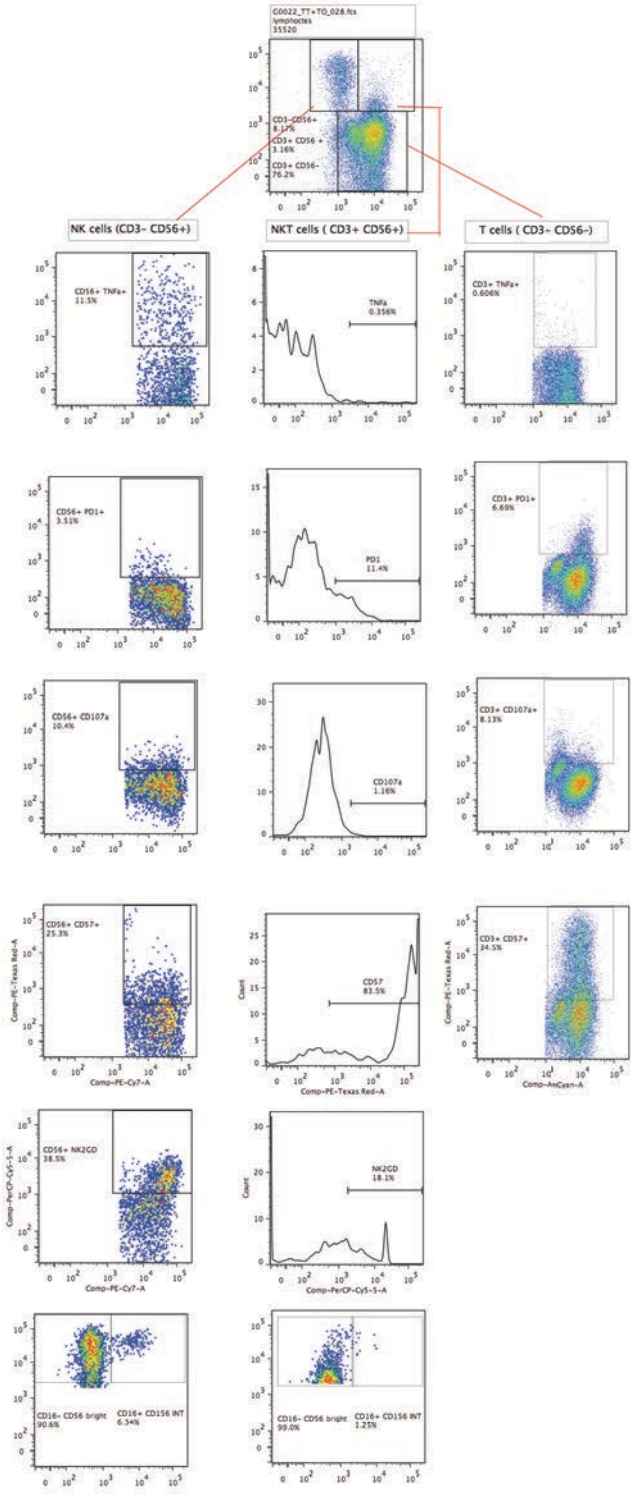

Figure 68 :Gating for Flow cytometer analysis: patient 22

Three cell population were gated based on CD3 and CD56 markers : (CD3+ CD56-) T cells , (CD3+ CD56+) NK-T cells and (CD3- CD56+) NK cells . TNF a, PD1 , CD107a and CD57, marker were measured for each population . NK2GD and CD16 were measured on NK and NK-T cells.

6.2.1.1 **The response of T cell (CD3+ CD56-)**

As presented in Figure 69a, there was no significant difference in the frequency of TNFa positive T-cells exposed to tumour or normal organoids, either after 6 hours or 10 days culture. Moreover, my results showed no differences of PD1 expression on T cells in between all groups or on TIL cells alone as presented in Figure 69b. The expression of CD107a on T cells was also analyzed to detect T cell degranulation. As show in Figure 69c, no cell surface CD107a was detected after six hours culture. In contrast, after ten days culture high CD107a expression was detected. However, Tumor TIL cells with tumor and non-tumor organoid had lower CD107a expression to TIL control. In Figure 69d the frequency of T cell expression of CD57 deceased after ten-day culture with tumor and non-tumor organoid in comparison with control.

6.2.1.2 **The response of NK cell (CD3- CD56+)**

Interestingly, as presented in Figure 70a the frequency of NK cells expressing TNFa+ was significantly greater in 10-day culture with tumor organoid ($p=0.0007$) and non-tumor organoid ($p=0.0018$) in comparison to TIL cells control. The level of response was significantly ($p<0.05$) increased after co-culture with both tumour and non tumour organoids cells., The frequency of TNFa positive NK cells with tumor organoid was higher than non-tumor but was not significantly different. In Figure 70b Immune checkpoint receptor PD1 expression was found to be increased after 10d culture in comparison to no expression with six-hour culture. Tthe frequency of PD1 with tumor organoid was greater than non-tumor. The frequency of CD107a expression on NK cells was increased after ten-day culture and the expression was found higher with tumor organoid than non-tumor as show in Figure 70c.

In Figure 70d, the expression of CD57 was increased after 10d culture but no differences were present in comparison to control cells. I also analyzed the expression of NKG2D on the surface of NK cells after co-culturing tumor TIL cells with organoids cells. My results show that NKG2D slightly increased after 10-day culture but no differences were seen between tumor and non-tumor organoids as presented in Figure 70e. After blocking NKG2D the NKG2D level decreased. As showed in Figure 70f I found that most of the NK cells population was (CD16- CD56 bright) cells.

6.2.1.3 **The response of NK- T cell (CD3+CD56+)**

The frequency of NK-T cells expressing TNFa were not-significantly different between tumor and non tumor organoids and compared to TIL cells control as presented in Figure 71a. The results indicated that no change in the expression of PD1 on NK-T cells, as has been noted with all groups and with culture time as show in Figure 71b, The same results were found with the expression of CD107a+ as presented in Figure 71c. However, my results show increased frequency of CD57+NK-T cells after co-culture for 10 days with both types of organoids as shown in Figure 71d. Finally, the results showed that there were no differences in the frequency of NK activation marker (NKG2D) even after included the blocking antibody as show Figure 71e.

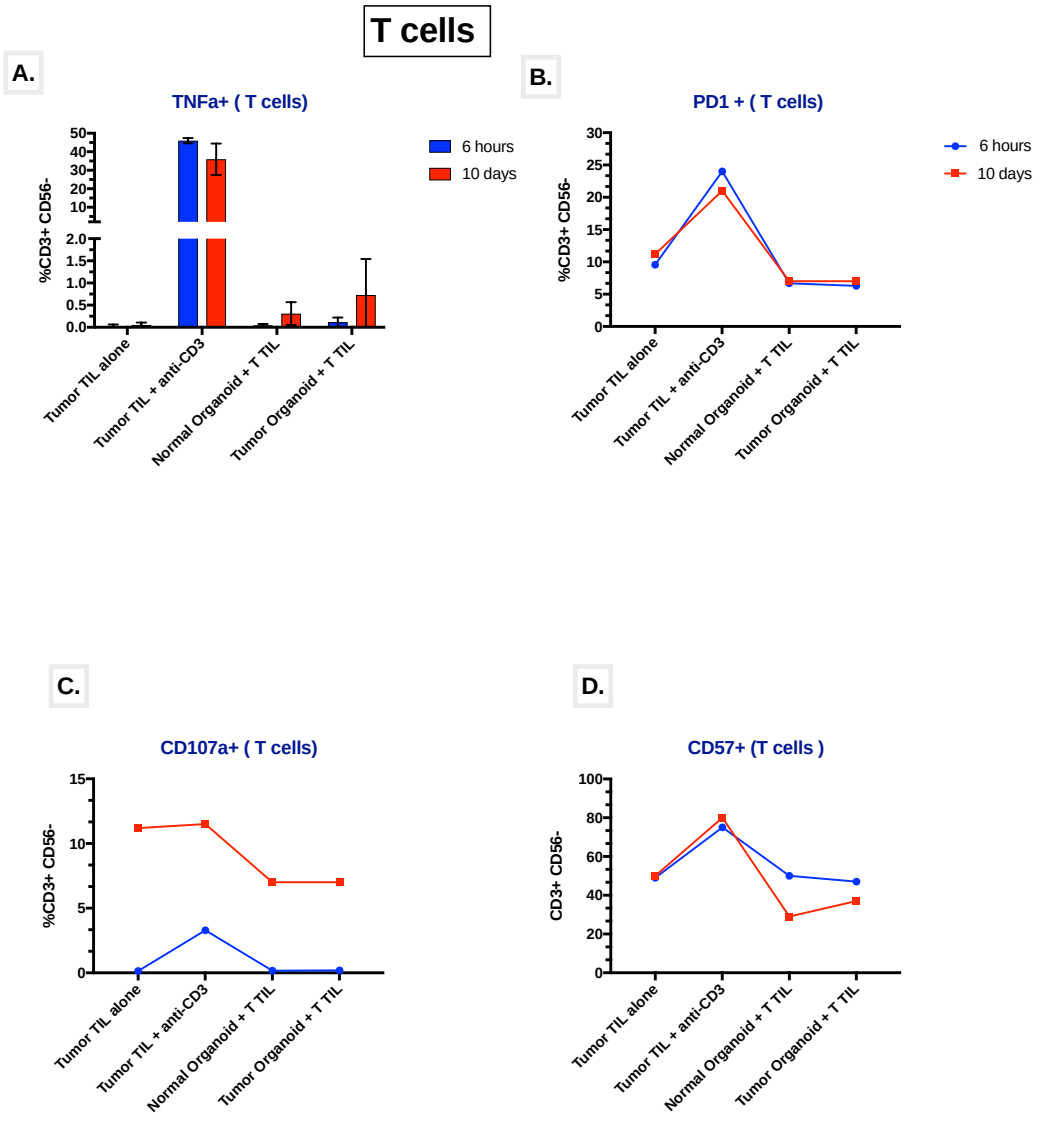

Figure 69: T cell response to 3D organoid

Tumor TIL (T TIL) were cultured with autologous tumor or non-tumor organoid for 6 hours or 10 days . A. to measure the response of T cells, anti-TNFa-APC antibody was added to culture well for 6 hrs then TNFa was measured on CD3+ T cells. TIL cells were also co-culture with organoid for 10 days then TIL cells were re-stimulated with fresh organoid in present of anti-TNFa antibody as described, all results were compared to negative control (TIL alone) (Sidak's multiple comparisons test) . B. PD1 expression on T cells. C, CD107a expression on T cells. D. CD57 expression. TIL cell alone were stimulated by anti-CD3 as positive control or without as negative control

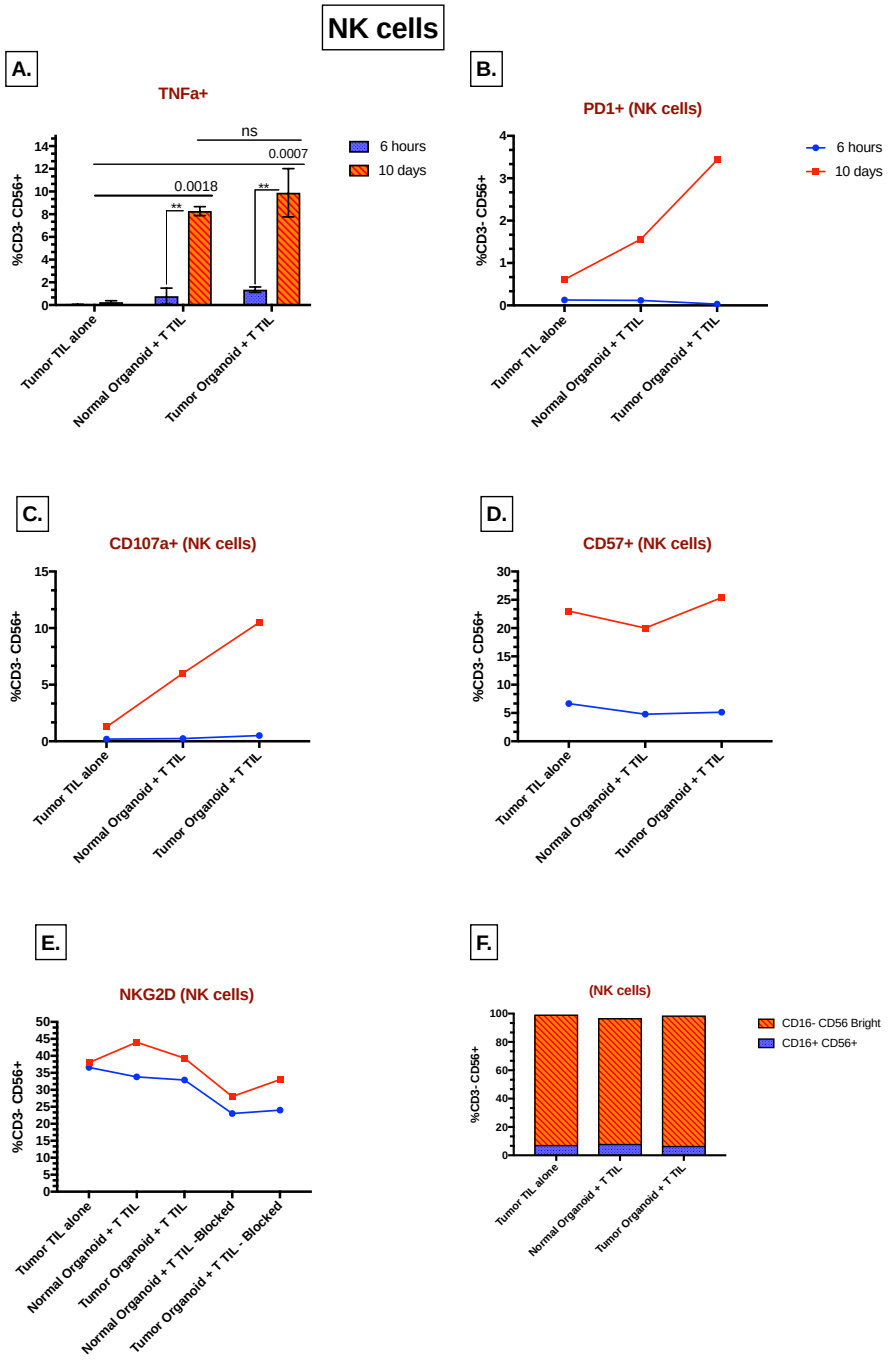

Figure 70 : The response of NK cell to 3D organoid

Tumor TIL (T TIL) were cultured with autologous tumor or non-tumor organoid for 6 hours or 10. A. to measure the response of NK cells, anti-TNFa-APC antibody was added to culture well for 6 hrs then TNFa was measured on the CD56+ NK cell population. TIL cells were also co-culture with organoid for 10 days then TIL cells were re-exposed to fresh organoid in present of TNFa antibody as described. all results were compared to negative control (TIL alone) Sidak's multiple comparisons test). B. PD1 expression on NK cells. C, CD107a expression on NK cells. D. CD57 expression. E. NKG2D expression on NK cells. F. Phenotyping of NK cells (CD16). TIL alone were used as negative control

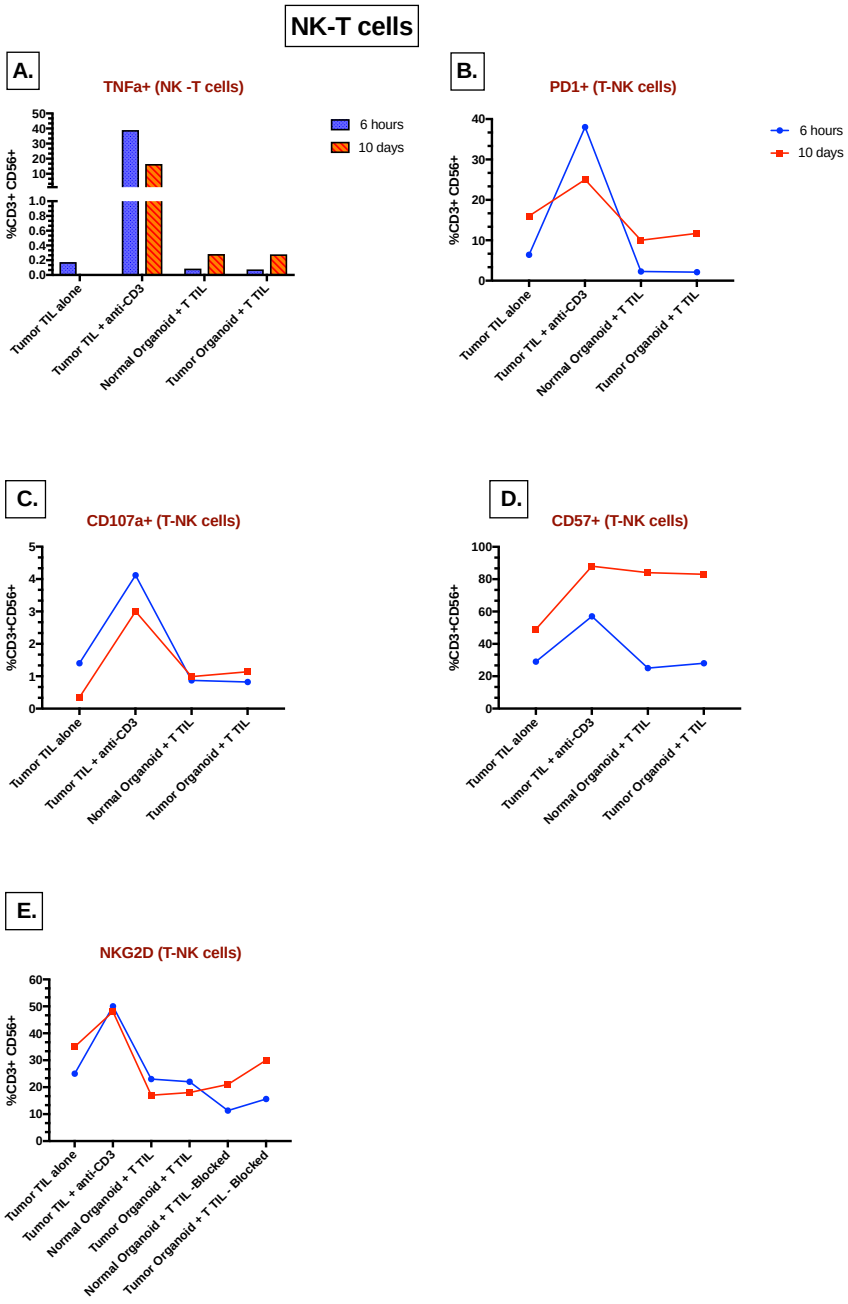

Figure 71: The response of NK-T cell to organoid

Tumor TIL (T TIL) were cultured to autologous tumor or non-tumor organoid for 6 hours and 10 days. A. To measure the response of NK-T cells, anti-TNFa-APC antibody was added to culture well for 6 hrs then TNFa was measured on CD3+CD56+ NK-T cell population. TIL cells were co-culture with organoid for 10 days then re-exposed to fresh organoid in presence of TNFa antibody as described all results were compared to negative control (TIL alone) Sidak's multiple comparisons test). B. PD1 expression on NKT cells. C, CD017a expression on NKT cells. D. CD57 expression on NKT cells. E. NKG2D expression on NK-T cells. TIL alone were used as negative control or stimulated by Anti-CD3 as positive control.

6.2.1.4 **Detection of intracellular secretion cytokines during TIL cells and organoid co-culture.**

During co-culture of TIL cells with organoids the supernatants were collected at different times to detect intracellular expression and secretion of IFNg which would indicate an immune response to organoid. For that, supernatants of culture were collected in different period times then tested by ELISA. As presented in ***Figure 72***a, culture supernatant collected after 6 and 20 hours of culture, the concentration of IFNg indicates significant differences between TILs and organoid and TIL alone cells after 6 hours. The result in the same figure also shows a significant increase in the response after 20 hours of culture with tumour and non-tumour organoid.

The concentration of IFNg were measured at day1, 7 and 10 as show in ***Figure 72***b, secreted IFNg was found significantly increased with both tumour and non-tumour organoids as culture time increased. This indicates a response of immune cells to organoid. As described above, after 10 days of culture TIL cells were cultured again with fresh organoids. In these experiments the supernatant was also collected after 6 and 24 hours. In ***Figure 72***c, the results show that the immune cells responded within 24 hours but the concentration of secreted IFNg was greater with tumor organoid in comparison to non-tumor. These results confirme the previous TNFa response which detected TNF-a expression on NK-cells, which can produce IFN-g.

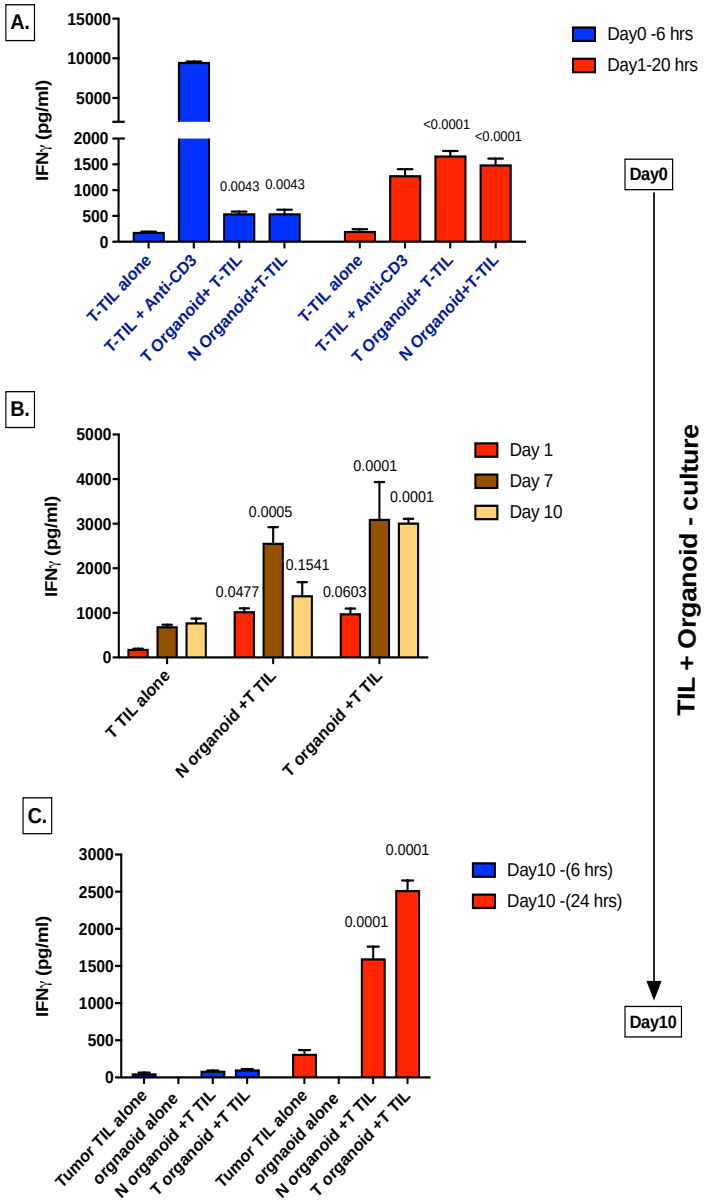

Figure 72 : Detection of intracellular secretion cytokines: patient 22

Cultured supernatants were harvested to measured secreted IFNg from TIL cells incubated with organoids using ELISA. A. Secreted IFNg was measured after 6 and 20 hours of culture. B. the supernatant was collected during co-culture at day 1, 7 and 10 and analysed. C. TIL cells were re-cultured with fresh organoid and the supernatant collected and tested after 6 and 24 hours. All results were compared to negative control (TIL alone) (Dunnett's multiple comparisons test)

6.2.2 Patient 21: the response of Tumor and non- tumor TIL cells to Tumor and non-tumor derived organoid cells.

In this study, tumor and non-tumor autologous TIL cells were co-cultured with tumor and non-tumor organoids. In this case, I tried to identify and compare the immune response from expanded tumor or non-tumor TIL cells to tumor or non-tumor gastric organoid. As presented in Figure 73 there are two cells population include T cells and NK cells. in my study, these cells have been analyzed separately as discussed below.

6.2.2.1 **The response of T cells to organoid cells**

The results showed no significant TNFa response from CD3+ CD56- cells exposed to tumor and non-tumor organoid as presented in Figure 74a . In Figure 74b , the expression of PD1 on CD3+ T cells was slightly decreased in tumor TIL after 10 days culture with organoid but there was no change in the frequency of PD1 in non-tumor TIL with all groups . The results also show that CD107a expression in tumor and non-tumor TIL cells were the same with all organoid as show in Figure 74e. Finally, a high frequency of CD57 was detected on TIL exposed to tumor organoid as shown in Figure 74d but no differences were present for TIL cells exposed to organoid and TIL alone.

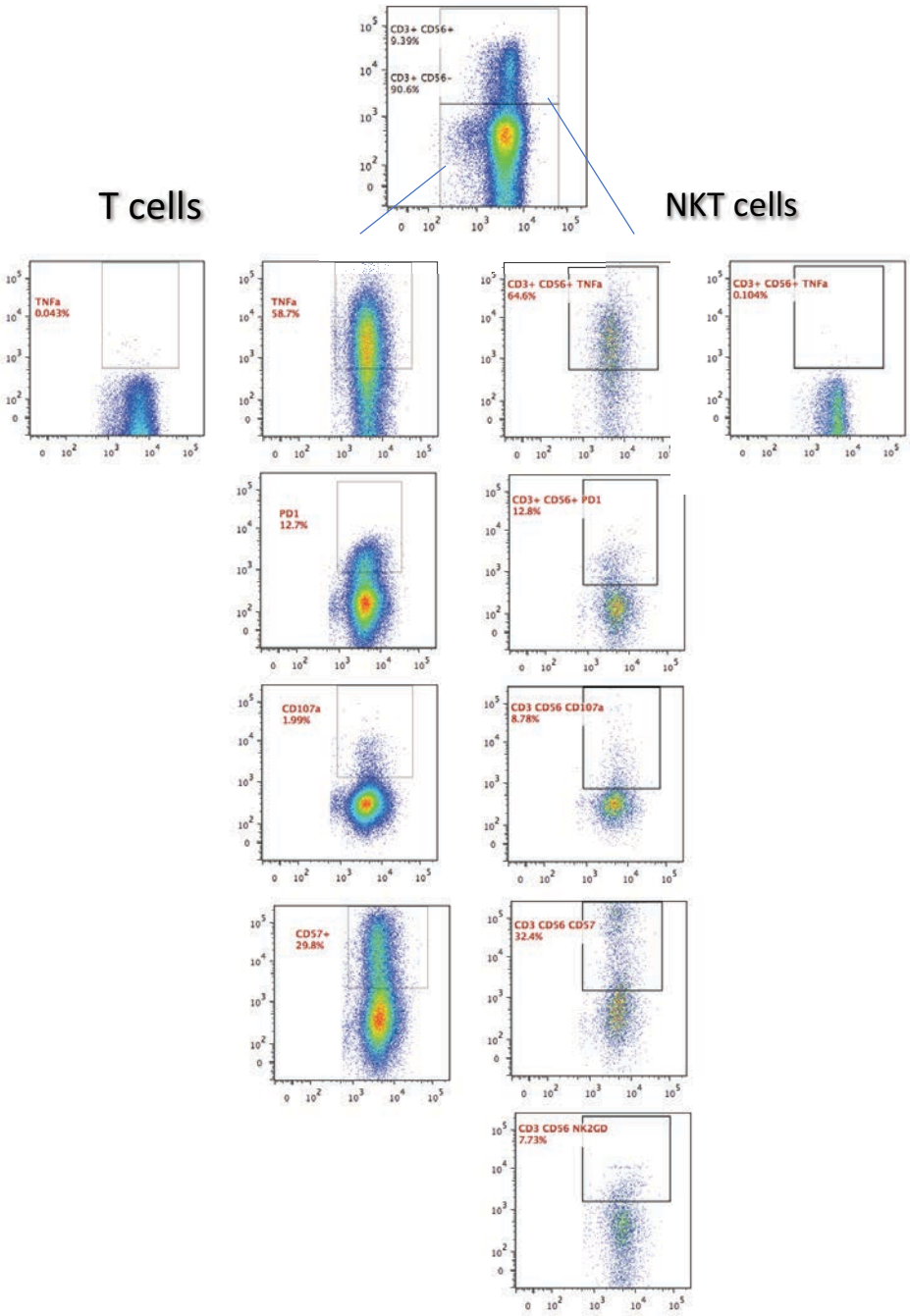

Figure 73 :Gating strategy for flow cytometer analysis of TIL cells

This gating is a sample of flow cytometer analysis for patient 21. two cells populations were gated, T cell (CD3+ CD56-) and NK-T cells (CD3+ CD56+) .

6.2.2.2 **The response of NK-T cells to organoid**

The frequency of TNFa+ NK-T cells indicates no NK-T cells responses were present in tumor and non-tumour TIL cells exposed to tumor or non-tumor organoids, even after 10-day co-culture as show in Figure 75a. As presented in Figure 75b, the was no change the frequency of PD1 expression on NKT cells with tumor and non-tumor cells exposed to the two different organoids. My result showed that no differences in the expression of CD107a+ from TIL cells after interaction with organoids as show in Figure 75c. My result found higher CD57 expression on NKT cells exposed to tumor TIL cells in comparison to non-tumor TIL cells where the expression slightly increased with tumor organoid as show in Figure 75d. The results also showe that the expression of NKG2D was slightly decreased on tumor and non-tumor TIL cells after culture with organoid as presented in Figure 75e but no differences between organoid groups were noted.

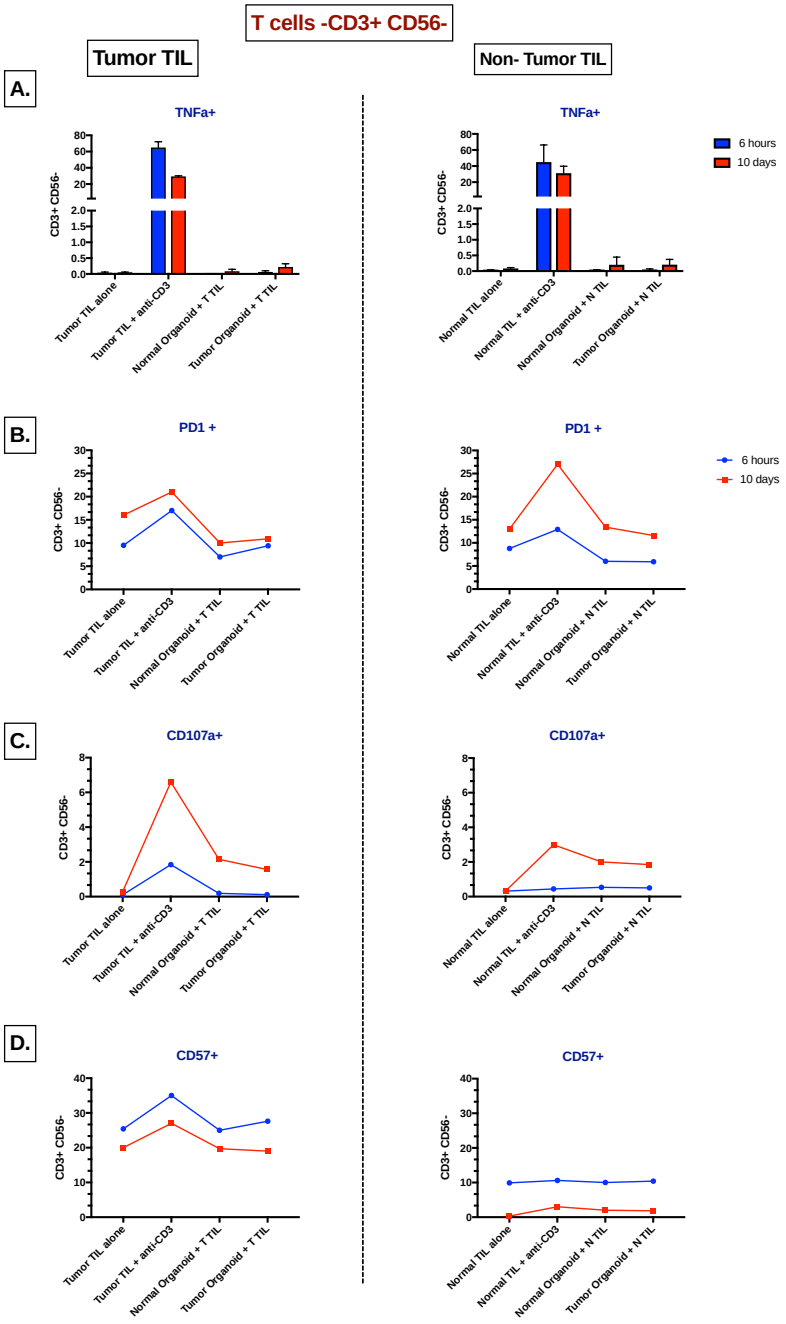

Figure 74: T cell response to 3D organoid: tumor and non-tumor TIL

Tumor TIL (T TIL) and non-tumor TIL (N TIL) were cultured with autologous tumor or non-tumor organoid for 6 hours and 10 days . A. to measure the response of T cells, TNFa antibodies were added to culture well for 6 hrs then TNFa was measured on the CD3+ T cell population. TIL cells were also co-cultured with organoid for 10 days then TIL cells were re-exposed to fresh organoid in present of TNFa antibody as described , all results were compared to negative control (TIL alone) Sidak's multiple comparisons test).. B. PD1 expression on T cells. C, CD107a expression on T cells. D. CD57 expression. TIL cell alone were stimulated by anti-CD3 as positive control or without as negative control

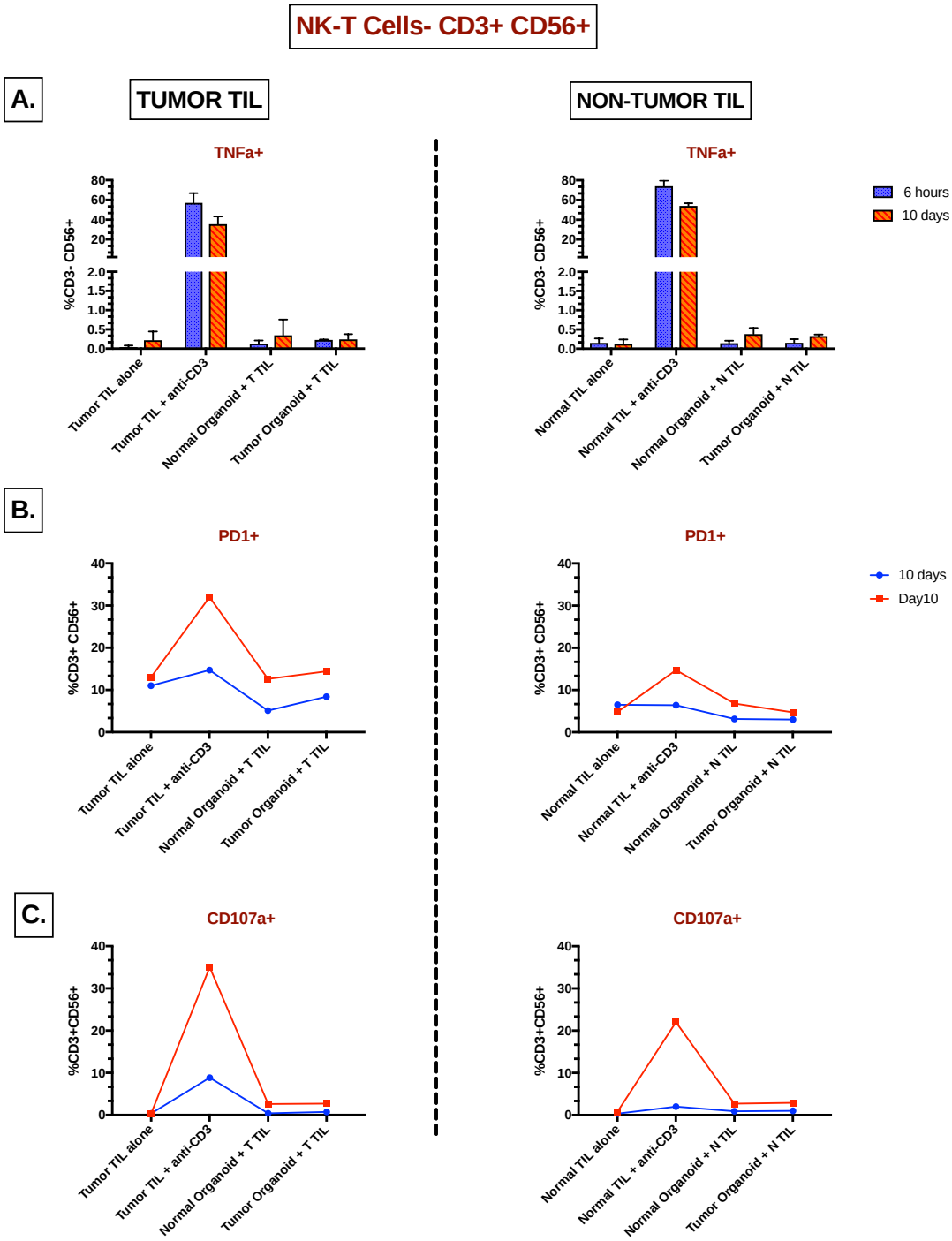
NK-T Cells- CD3+ CD56+
A.
TUMOR TIL
NON-TUMOR TIL
TNFa+
%CD3- CD56+
6 hours
10 days
Tumor TIL alone
Tumor TIL + anti-CD3
Normal Organoid + T TIL
Tumor Organoid + T TIL
Normal TIL alone
Normal TIL + anti-CD3
Normal Organoid + N TIL
Tumor Organoid + N TIL
B.
PD1+
%CD3+ CD56+
10 days
Day10
C.
CD107a+
%CD3+CD56+

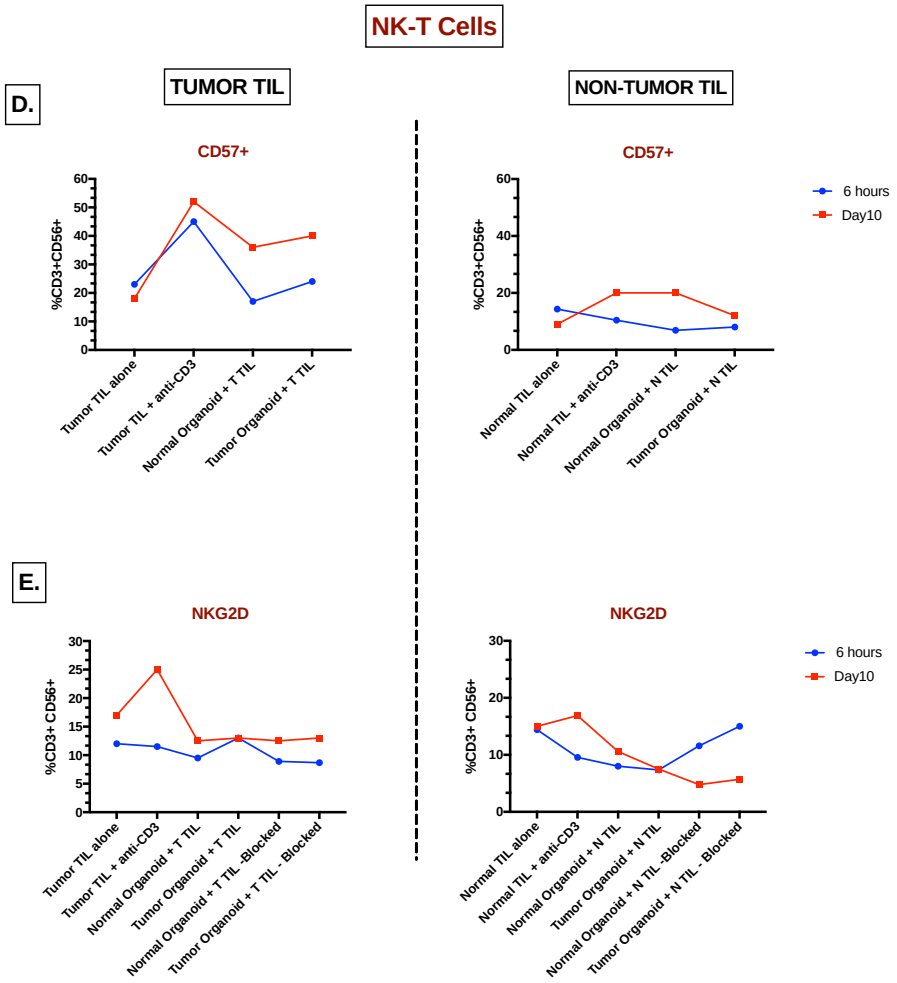

Figure 75 : The response of NK-T cell to organoid

Tumor TIL (T TIL) and non-tumor (N TIL) were cultured with autologous tumor or non-tumor organoid for 6 hours and 10 days . A. to measure the response of NK-T cells, anti-TNFa-APC antibody was added to culture well for 6 hrs then TNFa expression on CD3+CD56+ NK-T cells measured. TIL cells were co-culture with organoid for 10 days then TIL cells were re-exposed to fresh organoid in presence of TNFa antibody as described, all results were compared to negative control (TIL alone) Sidak's multiple comparisons test). . B. PD1 expression cells on NK-T cells. C, CD017a expression on NK-T cells. D. CD57 expression on NK-T cells. E. NKG2D expression on NK-T cells. TIL alone were used as negative control or stimulated by Anti-CD3 as positive control.

6.2.2.3 **Detection of intracellular secretion cytokines during TIL cells and organoid co-culture**

As described for the earlier patient, supernatant from the TIL+organoid experiments was analyzed using ELISA. The results in **Error! Reference source not found.**a show that no significant immune response was detected from tumor and non-tumor TIL cells with all groups of organoids after 6 or 20 hours of culture. In**Error! Reference source not found.**b, there were no significant differences in secreted IFNg in supernatant at day 1, 7 and 10 but increased IFNg was measured with tumor organoid and non-tumor organoid at the end of culture period. Finally, these results show that no significant differences between TIL cells alone and cultured TIL cells existed with all groups of fresh organoids culture as shown in ***Figure 76***c

6.3 T cell recognition of expressed MHC molecules by 3D gastric organoid

Because there were no responses from patient 21's T cells to organoid, either tumor or non-tumor, I analysed the expression of MHC molecules on organoid using T-cell clones in functional assays. The HLA type of the patients was unknown. Therefore, in this experiment, the organoid cells were pulsed with known EBV peptides and tested with CD4 and CD8 T cells clones including BARF1 TFF - specific CD4 cells (DR-51), GSL - specific CD4 cells (DR-17), LMP2 CLG – specific CD8 T cells (HLA-A2) and SSC – specific – CD8 T cells (HLA-A11). T cell responses were detected by measuring IFNg secreted into the supernatant using ELISA. The results showed that MHC molecules were present on tumor and non- tumor organoids from both patients. The results also show that HLA-A2 restricted CLG- specific CD8 T cell response were significantly greater in compare to control. this result indicated that organoid presented MHC-peptides to T cells.

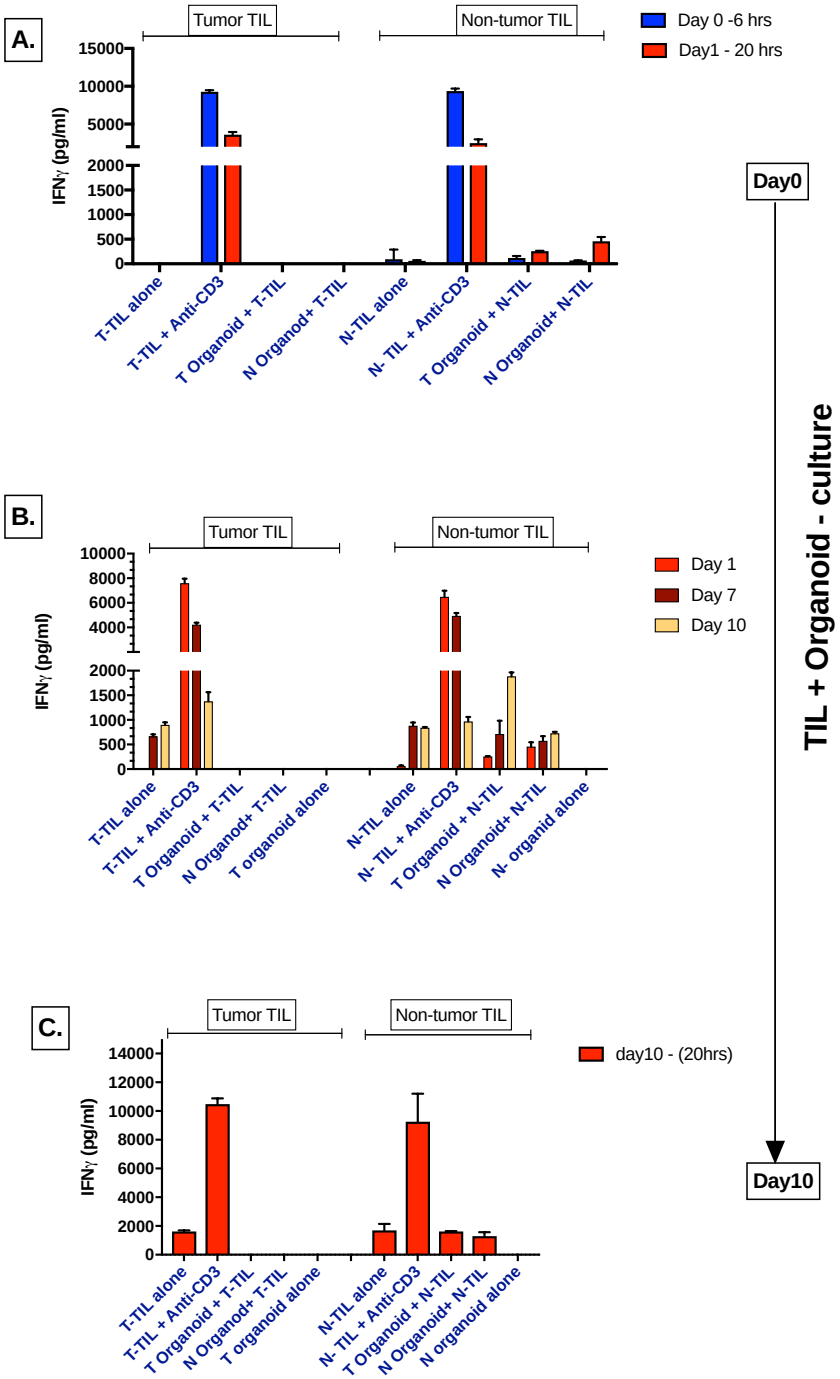

Figure 76 : Detection of intracellular secretion cytokines: patient 21

Cultured supernatants were harvested to measured secreted IFNg from TIL cells in organoid co-cultures using ELISA. A. Secreted IFNg was measured after 6 and 20 hours of culture. B. The supernatant was collected during co-culture at day 1, 7 and 10 and analysed. C. TIL cells were re-cultured with fresh organoid then the supernatant collected after 20 hours and tested. All results were compared to negative control (TIL alone) (Dunnett's multiple comparisons test)

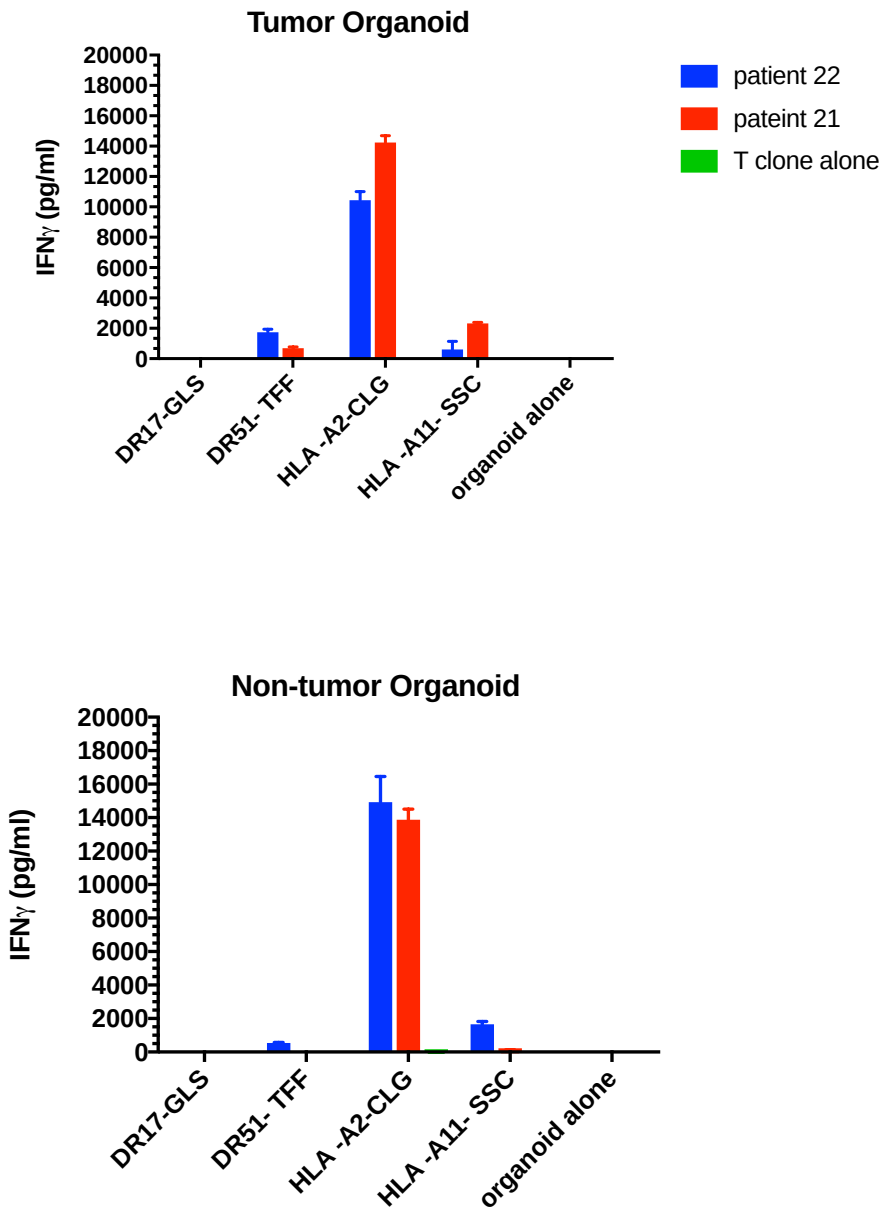

Figure 77 :T cell recognition of expressed MHC molecules by 3D gastric organoid

To study the expression MHC molecules on organoid, the organoid cells were pulsed with peptides and exposed to EBV-specific CD4 and CD8 T cells clones include BARF1 TFF - specific CD4 cells (DR-51), GSL - specific CD4 cells (DR-17), LMP2 CLG – specific CD8 T cells (HLA-A2) and SSC – specific – CD8 T cells (HLA-A11). Organoid alone and T cell clone alone were used as controls. IFNg was measured by ELISA.

6.4 Discussion

Despite the important role played by the interaction between tumor cells and neighbors in cancer development, only a small number of researchers have studied the interaction between immune and tumor cells using the 3D organoid co-culture system [249]. Conventionally, 2D monocultures have been used to study tumour cells, disregarding the importance of the 3-dimensional environment. However, most of those 3D cultures studies with components of tumor microenvironment depended on culture of fibroblasts with tumor cells for mimicking the tumor stroma[250, 251].

However, studying reaction of tumor cells in the presence cells which are related to tumor immunosuppression, progression and therapeutic failure such as infiltrateing lymphocytes, dendritic cells, MDSCs and TAMs have not been addressed[248, 252, 253]. To date, lymphocytes co-culture studies has mainly focused on tumor cells and their upregulated expression of markers of resistance to immune responses of T cell recognition [254] [253].

Until today, the interaction of TIL cells and matched gastric tumor organoid has not been studied. My work is therefore the first attempt to study the interaction and crosstalk between the immune response and 3D organoid in the setting of gastric cancer.

I have attempted to identify the TIL cells responsive to both tumor and non-tumor 3D organoids using the functional culture assay. In addition, I have analyzed upregulated expression markers for immunosuppression, activation and degranulation of TIL cells. My aim here has been to understand the immune response from TIL cells against organoid that can subsequently be developed as an immune therapy for gastric cancer patients.

TIL cells and organoid were isolated from two patients. TIL cells were cultured with 3D spheroid or early differentiated organoid to detect the response of immune cells. The TNFa response were detected after six hours and then after ten days culture the TIL cells were interacted with fresh organoid to detect the rapid immune response. TILs were marked with flow cytometry antibodies to distinguish T cells and NK cells populations and their response to organoids.

Flow cytometry analysis of patient 22 detected T, NK-T and NK cells whereas patient 21 had only T and NK-T cells. My results found no significant differences in T cells TNFa or NK –T TNFa responses between tumor and non-tumor organoids This result agrees with a previous report has showed 3D co-culture was assocaited with increased resistance to the T cell cytotoxic immune response [253].

Interestingly, NK cells from tumor TIL cells responded (NK+ TNFa+) to co-cultured tumor and non-tumor organoid. The frequency of TNFa with tumor organoid was found higher than non-tumor but no significant differences. However NK cells are considered antitumor immune cell as they have cytotoxic function and produce several cytokines include TNFa and IFNg [255] and NK cells are involved in tumor immunosurveillance [256]. The exact role of NK cell responses to tumor organoid models is still unclear but I have shown that the system can be used to begin to understand their role.

Expression marker were also analyzed in this study after co-cultureing organoid and TIL cells including expression of the PD1 immune checkpoint receptor which others have found increased on isolated tumor TIL cells in gastric cancer tissue [257] and different tumor tissue such as lung cancer[258]. CD107a expression is a degranulation marker indicating cytotoxic activity by NK and T cells[259]. The expression of CD57

as a marker of terminal differentiation and senescence has previously been reported to be increase on immune cells in gastric cancer[176] My results found no differences in PD1 and CD107a expression on T or NK-T cells after cultureing TIL cells from both patients. Whereas on T cells there were no differences with expression of CD57 on NK-T cells the expression of CD57 increased after culture with both types of organoid.

However, as noted above NK cells in TIL from patient 22 responded after exposure to the autologous organoids. The expression of PD1 was increased on the NK cell population incubated with tumor and non-tumor organoid but the expression was greater with tumor organoid. In a recent report, PD1 were found increase on tumor infiltrating NK cell in a digestive cancers [260] moreover, CD107a expression were upregulated on NK cells with tumor organoid but no differences have been seen on CD57 expression on these cells. A new study found high expression of CD107 and NKG2D on $PD1^{+}$ NK cells [261] [260]

During TIL cells and organoid co-culture, the supernatants were collected at different times starting from 6 hours until 10 days to detect expression and secretion of IFNg which would indicate an immune response to organoid. With patient 22, the results showed that high concentrations of IFNg was produced when Tumor TIL were co-cultured with organoids. Moreover, the concentration of secreted IFNg increased with co-culture time. After 10 day of co-culture, TIL cells were re-exposed to fresh organoid. IFNg was detected with tumour and non-tumour organoid but the concentration of IFNg was grater with tumour than non-tumour organoid. In contrast with patient 21, there were no significant differences in the concentration of IFNg in

the culture supernatant. These finding confirmed the flow cytometri measurement of TNFa .

The expression of MHC molecules on 3D organoid were analysed because there were no responses from T cells to organoid either tumor or non-tumor after cultured with TIL cells. My results clearly showed that a T cell clone responded to peptide exposed organoids, indicating that organoids could presented MHC-peptides to T cells.

Altogether, this study suggests that 3D organoid co-culture model will be a valuable tool to study critical factors affecting the interactions between immune cells and gastric cancer cells and that NK cells could potentially be useful for the immunotherapy of gastric cancer.

Chapter 7:

Conclusions and future work

7.1 Systematic investigation of T cells responses against EBV tumour antigens in Healthy Donors

Understanding the T cell response to the EBV tumor antigens is important for immune therapy. However, the T-cell response to these tumor antigens has previously been measured individually by different groups using different strategies and techniques. I therefore conducted a systematic analysis of the immune response to the four key EBV tumor antigens (EBNA1, LMP1, LMP2 and BARF1) in twenty-five healthy donors. While defining the immunogenicity of these antigens I found that the strongest response to LMP1 and LMP2 occurred in the same donor (who also had a high response to the EBNA1 antigen). I decided to characterize T cell responses for both latent membrane antigens in this healthy subject. Using seventy three peptides spanning the LMP1 sequence, I identified the LMP1 specific- CD8 T cell response was the already-defined YLQ epitope. Previous experience from others in the research group is that this response is weak; the strength of the YLQ response is therefore novel. Testing with ninety-eight LMP2 peptides identified novel CD4 and CD8 T-cell responses against the LMP2 antigen. Additional experiments testing seven uncharacterized CD4 and CD8 T cell clones specific for LMP2A pepmix revealed additional epitopes in LMP2. An important conclusion from my work is that the EBV tumour antigen response is incompletely characterised. This limits the ability of ourselves, and others in the field, to perform comprehensive immunomonitoring of immunotherapy trials and may also limit the development of effective immunotherapies. Therefore a concerted effort to map these antigens, both in White people but also in other ethnic groups that have different HLA alleles but have been little investigated is justified.

The T cell response to BARF1 antigen in ex vivo assays was weak in the healthy donors I studied. It remains to be seen if stronger responses exist in patients with EBV carcinomas that express BARF1 and this would be interesting to explore in future work. Nevertheless, because the main function of BARF1 during EBV infection is anti- apoptosis it may be difficult for tumours to react to BARF1-specific immune pressure by downregulating BARF1 expression. It is therefore important to explore BARF1 as a potential immunotherapy target.

I therefore searched for BARF1 T-cell responses using more sensitive cultured assays. The aim was to identify epitopes that, although inefficient at inducing T-cell responses in healthy donors could nevertheless potentially be used for immunotherapy by, for example, adoptive transfer of T-cells transduced with BARF1-specific T-cell receptors. Two factors are required for such an approach. First, T-cells bearing receptors with sufficient affinity need to be isolated. Second, the cognate epitope peptide needs to be naturally processed and presented on the tumour cells. I sought to address both rquirements in my work.

Using cultures assays, I confirmed that weak ex vivo T-cell responses to BARF1 were indeed real, based on the greater strength of these responses after the first and second stimulations. BARF1-specific T-cells from 5 healthy subjects were clones enabling me to study these responses in depth. I generated several novel BARF1 – specific CD4 T cell clones and identified the following new epitopes: HLA-DR51 restricted BARF1 (TFF), HLA-DR-53 restricted (GER), HLA-DP-2 restricted (TEV). HLA-DR17 restricted (GSL), and HLA-DR-103 restricted (TEV). To confirm these clones were indeed specific for these peptides, and not cross reactive low avidity responses, I

measured the functional avidity of these T cell clones against a range of peptide concentrations.

The avidity of BARF1 TFF- specific clones was low (>100 nM) with three T clones but other clones were high (16-53%). Importantly, some of the high avidity T cell clones were able to respond to naturally presented epitopes on LCLs. Using a panel of HLA – matched LCL and the epithelial NPC c666 cell line that expresses BARF1, I demonstrated that multiple T clones recognized naturally presented epitopes from these cell line.

BARF1 is a secreted protein. I therefore analyzed whether such recognition was the result of intercellular transfer of BARF1 protein, adding supernatant from these cells (which may contain secreted BARF1 protein) to B cells and epithelial cells and measuring CD4 T cell recognition. Using concentrated supernatant prepared from LCL and C666 as BARF1 positive, and supernatant prepared from the NP460 cells as a BARF1 negative control, I showed that BARF1 was transferred from LCL B cell to epithelial (c666), and this process yielded greater recognition than the reverse (epithelial to B cell).

The important step in development of TCR-based T cell immunotherapy is selection of target T cell epitope. Given that DR51 is a common HLA allele in the population, and that BARF1 (TFF) specific CD4 T-cells restricted by DR51 could recognize EBV-positive cells, I decided to examine this response in more detail.

I PCR amplified the TCRα/β genes and obtained the TCR sequences. Interestingly, all three clones had the same TCR sequence, despite having different avidities in T-cell assays. These differences were consistent over multiple assays. It is likely that other factors in the T-cells that contribute to T-cell binding to target cells, T-cell

activation or T-cell effector function account for these differences. These clones may be important tools for understanding these factors, which would help to improve T-cell immunotherapy.

Using newly generated BARF1 plasmids I found no recognition by BARF1- specific T clones (TFF) and (GSL) to all three transfected GC cell lines (YCCEL, MKN1 and MKN28) with BARF1 constructs even when expressed as an Invariant chain fusion. These epithelial cells were also not recognised after incubation with BARF1-containing cell supernatants. Interestingly, the B cell (SUDHL-5) transfects with the minimal BARF1-il- plasmid was recognized by the TFF-specific T clone.

I also transfected YCCEL cells with GFP-pcDNA plasmid (Full BARF1 gene), but no response was seen from T cell clones. At the same time, I treated some of the transfected YCCEL with Brefeldin A (BFA) to stop BARF1 secretion. After that, BARF1 protein was detected by monoclonal BARF1 antibody. I suggest BARF1 is secreted through classical pathway when block protein passage at specific stage with BFA via secretory pathway. these finding suggest that BARF1 protein is highly secreted in epithelial cells more than B cells, so T cells may not recognise the expressed antigen.

7.2 Involvement and Functional of Immune Cells in Patient Blood with Gastric Cancer: Features of Antigen -Specific T Cell Response to EBV And Tumour Antigens.

It is currently unclear what the status of EBV-specific immunity is in GCa patients. My study sought to understand how best to harness EBV-specific immunity to develop immunotherapy for patients with EBV-associated cancer by measuring T-cell immunity to the EBV tumor antigens that are expressed in the malignant cells of GCa. I have succeeded, through my study, in determining the T response in the blood to EBV antigens using a newly developed TNFa culture assay. However, these results may not reflect the full response of T cell to EBV tumour antigens in gastric cancer patients. It would be desirable to study more patients. I found that there were no significant differences in T cell response to EBV antigens between donors and patients according on the mean value of T cell responses.

It is unclear what the status of tumour antigens-specific immunity is in GC. So, in my study I also investigated T cell response to cellular tumour antigens including CEA, MUCIN1, MAGEA1, MAGEA3, MAGE4 and NY-ESO-1 all of which are reported to be expressed in gastric cancer tumours. My study is the first to compare the T response between these tumor antigens in GC patients' blood as well as comparing the response to HD blood. My results show that T cells from patients and donors responded to tumour antigens although there was variation in this recognition. While the T-cell response level was low, I observed differences between the mean value in GC and HD with some antigens. I found that T cell responses in GC patients to MAGEA1, MAGEA4, and NY-ESO-1 were more than HD. Interestingly, significant T cell response to MAGEA1 with GC patients compare to HD.

In my study I also examined lymphocytes subsets by flow cytometry. I found increased mean percentage of CD8 T-cells in PBMCs of GC patients compared to HD. I also found that the mean of the CD4/CD8 ratio was lower in GC patients compared to HD but the difference was not significant. The percentage of CD19+ B cells in the lymphocytes was significantly lower in GC patients compared to HD controls, I also studied the frequency of gamma delta T cells in GC patients and HD control and found that the mean frequency of gamma delta (γδ) T cells in the CD3+ population was increased in GC patients but this was not significant.

In recent years the field of immune checkpoint inhibition has advanced dramatically, with these agents now used to effectively treat several cancers. I therefore measured the expression of inhibitory receptors on CD4+ and CD8+ T cells in PBMCs from GC and HD. In this study, the expression of LAG3 and CTLA4 was significantly increased in GC on CD8 T cells whereas the mean of TIM-3 was found more in GC, No significant differences were seen with PD1 and CD57 expression. For the CD4 T-cell population, expression of TIM3 and CTLA4 was significantly higher in GC patients. I also found that the mean of PD1 and CD57 was higher in GC patients

Immune suppressor cells, including T reg and MDSCs, play important roles in cancer immunity. Analysing blood, I found a significant increase in the frequency of Treg cells in GC patients compared to HD. Moreover, CD45RA expression was lower on patients' T-regs which suggest these cells are effector Treg . Another way to determine if T-regs have been activated is to examine if they are proliferating, as detected by Ki67. I found the frequency of Ki67-positive T-reg cells was slightly higher in GC patients but this wan not significantly different.

I also studied the frequency of MDSCs, using PBMCs but also whole fresh blood to allow analysis of granulocytic cells. I found that the frequency of myeloid MDSCs in whole blood was elevated in some GC patients, but not all, suggesting heterogeneity in the patient population. In whole blood, I found no significant difference in myeloid MDSCS cell number. Analysing PBMCs I found that the frequency of myeloid MDSCs was increased in some patients although this was not significantly different compared to HD controls. Interestingly, granulocytic MDCSs were significantly higher in frequency in gastric patients‘ PBMCs. In cancer patients granulocytic MDSCs can have lower density and co-purify with PBMCs, and this appears to be the case in GC patients.

7.3 The function and phenotype of immune cells within gastric tumors

While analysis of blood samples can provide impotant insights into systemic immunity, arguably analysis of the tumour itself is more relevant for informing immunotherapy. Therefore, in addition to the blood analysis I also undertook detailed analysis of gastric cancer samples. I successfully isolated lymphocytes from tissue of gastric cancer patients by digestion, allowing them to be phenotypes. I was also able to isolate lymphocyes by culturing tissue in cytokine-containing medium. This approach allowed me to expand the intratumoural immune cells to prepare high number of tumour infiltrating lymphocytes (TILs).

A limited number of molecular and histological studies have reported the clinical prognostic impact of intra-tumoural lymphocytes in EBVaGC patients. Considering the specificity of the EBV-specific cells in GC, I found CD8 T cells specific for EBNA1, EBNA3A, LMP2 and LMP1 but no responses to BARF1 Further studies are necessary to detect whether these antigens were expressed in these tumours, and

whether such expression was in the tumour cells or in B cells infiltrating the tumour. Nevertheless, the presence of EBV antigen specific T-cells in tumors is encouraging for the potential treatment of the 10% of cases of gastric cancer positive for EBV.

No studies have investigated the response to cellular tumour associated antigens in gastric cancer tumours despite the fact that several antigens are expressed. My study provided me with the tools and samples to address this gap in our knowledge. I selected several tumour antigens for analysis (NY-ESO-1, MUCIN1, MAGEA1, MAGEA3, MAGEA4, CEA and PSMA) based on published evidence of expression in gastric cancer or detection of antibodies to the antigen in patient serum. I observed low PSMA–specific CD8 T cell responses in three of nine patients after short ex vivo stimulation of tumour lymphocytes but no response was found to the other antigens. No specific responses were detected after 10 days of in vitro culture except a MUCIN1– pecific CD8 T cell response in one of nine patients. These finding indicate that tumours infrequently contain T-cells specific for these classical tumour associated antigens.

Aanother aim of my study was to compare the function and phenotype of lymphocytes present in tumor and non-tumor tissues. I found the former had significantly higher CD4/CD8 ratio and higher EM and TEMRA CD4 and CD8 T cells. The frequency of gamma delta (γδ) T cells in the CD3+ population was statistically higher in tumor tissue than non-tumor tissue. I found no difference in the frequency of B cells between tumour and non-tumour tissues.

Measuring the expression of four immune checkpoints on lymphocytes isolated from tumor and non-tumor tissue, I found for CD8+ T cells that there were no significant differences in PD1, TIM3 or LAG3 expression between tumor and non-tumor tissues

but the expression of CTLA4 was significantly lower on CD8 T-cells isolated from tumor. For CD4+ T-cells the expression of immune checkpoint inhibitors was not significantly different for cells isolated from tumor and non-tumor tissue

comparing checkpoint expression on lymphocytes isolated from tumour tissue or PBMCs, I found that the expression of immune checkpoints was upregulated on both CD4 and CD8 T cells in tumor tissue.

Suppressive cells are important modulators of immunity within tumours. I found that the frequency of T reg CD4 T cells was significantly higher in tumor than non-tumor tissues. Moreover, the T regs in tumour tissue were antigen experienced (CD45RA) and had recently proliferated as determined by (KI67). For some patients, the frequency of monocytes-MDSCs and granulocyte- MDSCs were greater in tumour tissues compared to non-tumour tissue from the same patient.

Although I found little evidence for the presence of T-cells specific for cellular tumour antigens in gastric cancer tumours, it is possible that T-cells specific for other antigens, including private antigens such as neoantigens generated through mutations unique to the individuals cancer, could be present. Indeed, such T-cells may be more effective as they have not been negatively selected during the establishment of central tolerance. My results clearly show that gastric cancer intratumoural lymphocytes can readily be expanded to high numbers. I therefore examined the phenotype of these cells. My results show Expression of PD1 on CD T-cells was decreased on expanded TILs but LAG3 was; increased; the other inhbitors were unchanged.and was lower after in vitro expansion to generate TILs. The upregulation of LAG-3 expression in expanded TILs strongly suggests expression of this receptor is regulated differently.

Importantly, after in vitro culture the frequency of T reg cells significantly decreased in TILs. These results point to a role for T-reg in the tumour microenvironment.

Expanded TIL cells showed downregulation of M-MDSCs.

Overall, my results provide new insights into gastric cancer immunology and new leads for future investigation, both scientifically but also for immunotherapy development.

7.4 The functional assessment of Tumour infiltration lymphocytes with Three-Dimensional Organoid Derived from Gastric Cancer Patients tissue.

The ability for TIL cells to recognize gastric cancer cells has not been studied. Asa parallel project in the research team was generating organoids from gastric cancer, I decided to perform the first ever analysis of the interaction and crosstalk between the immune response and 3D organoids in the setting of gastric cancer. Because organoids are closer to tissues than conventional 2d cell cultures the use of organoids will provide better evidence for the use of TILs to treat gastric cancer patients.

Interestingly, NK cells in TILs prepared from tumor TIL responded to autologous tumor and non-tumor organoids. The frequency of TNFa-positive NK cells was higher after culture with tumor organoids although this was not significantly higher than the non-tumor organoids. The results found no significant differences in T cells TNFa or NK –T TNFa responses between tumor and non-tumor organoids.

The phenotype of TILs incubated with organoids was also analysed. The expression of PD1 was increased on the NK cell population incubated with tumor and non-tumor organoid and PD1 expression was greater for the former. Moreover, CD107a expression was higher on NK cells incubated with tumor organoid. During TIL + organoid co-cultures aliquots of supernatants were collected at different times starting

from 6 hours until 10 days after the start of the experiment. Detection of IFNg would indicate an immune response to organoid. The results showed that high concentrations of IFNg were produced when Tumor TIL were co-cultured with organoids. Moreover, the concentration of secreted IFNg increased with co-culture time. After 10 day of co-culture, TIL cells were re-exposed to fresh organoid. IFNg was detected with tumour and non-tumour organoid but the concentration of IFNg was grater with tumour than non-tumour organoid. These finding confirmed the flow cytometry data that measured TNFa.

Because there were no responses from T cells in TILs incubated with organoid, whether tumour or non tumour, I determined whether the organoids expressed functional MHC molecules. My results clearly showed that a CD8+ T cell clone responded to peptide exposed organoids, indicating that organoids could presented MHC-I restricted peptides to T cells, at least when high concentrations were used. It remains to be seen whether the efficiency of peptide presentation by tumor organoids is reduced Or whether defects in antigen processing and presentation are present; either could explain why T-cells failed to respond to organoids. Another explanation, of course, could be that TILs in gastric tumours are not specific for the tumour cells. My data show that is is feasible to study immune control of gastric cancer using the 3D organoid co-culture model. This will be a valuable tool to study critical factors affecting the interactions between immune cells and gastric cancer cells. My data also suggest that NK cells could potentially be useful for the immunotherapy of gastric cancer.

7.5 Future work

The following experiments naturally lead on from my work:

1- Characterizing the newly identified LMP1 and LMP2 specific CD8 and CD4 T cell responses.
2- Stratifying gastric cancer patients into EBV-positive and negative cases, and assessment of EBV protein expression in the former.
3- Developing BARF1 as a therapeutic T-cell target in EBV-assocaited cancers, including further characterization of the cloned T-cell receptor.
4- Determining if T-cells in TIL preparations are able to recognize autologous gastric cancer cells
5- Exploring the value of TIL NK cells to treat gastric cancer.

CHAPTER 8

REFERENCES

.1 Sonnenschein, C. and A.M. Soto, *The aging of the 2000 and 2011 Hallmarks of Cancer reviews: a critique.* J Biosci, 2013. **38**(3): p. 651-63.

.2 Berretta, R. and P. Moscato, *Cancer biomarker discovery: the entropic hallmark.* PLoS One, 2010. **5**(8): p. e12262.

.3 Vajaria, B.N. and P.S. Patel, *Glycosylation: a hallmark of cancer?* Glycoconj J, 2017. **34**(2): p. 147-156.

.4 Enderling, H. and P. Hahnfeldt, *Cancer stem cells in solid tumors: is 'evading apoptosis' a hallmark of cancer?* Prog Biophys Mol Biol, 2011. **1** :(2)06p. 391-9.

.5 Ebos, J.M. and R.S. Kerbel, *Antiangiogenic therapy: impact on invasion, disease progression, and metastasis.* Nat Rev Clin Oncol, 2011. **8**(4): p. 210-21.

.6 Munkley, J. and D.J. Elliott, *Hallmarks of glycosylation in cancer.* Oncotarget, .2016 :(23)7p. 35478-89.

.7 Arosa, F.A., *CD8+CD28- T cells: certainties and uncertainties of a prevalent human T-cell subset.* Immunol Cell Biol, 2002. **80**(1): p. 1-13.

.8 Ono, M. and R.J. Tanaka, *Controversies concerning thymus-derived regulatory T cells: fundamental issues and a new perspective.* Immunol Cell Biol, 2016. **94**(1): p. 3-10.

.9 Germain, R.N., *T-cell development and the CD4-CD8 lineage decision.* Nat Rev Immunol, 2002. **2**(5): p. 309-22.

.10 Morsheimer, M., et al., *The immune deficiency of chromosome 22q11.2 deletion syndrome.* Am J Med Genet A, 2017. **173**(9): p. 2366-2372.

.11 Huppler, A.R., S. Bishu, and S.L. Gaffen, *Mucocutaneous candidiasis: the IL-17 pathway and implications for targeted immunotherapy.* Arthritis Res Ther, 2012. **14**(4): p. 217.

.12 Kubo, M., *T follicular helper and TH2 cells in allergic responses.* Allergol Int, 2017. **66**(3): p. 377-381.

.13 Raje, N. and C. Dinakar, *Overview of Immunodeficiency Disorders.* Immunol Allergy Clin North Am, 2015. **35**(4): p. 599-623.

.14 Zloza, A., et al. ,*Workshop on challenges, insights, and future directions for mouse and humanized models in cancer immunology and immunotherapy: a report from the associated programs of the 2016 annual meeting for the Society for Immunotherapy of cancer.* J Immunother Cancer, 2017. **5**(1): p. 77.

.15 Chew, V., H.C. Toh, and J.P. Abastado, *Immune microenvironment in tumor progression: characteristics and challenges for therapy.* J Oncol, 2012. **2012**: p. 608406.

.16 Das, M. and H. Wakelee, *Angiogenesis and lung cancer: ramucirumab prolongs survival in 2(nd)-line metastatic NSCLC.* Transl Lung Cancer Res, 2014. **3**(6): p. 397-9.

.17 Romero Vielva, L., *Tumor lymphocytic infiltration in non-small cell lung cancer: the ultimate prognostic marker?* Transl Lung Cancer Res, 2016. **5**(4): p.2.-370

.18 Neves, H. and H.F. Kwok, *Recent advances in the field of anti-cancer immunotherapy.* BBA Clin, 2015. **3**: p. 280-8.

.19 Scott, A.M., J.D. Wolchok, and L.J. Old, *Antibody therapy of cancer.* Nat Rev Cancer, 2012. **12**(4): p. 278-87.

.20 Sharma, P., *Immune Checkpoint Therapy and the Search for Predictive Biomarkers.* Cancer J, 2016. **22**(2): p. 68-72.

.21 Sadelain, M., R. Brentjens, and I. Riviere, *The basic principles of chimeric antigen receptor design.* Cancer Discov, 2013. **3**(4): p. 388-98.

.22 Maude, S.L., et al., *CD19-targeted chimeric antigen receptor T-cell therapy for acute lymphoblastic leukemia.* Blood, 2015. **125**(26): p. 4017-23.

.23 Burd, E.M., *Human papillomavirus and cervical cancer.* Clin Microbiol Rev, 2003. **16**(1): p. 1-17.

.24 Di Bisceglie, A.M., *Hepatitis B and hepatocellular carcinoma.* Hepatology, 2009. **49**(5 Suppl): p. S56-60.

.25 Pieczonka, C.M., et al., *Sipuleucel-T for the Treatment of Patients With Metastatic Castrate-resistant Prostate Cancer: Considerations for Clinical Practice.* Rev Urol, 2015. **17**(4): p. 203-10.

.26 Clark, J.I., et al., *Impact of Sequencing Targeted Therapies With High-dose Interleukin-2 Immunotherapy: An Analysis of Outcome and Survival of Patients With Metastatic Renal Cell Carcinoma From an On-going Observational IL-2 Clinical Trial: PROCLAIM(SM).* Clin Genitourin Cancer, 2017. **15**(1): p. 31-41 e4.

.27 Weiland, F., et al., *Deciphering the molecular nature of ovarian cancer biomarker CA125.* Int J Mol Sci, 2012. **13**(8): p. 10568-82.

.28 Isaksson, S., et al., *CA 19-9 and CA 125 as potential predictors of disease recurrence in resectable lung adenocarcinoma.* PLoS One, 2017. **12**(10): p. e0186284.

.29 Westdorp, H., et al., *Immunotherapy for prostate cancer: lessons from responses to tumor-associated antigens.* Front Immunol :5 .2014 ,p. 191.

.30 Horm, T.M. and J.A. Schroeder, *MUC1 and metastatic cancer: expression, function and therapeutic targeting.* Cell Adh Migr, 2013. **7**(2): p. 187-98.

.31 Gutzmer, R., et al., *Safety and immunogenicity of the PRAME cancer immunotherapeutic in metastatic melanoma: results of a phase I dose escalation study.* ESMO Open, 2016. **1**(4): p. e000068.

.32 Konowalchuk, J.D. and B. Agrawal, *MUC1 is a novel costimulatory molecule of human T cells and functions in an AP-1-dependent manner.* Hum Immunol, .2012 :(5)73p. 448-55.

.33 *World Health Organization .Cancer: Fact Sheet No 297*. 2018; Available from: http://www.who.int/mediacentre/factsheets/fs297/en/.

.34 Maconi, G., G. Manes, and G.B. Porro, *Role of symptoms in diagnosis and outcome of gastric cancer.* World J Gastroenterol, 2008. **14**(8): p. 1149-55.

.35 Jemal, A., et al., *Global cancer statistics.* CA Cancer J Clin, 2011. **61**(2): p. 69-90.

.36 Siegel, R., D. Naishadham, and A. Jemal, *Cancer statistics, 2013.* CA Cancer J Clin, 2013. **63**(1): p. 11-30.

.37 Ryu, K.D., et al., *Treatment outcome for gastric mucosa-associated lymphoid tissue lymphoma according to Helicobacter pylori infection status: a single-center experience.* Gut Liver, 2014. **8**(4): p. 408-14.

.38 Lauren, P., *The Two Histological Main Types of Gastric Carcinoma: Diffuse and So-Called Intestinal-Type Carcinoma. An Attempt at a Histo-Clinical Classification.* Acta Pathol Microbiol Scand, 1965. **64**: p. 31-49.

.39 Shi, J., Y.P. Qu, and P. Hou, *Pathogenetic mechanisms in gastric cancer.* World J Gastroenterol, 2014. **20**(38): p. 13804-19.

.40 Tan, P. and K.G. Yeoh, *Genetics and Molecular Pathogenesis of Gastric Adenocarcinoma.* Gastroenterology, 2015. **149**(5): p. 1153-1162 e3.

.41 Ekstrom, A.M., et al., *Helicobacter pylori in gastric cancer established by CagA immunoblot as a marker of past infection.* Gastroenterology, 2001. **121**(4): p. 784-91.

.42 Farrell, P., *Pathogenesis: Infections causing gastric cancer.* Nat Microbiol, 2016. **1**: p. 16038.

.43 Hatakeyama, M., *Helicobacter pylori CagA and gastric cancer: a paradigm for hit-and-run carcinogenesis.* Cell Host Microbe, 2014. **15**(3): p. 306-16.

.44 Saju, P., et al., *Host SHP1 phosphatase antagonizes Helicobacter pylori CagA and can be downregulated by Epstein-Barr virus.* Nat Microbiol, 2016. **1**: p. 16026.

.45 Carneiro, F., et al., *Model of the early development of diffuse gastric cancer in E-cadherin mutation carriers and its implications for patient screening.* J Pathol, 2004. **203**(2): p. 681-7.

.46 Napieralski, R., et al., *Combined GADD45A and thymidine phosphorylase expression levels predict response and survival of neoadjuvant-treated gastric cancer patients.* Clin Cancer Res, 2005. **11**(8): p. 3025-31.

.47 Humar, B. and P. Guilford, *Hereditary diffuse gastric cancer: a manifestation of lost cell polarity.* Cancer Sci, 2009. **100**(7): p. 1151-7.

.48 Zulfiqar, M., et al., *Molecular diagnostics in esophageal and gastric neoplasms.* Clin Lab Med, 2013. **33**(4): p. 867-73.

.49 Wu, M.S., et al., *Correlation of histologic subtypes and replication error phenotype with comparative genomic hybridization in gastric cancer.* Genes Chromosomes Cancer, 2001. **30**(1): p. 80-6.

.50 Vollmers, H.P., et al., *Adjuvant therapy for gastric adenocarcinoma with the apoptosis-inducing human monoclonal antibody SC-1: first clinical and histopathological results.* Oncol Rep, 1998. **5**(3): p. 549-52.

.51 Jang, B.G. and W.H. Kim, *Molecular pathology of gastric carcinoma.* Pathobiology, 2011. **78**(6): p. 302-10.

.52 Motoshita, J., et al., *DNA methylation profiles of differentiated-type gastric carcinomas with distinct mucin phenotypes.* Cancer Sci, 2005. **96**(8): p. 474-9.

.53 Yang, W., A. Raufi, and S.J. Klempner, *Targeted therapy for gastric cancer: molecular pathways and ongoing investigations.* Biochim Biophys Acta, 2014. **1846**(1): p. 232-7.

.54 Cidon, E.U., et al., *Molecular targeted agents for gastric cancer: a step forward towards personalized therapy.* Cancers (Basel), 2013. **5**(1): p. 64-91.

.55 Kakiuchi, M., et al., *Recurrent gain-of-function mutations of RHOA in diffuse-type gastric carcinoma.* Nat Genet, 2014. **46**(6): p. 583-7.

.56 Guo, J., et al., *Genomic landscape of gastric cancer: molecular classification and potential targets.* Sci China Life Sci, 2017. **60**(2): p. 126-137.

.57 Wang, K., et al., *Whole-genome sequencing and comprehensive molecular profiling identify new driver mutations in gastric cancer.* Nat Genet, 2014. **46**(6): p. 573-82.

.58 Leite, M., et al., *MSI phenotype and MMR alterations in familial and sporadic gastric cancer.* Int J Cancer, 2011. **128**(7): p. 1606-13.

.59 Uozaki, H. and M. Fukayama, *Epstein-Barr virus and gastric carcinoma--viral carcinogenesis through epigenetic mechanisms.* Int J Clin Exp Pathol, 2008. **1**(3): p. 198-216.

.60 Lee, H.S., et al., *Epstein-barr virus-positive gastric carcinoma has a distinct protein expression profile in comparison with epstein-barr virus-negative carcinoma.* Clin Cancer Res, 2004. **10**(5): p. 1698-705.

.61 Kang, G.H., et al., *Epstein-barr virus-positive gastric carcinoma demonstrates frequent aberrant methylation of multiple genes and constitutes CpG island methylator phenotype-positive gastric carcinoma.* Am J Pathol, 2002. **160**(3): p. 787-94.

.62 Fukayama, M., *Epstein-Barr virus and gastric carcinoma.* Pathol Int, 2010. **60**(5): p. 337-50.

.63 Hino, R., et al., *Activation of DNA methyltransferase 1 by EBV latent membrane protein 2A leads to promoter hypermethylation of PTEN gene in gastric carcinoma.* Cancer Res, 2009. **69**(7): p. 2766-74.

.64 Hino, R., et al., *Survival advantage of EBV-associated gastric carcinoma: survivin up-regulation by viral latent membrane protein 2A.* Cancer Res, 2008. **68**(5): p. 1427-35.

.65 Saito, H., et al., *Increased PD-1 expression on CD4+ and CD8+ T cells is involved in immune evasion in gastric cancer.* J Surg Oncol, 2013. **107**(5): p. 517-22.

.66 Amedei, A., et al., *T cells in gastric cancer: friends or foes.* Clin Dev Immunol, 2012. **2012**: p. 690571.

.67 Lepone, L.M., et al., *Analyses of 123 Peripheral Human Immune Cell Subsets: Defining Differences with Age and between Healthy Donors and Cancer Patients Not Detected in Analysis of Standard Immune Cell Types.* J Circ Biomark, 2016. **5**: p. 5.

.68 Lee, A.J., et al., *gammadelta T cells are increased in the peripheral blood of patients with gastric cancer.* Clin Chim Acta, 2012. **413**(19-20): p. 1495-9.

.69 Adams, S., et al., *Prognostic value of tumor-infiltrating lymphocytes in triple-negative breast cancers from two phase III randomized adjuvant breast cancer trials: ECOG 2197 and ECOG 1199.* J Clin Oncol, 2014. **32**(27): p. 2959-66.

.70 Loi, S., et al., *Tumor infiltrating lymphocytes are prognostic in triple negative breast cancer and predictive for trastuzumab benefit in early breast cancer: results from the FinHER trial.* Ann Oncol, 2014. **25**(8): p. 1544-50.

.71 Lee, S. and K. Margolin, *Tumor-infiltrating lymphocytes in melanoma.* Curr Oncol Rep, 2012. **14**(5): p. 468-74.

.72 Ademuyiwa, F.O., et al., *NY-ESO-1 cancer testis antigen demonstrates high immunogenicity in triple negative breast cancer.* PLoS One, 2012. **7**(6): p. e38783.

.73 Fujiwara, S., et al., *NY-ESO-1 antibody as a novel tumour marker of gastric cancer.* Br J Cancer, 2013. **108**(5): p. 1119-25.

.74 Wang, X.T., et al., *MUC1 Immunohistochemical Expression as a Prognostic Factor in Gastric Cancer: Meta-Analysis.* Dis Markers, 2016. **2016**: p. 9421571.

.75 Hanson, R.L. and M.A. Hollingsworth, *Functional Consequences of Differential O-glycosylation of MUC1, MUC4, and MUC16 (Downstream Effects on Signaling).* Biomolecules, 2016. **6**(3).

.76 Kozakova, L., et al., *The melanoma-associated antigen 1 (MAGEA1) protein stimulates the E3 ubiquitin-ligase activity of TRIM31 within a TRIM31-MAGEA1-NSE4 complex.* Cell Cycle, 2015. **14**(6): p. 920-30.

.77 Sienel, W., et al., *Melanoma associated antigen (MAGE)-A3 expression in Stages I and II non-small cell lung cancer: results of a multi-center study.* Eur J Cardiothorac Surg, 2004. **25**(1): p. 131-4.

.78 Shinkins, B., et al., *The diagnostic accuracy of a single CEA blood test in detecting colorectal cancer recurrence: Results from the FACS trial.* PLoS One, 2017. **12**(3): p. e0171810.

.79 Chang, S.S., *Overview of prostate-specific membrane antigen.* Rev Urol, 2004. **6 Suppl 10**: p. S13-8.

.80 Haffner, M.C., et al., *Prostate-specific membrane antigen expression in the neovasculature of gastric and colorectal cancers.* Hum Pathol, 2009. **40**(12): p. 1754-61.

.81 Izumi, D ,.et al., *CXCL12/CXCR4 activation by cancer-associated fibroblasts promotes integrin beta1 clustering and invasiveness in gastric cancer.* Int J Cancer, 2016. **138**(5): p. 1207-19.

.82 Lin, L., et al., *CCL18 from tumor-associated macrophages promotes angiogenesis in breast cancer.* Oncotarget, 2015. **6**(33): p. 34758-73.

.83 Wang, H.C., et al., *Tumor-Associated Macrophages Promote Epigenetic Silencing of Gelsolin through DNA Methyltransferase 1 in Gastric Cancer Cells.* Cancer Immunol Res, 2017. **5**(10): p. 885-897.

.84 Kindlund, B., et al., *CD4(+) regulatory T cells in gastric cancer mucosa are proliferating and express high levels of IL-10 but little TGF-beta.* Gastric Cancer, 2017. **20**(1): p. 116-125.

.85 Alizadeh, D. and N. Larmonier, *Chemotherapeutic targeting of cancer-induced immunosuppressive cells.* Cancer Res, 2014. **74**(10): p. 2663-8.

.86 Liu, Y. and X. Cao, *Immunosuppressive cells in tumor immune escape and metastasis.* J Mol Med (Berl), 2016. **94**(5): p. 509-22.

.87 Postow, M.A., M.K. Callahan, and J.D. Wolchok, *Immune Checkpoint Blockade in Cancer Therapy.* J Clin Oncol, 2015. **33**(17): p. 1974-82.

.88 Prasad, V. and V. Kaestner, *Nivolumab and pembrolizumab: Monoclonal antibodies against programmed cell death-1 (PD-1) that are interchangeable.* Semin Oncol, 20 :(2)44 .17p. 132-135.

.89 Kumar, V., et al., *The Nature of Myeloid-Derived Suppressor Cells in the Tumor Microenvironment.* Trends Immunol, 2016. **37**(3): p. 208-220.

.90 Umansky, V., et al., *The Role of Myeloid-Derived Suppressor Cells (MDSC) in Cancer Progression.* Vaccines (Basel), 2016. **4**(4).

.91 Gorgun, G.T., et al., *Tumor-promoting immune-suppressive myeloid-derived suppressor cells in the multiple myeloma microenvironment in humans.* Blood, 2013. **121**(15): p. 2975-87.

.92 Fatehullah, A., S.H. Tan, and N .Barker, *Organoids as an in vitro model of human development and disease.* Nat Cell Biol, 2016. **18**(3): p. 246-54.

.93 Clevers, H., *Modeling Development and Disease with Organoids.* Cell, 2016. **165**(7): p. 1586-1597.

.94 Epstein, M.A., B.G. Achong, and Y.M. Barr, *Virus Particles in Cultured Lymphoblasts from Burkitt's Lymphoma.* Lancet, 1964. **1**(7335): p. 702-3.

.95 Henle, W. and G. Henle, *Epidemiologic aspects of Epstein-Barr virus (EBV)-associated diseases.* Ann N Y Acad Sci, 1980. **354**: p. 326-31.

.96 Thompson, M.P. and R. Kurzrock, *Epstein-Barr virus and cancer.* Clin Cancer Res, 2004. **10**(3): p. 803-21.

.97 Long, H.M., G.S. Taylor, and A.B. Rickinson, *Immune defence against EBV and EBV-associated disease.* Curr Opin Immunol, 2011. **23**(2): p. 258-64.

.98 Odumade ,O.A., K.A. Hogquist, and H.H. Balfour, Jr., *Progress and problems in understanding and managing primary Epstein-Barr virus infections.* Clin Microbiol Rev, 2011. **24**(1): p. 193-209.

.99 Kirschner, A.N., et al., *Soluble Epstein-Barr virus glycoproteins gH, gL, and gp42 form a 1:1:1 stable complex that acts like soluble gp42 in B-cell fusion but not in epithelial cell fusion.* J Virol, 2006. **80**(19): p. 9444-54.

.100 Dreyfus, D.H., et al., *Inactivation of NF-kappaB by EBV BZLF-1-encoded ZEBRA protein in human T cells.* Journal of Immunology, 1999. **163**(11): p. 6261-8.

.101 Hudnall, S.D., *Viruses and Human Cancer*. 2014.

.102 Tsurumi, T., M. Fujita, and A. Kudoh, *Latent and lytic Epstein-Barr virus replication strategies.* Rev Med Virol, 2005. **15**(1): p. 3-15.

.103 Altmann, M. and W. Hammerschmidt, *Epstein-Barr virus provides a new paradigm: a requirement for the immediate inhibition of apoptosis.* PLoS Biol, 2005. **3**(12): p. e404.

.104 Strockbine, L.D., et al., *The Epstein-Barr virus BARF1 gene encodes a novel, soluble colony-stimulating factor-1 receptor.* J Virol, 1998. **72**(5): p. 4015-21.

.105 Young, L.S. and A.B. Rickinson, *Epstein-Barr virus: 40 years on.* Nat Rev Cancer, 2004. **4**(10): p. 757-68.

.106 Amon, W. and P.J. Farrell, *Reactivation of Epstein-Barr virus from latency.* Rev Med Virol, 2005. **15**(3): p. 149-156.

.107 Babcock, G.J., D. Hochberg, and A.D. Thorley-Lawson, *The expression pattern of Epstein-Barr virus latent genes in vivo is dependent upon the differentiation stage of the infected B cell.* Immunity, 2 :(4)13 .000p. 497-506.

.108 Steven, N.M., et al., *Immediate early and early lytic cycle proteins are frequent targets of the Epstein-Barr virus-induced cytotoxic T cell response.* Journal of Experimental Medicine, 1997. **185**(9): p. 1605-17.

.109 Pudney, V.A., et al., *CD8+ immunodominance among Epstein-Barr virus lytic cycle antigens directly reflects the efficiency of antigen presentation in lytically infected cells.* Journal of Experimental Medicine, 2005. **201**(3): p. 349-60.

.110 Martorelli, D., et al., *Spontaneous T cell responses to Epstein-Barr virus-encoded BARF1 protein and derived peptides in patients with nasopharyngeal carcinoma: bases for improved immunotherapy.* International Journal of Cancer, 2008. **123**(5): p. 1100-7.

.111 Khanna, R., et al., *Localization of Epstein-Barr virus cytotoxic T cell epitopes using recombinant vaccinia: implications for vaccine development.* Journal of Experimental Medicine, 1992. **176**(1): p. 169-76.

.112 Murray, R.J., et al., *Identification of target antigens for the human cytotoxic T cell response to Epstein-Barr virus (EBV): implications for the immune control of EBV-positive malignancies.* Journal of Experimental Medicine, 1992. **176**(1): p. 157-68.

.113 Rickinson, A.B. and D.J. Moss, *Human cytotoxic T lymphocyte responses to Epstein-Barr virus infection.* Annu Rev Immunol, 1997. **15**: p. 405-31.

.114 Hislop, A.D., et al., *Cellular responses to viral infection in humans: lessons from Epstein-Barr virus.* Annu Rev Immunol, 2007. **25**: p. 587-617.

.115 Chapman, A.L., et al., *Epstein-Barr virus-specific cytotoxic T lymphocyte responses in the blood and tumor site of Hodgkin's disease patients: implications for a T-cell-based therapy.* Cancer Research, 2001. **61**(16): p. 6219-26.

.116 Lee, S.P., et al., *Conserved CTL epitopes within EBV latent membrane protein 2: a potential target for CTL-based tumor therapy.* Journal of Immunology, 1997. **158**(7): p. 3325-34.

.117 Levitskaya, J., et al., *Inhibition of antigen processing by the internal repeat region of the Epstein-Barr virus nuclear antigen-1.* Nature, 1995. **375**(6533): p. 685-8.

.118 Blake, N., et al., *Human CD8+ T Cell Responses to EBV EBNA1: HLA Class I Presentation of the (Gly-Ala)–Containing Protein Requires Exogenous Processing.* Immunity, 1997. **7**(6): p. 791-802.

.119 Lee, S.P., et al., *CD8 T cell recognition of endogenously expressed epstein-barr virus nuclear antigen 1.* Journal of Experimental Medicine, 2004. **199**(10): p. 1409-20.

.120 Iizasa, H., et al., *Epstein-Barr Virus (EBV)-associated gastric carcinoma.* Viruses, 2012. **4**(12): p. 3420-39.

.121 Shinozaki-Ushiku, A., A. Kunita, and M. Fukayama, *Update on Epstein-Barr virus and gastric cancer (review).* Int J Oncol, 2015. **46**(4): p. 1421-34.

.122 Nishikawa, J., et al., *Epstein-barr virus in gastric carcinoma.* Cancers (Basel), 2014. :(4)6p. 2259-74.

.123 Chen, J.N., et al., *Epstein-Barr virus-associated gastric carcinoma: a newly defined entity.* J Clin Gastroenterol, 2012. **46**(4): p. 262-71.

.124 Hino, R., et al., *Activation of DNA methyltransferase 1 by EBV latent membrane protein 2A leads to promoter hypermethylation of PTEN gene in gastric carcinoma.* Cancer Research, 2009. **69**(7): p. 2766-74.

.125 zur Hausen, A., et al., *Unique transcription pattern of Epstein-Barr virus (EBV) in EBV-carrying gastric adenocarcinomas: expression of the transforming BARF1 gene.* Cancer Research, 2000. **60**(10): p. 2745-8.

.126 Wang, Q., et al., *Anti-apoptotic role of BARF1 in gastric cancer cells.* Cancer Lett, 2006. **238**(1): p. 90-103.

.127 Wiech, T., et al., *Cyclin D1 expression is induced by viral BARF1 and is overexpressed in EBV-associated gastric cancer.* Virchows Arch, 2008. **452**(6): p. 621-7.

.128 Ribeiro, J., et al., *Epstein-Barr virus gene expression and latency pattern in gastric carcinomas: a systematic review.* Future Oncol, 2017. **13**(6): p. 567579.-

.129 Iwakiri, D. and K. Takada, *Role of EBERs in the pathogenesis of EBV infection.* Adv Cancer Res, 2010. **107**: p. 119-36.

.130 Shinozaki, A., et al., *Downregulation of microRNA-200 in EBV-associated gastric carcinoma.* Cancer Research, 2010. **70**(11): p. 4719-27.

.131 Wei, M.X. and T. Ooka, *A transforming function of the BARF1 gene encoded by Epstein-Barr virus.* EMBO J, 1989. **8**(10): p. 2897-903.

.132 Wang, Y., et al., *Relationship between Epstein-Barr virus-encoded proteins with cell proliferation, apoptosis, and apoptosis-related proteins in gastric carcinoma.* World J Gastroenterol, 2005. **11**(21): p. 3234-9.

.133 Chang, M.S., et al., *Epstein-Barr virus-encoded BARF1 promotes proliferation of gastric carcinoma cells through regulation of NF-kappaB.* J Virol, 2013. **87**(19): p. 10515-23.

.134 Wang, J., et al., *Identification of genes involved in Epstein-Barr virus-associated nasopharyngeal carcinoma.* Oncol Lett, 2016. **12**(4): p. 2375-2380.

.135 O'Grady, T., et al., *Global transcript structure resolution of high gene density genomes through multi-platform data integration.* Nucleic Acids Res, 2016. **44**(18): p. e145.

.136 Correia, S., et al., *Natural Variation of Epstein-Barr Virus Genes, Proteins, and Primary MicroRNA.* J Virol, 2017. **91**(15).

.137 Hitt, M.M., et al., *EBV gene expression in an NPC-related tumour.* EMBO J, 1989. **8**(9): p. 2639-51.

.138 Sbih-Lammali, F., et al., *Transcriptional expression of Epstein-Barr virus genes and proto-oncogenes in north African nasopharyngeal carcinoma.* J Med Virol, 1996. **49**(:(1p. 7-14.

.139 Decaussin, G., et al., *Expression of BARF1 gene encoded by Epstein-Barr virus in nasopharyngeal carcinoma biopsies.* Cancer Research, 2000. **60**(19): p. 5584-8.

.140 Stevens, S.J., et al., *Noninvasive diagnosis of nasopharyngeal carcinoma: nasopharyngeal brushings reveal high Epstein-Barr virus DNA load and carcinoma-specific viral BARF1 mRNA.* Int J Cancer, 2006. **119**(3): p. 608-14.

.141 Seto, E., et al., *Epstein-Barr virus (EBV)-encoded BARF1 gene is expressed in nasopharyngeal carcinoma and EBV-associated gastric carcinoma tissues in the absence of lytic gene expression.* J Med Virol, 2005. **76**(1): p. 82-8.

.142 Hoebe, E.K., et al., *BamHI-A rightward frame 1, an Epstein-Barr virus-encoded oncogene and immune modulator.* Rev Med Virol, 2013. **2** :(6)3p. 367-83.

.143 Xue, S.A., et al., *Epstein-Barr virus gene expression in human breast cancer: protagonist or passenger?* Br J Cancer, 2003. **89**(1): p. 113-9.

.144 Arbach, H., et al., *Epstein-Barr virus (EBV) genome and expression in breast cancer tissue: effect of EBV infection of breast cancer cells on resistance to paclitaxel (Taxol).* J Virol, 2006. **80**(2): p. 845-53.

.145 Xue, S.A., et al., *Promiscuous expression of Epstein-Barr virus genes in Burkitt's lymphoma from the central African country Malawi.* International Journal of Cancer, 2002. **99**(5): p. 635-43.

.146 Zhang, Y., et al., *Transcriptional profiling of Epstein-Barr virus (EBV) genes and host cellular genes in nasal NK/T-cell lymphoma and chronic active EBV infection.* Br J Cancer, 2006. **94**(4) :p. 599-608.

.147 Frumento, G., et al., *Cord blood T cells retain early differentiation phenotype suitable for immunotherapy after TCR gene transfer to confer EBV specificity.* Am J Transplant, 2013. **13**(1): p. 45-55.

.148 Wang, A., et al., *Differential expression of EBV proteins LMP1 and BHFR1 in EBVassociated gastric and nasopharyngeal cancer tissues.* Mol Med Rep, 2016. **13**(5): p. 4151-8.

.149 Lin, X., et al., *CD4 and CD8 T cell responses to tumour-associated Epstein-Barr virus antigens in nasopharyngeal carcinoma patients.* Cancer Immunol Immunother, 2008. **57**(7): p. 963-75.

.150 Fiorini, S. and T. Ooka, *Secretion of Epstein-Barr virus-encoded BARF1 oncoprotein from latently infected B cells.* Virol J, 2008. **5**: p. 70.

.151 Hegde, N.R., et al., *Endogenous human cytomegalovirus gB is presented efficiently by MHC class II molecules to CD4+ CTL.* J Exp Med, 2005. **202**(8): p. 1109-19.

.152 Taylor, G.S., et al., *A role for intercellular antigen transfer in the recognition of EBV-transformed B cell lines by EBV nuclear antigen-specific CD4+ T cells.* J Immunol, 2006. **177**(6): p. 3746-56.

.153 Leung, C.S., et al., *Nuclear location of an endogenously expressed antigen, EBNA1, restricts access to macroautophagy and the range of CD4 epitope display.* Proc Natl Acad Sci U S A, 2010. **107**(5): p. 2165-70.

.154 Lautscham, G., et al., *Identification of a TAP-independent, immunoproteasome-dependent CD8+ T-cell epitope in Epstein-Barr virus latent membrane protein 2.* J Virol, 2003. **77**(4): p. 2757-61.

.155 Straathof, K.C., et al., *Characterization of latent membrane protein 2 specificity in CTL lines from patients with EBV-positive nasopharyngeal carcinoma and lymphoma.* J Immunol, 2005. **175**(6): p. 4137-47.

.156 Snyder, J.T., et al., *Molecular mechanisms and biological significance of CTL avidity.* Curr HIV Res, 2003. **1**(3): p. 287-94.

.157 McKee, M.D., J.J. Roszkowski, and M.I. Nishimura, *T cell avidity and tumor recognition: implications and therapeutic strategies.* J Transl Med, 2005. **3**: p. 35.

.158 Xue, S.A., et al., *Human MHC Class I-restricted high avidity CD4(+) T cells generated by co-transfer of TCR and CD8 mediate efficient tumor rejection in vivo.* Oncoimmunology, 2013. **2**(1): p. e22590.

.159 Zheng, Y., et al., *Human Leukocyte Antigen (HLA) A*1101-Restricted Epstein-Barr Virus-Specific T-cell Receptor Gene Transfer to Target Nasopharyngeal Carcinoma.* Cancer Immunol Res, 2015. **3**(10): p. 1138-47.

.160 Cho, H.I., et al., *A novel Epstein-Barr virus-latent membrane protein-1-specific T-cell receptor for TCR gene therapy.* Br J Cancer, 2018.

.161 Hoebe, E.K., et al., *Purified hexameric Epstein-Barr virus-encoded BARF1 protein for measuring anti-BARF1 antibody responses in nasopharyngeal carcinoma patients.* Clin Vaccine Immunol, 2011. **18**(2): p. 298-304.

.162 Burke, A.P., et al., *Lymphoepithelial carcinoma of the stomach with Epstein-Barr virus demonstrated by polymerase chain reaction.* Mod Pathol, 1990. **3**(3): p. 377-80.

.163 Tsai, C.Y., et al., *Comprehensive profiling of virus microRNAs of Epstein-Barr virus-associated gastric carcinoma: highlighting the interactions of ebv-Bart9 and host tumor cells.* J Gastroenterol Hepatol, 2017. **32**(1): p. 82-91.

.164 Chen, X.Z., et al., *Epstein-Barr virus infection and gastric cancer: a systematic review.* Medicine (Baltimore), 2015. **94**(20): p. e792.

.165 Truong, C.D., et al., *Characteristics of Epstein-Barr virus-associated gastric cancer: a study of 235 cases at a comprehensive cancer center in U.S.A.* J Exp Clin Cancer Res, 2009. **28**: p. 14.

.166 Hoshikawa, Y., et al., *Evidence of lytic infection of Epstein-Barr virus (EBV) in EBV-positive gastric carcinoma.* J Med Virol, 2002. **66**(3): p. 351-9.

.167 Cainap, C., et al., *Classic tumor markers in gastric cancer. Current standards and limitations.* Clujul Med, 2015. **88**(2): p. 111-5.

.168 Futawatari, N., et al., *Early gastric cancer frequently has high expression of KK-LC-1, a cancer-testis antigen.* World J Gastroenterol, 2017. **23**(46): p. 8200-8206.

.169 Boltin, D. and Y. Niv, *Mucins in Gastric Cancer - An Update.* J Gastrointest Dig Syst, 2013. **3**(123): p.15519.

.170 Jung, E.J., et al., *Expression of family A melanoma antigen in human gastric carcinoma.* Anticancer Res, 2005. **25**(3B): p. 2105-11.

.171 Xie, C., et al., *Melanoma associated antigen (MAGE)-A3 promotes cell proliferation and chemotherapeutic drug resistance in gastric cancer.* Cell Oncol (Dordr), 2016. **39**(2): p. 175-86.

.172 He, Q., et al., *Impact of the immune cell population in peripheral blood on response and survival in patients receiving neoadjuvant chemotherapy for advanced gastric cancer.* Tumour Biol, 2017. **39**(5): p. 1010428317697571.

.173 Tsujimoto, H., et al., *Roles of inflammatory cytokines in the progression of gastric cancer: friends or foes?* Gastric Cancer, 2010. **13**(4): p. 212-21.

.174 Ohta, M., et al., *Monocyte chemoattractant protein-1 expression correlates with macrophage infiltration and tumor vascularity in human gastric carcinomas.* Int J Oncol, 2003. **22**(4): p. 773-8.

.175 Kai, H., et al., *Involvement of proinflammatory cytokines IL-1beta and IL-6 in progression of human gastric carcinoma.* Anticancer Res, 2005. **25**(2A): p. 709-13.

.176 Akagi, J. and H. Baba, *Prognostic value of CD57(+) T lymphocytes in the peripheral blood of patients with advanced gastric cancer.* Int J Clin Oncol, 2008. **13**(6): p. 528-35.

.177 Sagiv, J.Y., S. Voels, and Z. Granot, *Isolation and Characterization of Low- vs. High-Density Neutrophils in Cancer.* Methods Mol Biol, 2016. **1458**: p. 179-93.

.178 Li, G.C., et al., *Are biomarkers correlated with recurrence patterns in patients with resectable gastric adenocarcinoma.* Mol Biol Rep, 2012. **39**(1): p. 399-405.

.179 Liu, K.J., et al., *Generation of carcinoembryonic antigen (CEA)-specific T-cell responses in HLA-A*0201 and HLA-A*2402 late-stage colorectal cancer patients after vaccination with dendritic cells loaded with CEA peptides.* Clin Cancer Res, 2004. **10**(8): p. 2645-51.

.180 Lee, K.A., et al., *A multimeric carcinoembryonic antigen signal inhibits the activation of human T cells by a SHP-independent mechanism: a potential mechanism for tumor-mediated suppression of T-cell immunity.* Int J Cancer, 2015. **136**(11): p. 2579-87.

.181 Lu, X., et al., *Tumor antigen-specific CD8(+) T cells are negatively regulated by PD-1 and Tim-3 in human gastric cancer.* Cell Immunol, 2017. **313**: p. 43-51.

.182 Gnjatic, S., et al., *Survey of naturally occurring CD4+ T cell responses against NY-ESO-1 in cancer patients: correlation with antibody responses.* Proc Natl Acad Sci U S A, 2003. **100**(15): p. 8862-7.

.183 Cesson, V., et al., *MAGE-A3 and MAGE-A4 specific CD4(+) T cells in head and neck cancer patients: detection of naturally acquired responses and identification of new epitopes.* Cancer Immunol Immunother, 2011. **60**(1): p. 23-35.

.184 Hanagiri, T., et al., *Analysis of a rare melanoma patient with a spontaneous CTL response to a MAGE-A3 peptide presented by HLA-A1.* Cancer Immunol Immunother, 2006. **55**(2): p. 178-84.

.185 Cho, Y., et al., *CD4+ and CD8+ T cells cooperate to improve prognosis of patients with esophageal squamous cell carcinoma.* Cancer Res, 2003. **63**(7): p. 1555-9.

.186 Caras, I., et al., *Evidence for immune defects in breast and lung cancer patients.* Cancer Immunol Immunother, 2004. **53**(12): p. 1146-52.

.187 Takano, S., H. Saito, and M. Ikeguchi, *An increased number of PD-1+ and Tim-3+ CD8+ T cells is involved in immune evasion in gastric cancer.* Surg Today, 2016. **46**(11): p. 1341-7.

.188 Takaya, S., H. Saito, and M. Ikeguchi, *Upregulation of Immune Checkpoint Molecules, PD-1 and LAG-3, on CD4+ and CD8+ T Cells after Gastric Cancer Surgery.* Yonago Acta Med, 2015. **58**(1): p. 44.-39

.189 Shiraki, T., et al., *Altered cytokine levels and increased CD4+CD57+ T cells in the peripheral blood of hepatitis C virus-related hepatocellular carcinoma patients.* Oncol Rep, 2011. **26**(1): p. 201-8.

.190 Iida, M., et al., *Increase of peripheral blood CD57+ T-cells in patients with oral squamous cell carcinoma.* Anticancer Res, 2014. **34**(10): p. 5729-34.

.191 Ichihara, F., et al., *Increased populations of regulatory T cells in peripheral blood and tumor-infiltrating lymphocytes in patients with gastric and esophageal cancers.* Clin Cancer Res, 2003. **9**(12): p. 4404-8.

.192 Maruyama, T., et al., *Distribution of Th17 cells and FoxP3(+) regulatory T cells in tumor-infiltrating lymphocytes, tumor-draining lymph nodes and peripheral blood lymphocytes in patients with gastric cancer.* Cancer Sci, 2010. **101**(9): p. 1947-54.

.193 Mizukami, Y., et al., *CCL17 and CCL22 chemokines within tumor microenvironment are related to accumulation of Foxp3+ regulatory T cells in gastric cancer.* Int J Cancer, 2008. **122**(10 :(p. 2286-93.

.194 Wang, L., et al., *Increased myeloid-derived suppressor cells in gastric cancer correlate with cancer stage and plasma S100A8/A9 proinflammatory proteins.* J Immunol, 2013. **190**(2): p. 794-804.

.195 Gabitass, R.F., et al., *Elevated myeloid-derived suppressor cells in pancreatic, esophageal and gastric cancer are an independent prognostic factor and are*

associated with significant elevation of the Th2 cytokine interleukin-13. Cancer Immunol Immunother, 2011. **60**(10): p. 1419-30.

.196 Weber, C.E. and P.C. Kuo, *The tumor microenvironment.* Surg Oncol, 2012. **21**(3): p. 172-7.

.197 Hanahan, D. and L.M. Coussens, *Accessories to the crime: functions of cells recruited to the tumor microenvironment.* Cancer Cell, 2012. **21**(3): p. 309-22.

.198 Weigelin ,B., M. Krause, and P. Friedl, *Cytotoxic T lymphocyte migration and effector function in the tumor microenvironment.* Immunol Lett, 2011. **138**(1): p. 19-21.

.199 Stojanovic, A. and A. Cerwenka, *Natural killer cells and solid tumors.* J Innate Immun, 2011. **3** :(4)p. 355-64.

.200 Aktas, O.N., et al., *Role of natural killer cells in lung cancer.* J Cancer Res Clin Oncol, 2018.

.201 Qin, Z., et al., *A critical requirement of interferon gamma-mediated angiostasis for tumor rejection by CD8+ T cells.* Cancer Res, 20 :(14)63 .03p. 4095-100.

.202 Ostrand-Rosenberg, S. and P. Sinha, *Myeloid-derived suppressor cells: linking inflammation and cancer.* J Immunol, 2009. **182**(8): p. 4499-506.

.203 Zou, W., *Regulatory T cells, tumour immunity and immunotherapy.* Nat Rev Immunol :(4)6 .2006 ,p. 295-307.

.204 Porembka, M.R., et al., *Pancreatic adenocarcinoma induces bone marrow mobilization of myeloid-derived suppressor cells which promote primary tumor growth.* Cancer Immunol Immunother, 2012. **61**(9): p. 1373-85.

.205 Yu, J., et al., *Myeloid-derived suppressor cells suppress antitumor immune responses through IDO expression and correlate with lymph node metastasis in patients with breast cancer.* J Immunol, 2013. **190**(7): p. 3783-97.

.206 Raychaudhuri, B., et al., *Myeloid derived suppressor cell infiltration of murine and human gliomas is associated with reduction of tumor infiltrating lymphocytes.* J Neurooncol, 2015. **122**(2): p. 293-301.

.207 Nishikawa, H. and S. Sakaguchi, *Regulatory T cells in cancer immunotherapy.* Curr Opin Immunol, 2014. **27**: p. 1-7.

.208 Chaudhary, B. and E. Elkord, *Regulatory T Cells in the Tumor Microenvironment and Cancer Progression: Role and Therapeutic Targeting.* Vaccines (Basel), 2016. **4**(3).

.209 Nirschl, C.J. and C.G. Drake, *Molecular pathways: coexpression of immune checkpoint molecules: signaling pathways and implications for cancer immunotherapy.* Clin Cancer Res, 2013. **19**(18): p. 4917-24.

.210 Buchbinder, E.I. and A. Desai, *CTLA-4 and PD-1 Pathways: Similarities, Differences, and Implications of Their Inhibition.* Am J Clin Oncol, 2016. **39**(1): p. 98-106.

.211 Radvanyi, L.G., et al., *Specific lymphocyte subsets predict response to adoptive cell therapy using expanded autologous tumor-infiltrating lymphocytes in metastatic melanoma patients.* Clin Cancer Res, 2012. **18**(24): p. 6758-70.

.212 Syn, N.L., et al., *De-novo and acquired resistance to immune checkpoint targeting.* Lancet Oncol, 2017. **18**(12): p. e731-e741.

.213 Iacopetta, B., F. Grieu, and B. Amanuel, *Microsatellite instability in colorectal cancer.* Asia Pac J Clin Oncol, 2010. **6**(4): p. 260-9.

.214 Lee, H.E., et al., *Prognostic implications of type and density of tumour-infiltrating lymphocytes in gastric cancer.* Br J Cancer, 2008. **99**(10): p. 1704-11.

.215 Grogg, K.L., et al., *Lymphocyte-rich gastric cancer: associations with Epstein-Barr virus, microsatellite instability, histology, and survival.* Mod Pathol, 2003. **16**(7): p. 641-51.

.216 Murphy, G., et al., *Meta-analysis shows that prevalence of Epstein-Barr virus-positive gastric cancer differs based on sex and anatomic location.* Gastroenterology, 2009. **137**(3): p. 824-33.

.217 Ohue, Y., et al., *Antibody response to cancer/testis (CT) antigens: A prognostic marker in cancer patients.* Oncoimmunology, 2014. **3**(11): p. e970032.

.218 Chen, X.H., et al.,]*Expression of MAGE-1 and MAGE-3 genes in gastric cancer and gastric biopsy tissues and its clinical significance].* Xi Bao Yu Fen Zi Mian Yi Xue Za Zhi, 2004. **20**(3): p. 310-3.

.219 Honda, T., et al., *Demethylation of MAGE promoters during gastric cancer progression.* Br J Cancer, 2004. **90**(4): p. 838-43.

.220 Sisik, A., et al., *CEA and CA 19-9 are still valuable markers for the prognosis of colorectal and gastric cancer patients.* Asian Pac J Cancer Prev, 2013. **14**(7): p. 4289-94.

.221 Ruffini, E., et al., *Clinical significance of tumor-infiltrating lymphocytes in lung neoplasms.* Ann Thorac Surg, 2009. **87**(2): p. 365-71; discussion 371-2.

.222 Yu, P. and Y.X. Fu, *Tumor-infiltrating T lymphocytes: friends or foes?* Lab Invest, 2006. **86**(3): p. 231-45.

.223 Erdag, G., et al., *Immunotype and immunohistologic characteristics of tumor-infiltrating immune cells are associated with clinical outcome in metastatic melanoma.* Cancer Res, 2012. **72**(5): p. 1070-80.

.224 Linnebacher, M. and C. Maletzki, *Tumor-infiltrating B cells: The ignored players in tumor immunology.* Oncoimmunology, 2012. **1**(7): p. 1186-1188.

.225 Woo, J.R., et al., *Tumor infiltrating B-cells are increased in prostate cancer tissue.* J Transl Med, 2014. **12**: p. 30.

.226 Rei, M., D.J. Pennington, and B. Silva-Santos, *The emerging Protumor role of gammadelta T lymphocytes: implications for cancer immunotherapy.* Cancer Res, 2015. **75**(5): p. 798-802.

.227 Silva-Santos, B., K. Serre, and H. Norell, *gammadelta T cells in cancer.* Nat Rev Immunol, 2015. **15**(11): p. 68391.-

.228 Wu, X., et al., *IL-17 promotes tumor angiogenesis through Stat3 pathway mediated upregulation of VEGF in gastric cancer.* Tumour Biol, 2016. **37**(4): p. 5493-501.

.229 Zhao, Y., C. Niu, and J. Cui, *Gamma-delta (gammadelta) T cells: friend or foe in cancer development?* J Transl Med, 2018. **16**(1): p. 3.

.230 Kabelitz, D., et al., *Human Vdelta2 versus non-Vdelta2 gammadelta T cells in antitumor immunity.* Oncoimmunology, 2013. **2**(3): p. e23304.

.231 Georgiannos, S.N., et al., *The immunophenotype and activation status of the lymphocytic infiltrate in human breast cancers, the role of the major histocompatibility complex in cell-mediated immune mechanisms, and their association with prognostic indicators.* Surgery, 2003. **134**(5): p. 827-34.

.232 Al-Shibli, K ,.et al., *The prognostic value of intraepithelial and stromal innate immune system cells in non-small cell lung carcinoma.* Histopathology, 2009. **55**(3): p. 301-12.

.233 Gras Navarro, A., A.T. Bjorklund, and M. Chekenya, *Therapeutic potential and challenges of natural killer cells in treatment of solid tumors.* Front Immunol, 2015. **6**: p. 202.

.234 Pauken, K.E. and E.J. Wherry, *Overcoming T cell exhaustion in infection and cancer.* Trends Immunol, 2015. **36**(4): p. 265-76.

.235 Moehler, M., et al., *Immunotherapy in gastrointestinal cancer: Recent results, current studies and future perspectives.* Eur J Cancer, 2016. **59**: p. 160-170.

.236 Barbee, M.S., et al., *Current status and future directions of the immune checkpoint inhibitors ipilimumab, pembrolizumab, and nivolumab in oncology.* Ann Pharmacother, 2015. **49**(8): p. 907-37.

.237 Lindau, D., et al., *The immunosuppressive tumour network: myeloid-derived suppressor cells, regulatory T cells and natural killer T cells.* Immunology, 2013. **138**(2): p. 105-15.

.238 Choi, H.S., et al., *The prognostic effects of tumor infiltrating regulatory T cells and myeloid derived suppressor cells assessed by multicolor flow cytometry in gastric cancer patients.* Oncotarget, 2016. **7**(7): p. 7940-51.

.239 Grapin-Botton, A., *Three-dimensional pancreas organogenesis models.* Diabetes Obes Metab, 2016. **18 Suppl 1**: p. 33-40.

.240 Lancaster, M.A. and J.A. Knoblich, *Organogenesis in a dish: modeling development and disease using organoid technologies.* Science, 2014. **345**(6194): p. 1247125.

.241 Ader, M. and E.M. Tanaka, *Modeling human development in 3D culture.* Curr Opin Cell Biol, 2014. **31**: p. 23-8.

.242 Dekkers, J.F., et al., *A functional CFTR assay using primary cystic fibrosis intestinal organoids.* Nat Med, 2013. **19**(7): p. 939-45.

.243 McCracken, K.W., et al., *Modelling human development and disease in pluripotent stem-cell-derived gastric organoids.* Nature, 2014. **516**(7531): p. 400-4.

.244 Barker, N., et al., *Lgr5(+ve) stem cells drive self-renewal in the stomach and build long-lived gastric units in vitro.* Cell Stem Cell, 2010. **6**(1): p. 25-36.

.245 Li, X., et al., *Oncogenic transformation of diverse gastrointestinal tissues in primary organoid culture.* Nat Med, 2014. **20**(7): p. 769-77.

.246 Nadauld, L.D., et al., *Metastatic tumor evolution and organoid modeling implicate TGFBR2 as a cancer driver in diffuse gastric cancer.* Genome Biol, 2014. **15**(8): p. 428.

.247 Dolznig, H., et al., *Modeling colon adenocarcinomas in vitro a 3D co-culture system induces cancer-relevant pathways upon tumor cell and stromal fibroblast interaction.* Am J Pathol, 2011. **179**(1): p. 487-501.

.248 Sugihara, H., et al., *Identification of miR-30e* regulation of Bmi1 expression mediated by tumor-associated macrophages in gastrointestinal cancer.* PLoS One, 2013. **8**(11): p. e81839.

.249 Hirt, C., et al., *"In vitro" 3D models of tumor-immune system interaction.* Adv Drug Deliv Rev, 2014. **79-80**: p. 145-54.

.250 Unger, C., et al., *Modeling human carcinomas: physiologically relevant 3D models to improve anti-cancer drug development.* Adv Drug Deliv Rev, 2014. **79-80**: p. 50-67.

.251 Alonso-Nocelo, M., et al., *Development and characterization of a three-dimensional co-culture model of tumor T cell infiltration.* Biofabrication, 2016. **8**(2): p. 025002.

.252 Gajewski, T.F., H. Schreiber, and Y.X. Fu, *Innate and adaptive immune cells in the tumor microenvironment.* Nat Immunol, 2013. **14**(10): p. 1014-22.

.253 He, W., et al., *Proteomic comparison of 3D and 2D glioma models reveals increased HLA-E expression in 3D models is associated with resistance to NK cell-mediated cytotoxicity.* J Proteome Res, 2014. **13**(5): p. 2272-81.

.254 Florczyk, S.J., et al., *3D porous chitosan-alginate scaffolds: a new matrix for studying prostate cancer cell-lymphocyte interactions in vitro.* Adv Healthc Mater, 201 :(5)1 .2p. 590-9.

.255 Caligiuri, M.A., *Human natural killer cells.* Blood, 2008. **112**(3): p. 461-9.

.256 Zingoni, A., et al., *Natural Killer Cell Response to Chemotherapy-Stressed Cancer Cells: Role in Tumor Immunosurveillance.* Front Immunol, 2017. **8**: p. 1194.

.257 Chang, H., et al., *Programmed death-ligand 1 expression in gastric adenocarcinoma is a poor prognostic factor in a high CD8+ tumor infiltrating lymphocytes group.* Oncotarget, 2016. **7**(49): p. 80426-80434.

.258 He, Y., et al., *PD-1, PD-L1 Protein Expression in Non-Small Cell Lung Cancer and Their Relationship with Tumor-Infiltrating Lymphocytes.* Med Sci Monit, 2017. **23**: p. 1208-1216.

.259 Aktas, E., et al., *Relationship between CD107a expression and cytotoxic activity.* Cell Immunol, 2009. **254**(2): p. 149-54.

.260 Liu, Y., et al., *Increased expression of programmed cell death protein 1 on NK cells inhibits NK-cell-mediated anti-tumor function and indicates poor prognosis in digestive cancers.* Oncogene, 2017. **36**(44): p. 6143-6153.

.261 Pesce, S., et al., *Identification of a subset of human natural killer cells expressing high levels of programmed death 1: A phenotypic and functional characterization.* J Allergy Clin Immunol, 2017. **139**(1): p. 335-346 e3.